WET PHYSICAL SEPARATION OF MSWI BOTTOM ASH

LENKA MUCHOVÁ

WET PHYSICAL SEPARATION OF MSWI BOTTOM ASH

Proefschrift

ter verkrijging van de graad van doctor
aan de Technische Universiteit Delft,
op gezag van de Rector Magnificus prof. ir. K.C.A.M. Luyben,
voorzitter van het College voor Promoties,
in het openbaar te verdedigen op maandag 13 december 2010 om 10:00 uur

door

Lenka MUCHOVÁ

Master of Science in Engineering
VŠB Technical University Ostrava, Czech Republic
geboren te Opava, Czech Republic.

Dit proefschrift is goedgekeurd door de promotor:

Prof. dr. ir. K. van Breugel

Copromotor: Dr. P. C. Rem

Samenstelling promotiecommissie:

Rector Magnificus	voorzitter
Prof. dr. ir. K. van Breugel	TU Delft, CiTG, promotor
Dr. P. C. Rem	TU Delft, CiTG, copromotor
Prof. dr. ir. G. Bonifazi	University La Sapienza, Roma
Prof. dr. K. Vrancken	University Antwerpen
Prof. dr. ir. M. Haas	TU Delft, CiTG
Prof. dr. ir. R. N. J. Comans	University Wageningen
Ir. M. A. J. van Berlo	Afvalenergiebedrijf, Amsterdam
Prof. dr. R. B. Polder	TU Delft, CiTG, reservelid

The research described in this thesis was supported by the Afval Energie Bedrijf, SenterNovem and LIFE.

Publisher: Ponsen & Looijen b.v.

Cover design: Michiel Nieuwenhuijse, Artic, b.v.

Keywords: bottom ash, leaching, physical separation, municipal solid waste, building products.

ISBN 978-90-6464-440-5

Contents

Executive Summary

Bottom ash (BA) from municipal solid waste incineration (MSWI) has high potential for the recovery of valuable secondary materials. For example, the MSWI bottom ash produced by the incinerator at Amsterdam contains materials such as non-ferrous metals (2.3%), ferrous metals (8-13%), gold (0.4 ppm), silver (10 ppm), stainless steel (0.1%) and minerals that can be converted into building products such as aggregates utilized for concrete, asphalt, etc. Since the composition of BA varies from country to country, the first step in valorizing it should be characterization. Therefore, this thesis proposes a new system for analysing BA, which concentrates on properties of fractions related to their ease of separation and material value.

A common practice in BA treatment in Western Europe is to separate coarse metal particles from the rest of the material by dry physical separation and to use the residue as a low-value construction material (road fillers) in controlled applications. Unrestricted re-use of this residue as a mineral resource is not possible in most EU countries because, generally, some of the leaching values for salts and metals exceed regulatory limits. In the Netherlands, the quality of building materials must be measured according to the Soil Quality Decree (SQD), which mandates strict environmental limits. Therefore, a new separation solution, based on wet physical treatment, was developed and tested to recover more metals and at the same time produce environmentally clean products that are suitable for various building applications.

Wet physical separation processes are preferable to dry methods of mineral processing due to the fact that they allow for more efficient and accurate classifications of size and density. The wet separation system can recover more metals of all size fractions down to 0.3 mm. Wet separation provides an important advantage through the wet screening process, as fine particles and organics are washed out from the granulate fractions, thereby improving the environmental quality of building products. The high recovery of metals provides financial benefits, and in combination with the washing and removal of organics it also has positive environmental effects. This thesis describes a new separation system, based on wet treatment, which was developed and implemented in a pilot plant in Amsterdam between 2003 and 2006. Furthermore, in addition to the treatments applied in the pilot plant, techniques to separate precious metals, separate stainless steel and improve the quality of the recovered sand were developed, all of which, when implemented, should increase the value of bottom ash.

Wet treatment is also able to decrease leaching values to close to, legislative limits in order to produce building materials from BA of a category for which no extra isolation is needed. Nevertheless, leaching values of some contaminants such as copper, molybdenum, antimony, sulphate and chloride still occasionally exceeded the limits. Therefore, this research focused on the correlation between contaminants (salts and metals) and separation settings, composition and input

materials, in aim to find the factors which can minimise leaching values. Another objective was to develop a convenient quality control system for building products generated from BA capable of rapidly providing accurate results based on measurements obtained using the column test. A model based on physical parameters such as diffusion, contaminant levels and dissolving factors was developed and demonstrated that it is possible to decrease the time consumed by the column test while still obtaining accurate predictions. The quality of building materials can determine their future utilization, therefore this study also examined the chemical, geometrical and mechanical properties of building materials such as sand and aggregates. Initial tests in which those aggregates and sand were utilized in asphalt, concrete and lime-sand stone were then conducted in attempts to identify the optimal utilization route for such materials.

The last part of this thesis presents a financial overview of the process, products and environmental impacts of BA treatment. The wet separation system was compared in these terms with the existing, commonly used dry separation system, using Life Cycle Assessment (LCA). This analysis showed that the wet process has less adverse environmental impacts, of diverse kinds (e.g. global warming and human toxicity potential), than the dry system. The investment and process costs of the pilot system in Amsterdam were also calculated under several scenarios, with various modelled separation capacities, to identify the most financially beneficial scheme for treating (and utilizing) BA.

Samenvatting

Bodemas (BA) afkomstig van afvalenergiecentrales heeft een hoge potentie voor het terugwinnen van waardevolle secundaire materialen. Bijvoorbeeld, bodemas geproduceerd bij de Amsterdamse afvalenergiecentrale bevat materialen zoals non-ferrous metalen (2.3%), ferrous metalen (8-13%), goud (0.4 ppm), zilver (10 ppm) en roestvrij staal (0.1%) en mineralen die geschikt zijn om als grondstof te dienen bij de productie van beton, asfalt, enz. Omdat de samenstelling van BA van land tot land kan variren, zal eerst een karakterisatie van de BA moeten plaatsvinden, waarna een valorisatie strategie kan worden vastgesteld. Dit proefschrift introduceert een nieuw systeem voor de analyse van BA, dat zich focusseert op deeltjes eigenschappen die gerelateerd zijn aan scheidbaarheid en de waarde van de materialen.

Het huidige verwerkingsproces voor BA in West Europa onttrekt de grove metalen delen uit de BA door gebruikmaking van droge fysische scheidingsmethoden en het residu wordt ingezet als laagwaardig constructie materiaal (opvulmateriaal voor wegen) bij gecontroleerde toepassingen. Hergebruik van het residu als minerale grondstof is in de meeste EU landen niet zonder beperkingen vanwege het overschrijden van de limiet betreffende het uitlogen van zouten en metalen. In Nederland moet de kwaliteit van bouwmaterialen worden bepaald aan de hand van Bouwstoffenbesluit waarin strikte milieu limieten worden gehanteerd. Een nieuwe oplossing voor de scheiding van BA, de natte fysische scheidingsmethode, is ontwikkeld en getest, waarbij meer metalen worden terug gewonnen en tegelijkertijd milieuvriendelijke schone bouwmaterialen worden geproduceerd met een scala aan toepassingsmogelijkheden.

Natte fysische scheidingsmethoden zijn te verkiezen boven droge methodes vanwege het feit dat ze efficinter en nauwkeuriger classificeren naar grootte en dichtheid. Het natte scheidingssysteem kan meer metalen terugwinnen in alle grootte fracties tot aan 0.3 mm. Natte scheiding heeft een belangrijk voordeel met het natte zeef proces, waarbij fijne deeltjes en organisch materiaal van het granulaat worden verwijderd. Hierdoor verbetert de milieutechnische kwaliteit van de bouw materialen. De hoge terugwinninggraad van het metaal geeft een financieel voordeel en in combinatie met het wassen en de verwijdering van organisch materiaal ook een positief milieu effect. Dit proefschrift beschrijft een nieuw scheidingssysteem dat gebruik maakt van natte processen, ontwikkeld en gebouwd als proef installatie in Amsterdam tussen 2003 en 2008. Verder zijn er, naast de proef installatie, additionele scheidingsstappen ontwikkeld, zoals de scheiding voor edelmetalen en roestvrij staal en een speciale toepassing voor zand, die er zorg voor dragen dat, wanneer ze worden gemplementeerd, de waarde van bodemas toeneemt.

De natte scheidingsmethode is ook in staat om door lagere uitloogwaarden tot bij of onder de toegestane limiet waarde, bouwmaterialen van BA te produceren, zonder dat extra isolatie nodig is. Enkele contaminanten, zoals koper, molybdeen, antimoon, sulfaat en chloride overschrijden soms de limieten. Dit

onderzoek richt zich op de correlatie tussen contaminanten (zouten en metalen) en scheidingsinstellingen, compositie en ingang materiaal, met als doel het vinden van factoren die leiden tot minimale uitloogwaarden. Een ander aspect is de ontwikkeling van een goed kwaliteitscontrole systeem voor bouwmaterialen van bodemas, dat snel en accuraat resultaat geeft op basis van metingen met de kolom test. Een model dat gebaseerd is op fysische parameters, zoals diffusie, contaminant concentraties en oplossings factoren is ontwikkeld. Met dit model is het mogelijk om de benodigde tijd voor metingen met de kolom test in te korten, terwijl een hoge accuraatheid van de voorspelling behouden blijft. De kwaliteit van bouw materialen bepaald de toekomstige gebruiksmogelijkheden en daarom richt deze studie zich ook op de chemische, geometrische en mechanische eigenschappen van bouw materialen, zoals zand en aggregaten. Met deze reden zijn er eerste testen uitgevoerd, waarbij deze aggregaten en zand zijn gebruikt bij de productie van asfalt, beton en kalkzandsteen, om zo de beste gebruiksroute te bepalen voor deze materialen.

Het laatste deel van dit proefschrift geeft zowel een financieel overzicht van de processen en producten als ook de milieu impact van BA behandeling. De natte scheidingsmethode wordt vergeleken met de bestaande, vandaag de dag gebruikte droge scheidingsmethode met gebruikmaking van Life Cycle Assesment (LCA). BA die is gescheiden met de natte scheidingsmethode is beter ten opzichte van de droge scheidingsmethode in vele milieu impacts. De investeringskosten en proceskosten van de proef installatie in Amsterdam zijn doorgerekend voor verschillende scenario's en verschillende installatie groottes gebaseerd op de scheidingscapaciteit om de meest geschikte financile route van bodemas te demonstreren.

Abreviations

AEB Afval Energie Bedrijf (incinerator of Amsterdam)

BA Bottom Ash

MSW Municipa Solid Waste

MSWI Municipa Solid Waste Incineration

LME London's Metals Exchange

MDS Magnetic Density Separator

WEEE Waste Electrical and Electronic Equipment

PCB's Polychlorinated Biphenyls

HNF Heavy Non-ferrous Metals

XRF X-ray Fluorescence

WECS Wet Eddy Current Separator

KGS Kynetic Gravity Separator

ECS Eddy Current Separator

CCS Cut Size (by hydrocyclone)

Chapter 1

Introduction

Summary

Bottom ash (BA) from municipal solid waste incineration (MSWI) has considerable potential for the recovery of valuable secondary materials, since it contains ferrous metals, non-ferrous metals, and minerals that can be used in the manufacture of building products. In 2006, a tonne of Amsterdam's BA contained about 130 kg of ferrous metals, 10 kg of aluminium, 7 kg of copper, zinc and lead, 4 kg of stainless steel, 20 g of silver and 0.4 g of gold. The total annual amounts in the BA represent 3% to 10% of the Dutch consumption of these metals.

A new wet physical separation plant with a capacity of 50 t/h was built in Amsterdam to recover ferrous and non-ferrous metals from three different size fractions of the ash with superior grades and recoveries to those yielded by conventional dry methods. The process uses standard technologies, like magnetic and eddy-current separation, as well as several new separation techniques, such as kinetic gravity separation and wire separation. Simultaneously, the plant produces building products (aggregates, sand) with low concentrations of metals and organics that can replace natural aggregate in a wide range of applications. An important criterion for these building products is that they should comply with civil technical engineering and environmental requirements for use as unrestricted construction materials.

General application of this novel type of Sorting After Incineration (SAI) would make a significant contribution to the environmental performance of Waste-to-Energy programs in Europe. The main ecological advantage of wet technologies is the increased recovery of metals, which helps to conserve primary resources. A second advantage is that the residual aggregates they generate have better leaching characteristics, and thus pose less environmental risks, than the corresponding materials produced by dry processes.

1.1 MSWI Bottom Ash

Municipal solid waste (MSW) is increasingly being pre-separated and incinerated in Europe, resulting in a flow of 20 million metric tonnes per year of bottom ash (BA), while the total amount of MSW deposited in land fills has gradually decreased in recent years. The increases in the separate collection and recycling of municipal solid waste, and the steady rise of incineration, are illustrated in (Figures 1.1, and 1.2).

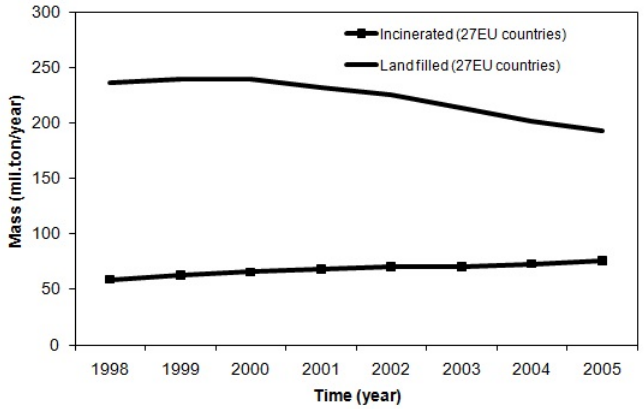

Figure 1.1: Amounts of municipal waste incinerated and land-filled in the EU 27 countries from 1998 to 2005 (Statistics 2007).

The largest producers of BA in the EU 24 countries are France and Germany, based on amounts of municipal solid waste incinerated (Figure 1.3). About 1.1 million tonnes per year of BA is produced in the Netherlands.

BA is by far the largest residue fraction (20-25% of the total residue) after the incineration of household waste. During the incineration the temperature is high enough to break the waste down into particles of various component materials, but not high enough to agglomerate these particles, therefore over 80% of the metals are free from other residues.
Most incinerators in Europe are of the stoker furnace type, as is the incinerator in Amsterdam. These produce a relatively coarse BA, in which ca. 50% of the material consists of fragments larger than 2 mm. Therefore, metals, minerals and organics can be easily separated from each other. A major problem after incineration is that the BA is cooled with water, which considerably complicates its classification into particle size fractions (an essential step prior to separating materials).The average composition of western European BA is shown in Table 1.1.

The major component of BA is aggregate (stone, glass, ceramics), which has similar engineering properties to primary building materials (gravel, sand) and is therefore often used in infrastructural projects. The value of the material ranges from negative costs (if the material has to be isolated to protect the environment) to 60% of the value of the primary building material with which it competes. The steel scrap from BA typically contains residual stone, which reduces the value of the scrap by €20-40 per tonne with respect to clean scrap.

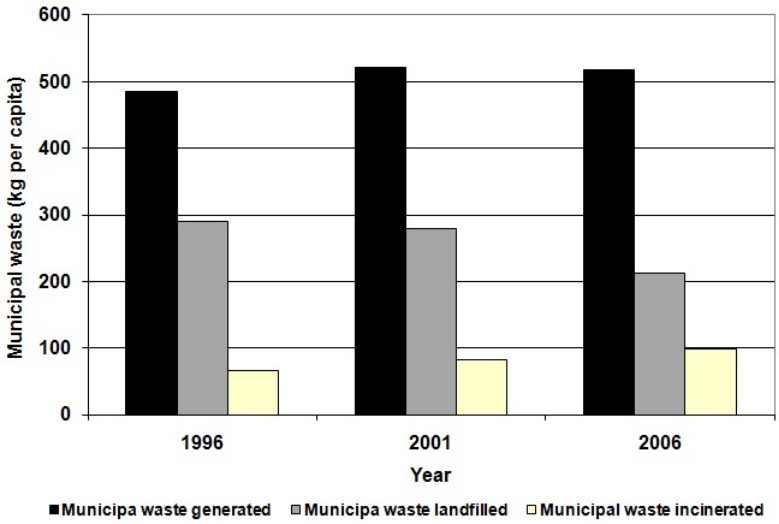

Figure 1.2: Amounts of municipal waste generated, incinerated and land-filled in the EU 27 countries per capita from 1996 to 2006 (Statistics 2007).

Table 1.1: Average composition of BA and typical values of its components per tonne in Western Europe.

Aggregate (stone, glass, ceramics)	± 80%	4 €/t
Iron scrap	5-13%	12 €/t
Non-ferrous metals (Cu, Al, Pb, Zn, brass)	1.7-5%	24 €/t
Precious metals	0.001%	10 €/t
Organic (paper, textile, plastic)	1-5%	

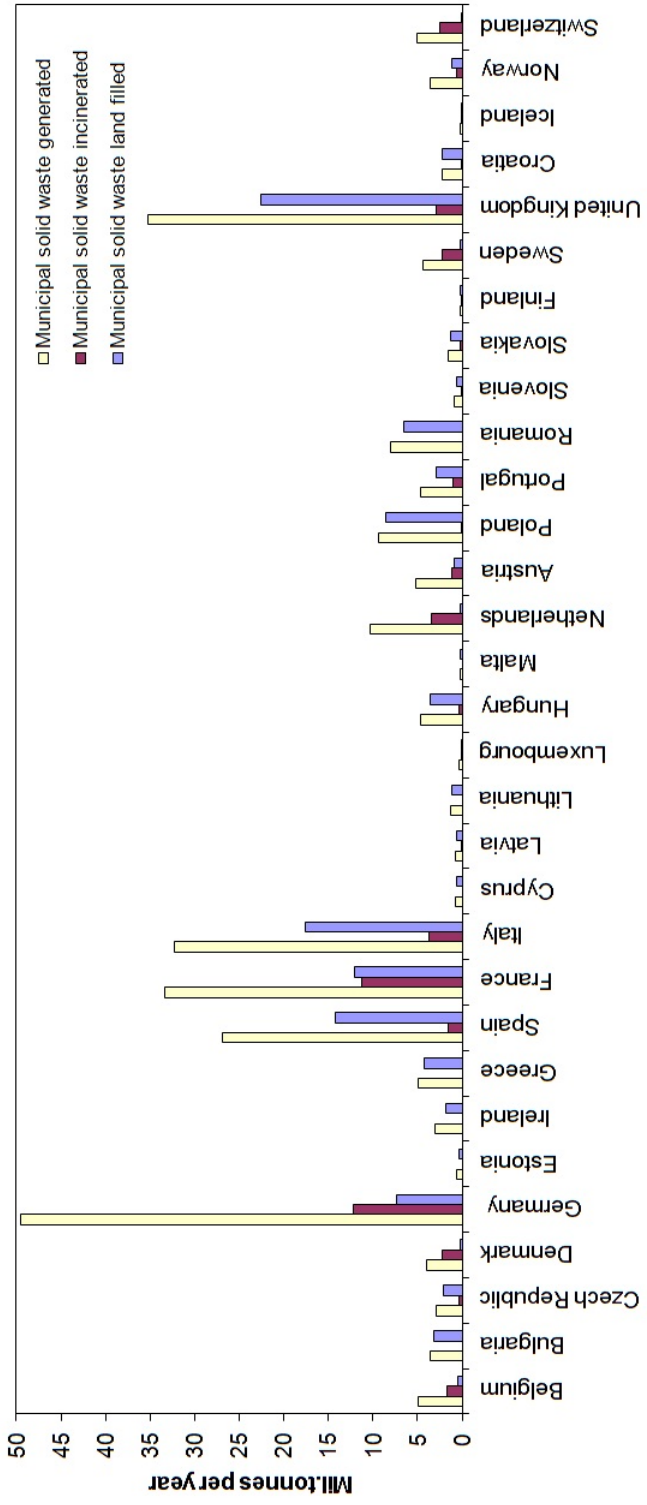

Figure 1.3: Amounts of municipal solid waste land filled and incinerated in the EU-24 countries in 2005 (Statistics 2007).

About 1% of copper and zinc from waste electrical appliances and batteries can also be found in the steel scrap. Modern technologies are able to remove these contaminants from the scrap. The main non-ferrous metal is aluminium which can be found throughout the entire particle size range of the ash. An important issue is the metallic aluminium found in the very fine fraction (<2 mm) of BA. This aluminium is currently lost in the BA and may represent the largest single loss in the aluminium cycle (RIVM 1994). Table 1.2 shows the estimated aluminium content of Dutch BA and land-filled household waste in 2000. This aluminium is presently lost in the BA.

Table 1.2: Estimated aluminum contents (ktonnes) of Dutch BA and land filled household waste in 2000, originating from various sources, based on composition and recovery estimates derived from a detailed analysis of data for 1996 and the overall non-ferrous content, household waste and incinerator data for 2000 (extrapolated from RIVM data of 1998 and 1999) (RIVM 1994).

Fraction	Incinerated	Bottom ash (BA)	Land-filled
Foil and Flexible Packaging	9.0	2.2	1.8
Other aluminium	5.9	5.9	1.2

Table 1.2 shows the aluminium content in BA lost from foil and flexible packaging. The difference between the amounts in foil and flexible packaging that were incinerated (9 ktonnes) and found in the BA (2.2 ktonnes) shows a gap of 6.8 ktonnes. In the sand product from Amsterdam BA the aluminium content was found to be 2%, which extrapolates to 6.6 ktonnes for the BA annually generated in the Netherlands; very similar to the loss in the aluminium cycle. This fine metallic aluminium is very difficult to separate. However, several options for its utilization are outlined in Chapter 4.

The remaining metals are mixtures of copper, brass, zinc, lead, stainless steel and precious metals. The concentration of ferrous and non-ferrous metals in MSWI BA varies for each country and for each incinerator. The BA from the incinerator of Rotterdam contains 1.2% aluminium, 0.2% copper, 0.2% heavy alloys and 9.9% ferrous metals (Waterman and van Houwelingen 1997). Chimenos (Chimenos et al. 1999) investigated two kinds of BA from different locations in Spain. The concentration of non-ferrous metals found in the Spanish BA varies between 2% and 5% and the concentration of ferrous metals varies between 5% and 12%. Raw Amsterdam BA contains 13% ferrous metals and 2.3% non-ferrous metals, 0.4 ppm of gold and 10 ppm of silver. Most of the precious metals in it are alloys from jewellery in the 2-6 mm fraction and residues of electronic components in the 0-2 mm fraction (Muchova and Rem 2006b, Muchova et al. 2008). The prices of various metals have increased sharply in recent years, so the recovery of metals from BA is an increasingly attractive option.

1.2 Valorisation Strategy of MSWI Bottom Ash

The presence of valuable products makes the BA interesting from the commercial point of view. The valorisation strategy depends on several factors (Figure

1.4).

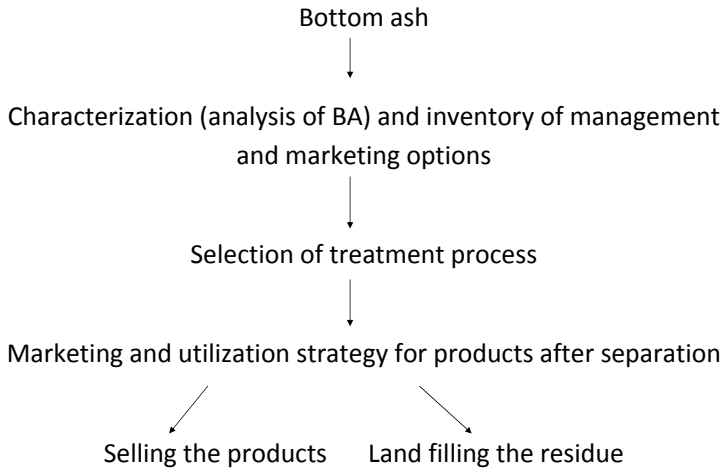

Figure 1.4: Valorisation scheme for MSWI BA.

The composition of the BA generated differs between countries, therefore the valorisation strategy should start with characterising the BA. The system used to characterize Amsterdam BA is described in Chapter 2. Chapter 2 also compares the composition of BA from Germany, Belgium and the Eastern part of the Netherlands. The management of BA depends on the market opportunities and legal requirements stipulated in legislation and regulations, regarding aspects such as the leaching tests that must be applied and leaching limits that must be met. For example, in Switzerland BA is mainly land-filled, whereas it is used as road filler in the Netherlands and Denmark - both of these countries have extensive legislation controlling the application of BA in infrastructure. When both issues, the analyzed composition and the marketing system, are determined then the optimal system of separation for such characteristics should be decided. The next step after separation is finding the optimal marketing systems for the products or waste streams.

1.3 Management, Legislation and Marketing of Bottom Ash

The recycling of BA is not regulated at the EU level, thus the market for the aggregate is determined by local legislation. In countries like Belgium, the Netherlands, France, Germany and Denmark civil and environmental regulations have been developed and adjusted to allow the use of BA residue in road construction (van Gerven et al. 2005). The costs of the land filling alternative in Europe vary between €30-80 per tonne of BA. Recycling of the stony fraction

(aggregate) is complicated due to the safety and quality levels of the residue. Many countries have strict leaching limits, hence the utilization of BA in those countries is very limited. EU legislation established the Waste Framework Directive (2008/98/EC 2008) where land filling requirements are proposed based on different leaching tests and leaching limits. However, the mineral fraction of BA has high potential for recycling, inter alia as a building material. Therefore, many EU countries have developed their own legislation and regulations for building materials. The main rule is to perform a standardized leaching test to determine if the BA meets the required leaching limits, and thus can be used as a building material. One of the complicating aspects is that the leaching tests and limit values differ somewhat from country to country. In the Netherlands, BA used for applications in civil industry has to meet certain leaching limits. In practice, the limits pose problems for unrestricted applications since the leaching values of MSWI BA processed in a conventional dry manner often exceed the defined ('Granulate construction material limit') limit values for Cu, Mo, Sb, Cl, Br and SO_4 (Chapter 5). In the Netherlands, a column test system has been long used for measuring leaching values, which was first introduced in legislation in the Building Materials Decree in 1989 (BMD 1989), when its use for granular applications was stipulated. The test reportedly simulates actual environmental conditions accurately (Chandler et al. 1997), (van der Sloot 2002). Hence, the results are likely to be more precise than, for example, those of a batch test (shaking test). The disadvantages of the column test are that it takes a long time (21 days) and analyzing all leachates is costly. In 2007 the Dutch government introduced further legislation, and amended previous regulations, in the Soil Quality Decree (SQD) (SQD 2007), which is based on experience from the previous legislation (BMD 1989), and retains use of the column test in practice. Due to its more reliable results and positive experience, the column test was chosen for use in this research.

1.3.1 EU Legislation

BA is classified as waste according to Directive 2001/118/EC (2001/118/EC 2001). The EU legislation in Directive 2008/98/EC (2008/98/EC 2008) on waste recommends the recovery of waste, but unfortunately there are no regulations for BA. The recycling of incinerator residue is not yet regulated at the EU level but the policy on land filling waste was developed and implemented for the waste material in our case for the BA. Two land filling types are applicable to incinerator residues. The European Directive established licensing criteria for landfills and acceptance procedures for receiving waste at these landfills. Table 1.3 shows the limit values (for granular waste) for two types of landfill and inert material. The member states are each supposed to establish criteria for monolithic waste, to provide the same level of environmental protection as set by the limit values for granular waste. The EU proposed three leaching tests (EN12457/1 2002), (EN12457/2 2002), (EN12457/3 2002), (EN12457/4 2002) and (prEN 14405 n.d.) and allows the member states to decide which of these tests will be used.

Each EU country has different regulatory tools, which mainly differ in leaching limits and the leaching tests applied. The leaching tests can be divided into column leaching tests and batch leaching (shaking) tests, or a combination of both. An overview of the leaching tests is presented in Table 1.4.

Table 1.3: Leaching limit values (emissions), for three kinds of land fills (2003/33/EC 2003) as measured by a compliance test (shaking test according to (EN12457/1 2002), (EN12457/2 2002), (EN12457/3 2002), (EN12457/4 2002) for L/S of 1 and 10l/kg) or percolation test (column test (prEN 14405 n.d.)) for L/S=0.1l/kg.

	Inert waste			Non-hazardous waste			Hazardous waste		
	L/S=2 (mg/kg)	L/S=10 (mg/kg)	L/S = 0.1 (mg/l)	L/S=2 (mg/kg)	L/S=10 (mg/kg)	L/S=0.1 (mg/l)	L/S=2 (mg/kg)	L/S=10 (mg/kg)	L/S = 0.1 (mg/l)
As	0.1	0.5	0.06	0.4	2	0.3	6	25	3
Ba	7	20	4	30	100	20	100	300	60
Cd	0.03	0.04	0.02	0.6	1	0.3	3	5	1.7
Cr total	0.2	0.5	0.1	4	10	2.5	25	70	15
Cu	0.9	2	0.6	25	50	30	50	100	60
Hg	0.003	0.01	0.002	0.05	0.2	0.03	0.5	2	0.3
Mo	0.3	0.5	0.2	5	10	3.5	20	30	10
Ni	0.2	0.4	0.12	5	10	3	20	40	12
Pb	0.2	0.5	0.15	5	10	3	25	50	15
Sb	0.02	0.06	0.1	0.2	0.7	0.15	2	5	1
Se	0.06	0.1	0.04	0.3	0.5	0.2	4	7	3
Zn	2	4	1.2	25	50	15	90	200	60
Chloride	550	800	460	10000	15000	8500	17000	25000	15000
Fluoride	4	10	2.5	60	150	40	200	500	120
Sulphate	560	1000	1500	10000	20000	7000	25000	50000	17000
DOC	240	500	160	380	800	250	480	1000	320

Table 1.4: Leaching tests used in different countries.

Type of tests	Test procedure	Country/Region
Column tests	NEN 7373 Column Test	The Netherlands, part of Belgium
	Nordtest Procedure: Column test.	Scandinavia
	Combined column and batch leaching test	Denmark
	European standard prEN 14405	Europe
Batch tests	DIN 38414 S4	Germany
	AFNOR X31-210	France
	JST-13	Japan
	European Standard prEN 12457 (Compliance batch leaching test)	Europe
	Nordtest Procedure: Single or two-stage batch test	Europe
	ENA Skaktest	Sweden
	TVA-Eluattest	Switzerland
	WRU Batch Extraction	United Kingdom
	EP Tox Method 1310	USA
	TCLP Method 1311	USA

In Germany waste is divided into seven categories (designated Z_o, $Z_{1.1}$, $Z_{1.2}$, Z_2, Z_3, Z_4 and Z_5) depending on their composition and leachability. The latter is measured according to DIN 38414-S4 (extraction test) (DIN38414S4 1984), with 24 h agitation and a liquid/solid (L/S) ratio of 10 l/kg. BA can be recycled for road construction. Besides the abovementioned categories, a special category for BA has been created, since leaching of salts from MSWI ash does not comply with the relevant Z_2 limit values. When recycling is not possible, the BA should be land filled as non-hazardous waste.

In France waste is divided into three types based on the NFX31-210 (extraction test) (NFX31-210 2004) run for 16 h at an L/S of 30 l/kg. BA with low leachability is classed as V-type (valorization) and can be recycled in road and other construction materials without applying isolation measures. The second type is M-type (maturation), which has medium leachability and needs treatment (solidification) before recycling. Without treatment this BA has to be land filled in a category II landfill. The third is S-type (storage), which has to be land filled in a category II landfill, with prior stabilization if needed.

Denmark introduced statutory limit values in January 2001, which should be determined by a batch test according to EN 12457/4 at L/S=2 l/kg.

In Flanders (Belgium) a Dutch leaching test, NEN 7373 (column test) (NEN7373 2004), is used for inorganic compounds. The leaching limit values are valid for granular materials with a density of 1550 kg/m^3. When the results comply with the limit values, the BA can be used as is, or as an aggregate in monolithic application. Granular materials that do not comply with the limit leaching values for granular applications can be recycled in monolithic form, calculated from the result obtained using the NEN 7345 (diffusion test) (NEN7345 1995).

The variations in leaching tests and leaching limits applied in different countries make it very difficult to compare the quality of BA between member states. The vision of the EU is to introduce a single, standardized test for all EU member states. This strategy will facilitate comparisons of the quality of the BA generated in different countries, and control of its utilization, to avoid the illegal transportation of waste materials that may be suitable in one country but not another that has stricter leaching limits.

1.3.2 Legislation in the Netherlands

In the Netherlands the waste management hierarchy is described in the Waste Chapter of the Environmental Management Act. The third National Environmental Policy Plan (NEPP3) set targets of 2000 ktonnes as the maximum amount of waste to be land filled in 2010. According to the waste management hierarchy, only waste that is unsuitable for recovery or incineration with energy recovery should be land filled. The target in the third National Environmental Policy Plan was that in 2010 a maximum of 9000 ktonnes would be incinerated. That assumes that no combustible waste would be land filled. The waste incinerator residues plan was published in 1995. This plan deals with solid residues from household waste and non-hazardous commercial waste incinerators. The target for BA recycling in 1999 was 1200 ktonnes: it resulted in a record level of almost 100% recycling.

BA is separated in the Netherlands and one of the recycled products (aggregate) is utilised in road bases, with a number of restrictions. The chemical composition of raw BA makes it highly reactive in ambient conditions due to

its high chloride, heavy metals and alkali sulphate and oxides contents. These components can cause severe environmental problems by contaminating surface water via leachate, and can be transferred to the soil and groundwater. To avoid this problem several environmental requirements have been applied to BA in the Netherlands. The first were introduced in the Building Materials Decree (BMD) 1995/1999, which was subsequently replaced by the Soil Quality Decree (SQD) in 2007, both based on the Soil Protection Law (WBB 1986), the Waste Disposal Act (1993/31/EU 1993) and the Surface Water Protection Law (WVO 1969).

The Building Materials Decreen (BMD) and Soil Quality Decree (SQD)
The first regulations of the quality of building products were introduced in 1995-1999, when the Building Materials Decree (BMD) came into force. The BMD was subsequently superseded, in 2007 by the Soil Quality Decree (SQD), which imposes general regulations for the application of building materials, soil and dredged material, (inter alia) setting maximal values for leaching and the composition of materials in order to limit their effects on land and surface water. The Decree also introduced the process to relevant parties and established the declaration, production and functional control systems.

According to the SQD the construction products are defined as solid moulded (monolithic) or granular products. The SQD introduced several rules with the following main features:

- The total content of silica, aluminium and calcium measured according to ASTM D 3682-01 (ASTMD3682-01 n.d.), NPR 6416 (NPR6416 1995) and NPR 6417 (NPR6417 1997) should not exceed 10% (m/m).
- A new system for classifying construction materials as solid, moulded (vormgegeven), granular construction materials (niet-vormgegeven) and granular IBC (isolation and controlling system required), illustrated in Table 1.5.
- Maximal leaching of granulate and moulded materials must be measured, according to the column test and the diffusion test.

Immission values must be calculated from results obtained with the NEN 7375 diffusion test for moulded (monolithic) applications and either the NEN 7373 (NEN7373 2004) or NEN 7383 column test (NEN7383 2004) for granular applications. Table 1.5 shows the immisions limits for categories N1 and N2 according to the BMD* and the new emission limits according to the SQD, valid from 2007.

Column test
In the Netherlands the immission values must be calculated from the test results obtained with the column test (NEN 7343, superseded by NEN 7373 in 2004)

*When the material complies with the immission limit values for category N1 construction material, it is decreed that no isolation precautions are needed to prevent contact with water. When the immision limit values for category N1 are exceeded, but the category N2 limit values are complied with, the waste can be recycled as category N2 construction material provided necessary isolation measures are taken.

for granular applications. For the NEN 7373 test a column (minimum length 20 cm, internal diameter 5 cm) is filled with material, which has been previously crushed to a particle size less than 4 mm. Distilled water is percolated through the column from bottom to top with a maximum flow of 2 cm/h. The eluate is collected in several fractions depending on the total L/S ratio that must be reached. According to the Soil Quality Degree the total L/S has to be 10. Seven fractions are collected, corresponding to L/S ratios of 0.1 (K1), 0.2 (K2), 0.5 (K3), 1 (K4), 2 (K5), 5 (K6) and 10 (K7).

During this research the old column test according to NEN 7343 was used. The new test (NEN 7373) is very similar to the one it replaced, except for a change in the water pH (pH 4 rather than pH 7) and a more detailed procedure for filling the column with the material and measuring specifications. During this research several problems were encountered that could influence the leaching results. One is related to milling and screening the samples before use in the column. During experimental work at TU Delft it was found that for larger size fractions (6-20 mm and larger) it is important to mill a larger amount of the sample and then split it with a splitter. Each fraction should be screened to < 4 mm before milling, then only the oversize fraction should be milled and screened again until the entire sample is < 4 mm. This reduction in particle size increases the specific area of the solid exposed to the leachant. Milling (grinding), therefore, increases surface accessibility and thus leaching (Todorovic and Ecke 2006).

Diffusion Test

The NEN 7345 diffusion test (NEN7345 1995) was replaced by the NEN 7375 test (NEN7375 2004) in 2004. The purpose of this test is to simulate the leaching of inorganic components from moulded and monolithic materials under aerobic conditions as a function of time over a period of 64 days. The nature and properties of the material matrix under investigation are determined in the test by placing a complete sample in a leaching fluid (demineralised, pH-neutral water) and replenishing the eluate at specific times. The concentrations of specifies ions in the leachate are measured. On the basis of the diffusion test results, the quantity leached per unit mass can be calculated for each component analysed.

Land Filling in the Netherlands

If the limit values are exceeded even for applications with isolation measures, the waste has to be land filled. Hazardous waste must be land filled in a C2 or C3 landfill. The selection of the landfill category depends on the leachability of several compounds according to the short NEN 7343 column test with L/S = 1 l/kg. Limit values are given in Table 1.6. If concentrations in the leachate are below the limit values, the waste is categorized as C3. If one or more of the leaching values are equal to or exceed the corresponding limit value, the waste has to be categorized as C2. C1 waste is a category of very specific hazardous waste (mercury containing waste, etc.).

Dutch Standards for Prospective Building Products

The residue after BA separation should be used as road filler in the Netherlands or as a replacement for building products (concrete, asphalt, lime-sand stone, aerated autoclaved concrete, etc.) as described in Chapter 6. There

Table 1.5: Immision limits according to the BMD in 1998 and emission limits according to the SQD in 2007 (in mg/kg).

	1998		2007		
	N1[6]	N2[6]	Moulded construction materials (E_{64d})[4]	Granulate construction materials[5]	IBC[5]
Cu	0.72	3.3	98	0.9	10
Mo	0.28	0.84	144	1	15
Sb	0.045	0.41	8.7	0.16	0.7
Br	4.4[7]	44[7]	670[2]	20[2]	34
As	0.88	7.0	260	0.9	2
Ba	5.50	55	1500	22	100
Cd	0.032	0.061	3.8	0.04	0.06
Cl	600[7]	8790[7]	110000[2]	616[2]	8800
Cr	1.3	12	120	0.63	7
Co	0.42	2.3	60	0.54	2.4
F	13[7]	96[7]	2500[2]	55[2]	1500
Hg	0.018	0.075	1.4	0.02	0.08
Pb	1.9	8.1	400	2.3	8.3
Ni	1.1	3.5	81	0.44	2.1
Se	0.044	0.094	4.8	0.15	3
SO_4	750[7]	22000[7]	165000[2]	1730[2,3]	20000
Sn	0.27	2.3	50	0.4	2.3
V	1.6	32	320[1]	1.8[1]	20
Zn	3.8	14	800	4.5	14

[1] Requirement of 460 mg/m^2 for vanadium applies in the case of the use of solid building materials in large surface water and a requirement of 4.6 mg/kg dry matter applies in the case of granulate materials.
[2] The following applies to the use of building materials in places where direct contact is (possible) with seawater or brackish surface water with a natural chloride content of more than 5.000 mg/l: a) no emission requirements for chloride and bromide, and b) the emission requirements given in the Table for fluoride and sulphate multiplied by a factor of 4.
[3] For a period as indicated in article 5.1.9 (2), an emission requirement of 2.430 mg/kg d.m. applies.
[4] Measured by diffusion test in mg/m^2
[5] Measured by column test in mg/kg
[6] Immision values which must be calculated from the emissions values according to the BMD.
[7] Other limit values apply for specific conditions (for more details see the BMD).

are standards, with geometrical, physical and chemical requirements, for each application.

1.4 Treatment and Utilization

MSWI BA treatment in Europe is based on one of four basic solutions:

- Land filling, possibly after partial recovery of ferrous and non-ferrous metals (> 10 mm) by dry physical separation (using magnetic and eddy current separators) (Switzerland, Italy)
- Partial recovery of ferrous and non-ferrous metals (> 10 mm) by dry physical separation, followed by use of the residue in infrastructure (the Netherlands, Germany, France)
- Deep dry recovery of metal particles (> 4 mm) by dry physical methods, followed by use of the residue in infrastructure (Denmark)
- Wet treatment of the BA to remove organics and metals down to 0.3 mm, while leaving a clean aggregate for the building industry (Amsterdam, the Netherlands). (This technology is at the testing stage and has not yet been applied.)

BA is commonly separated by dry physical methods (coarse screening, size reduction, magnetic separation, eddy current separation) and using aging or washing to stabilize the residue in terms of leaching capacity. France provides some good practical examples of these procedures, including some incinerators in which ferrous metals are separated directly on site. The country has over 50 BA management facilities for treatment and maturation. The facilities screen and crush the ash, use sifters to eliminate light unburned fractions, magnetic separators to recover ferrous metals and eddy current separators to recover aluminium and other non-ferrous metals. Off-site, secondary separation facilities recover another 5.3% of ferrous metals and 0.5% of non-ferrous metals (Autret et al. 2007).
In Germany, BA is also treated by magnetic separation and eddy current separation.

After separation the residue is sprayed with water and stored in an enclosed facility for about three months. It is believed that after this treatment the BA is stabilized and can be used for road construction.
Other EU member countries are using identical or similar procedures to improve the quality of BA residue. Danish facilities are able to separate a higher proportion of metals from BA. In 2007, the company Melgaard recovered 1.5% of non-ferrous metals. Fine metals, down to 4 mm, are separated by dry physical separation after intensive screening, depending on the moisture content of the ash. The coarse magnetic fraction is processed by hand to recover copper from electric appliances. The residue is then used as road filler if the leaching values are within the required limits. Attempts are being made in many countries to find ways to reduce leaching to proposed levels. Several alternatives have been examined in recent years, mainly focusing on the immobilization of mobile metals and other elements. Some of the immobilization processes take place at a low temperature (natural weathering, carbonation, reaction with phosphate,

etc.) and others at a high temperature (clinker production, vitrification, sintering, calcination, co-smelting with glass and artificial stone formation). However, immobilization strategies that have been tested on BA have not completely met the required criteria, in terms of leaching values. Outside Europe, expensive thermal treatment or a combination of separation and high temperature processing are considered options.

1.4.1 Wet Physical Separation Plant

In the Netherlands, projected changes in legislation have posed challenges, requiring improvements in the separation of BA. Consequently, a wet physical separation pilot plant was built in Amsterdam (Figure 1.5).

Table 1.6: Dutch land filling limits (below the category C3 thresholds, but higher than C2 thresholds).

	for L/S=1 in mg/kg
As	9
Ba	60
Cd	0.2
Cr total	30
Cu	10
Hg	0.1
Mo	3
Ni	10
Pb	25
Sb	0.8
Se	0.3
Zn	40
Chloride	50000
Fluoride	280
Sulphate	80000

The treatment facility in Amsterdam consists of two distinct separation units (Figure 1.6). The first is the existing dry physical separation plant and the second is a new pilot plant based on wet physical separation. The dry BA treatment plant shreds and separates the > 20 mm ferrous scrap (7% of the total BA), the > 15 mm non-ferrous metals (1.1%) and the organic materials (5%) fractions. The 0-40 mm residue fraction continues to the new wet pilot plant which applies wet physical separation treatments. The pilot plant can separate yet another fraction of metals and organics, and produce quality building products (Chapters 3 and 6).

The wet treatment plant consists of a screening section, where the BA is separated into five fractions: sludge, sand, the fine fraction, the coarse fraction and the > 20 mm fraction. The > 20 mm fraction was not further investigated during the research this thesis is based upon, and therefore was not included in the detailed mass balance analyses. This wet technology can recover virtually all metals from the size fraction > 0.3 mm (Table 1.7) and remove organic and

Figure 1.5: Pilot plant for wet physical separation of BA with a capacity of 50 t/h.

fine particles from the residue.

This combination of screening, metals recovery and washing considerably improves the quality of the residue in terms of leaching of most of the elements (Table 1.8).

Another advantage is the recovery of precious metals from the 0-6 mm fraction by new developments in sink-floating using a magnetic density separator (Chapter 4). The magnetic density separator provides the possibility for relatively small processors, like BA treatment plants, to concentrate precious metals and produce non-ferrous metal fractions that are directly suitable for smelters.

High recovery of metals is essential to ensure that the stony fraction has sufficient quality for high value construction applications because metals are problematic even at very low concentrations. The most difficult metal components to remove are wires and stainless steel parts (Chapter 3 and 4). The mechanical properties of the aggregate generally meet relevant criteria, and thus are not problematic. Hence, the wet physical separation process has many positive economic and environmental advantages (Chapter 7 and 8).

1.4.2 Wet Versus Dry Physical Separation

The advanced treatment systems (dry and wet) currently on the market can have a significant, positive impact on the economics and recycling efficiency of MSWI BA. Therefore, the efficiency of wet physical separation and typical dry physical methods was compared by comparing the BA generated in the Amsterdam pilot plant and BA from the Eastern part of the Netherlands. The grades and recoveries of the magnetic fraction, the fine and coarse non-ferrous fractions separated by dry physical and wet methods are shown in Table 1.9.

The grade of ferrous metals recovered by wet physical methods is higher than that of metals recovered by dry methods, while recoveries of ferrous metals by wet and dry methods are similar. However, recoveries of non-ferrous metals are

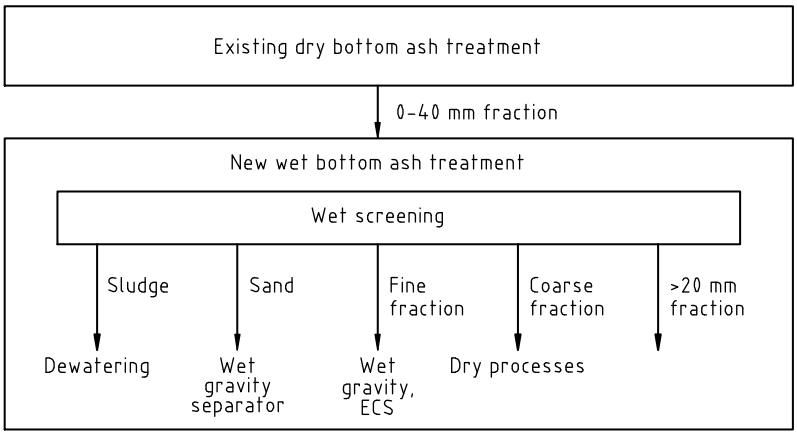

Figure 1.6: Flow sheet of the Amsterdam pilot.

Table 1.7: Grades and recoveries of the magnetic, non-ferrous and aluminium fractions from the wet separation pilot plant (after pre-treatment in the dry separation plant).

	Magnetic fraction[1]		Non-ferrous fraction		Aluminium fraction	
	Grade (%)	Recovery (%)	Grade (%)	Recovery (%)	Grade (%)	Recovery (%)
6-20 mm	62	90	87	77	n.d.	n.d.
2-6 mm	n.d.	n.d.	80	81	82	83
<2 mm	98	29	29	40	n.r.	n.r.

[1] the magnetic fraction refers to all magnetic particles removed by a magnetic separator. n.d. - not determined; n.r. - not recovered. The >20 mm fraction was not processed during the research, and therefore is not included in the table.

Table 1.8: Comparison of leaching values for critical elements from Amsterdam BA without treatment (column 2) and values after wet physical separation for three fractions (sand, fine aggregate and coarse aggregate) in mg/kg measured by the NEN 7343 column test in 2005.

Leachate	BA	Sand product	Fine aggregate	Coarse aggregate
Cu	5.4 ± 3.2	1	1	0.9
Mo	1.2 ± 0.4	0.2	0.9	0.5
Sb	0.21 ± 0.13	0.27	0.2	0.18
SO4	6100 ± 1838	1600	3000	1550
Cl	4150 ± 495	165	400	800

Figure 1.7: An examples of a product from BA, the 2-6 mm heavy non-ferrous metals.

considerably higher for wet methods. This is because wet treatment can separate fragments of non-ferrous metals down to 0.3 mm. In the short term, the choice of wet or dry separation is determined by the local market for aggregate and sand versus the costs of land filling the residue or the isolation measures required for using it in roads. In the somewhat longer term, wet treatment technologies offer substantial advantages, including superior metal recovery (particularly of copper and precious metals), smaller amounts of residue and greater flexibility with respect to the moisture content of the input ash.

1.5 Products from Bottom Ash

The largest fraction (aggregate) can be used for a variety of building applications (foundations, road construction, concrete, bituminous concrete aggregates, asphalt, etc.) as illustrated in Figures (Figures 1.8a, 1.8b). The fine fractions of BA are somewhat pozzolanic as a result of the incineration process. A new application related to this property is in finely crushed aggregate as a replacement for cement.

Table 1.9: Comparison of grades and recoveries of metals obtained by wet physical separation (in the Amsterdam pilot plant) and typical treatment using dry physical methods (in percentage).

	Wet pilot plant in Amsterdam		Typical dry separation plant	
	Grade	Recovery	Grade	Recovery
Ferrous metals	>80	83	98	82
Non-ferrous metals	>80	73	75-84	9-28
Aluminium	>80	80	Not separated	Not separated

The other main products are steel and non-ferrous scrap. The steel scrap is

(a) Aggregates from BA.

(b) Concrete blocks made from the BA aggregate.

Figure 1.8: An example of aggregate products from BA.

usually sold to shredding companies to upgrade for smelting. The non-ferrous scrap is sold to sink-floaters to produce aluminium and heavy metal fractions to various types of non-ferrous smelters. Now that increasingly fine non-ferrous fractions are produced, with relatively high concentrations of heavy non-ferrous alloys, including precious metals, it may become attractive for BA treatment plants to separate the heavy alloys from the aluminium in a jig or a kinetic gravity separator. The precious metals can also be concentrated by a magnetic density separator. The resulting heavy 2-6 mm fraction (Figure 1.7) can then be sold directly to a copper/brass smelter and the precious metals concentrate to a precious metals smelter.

1.6 Ecology

In Western Europe MSWI BA has long been recycled as a source of road construction materials instead of being land filled. Apart from the environmental benefits it offers, by saving resources, the separation method can also contribute to reducing the EU's dependence on imported ores and concentrates. However, the currently used method for BA processing, dry separation, while ranking higher in the waste hierarchy than land filling, poses several environmental problems (Birgisdottir et al. 2007). Therefore, the two methods were subjected to LCA analyses, which indicated that wet methods are superior to dry methods in terms of all considered environmental impacts, in addition to saving more resources (Chapter 8).

1.7 Aims and objectives of the research

The objective of the research this thesis is based upon was to develop a wet system for separating MSWI bottom ash in Amsterdam and process the bottom ash into high-quality building materials and valuable light and heavy non-ferrous concentrates. It involved monitoring and operational optimization of the full-scale plant with an emphasis on understanding the relationships between the techniques applied and product quality. Some of the research was performed at the plant itself, and some in the laboratories of TU Delft and AEB, which

provided the scientific tools to investigate the performance of processes and the quality of products. The main questions addressed were:

- To what extent can separation technology increase product quality, and what plant processes contribute strongly to the quality of the building product (aggregate and sand product)?
- What components affect the engineering quality of the aggregate fraction in concrete?
- What arrangement of separation steps (cyclones, upstream column, jig) is most suitable for obtaining a high quality sand product?
- What factors influence leaching from aggregate and sand products, and what are acceptably low content levels for metals and organics in building materials derived from BA to produce high-quality products?
- What is the best utilization route for the metals and how can the desired quality of the non-ferrous concentrates be achieved?
- What are possible outlets for the sludge fraction?
- Is it possible to predict the quality of products based on the input composition?

Chapter 2

Characterisation of MSWI Bottom Ash

Summary

The composition of bottom ash (BA) resulting from municipal solid waste incineration (MSWI) varies amongst countries and incinerators (Waterman and van Houwelingen 1997, Chimenos et al. 1999, Schmelzer et al. 1996). Different options are also available for its utilization in different countries (Muchova and Rem 2007a). Therefore, the strategy for utilizing BA should be determined after analysing its composition and considering marketing options (Figure 2.1).

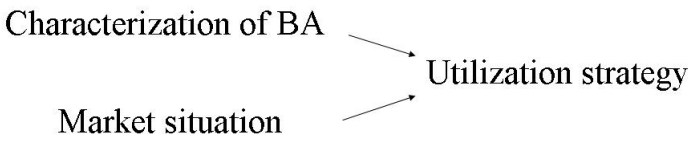

Figure 2.1: Utilazation strategy.

The first step of the valorisation strategy should be characterization of the BA by an appropriate system of sampling and analysis. This chapter proposes a new system for analysing BA, focusing on properties of the particles related to their ease of separation and material value. The results of such analysis indicate the viability of BA separation and utilization. The majority of the analyses described in this chapter were applied to Amsterdam BA. However, bottom ashes from Germany, Belgium and the Eastern part of the Netherlands were also tested, and showed comparable composition to Amsterdam BA.

2.1 Introduction

Bottom ash (BA) can be analysed in various ways. Most authors have focused on analysing and measuring its elemental composition (Chung et al. 2007, Song et al. 2004). This kind of analysis is interesting from an environmental perspective. Examples are studies of leaching of harmful elements, heavy metals, salts, etc. from BA into the environment. However, elemental analysis generally does not provide indications of the content of valuable products that can be recycled. For this, it is essential to know the grain size distribution of valuable metallic particles and organic pollutants, since this information indicates the economic value and recyclability of the ash. Figure 2.2 shows particle size distribution curves for metals (gold, aluminium and heavy non-ferrous metals) found in Amsterdam BA.

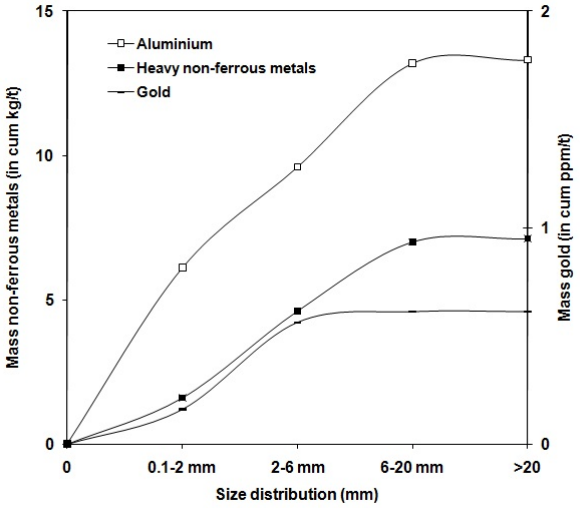

Figure 2.2: Size distributions of base metals, heavy non-ferrous metals (Cu, brass, Zn, Pb), aluminium and gold, in 1 ton of Amsterdam's BA.

One of the main recycling issues for BA is the presence of metals (non-ferrous, precious and ferrous), followed by the aggregate (stone, glass, ceramics) and the organic content (plastic, foils, textile, wood, etc.) which has a negative impact on the engineering and environmental quality of possible building products.

Since we are interested in the particulate nature of the ash, analysis of any finite proportion of sample introduces a statistical error of the kind studied by Gy (Gy 1999). This chapter describes a sampling strategy, including specifications of the amounts of sample that are required to control this statistical error. A complete BA analysis system was developed at TU Delft in order to document the valorisation potential of Amsterdam BA, and BAs from several incinerators in Western Europe were analyzed in the same way to determine if there were significant differences in composition amongst them.

2.2 Sampling and Analysis

The sampling and analysis strategy described in this chapter was used throughout this research. Therefore, the results from different tests can be compared. The outlined procedure can be applied to BA of any origin. This system can be used to ensure that statistical errors can be kept within acceptable limits, and the analyses focus on the economic and environmental value of the BA.

2.2.1 Sampling Strategy

BA can be analysed by collecting samples at two points:

- after incineration (from the mixture of BA after cooling without any further separation treatment)
- after incineration and separation steps have been applied (the ferrous fraction, non-ferrous fraction, residue, etc.)

In the first option the amount of the analysed sample will be larger than the amounts analyzed in the second option. In the second option, BA is distributed into several fractions of varying value and sizes, in which the final products are concentrated. To avoid substantial errors during sampling it is important to follow certain basic rules. Representative samples should be collected in different time periods, homogenised and split. The size of the samples required depends on the size distribution and content of the desired material (non-ferrous metals, precious metals, organic, etc.). Larger samples will be required for fractions with large size distributions than for fractions with fine size distributions. The relationship between size distribution and sampling errors is illustrated in Figure 2.3.

Figure 2.3 shows that error levels depend on the number of particles in the sample (sample mass/average particle mass) and the concentration. The sampling errors were calculated according to Gy's formula for a material consisting of two components:

$$c = \frac{\sigma}{aL} \text{ in cases where } aL < 10\% \text{ (most cases)} \tag{2.1}$$

$$c = (1 - aL)\sigma g \text{ in cases when } aL > 90\% \text{ (concentrates)} \tag{2.2}$$

$$c = \frac{1 - aL}{aL}\left[(1 - aL)\sigma A + aL\sigma G\right]\,[\mathrm{g/cm^3}] \tag{2.3}$$

$$aL = \frac{MA}{ML} \tag{2.4}$$

aL the proportion of A in the lot (e.g. 0.10)
σA the density of the critical component
σG the density of the other material

The average particle mass for each size fraction and product obtained from the BA was experimentally determined (Annex A, Table A.1, A.2, and A.3) and used for the error calculations.

The average content of non-ferrous metals in Amsterdam BA is approximately 2%, including approximately 0.0004% of gold. Calculated errors for the

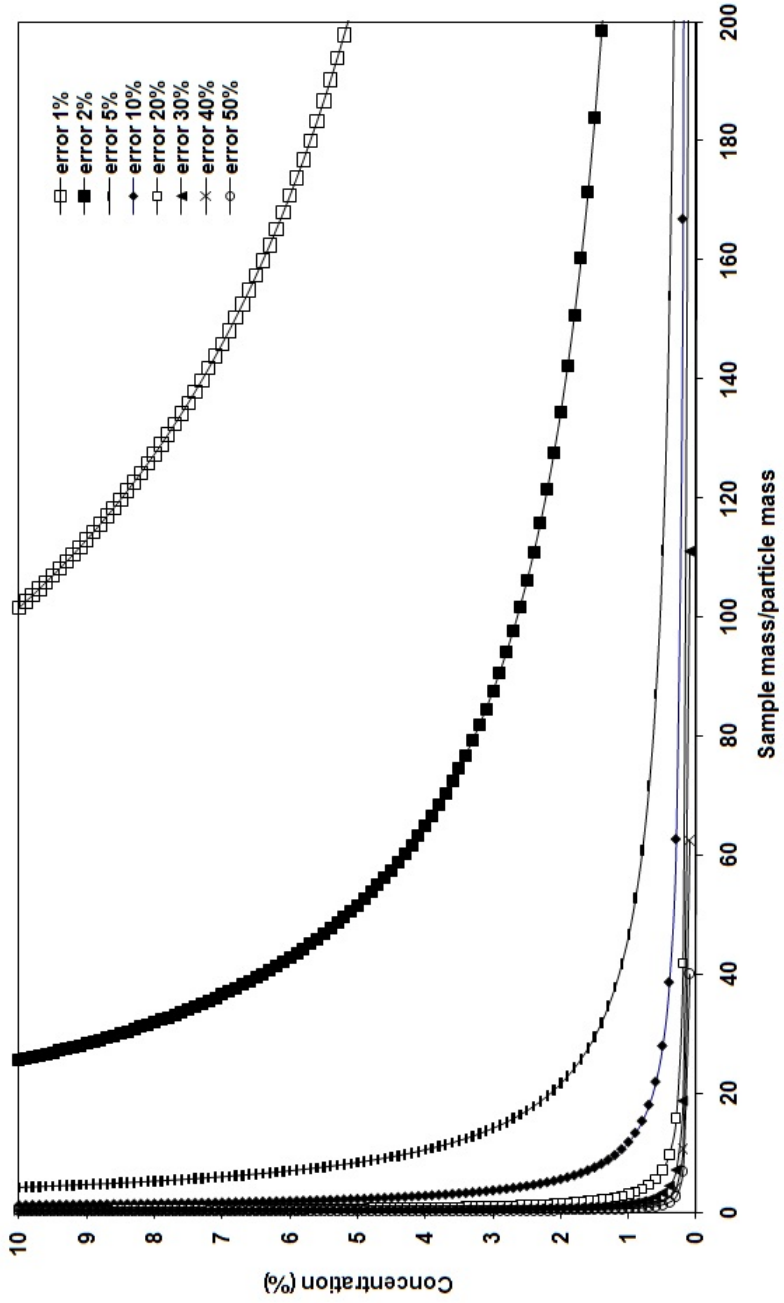

Figure 2.3: Statistical error related to the amount of particles and the sample concentration.

non-ferrous fraction and the gold found in the sample mass is shown in Table 2.1.

Table 2.1: Effects of varying the mass of BA analyzed on errors of estimated non-ferrous metals and gold contents (assuming the non-ferrous metals and gold contents of the BA, overall, are 2% and 0.0004%, respectively).

Mass BA (kg)	Non-ferrous metals error (%)	Gold error (%)
25	15.5%	1000%
50	11.0%	707%
100	7.7%	500%
200	5.5%	354%
500	3.5%	224%
1000	2.4%	158%

Table 2.1 shows that the errors for gold contents are very large even when 1 tonne of BA is collected. However, the sampling errors can be reduced in several ways, for example by dividing the sample into several sizes and different products. Sample size is closely related to sampling error. Therefore one should focus on the composition of BA initially, and decide what the main product(s) of interest will be. Even a 100 kg sample of BA containing 2% of non-ferrous metals will give an error of about 8%. If one is interested in the precious metals content then the sample should be very large to avoid potentially substantial statistical errors.

2.2.2 Analysis System

The analytical strategy is illustrated for a case in which the total BA collected from the incinerator is sampled. Samples collected from the incinerator contain large pieces of metals and organics (bicycles, carpets, etc.), therefore it is best to remove such particles before analysis. The rest should be wet screened in several size fractions (<CCS*, CCS-2 mm, 2-6 mm, 6-20 mm, 20-40 mm)†. The dry mass of each size fraction should be measured. Each fraction is then separately analysed according to Figure 2.4 and the procedures defined below.

2.2.2.1 Analysis of the 0-CCS fraction

The <CCS fraction (sludge) is difficult to separate into different materials due to its very fine grain size distribution. As a waste material this fraction is usually land filled. For land filling the environmental quality of the fraction has to be measured according to the landfill waste directive (2006/12/EC), which states the quality requirements (leaching limits, etc.) for different waste materials (Chapter 1). Sometimes the organic content (determined by LOI measurement) must also be measured. This can be done according to Procedure 2 described in this section.

*The hydrocyclone cut size

†These size distributions are related to the pilot plant for wet physical separation because the installation produces fractions of the same sizes. More details related to this subject are presented in Chapter 3

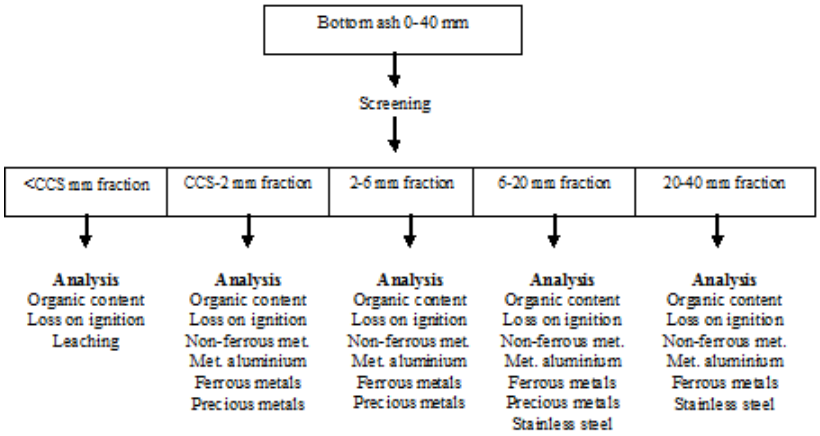

Figure 2.4: Schema of the analysis system.

2.2.2.2 Analysis of the CCS-2 mm fraction

The CCS-2 mm fraction (sand fraction) contains valuable heavy non-ferrous metals, aluminium, ferrous metals, organics and minerals. It is best to split the sample into three sub-samples and analyse each part separately for their heavy non-ferrous and ferrous metals, metallic aluminium content and organic content (or loss on ignition).

Heavy non-ferrous and ferrous metals contents: the first sub-sample is analysed according to Procedure 3 (heavy density solution) in which the product is divided into heavy and light fractions. The heavy fraction can be milled or smelted then analysed by X-ray fluorescence (XRF). The magnetic (ferrous fraction) can be removed by a magnet before XRF analysis to determine the magnetic content.

Metallic aluminium content: the second sub-sample can be split and the metallic aluminium content of approximately 15 g can be analysed (Procedure 4).

Organic content or loss on ignition (LOI): the third sample should be used to determine its organic content or LOI. There is a distinction between these parameters: the organic content is the incinerated mass of organic compounds while LOI is the total amount of material lost on ignition, which will include losses of CO_2 from carbonates. The measurement of organic content and LOI is described in Procedures 1 and 2.

2.2.2.3 Analysis of the 2-6 mm fraction

The 2-6 mm fraction contains heavy non-ferrous metals, ferrous metals, aluminium, organics and granulate (aggregate for building uses). It is simplest to first mill the fraction in a roller mill and sieve it with a 2 mm screen. Most of the particles will be crushed and pass through the screen, while the metallic particles, ferrous metals and non-ferrous metals (brass, Cu, Pb, Al) will remain on top of the sieve.

Magnetic content: the over-sieve fraction (> 2 mm) should be analysed by a magnet to remove magnetic particles (scrap iron). The main interest is not in the total magnetic content, but only the scrap iron content, which in some cases will be attached to stone. Therefore, all magnetic particles should be milled or crushed by a hammer to separate the scrap iron from the magnetic stone. The scrap iron should be then hand-picked from the milled residue.

Heavy non-ferrous metals content: The rest (> 2 mm) should be analysed according to Procedure 3 (heavy density solution). The heavy non-ferrous fraction can be hand-picked according to colour to analyse its copper, brass, zinc or stainless steel contents. A second option is to mill the particles and analyse them by XRF. A third option is to smelt the heavy non-ferrous fraction and then analyse the metals content by drilling several holes through the smelt (from top to bottom), mill it and analyse it by XRF.

Metallic aluminium content: The light fraction after Procedure 3 is composed of aluminium, organics and aggregate (stone, glass, etc). This fraction can be milled and a small sample can be analysed according to Procedure 4. The second option is to smelt the fraction, drill holes through the smelt (from top to bottom) and analyse it by XRF.

Organic content: Two size fractions should be investigated to determine organic contents. The over-sieve fraction (> 2 mm) contains larger organic particles. This fraction should be investigated according to Procedures 1 or 2. The fraction that passes through the screen (< 2 mm) also contains very fine organic particles. This fraction should be split and also analysed according to Procedures 1 or 2. The measured masses of the organic content or LOI in the > 2 mm and < 2 mm fractions should then be combined to estimate the total organic content or total LOI.

2.2.2.4 Analysis of the 6-20 mm fraction

Non-ferrous metals content: this fraction can be initially processed using an eddy current separator (ECS) to remove the non-ferrous metals (both light and heavy) from the magnetic fraction and the stony residue. The non-ferrous fraction can be analysed using heavy density solution (Procedure 3) to separate the aluminium from the heavy non-ferrous fraction. The second option is to hand pick the light particles from the heavy particles. The heavy non-ferrous fraction and the aluminium fraction can then be separately smelted and analysed by drilling holes through the smelt. The filings after drilling should be analysed by XRF.

Magnetic content: the magnetic fraction is attracted to the ECS drum and thus removed. If ECS is not used, the magnetic particles can also be removed by a magnet, which will separate all magnetic particles from the residue. The main interest is not in the total magnetic content, but only the scrap iron content which is often attached to stone. Therefore all magnetic particles should be milled or crushed by a hammer to separate the iron scrap from the magnetic stone. The iron scrap should be then hand-picked from the milled residue.

Organic content: the large organic particles should be hand-picked from every 6-20 mm fraction (magnetic, non-ferrous and stony). The stony fraction separated by the ECS should then be milled and a small sample analysed for fine organic content by Procedures 1 or 2. The sum of the large organic and fine organic content (after Procedures 1 or 2) will be the total organic content or total LOI.

2.2.2.5 Analysis of the 20-40 mm fraction

The procedure to apply to this fraction is the same as that outlined for the 6-20 mm fraction.

Procedure 1 (organic content analysis)
Split the sample (approximately 100 g),
Measure the dry mass of the sample (m_1),
Add the sample to a 5% HCl solution (the sample should be completely submerged in the liquid),
Allow the acid to react with the sample (for approximately 20 minutes),
Filter the sample from the liquid and rinse it thoroughly with water,
Dry the sample in an oven at a temperature not exceeding 110 °C,
Measure the mass of the sample (m_2)
Incinerate the sample in an oven at 550°C for 4 hours.
Weigh the sample (m_3)

Calculate the organic content in %, as follows:

$$C = \frac{m_2 - m_3}{m_1} 100 \tag{2.5}$$

Procedure 2 (LOI analysis)
Split the sample (approximately 100 g),
Measure its dry mass (m_1),
Incinerate it in an oven at 550 °C for 4 hours.
Weigh the sample (m_2)

Calculate the LOI content in %, as follows:

$$C = \frac{m_1 - m_2}{m_1} 100 \tag{2.6}$$

Procedure 3 (heavy density solution)
Take a sample of approximately 100 g, measure its dry mass (m)

Create a sodium polytungstate solution with a density of at least 2800 kg/m^3.
Add the sample to the heavy density solution.
Mix the sample thoroughly in the liquid and wait until the heavy particles segregate.
Heavy particles (density > 2800 kg/m^3 will sink), while light particles (< 2800 kg/m^3 will float).
Remove the light particles with a spoon, rinse them with water, dry them and measure their mass (m_1).
Remove the heavy particles by filtering the liquid, rinse them with water, dry them and measure their mass (m_2).

Calculate the % of heavy particles and light particles, as follows:

$$M_{\text{heavy}} = \frac{m_2}{m}100 \tag{2.7}$$

$$M_{\text{light}} = \frac{m_1}{m}100 \tag{2.8}$$

Procedure 4 (metallic aluminium analysis)
The aluminium content in the BA should be measured by the following method (Figure 2.5). Approximately 15 g of fine particles (larger particles should be milled) should be added to a glass beaker (a) together with a stirring magnet. This beaker should be placed in a larger glass beaker (b) covered with a volumetric measuring cylinder (c). A solution of sodium hydroxide should then be added to the beakers until it reaches the top of the graduated cylinder and then air in the top of the cylinder should be removed with a suction device inserted through the rubber top. No air should remain inside the beakers when the procedure begins. The entire device should be heated and stirred by a magnet placed in the first glass beaker. The reaction of the sodium hydroxide and aluminium creates hydrogen gas, which is collected in the graduated cylinder, and the aluminium content can be calculated from the volume of hydrogen collected.

The metallic aluminium content in the sample should be calculated in the following way:

$$M_{H_2(\text{mol})} = \frac{\left(\frac{V_{H_2(\text{ml})}}{1000}\right)}{23} \tag{2.9}$$

$$M_{al(\text{mol})} = \frac{2}{3}V_{H_2(\text{mol})} \tag{2.10}$$

$$M_{al(\text{g})} = M_{al(\text{mol})}27 \tag{2.11}$$

$$M_{al(\%)} = \frac{M_{al(\text{g})}}{m} \tag{2.12}$$

m (g)	input mass (g)
$V_{H_2(ml)}$ (ml)	gas collected in the glass beaker in ml
$V_{H_2(mol)}$ (mol)	gas collected in the glass beaker in mol
$M_{al(mol)}$ (mol)	amount of aluminium in mol
$M_{al(g)}$ (g)	amount of aluminium in grams
$M_{al(\%)}$ (%)	amount of aluminium in the sample in mass %

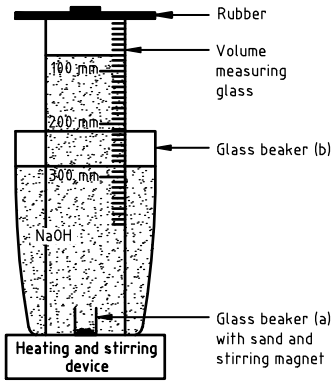

Figure 2.5: Laboratory set-up for hydrogen measurement (Muchova and Rem 2007b).

2.3 Characterization of Amsterdam Bottom Ash

The composition of Amsterdam BA is influenced by the composition of the household waste incinerated, the incineration system (stoker furnace) and the parameters of the incineration process (temperature, moisture content, etc). Table 2.2 shows the composition of waste incinerated from 2004 to 2007 in Amsterdam. The missing component in Table 2.2 is the dry separated coarse organic fraction of the BA that was reintroduced into the incinerator together with the waste. The composition of waste incinerated in this period did not change much, except for the amount of sewage sludge, which increased from 2005.

Table 2.2: Composition of waste incinerated in the Amsterdam incinerator from 2004 until 2007.

	2004	2005	2006	2007
Municipal waste	47%	60%	40%	47%
Waste from offices	25%	22%	24%	24%
Waste from hospitals	1%	1%	1%	1%
Sewage sludge	2%	11%	8%	9%

Most incinerators in Europe are of the Stoker furnace type. The incinerator in Amsterdam is also of this type, and produces relatively coarse BA in which about 50% of the particles are larger than 2 mm. This allows relatively easy separation of metals, minerals and organics. A major problem is that BA is usually quenched in water before further processing. This step considerably complicates

the classification into particle size fractions; an essential step to take prior to materials separation. Due to the conditions of incineration, the structure of the waste is broken down into various materials, but temperatures (the heart of the oven is ±800 °C) are generally not high enough to melt metals and slag, turning them into aggregated particles. Therefore, the material has a high degree of liberation (> 80% of the metals are free). The average composition of Amsterdam BA is shown in Table 2.3.

Table 2.3: Average composition of BA from Amsterdam (%, by mass).

Aggregate (stone, glass, ceramics)	±80%
Iron scrap	8-13%
Non-ferrous metals (Cu, Al, Pb, Zn, brass)	2.3%
Precious metals	0.001%
Organics (paper, textile, plastic)	1-5%

2.3.1 Grain Size Distribution

The grain size distribution is an important factor when considering options for further utilization of BA. Many incinerators use dry physical separation as their primary separation system, whereby big particles such as large pieces of metals are removed and the rest are shredded to below 40 mm. For example, the Amsterdam incinerator removes approximately 8-10% of big particles and shreds the rest for easy utilization. An average grain size distribution of 0-40 mm BA from Amsterdam measured from 2004 until 2006 is shown in Figure 2.6.

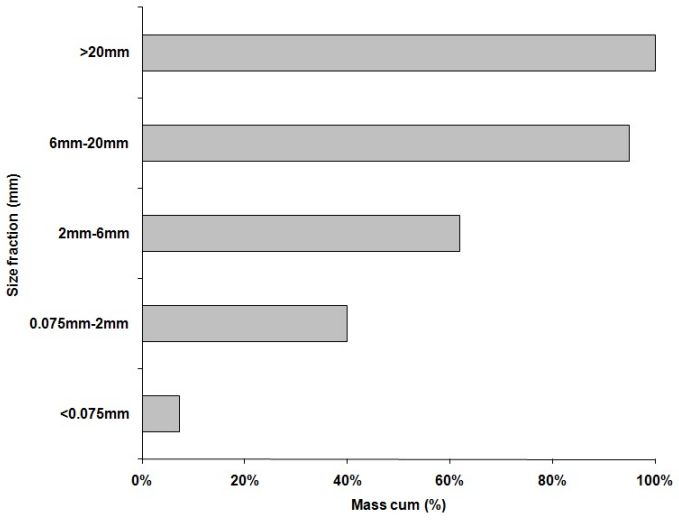

Figure 2.6: Grain size distribution (in %, by mass) of Amsterdam BA (0-40 mm fraction) analysed after wet physical separation in 2004.

The size distribution has an effect on value. For example, metals and gravel in larger size fractions are more valuable than those in fine fractions. It is also an important consideration for the utilization of aggregate or sand for building applications (concrete, lime-sand stone), since the grain size distribution should comply with standards for building materials (Chapter 6).

2.3.2 Metal Content

This section presents metals contents found in bottom ash collected from the Amsterdam incinerator from 2003 to 2007. The non-ferrous metals contents were measured as the mass of metallic particles in the fraction, as determined by hand-picking or smelting the metals followed by XRF. For assessing the economic value of the fraction, the most accurate option is smelting and XRF.

2.3.2.1 Heavy Non-ferrous Metals and Precious Metals Contents

The non-ferrous metals fraction in BA should be divided into two size fractions. The $>$ 20 mm and $<$ 20 mm fractions contained on average 1.1% and 1.2% of non-ferrous metals, respectively. In addition, the $<$ 20 mm fraction was divided into three size categories (CCS-2 mm, 2-6 mm and 6-20 mm), the non-ferrous and precious metals contents of which were separately analysed.

The CCS-2 mm heavy non-ferrous fraction amounts to approximately 0.1-0.2% of the 0-40 mm BA. This fraction was smelted, analysed by XRF and found to contain mainly copper (90%), zinc, lead and precious metals (approximately 100 ppm of gold and 2400 ppm of silver).

The heavy 2-6 mm non-ferrous fraction amounts to approximately 0.2-03% of the 0-40 mm BA fraction. Its main chief constituents are copper (38%), zinc (18%), lead (6%), iron, tin, silver (3000 ppm), gold (100 ppm) and platinum (14 ppm) (Bakker et al. 2007b) and the remaining are stone and glass (20-30%).

The 6-20 mm non-ferrous fraction, after mineral removal, amounts on average to 0.5-0.7% of the 0-40 mm fraction of BA. It contains mainly aluminium (61%), followed by heavy non-ferrous metals (38%) and stainless steel (1%), based on hand-picking the particles. This metallic fraction was also smelted and analysed by XRF and the results are shown in Table 2.4.

The smelting was performed at higher temperatures, therefore the Pb and Zn contents in the mass balance will be higher than shown in Table 2.4. The vaporised mass of 8% shown in Table 2.4 pertains to metals with a low vaporizing temperature (Zn and Pb). Therefore, the Zn and Pb content will be on average 18.7% of the smelted mass. The mass of minor elements (3%) shown in Table 2.4 pertains to Ni, Sn, etc.

Aluminium Content

Each size fraction was analysed for aluminium content. The sand fraction was analysed according to Procedure 4, and its average metallic aluminium content was found to be around 1.8% (Muchova and Rem 2007b). The 2-6 mm fraction contains approximately 1.4% of aluminium (in particle form), which after smelting is about half, the rest is stone or aluminium oxide. The 6-20 mm fraction contains 1.6% of aluminium (analysed by hand picking) which after smelting is on average 1.4%.

Table 2.4: Composition of the 6-20 mm non-ferrous metals fraction, analyzed by smelting and XRF.

	Mass (%)
Cu	19%
Zn	10%
Pb	0.7%
Fe	1%
Al	58%
Stainl. steel[1]	1%
Ag	0.1%
Vaporized	8%
Minor elements	3%
Total	100%

[1] Stainless steel was not analyzed by smelting, this value is the hand-picked mass.

Ferrous Metals Content

The magnetic fraction in BA was usually collected by a magnet, therefore mass balances reflect all particles attracted to the magnet rather than the amount of scrap iron. Hence, the fraction is called the magnetic fraction, and it can be milled to crush the stony particles and release the scrap iron (which is the real target, and should be considered as a valuable product). The scrap iron contents of the 20-40 mm and 6-20 mm fractions were analyzed. Fractions smaller than 6 mm were not analysed for scrap iron contents during this research. Table 2.5 shows the masses of iron scrap obtained from each size fraction and their grade (in %).

Table 2.5: Amsterdam BA fractions containing scrap iron, with average grades of scrap iron, from 2004 and 2005.

	Mass (%)	Grade (%)
> 40 mm	7	80-90
$20 - 40$ mm	5	20-30
$6 - 20$ mm	7	20
$2 - 6$ mm	1	n.m.
< 2 mm	7	n.m.

n.m. - not measured

2.3.3 Organic Content

The 0-40 mm fraction contains a portion of unburned organic matter, the amount of which (in each size fraction) was measured separately by three different methods (hand picking organics, LOI and organic content analysis). The methodology of the analyses is described above (Procedures 1 or 2). The organic content was measured after separating the BA into several sizes and products. The results for each fraction are shown in Table 2.6.

Table 2.6: Organic contents, hand-picked, in %, incinerated according to Procedure 1 and measured as LOI according to Procedure 2. Expressed as the %, by mass, of each stream after wet physical separation of Amsterdam BA (0-40 mm fraction after dry physical separation) in 2004, 2005 and 2006.

	2004			2005			2006		
	Organic hand picked	Organic content (incinerated)	LOI	Organic hand picked	Organic content (incinerated)	LOI	Organic hand picked	Organic content (incinerated)	LOI
Sludge	n.m.	n.m.	n.m.	n.m.	0.15 ± 0.1	21.6 ± 0.9	n.m.	n.m.	20 ± 0.5
Sand total	n.m.	n.m.	n.m.	n.m.	n.m.	n.m.	n.m.	n.m.	n.m.
Sand product	n.m.	0.6 ± 0.2	1.9 ± 0.1	n.m.	n.m.	n.m.	n.m.	3.9 ± 1.8	21.9 ± 2.2
2-6 mm total	n.m.	n.m.	n.m.	n.m.	n.m.	n.m.	n.m.	n.m.	n.m.
2-6 mm aggregate	1.2 ± 0.4	n.m.	n.m.	n.m.	n.m.	n.m.	n.m.	1.8 ± 0.4	8.5 ± 1.3
2-6 mm metals	n.m.	n.m.	n.m.	n.m.	n.m.	n.m.	n.m.	n.m.	n.m.
6-20 mm total	2.0 ± 0.2	n.m.	1.25 ± 0.2	n.m.	n.m.	n.m.	n.m.	n.m.	n.m.
6-20 mm aggregate	1.1-2.2	0.64 ± 0.4	n.m.	n.m.	n.m.	n.m.	0.4 ± 0.1	2.0 ± 0.2	5.7 ± 1.6
6-20 mm metals	0.8 ± 0.2	n.m.	n.m.	n.m.	n.m.	n.m.	n.m.	n.m.	n.m.
6-20 mm ferrous metals	n.m.	n.m.	n.m.	n.m.	n.m.	n.m.	n.m.	n.m.	n.m.
>20 mm	2.1 ± 1.6	n.m.	n.m.	n.m.	n.m.	n.m.	n.m.	n.m.	n.m.

The organic content and LOI in the sand product (CCS-2 mm) changed over time, as shown in Table 2.7.

Table 2.7: Organic content (in %) and LOI (in %) in the sand fraction in 2002, 2004 and 2006.

Year	LOI (%)	Organic content (%)
2002	2.2-2.4	0.5-0.6
2004	1.9-2	0.6-0.8
2006		2.7-4.3 (7%[1])

[1] in one case the organic content was 7%.

The organic content should be considered an important quality factor for further utilization (Muchova and Rem 2007c). The amount of large (> 6 mm) organic particles as well the amount of fine organic particles will affect both the engineering and environmental quality (leaching values) of the residues.

2.3.4 Water Content

The water content in the 0-40 mm fraction of raw BA varies mainly depending on the season. In summer it is between 15-18% and in winter it can increase up to 25%. The water content of the BA was determined by weighing a sample (approximately 200 g), drying it at 105 °C for 24 hours and re-weighing. The moisture content also depends on further separation (dry or wet). Each fraction after the wet physical treatment has a different moisture content: sludge has the highest moisture content (50-55%), followed by sand (25-35%), the 2-6 mm fraction (12-18%), the 6-20 mm fraction (5-8%) and the 20-40 mm fraction (2-8%).

The moisture content affects the sampling, separation options (wet or dry), mass balance and estimated prices.

2.3.5 Elemental Composition

The main elements in 0-40 mm BA are Si, Ca, Al, Fe, Na, which collectively account for 80-90% (w/w) of the total content. Therefore, the high Si and Ca content make BA interesting as a secondary source for building products. The main use of BA in the past was as a road filler. Amsterdam BA was first separated by dry physical methods (large particles of iron scrap and non-ferrous metals were removed) and the residue, if it met environmental regulations (leaching limits), could be used as road filler. Therefore, the elemental composition was measured. Amsterdam BA was also analysed by a leaching test (column test) several times each year and the average results are shown in Table 2.8.

The results show that leaching values of several elements (such as Cu, Mo, Sb, SO_4 and Cl) were high, exceeding Soil Quality Decree (SQD) limits (Muchova and Rem 2006a, Muchova and Rem 2007c). Further details about environmental regulations and leaching investigation are presented in Chapters 1 and 5.

Table 2.8: Leaching values in mg/kg and standard deviations for Amsterdam BA from 2000 until 2005.

	2000		2001		2002		2003		2004		2005	
	Unit	St.dev.	Unit	St.dev.	Unit	St.dev.	Unit	St.dev.	Unit	St.dev.	Unit	St.dev.
pH	11.2	0.4	10.4	1.1	10.0	1.2	8.8	0.6	8.3	0.5	8.5	0.5
Conductivity (microS/cm)	2590	534	2227	576	2677	888	2444	418	2768	575	2543	365
	mg/kg	St.dev.	mg/kg	St.dev.	mg/kg	St.dev.	mg/kg	St.dev.	mg/kg	St.dev.	mg/kg	St.dev.
Cu	4.0	1.5	6.8	1.5	5.5	2.8	6.9	3.3	6.2	3.7	5.4	3.2
Mo	1.2	0.3	1.1	0.3	1.4	0.5	1.4	0.3	1.4	0.4	1.2	0.4
Sb	0.11	0.04	0.17	0.07	0.14	0.06	0.17	only one nr.	0.38	0.13	0.21	0.13
Cl	3089	794	2651	521	3374	834	4300	only one nr.	4050	1061	4150	495
Br	10.3	4.9	9.2	1.8	16.5	5.7	14.0	only one nr.	14.5	2.1	8.4	10.7
SO_4	3896	1323	4483	1091	5395	700	5200	only one nr.	4200	141	6100	1838
Pb	0.4	0.3	0.3	0.0	0.5	0.2	0.1	0.1	0.0	0.1	0.0	
Hg	<0.005	<0.005	<0.005	<0.005	<0.005	<0.005						
Cd	<0.007	<0.007	<0.007	<0.007	<0.007	<0.007						
As	<0.2	<0.2	<0.2	<0.1	<0.1	<0.1						
Cr	<0.1	<0.1	<0.1	<0.5	<0.05	<0.05						
Co	<0.07	<0.07	<0.07	<0.05	<0.05	<0.05						
V	<0.3	<0.3	<0.3	<0.1	<0.1	<0.1						
Zn	<0.79	<0.72	<0.7	<0.2	<0.2	<0.2						

Note: missing numbers in the table could not be calculated due to uncertainty or too few measurements.

2.4 Composition of Bottom Ash in some European Countries

BAs from Western Germany, Northern Belgium and the Eastern part of the Netherlands were also analysed, to assess the similarity of their composition to that of Amsterdam BA. In each case the BA was analysed according to the methodology outlined above to obtain results that could be validly compared to those obtained for Amsterdam BA.

2.4.1 Composition of German Bottom Ash

The German BA analysed in 2005 was collected after the incineration of household waste. The amount analysed was 56 kg (d.s.), which proved to be too little to obtain statistically reliable mass balances for all components of interest. Therefore, the analysis focused on the BA's non-ferrous and ferrous metals contents. Table 2.9 shows the distributions of these constituents in several size fractions, and products in kg.

Table 2.9: Mass balance of German BA in kg d.s.

	Sludge	Sand (-2 mm)	2-6 mm	6-20 mm	>20 mm	Total
Aggregate						48.2
Steel		not analyzed	0.2	2.8	3.7	6.7
Aluminium		not analyzed	0.53		0.14	
Heavy non-ferrous met.		0.04	0.22	0.21	0	1.18
Stainless st.					0.04	
Total	2.5	11.2	20.8	13.1	8.5	56.1

Table 2.10 shows the summarized masses of items in Table 2.9 with statistical errors. The masses of heavy non-ferrous metal, aluminium and stainless steel were combined because there was insufficient sample to estimate percentage masses with satisfactorily low statistical errors.

Table 2.10: Composition of BA from Germany; total mass analysed 56 kg (d.s.).

Granulate (stone, glass, ceramics, etc.)	
Organics (paper, plastic, bones)	86.0% ± 1.3%
Ferrous metals	11.9% ± 5%
Heavy non-ferrous (cu, zn)	
Aluminium	2.1% ± 0.1%
Stainless steel	

The results of the analysis show that the German BA had a similar composition to Amsterdam BA. The silver content of the non-ferrous 2-6 mm fraction was also analysed, and found to be 0.4%. The gold and platinum contents could not be measured since the sample mass was too small.

2.4.2 Composition of Bottom Ash from Belgium

A sample of approximately 36 kg was also collected from one of the Belgian incinerators and analysed as outlined below. The sample was again too small to obtain an accurate mass balance. The results are shown in Table 2.11.

Table 2.11: Composition of BA from Belgium; total mass analyzed 35.9 kg (d.s.).

	Mass (kg)	Mass (%)
Aggregate (stone, glass, ceramics, etc.)	30.6	85.4% ± 2%
Non-ferrous metals + st.st. (2-40 mm)	1.5	4.1% ± 0.3%
Non-ferrous metals + st.st. (> 40 mm)	0.4	1.1% ± 0.5%
Magnetic fraction	3.4	9.4% ± 2.5%
Total	35.9	100.0%

The results show that the non-ferrous metals contents of the 2-40 mm and > 40 mm fractions were approximately 4.1% and 1.1%, respectively. The errors for the latter are high, therefore it is difficult to estimate the non-ferrous content accurately. The magnetic fraction (all magnetic particles attracted to the magnet) was found to be 9.4%, with an error (standard deviation) of 7%. The amount of precious metals was not analysed since the sample mass was too low.

2.4.3 Bottom Ash Composition from the Eastern Part of the Netherlands

The BA from the Eastern part of the Netherlands was first processed by dry physical separation, resulting in four different products, each of which was sampled and analysed by the above analytical system. The first sample collected and analysed was a stream designated 'building product' (480 kg d.s.), the second stream was called coarse non-ferrous product (118 kg d.s.), the third stream was called fine non-ferrous product (132 kg d.s.) and the last stream was called ferrous product (172 kg d.s.). Each fraction was analysed separately, then a mass balance was created by considering the composition of each fraction 2.12.

Table 2.12: Composition of BA from the Netherlands (Eastern part).

Aggregate (stone, glass, ceramics, etc.)	85.0% ± 0.9%
Organics (paper, plastic, bones)	0.5% ± 0.3%
Magnetic	11.6% ± 0.1%
Heavy non-ferrous (cu, zn)	1.0% ± 0.3%
Aluminium	1.6% ± 0.4%
Stainless steel	0.3% ± 0.2%

The composition shows a similar metals content to the BA from Amsterdam. The organic content in this case was lower than in Amsterdam BA. The precious metals were not measured.

2.5 Conclusion

Raw Amsterdam BA contains 8-13% of ferrous metals, 2.3% of non-ferrous metals and 0.001% of precious metals (Rem et al. 2004, Muchova and Rem 2006b, Bakker et al. 2007b). Amsterdam BA was monitored and analysed several times from 2003 until 2007 and the metals content was found to be quite constant. Non-ferrous metals were distributed in several size fractions: 0-2 mm, 2-6 mm, 6-20 mm and 20-40 mm. Hence, each size fraction has value and can be separated. The precious metals in the BA were found in three different size fractions: 0.1-2 mm, 2-6 mm and 6-20 mm, with total contents of approximately 0.4 ppm of gold and 10 ppm of silver (Muchova et al. 2008). The organic content changed in the period from 2003-2007 due to changes in the waste incinerated and incinerator settings. The BA from Germany, Belgium and different incinerators in the Netherlands showed very similar composition. The average composition in Western Europe is shown in Table 1.1, Chapter 1. These findings indicate that western European BA has high economic value and thus should be further separated to obtain valuable products instead of land filled or used as a cheap material for road basement solutions.

Chapter 3

Physical Separation of Bottom Ash

Summary

Bottom ash is a moist material; the particles making up the ash are strongly bound by water bridges below a grain size of 8 mm. In order to recover metals and minerals from the ash down to very fine particle sizes, the material should either be dried to eliminate the water bridges or immersed in water to obtain a slurry with freely moving particles. Wet physical processes avoid the cost of drying the ash and are generally superior to dry methods because they allow more efficient and accurate classifications based on size and density. An important advantage of wet screening is that fine particles and organics are washed out from the granulate fractions (aggregates), thereby improving the environmental quality of building products. The high recovery of metals provides financial benefits and, in combination with the washing and removal of organics, it also has positive environmental effects. The majority of contaminants are found in the sludge stream, which accounts for 5-10% of the solids input. Therefore, it is recommended to dewater and land fill the sludge. The relatively small amounts of organics that are separated out must be incinerated again or land filled. The wet system recycles water, which is collected in the process tank and reintroduced as input water. During the final separation steps, building products are rinsed with fresh water which should reduce the leaching values of the final products.
This chapter documents the treatment system developed in a series of pilot plants for wet physical separation of BA that were built in Amsterdam between 2003 and 2008. The aim of the treatment system in each case was to employ the most suitable separation steps to achieve three main goals:

- To create environmentally clean building products (aggregate, sand), which can be utilized without any special restrictions (i.e. no need for a protection layer to prevent leaching, etc.).
- To recover high-grade, marketable metal fractions.
- To improve the financial value of BA with respect to the traditional treatment (road fillers €-9 per tonne, land filling €-30 per tonne, pre-processing by dry separation €-15 per tonne, in the Netherlands).

3.1 Introduction

Bottom ash from municipal solid waste incinerators is generally quenched immediately after exiting the furnace. The result is a moist, agglomerated material, in which the finer particles are strongly bound by water bridges. These features make it difficult to process the material below a grain size of 8 mm. In order to recover metals and minerals from the ash down to very fine particle sizes, the material should either be dried to eliminate the water bridges or immersed in water to obtain a slurry with freely moving particles. Drying the ash requires a considerable amount of energy; 750-1000 MJ of energy per tonne since the water content amounts to about 150 to 200 kg per tonne. Furthermore, for the production of mineral products, it is important to reduce the soluble chloride and sulphate contents, which is difficult starting from a dry material. Wet physical processes are also generally superior for separating organic and heavy metal particles because they allow more efficient and accurate classifications based on size and density.

MSWI BA incinerated at Afval Energie Bedrijf (AEB) in Amsterdam is separated on-site using a basic dry BA treatment. The main purposes of this step are to remove the ferrous scrap, return the large, ill-burnt pieces back to the incinerator and reduce the size of the ash to below 40 mm. The installation also recovers most of the coarse (>15 mm) fragments of non-ferrous metals. A schema of the complete dry separation at the dry plant at AEB is shown in Figure 3.1. The main products after dry physical separation in 2005 are shown in Table 3.1. The residue from the dry treatment, with or without dry non-ferrous recovery, was used as the feed material for a series of wet pilot plants during this research (Figure 3.2).

Table 3.1: Fractions produced in the dry BA separation plant in 2005.

	Tons /Year
Total household waste	865000
BA	205000
Ferrous scrap from BA	15200
Non-ferrous scrap from BA	2100

The concept of wet BA separation was tested from 2003-2008, following initial tests in 2002, when BA was processed in a provisional installation of 20 t/h (Kooy et al. 2002). The preliminary results obtained helped to develop the basic separation layout of the first pilot plant (Pilot plant I), which had a capacity of 50-100 t/h and was built from 2003 to 2004 adjacent to an existing installation for dredging sludge treatment. The equipment of the sludge treatment plant (upstream column, trommel screen, etc.) was employed for size classification and treatment of the <2 mm fraction of the BA. Some of the equipment installed in Pilot I was later transferred to the Amsterdam incinerator (AEB) and combined with a new wet classification and sand treatment line, resulting in Pilot plant II.

This chapter discusses each of the three wet implementations, their mass balances and the step-by-step improvements of the process concept. The chapter concludes with an evaluation of the results obtained from Pilot plant II.

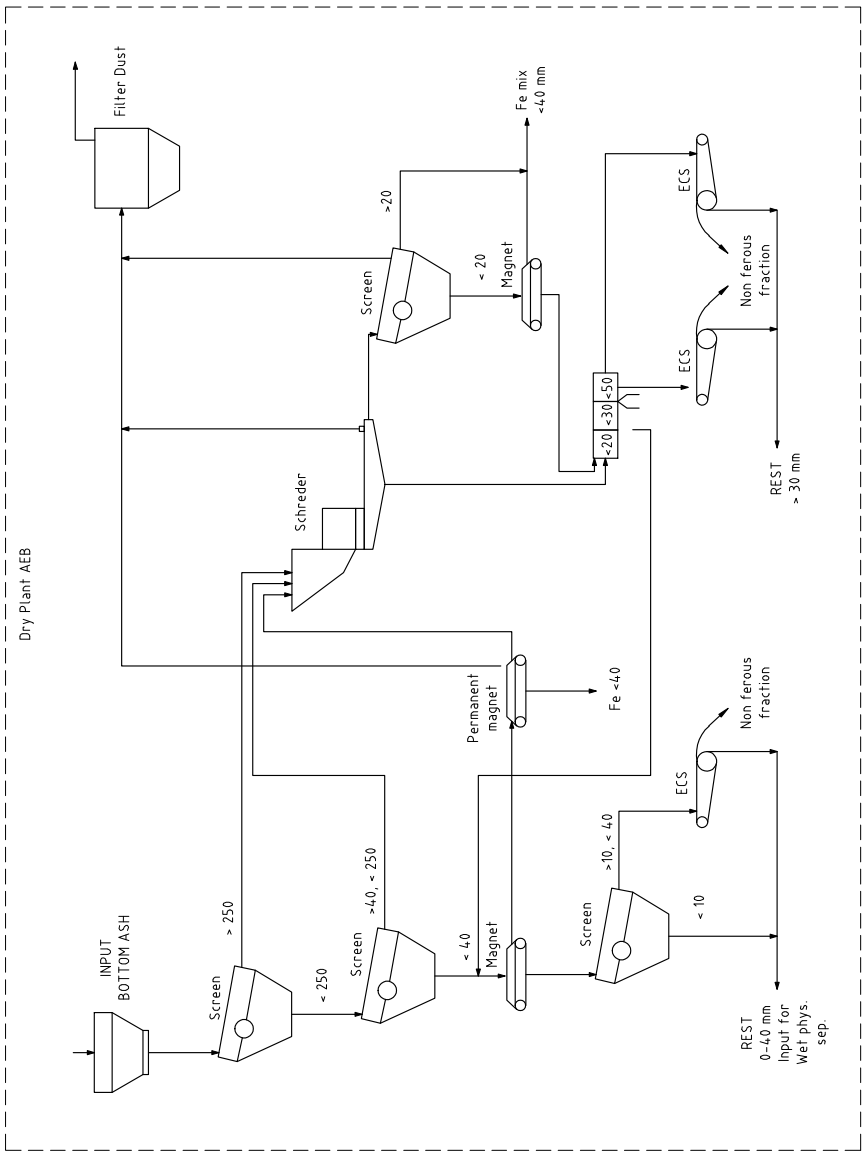

Figure 3.1: Schema of the dry treatment plant at AEB.

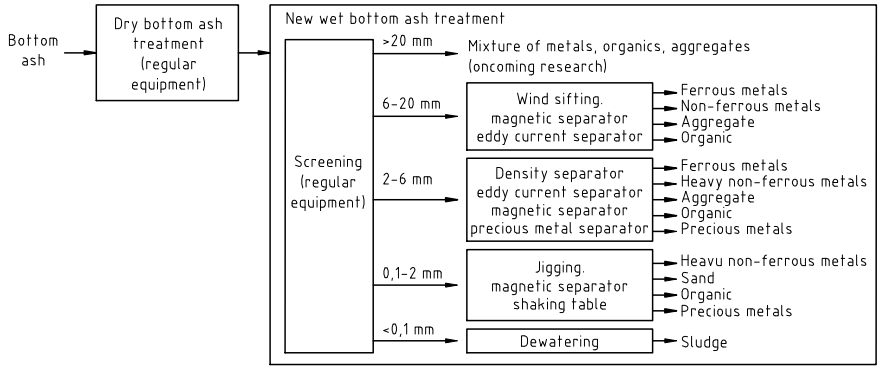

Figure 3.2: Schema of the dry and wet physical separation at AEB.

Wet process: basic concept

The basic layout of the wet BA treatment processes studied in this research consists of a combination of size classification and physical separations according to density and the magnetic and conductive properties of the treated materials. Rinsing steps are added at the end of process lines to reduce the level of contaminants dissolved in the process water that comes with the products. Each of the three basic modules of the process (size classification, physical separation and rinsing) is discussed in this section.

Physical separation based on density and electrical conductivity also depends strongly on particle size. Size classification of BA is therefore the most important step to achieve high grades and recoveries of non-ferrous metals as well as minerals free of organics in the subsequent processes. The best results are obtained by screening into narrow size fractions (optimally with a factor of two between size limits). However, economy of scale is best served by a small number of size categories. For BA treatment, screening into five size categories seems a good compromise:

< hydrocyclone cut size (CCS)

The ideal CCS represents a compromise between the ideal sizes for minimizing leaching values of the fine mineral (sand) product and the amount of sludge cake that must be disposed of or thermally treated by expensive process routes. Mechanical processing of the sludge is limited to particles 60-80 μm, as larger particles make the sludge more difficult to transport, while the $< 45\,\mu$m fraction is the fraction that is most heavily contaminated by heavy metals and organics, therefore it is a priority to separate it out. Hence, the optimal cut size is around 60 μm.

CCS - 2 mm

The 2 mm cut point was chosen partly because civil engineering applications demand that the maximum size of sand products must be between 2-4 mm. Another reason is that BA has high metallic aluminium contents (which must be minimized in aggregate used for most building products) and wet eddy current separation (WECS) can separate out aluminium particles down to 2 mm.

2-6 mm
Density separators like the kinetic gravity separator (KGS) which separate heavy metals from the residue cannot deal with more than a factor of 3 between minimal and maximal size, therefore this fraction is limited by 6 mm. Another reason is the dry separation by ECS for the 6-20 mm fraction because this separator functions optimally with a minimum particle size of 5 mm at normal capacities.

6-20 mm
Stainless steel, which cannot be efficiently separated with ECS, is mainly concentrated in the small amount of ash that makes up the >20 mm fraction. Therefore, if the coarse fraction is to be used for building applications it is important to reduce the stainless steel content by cutting this fraction at 20 mm (unless the aggregate product is passed over a stainless steel sensor sorter, in which case the upper limit could be raised to 40 mm). However, a second reason for limiting this fraction to 20 mm is the limitations of organics removal by wind sifters, which cannot separate organics from minerals in fractions with more than a ca. 3-fold size range.

20-40 mm
This fraction, accounting for about 5% of the input ash, can either be sold to sink floaters or broken by impact crushing to screen out the metals. The 40 mm limit was selected because it matches that of the previous dry separation plant used in Amsterdam.

Physical Separation

The CCS-2 mm (sand) can be separated by a jig, spiral, wet tabling or upstream column. Each of those options has both advantages and disadvantages. Wet tabling requires a large area for such large amounts of BA sand, and thus was not considered, and an upstream column was excluded since such columns can only separate the light fraction (organics) from the minerals (separation of heavy metals from sand requires enormous water flows, due to the high density of particles). Therefore, the utility and performance of a spiral and jig were tested during this research, and their advantages are discussed in this chapter.

The 2-6 mm fraction must be separated by gravity separation. One option is to use jigging or a KGS. The jigging option caused many difficulties due to the presence of wires, which affect the operation of the jig, therefore KGS was selected for this research. The non-ferrous metals must be further separated by a WECS or a Magnus separator. These two options are compared in this chapter.

The 6-20 mm fraction must be first separated by magnetic separators. During the next step, ECS, it is essential to have removed all magnetic particles because they can cause damage. For this reason a drum magnetic separator was chosen to separate out all magnetic particles. The grade of the scrap iron can be further improved by using an additional cross-belt magnetic separator. The non-ferrous metals must be separated by ECS and the organic fraction can be

separated by wind sifting, a ballistic separator or flotation. However the ballistic separator is sensitive to moisture content and flotation requires an extra step in which additional water is needed. Therefore, in this research a simple wind sifter that was not sensitive to the moisture level of the 6-20 mm fraction was used.

3.2 Pilot Plants

The experimental work presented in this chapter was divided into three stages between 2003 and 2008 which are shown in Table 3.2.

Table 3.2: Developmental stages of the wet physical separation system from 2003-2008.

2003	Preliminary wet pilot
2004-2005	Pilot plant I
2006-2008	Pilot plant II

3.2.1 Preliminary Wet Pilot and Pilot Plant I

The preliminary wet pilot installation was built in 2003 in Amsterdam, and used to separate, in total, 116 tonnes of BA with an 18% moisture content into several products 3.3).

Table 3.3: Mass balance of the treatments applied, (to 116 tonnes of BA in total) at the first DWR installation in Amsterdam in 2003 (Kooy et al. 2002)

Products	Non-ferrous		Iron	Building products (granulate)				Sludge
	coarse	fine		coarse	Magn.	non.mag	sand	
Total NF	1.25	0.078		0.38	0.23	0.26	0.07	
Al	0.90	0.036		0.20	0.15	0.12		
Cu/Zn	0.30	0.042		0.07			0.07	
St.steel	0.05			0.11	0.08	0.14		
Total BS	0.12	0.097		35.5	15.7	4.7	32.7	
Stone				4.0				
Glass				4.7				
Sludge				26.8				
Organic				0.1				
Fe			0.68	0.25	0.40			
Sludge(dry)								5.1
Water	0.05	0.01		1.1	1.0	0.3	12.4	6.5

The results, presented in Table 3.3 show that the non-ferrous and ferrous metal contents of the BA were 2.3% and 14%, respectively. The $< 45\,\mu$m fraction accounted for 5% of the solid input.

The installation at DWR gave an opportunity to use the existing separation machines (screening, dewatering and drying, upstream column, hydrocyclone) that had been previously used for separating dredging sludge. Next to the existing machines a new process line was installed to handle the > 2 mm fraction (by eddy current separation, gravity separation, magnetic separation, etc).

The separation was based on wet screening. The BA was screened by a trommel screen with circular openings of 20 mm. The >20 mm fraction was not further separated, but if desired this fraction could be milled and fed at the beginning of the process.

The < 20 mm fraction was screened by a 2 mm flat screen (wet screening). The < 2 mm fraction was separated by a hydrocyclone to remove $<$ CCS mm particles (sludge) and the $>$ CCS mm particles were separated by an upstream column. The sludge fraction was dewatered by a belt filter press and land filled. The upstream column removed organic particles from the CCS-2 mm fraction. The residue (sand) had to be separated by jigging. However, at this stage the jig was not implemented.

The 2-20 mm fraction was screened by a 6 mm screen (wet screening). The 2-6 mm fraction was separated by a WECS (a specially constructed ECS for fine particles; (Rem 1999)). The WECS separated the 2-6 mm fraction into a non-ferrous metals fraction and a residue mixture of aggregate (stone, glass), organic particles and magnetic particles. The non-ferrous fraction was further processed by a wire separator to remove long particles (> 150 mm) from the residue, since wires caused several problems during gravity separation (see 'Wire Separation' in this section, below). The non-ferrous fraction without wires was separated by a kinetic gravity separator (KGS) where the light particles were separated from the heavy particles. The heavy non-ferrous fraction (Cu, Zn, brass) was the final product. The light 2-6 mm non-ferrous fraction was separated initially by a Magnus separator and subsequently by another WECS. The processing of the 2-6 mm fraction resulted in an aluminium product, heavy non-ferrous product, organic fraction, wires, and granulate mixed with organic and magnetic particles.

The 6-20 mm fraction was separated by a magnetic separator in which the magnetic particles were removed and the rest was processed by the ECS, which separated non-ferrous metals from the aggregate fraction. The aggregate fraction contained minerals, organics and stainless steel particles. The organic content was separated by a ramp (see "Organic separation of the 6-20 mm fraction" in this chapter).

During a one-year period of development, improvement and tests of set-ups for the wet physical treatment several mass balances were compiled, and an overall mass balance, as shown in (Table 3.4).

The mass balance shown in Table 3.4 used data from Pilot I and from a laboratory experiment for sand and precious metals. The precious metals and sand separation was at this time not implemented in Pilot I. The aluminium content in the sand product was also measured in the laboratory and was included in this mass balance. The organic content was measured using three different methods. This mass balance should be regarded as an example of the optimal output of the wet pilot plant, resulting from the improved scenario from

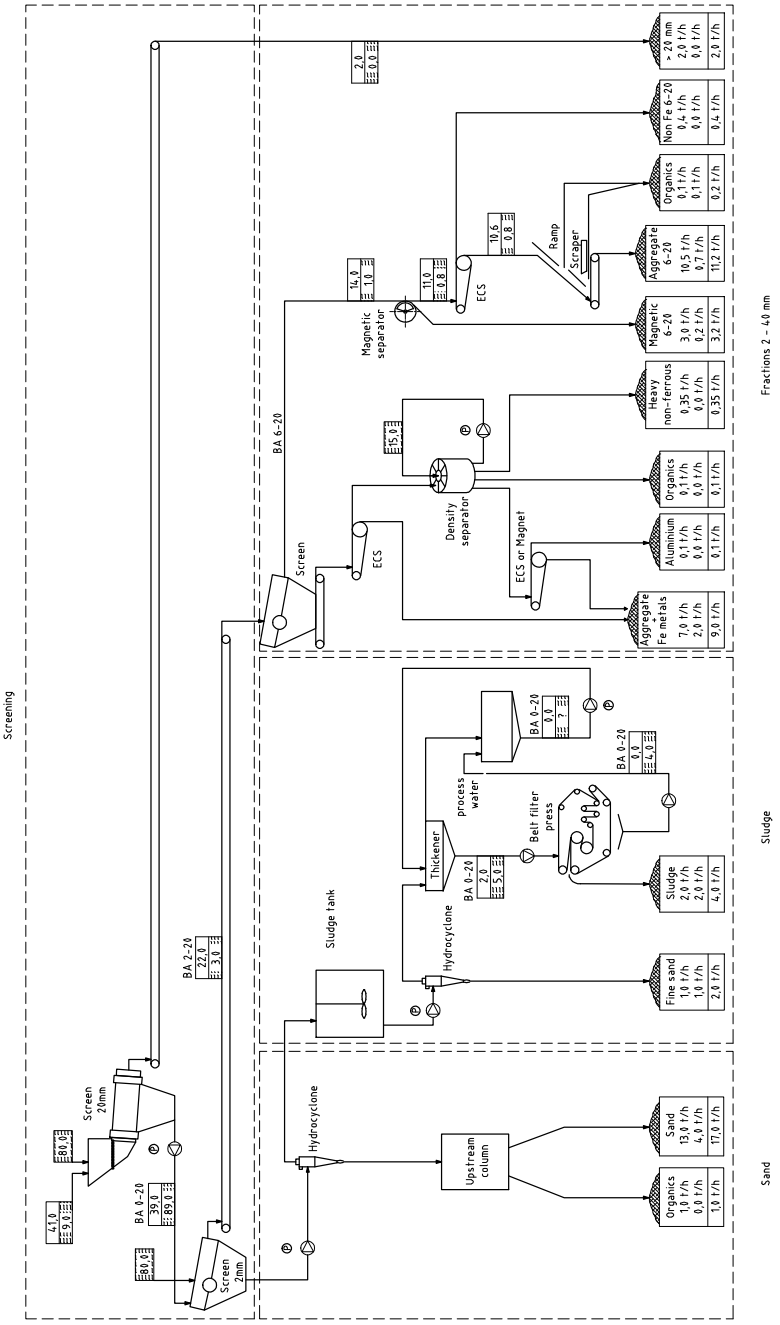

Figure 3.3: Scheme of the wet separation pilot plant (Pilot plant I.)

Table 3.4: Overall mass balance of the new wet pilot plant at DWR Amsterdam in 2004 and 2005, in kg.

		Dry mass (kg)	Dry mass (%)	Non ferrous heavy (kg)	Al Al (kg)	St. steel (kg)	Minerals (kg)	Magnetic (kg)	Organic (kg)	Gold (g)	Silver (g)
<CCS mm		100	10%				80[4]		20[1]		
CCS-2 mm	Heavy non-ferrous fraction[5]	2.4	0.24%	1.0	0	n.m.	1.5	0		0.16	6
	Magnetic fraction[6]	3.1	0.3%	0	0	n.m.	1.3	1.8		n.m.	n.m.
	Sand product	338	34%	0.6	6.1	n.m.	315	13	3.8[2]	n.m.	n.m.
	Light fraction[7]	20	2%	0	0	n.m.	18	n.m.	2.1[2]	n.m.	n.m.
2-6 mm	Heavy non-ferrous fraction	3	0.3%	2.4	n.m.	n.m.	0.3	0.3	n.m.	0.24	8
	Magnetic fraction	4	0.4%	n.m.	n.m.	n.m.	1.0	3.0	n.m.		
	Aggregate	210	21%	0.6	0.7	n.m.	207	0.7	1.2[3]		
	Aluminium fraction	3	0.3%	n.m.	2.8	n.m.	0.2	n.m.	n.m.		
	Light fraction[7]	30	3%	n.m.	n.m.	n.m.	27.5	n.m.	2.5[3]		
6-20 mm	Non-ferrous fraction	7	0.7%	5.3		n.m.	1.6	0.1	n.m.	n.m.	6
	Magnetic fraction	70	7%				22	48	n.m.	n.m.	n.m.
	Aggregate	145	15%	0.7		n.m.	141	1.9	1.8[1]	n.m.	n.m.
	Light fraction[7]	7.6	0.8%	n.m.	n.m.	n.m.	6.5	n.m.	1.1[1]	n.m.	n.m.
20-40 mm	Total	50	5%		0.2	4.5	44	n.m.	1[3]	n.m.	n.m.
Total		1000	100%	10.6	9.8	4.5	867	69	34	0.4	20

[1] Measured as loss on ignition (LOI) (LOI, according to 2, Procedure 2)
[2] Measured as organic burned (according to Chapter 2, Procedure 1)
[3] Measured as organic hand-picked
[4] Sludge content
[5] Mass after processing by jig and LIMS
[6] Mass after processing by LIMS
[7] Light fraction here refers to all light materials (mainly organics) removed based on density

2004.

3.2.2 Pilot Plant II

Some of the Pilot plant I equipment was transferred and reinstalled at Afval Energie Bedrijf (AEB), resulting in Pilot plant II, which included the best separation equipment for processing the 2-20 mm fraction as tested in Pilot plant I, as well as new, additional equipment for treating sand and sludge that was built and implemented. Pilot plant II was designed to process 50 t/h of input of wet BA, but during its operation an input of only 35 t/h was reached due to the limited capacity of the sludge and sand equipment. However, by improving the capacity for the <2 mm fraction (sand and sludge) the installation would be suitable for processing 50 t/h.

The separation of 0-40 mm BA was based on the same principles as in Pilot plant I. The BA was first screened by a 20 mm vibrating screen (wet screening) instead of a trommel screen as in Pilot plant I. The >20 mm fraction was larger than in Pilot I due to a change in the screen implementation. The 0-20 mm fraction was processed by the same screening system as in Pilot plant I. The fraction was separated by a hydrocyclone where the <CCS particles (sludge) were removed and the CCS-2 mm fraction was further separated by a specially-constructed jig (for more details see the jig separation section of this chapter). With the purchase and installation of a new hydrocyclone in Pilot plant II, the cut point was raised to 0.1 mm and thus more fine particles were generated. This step created technical problems during processing and increased the cost of land filling the extra sludge. The jig separated the heavy metals (ferrous and non-ferrous), the organics and the sand product from the CCS-2 mm fraction. The heavy fraction could have been further separated by a wet low-intensity magnetic separator (LIMS) and a shaking table. However, this step was tested only in the laboratory and was never implemented in the plant. Further research is needed to optimize this separation step.

The 2-20 mm fraction was screened by a vibrating 6 mm screen into 2-6 mm and 6-20 mm fractions. A screen 50% larger than that applied in Pilot plant I was used to improve the cut based on particle size. The 6-20 mm fraction was separated by a wind sifter (organics separation), magnetic separator (magnetic particle separation) and ECS (non-ferrous metals separation). The organics in the aggregate fraction were further separated by a ramp and scraper (for further details see the organic separation section). The 2-6 mm fraction was first processed by use of a wire separator that removed long wire particles (mainly copper and steel), which can complicate further separation. Then the 2-6 mm fraction was separated by the kinetic gravity separator (Kooy et al. 2004), which separated the 2-6 mm fraction into three products (heavy non-ferrous/ferrous metal, aluminium/aggregate and organic fractions). The kinetic gravity separator was used in Pilot plant I after the eddy current separation, however placing the kinetic separator before the WECS provides more advantages (further information can be found in section '2-6 mm Fraction'). Furthermore, the heavy non-ferrous fraction was separated by the WECS, yielding non-ferrous and magnetic fractions. The aluminium/aggregate fraction was then separated by another WECS where the aluminium was separated from the aggregate. The organic fraction was dewatered and could have been incinerated again, or land filled.

Pilot plant II was not completely optimised in 2007 due to several technical

difficulties, however a mass balance from this period (Figure 3.5) gives a first impression of the whole process of continuously separating the entire BA fraction (0 to 40 mm) and shows the masses of its resulting streams.

Table 3.5: Mass balance of the Pilot plant II in Amsterdam in 2006 (from July until November 2006, total processed 4700 tonnes).

		Mass total (kg)	Mass total (%)
<CCS mm		150	15%
CCS-2 mm	Heavy non-ferrous fraction	5.5	0.55%
	Heavy magnetic fraction	24	2.4%
	Light fraction	196	19.6%
	Organic fraction	10	1.0%
2-6 mm	Heavy fraction	4.5	0.5%
	Magnetic fraction	11	1.1%
	Aggregate	223	22.3%
	Aluminium fraction	4	0.4%
	Organics	28	2.8%
6-20 mm	Non-ferrous fraction	7	0.7%
	Magnetic fraction	53	5%
	Aggregate	152	15%
	Organics	22	2.2%
20-40 mm	Total	110	11%
Total		1000	100%

The mass balance obtained from Pilot plant II differs from that obtained from Pilot plant I. The main differences are in the >20 mm and sludge fractions. The >20 mm fraction increased by a factor of two due to screening differences (the screen used was not optimal for this application) and screening capacity difficulties (small screening area). The mass of the sludge fraction increased by a factor of two because of changes in hydrocyclone settings. In 2003 the hydrocyclone cut-off point was 45 μm, in 2004 it was 70 μm and from 2005 to 2008 (Pilot plant II) it was 100 μm. This change in 2005 increased the amount of sludge and created difficulties with pumping. The masses of organic fractions also increased, which had a negative financial effect. The metals masses remain constant. However, the mass balance shown in Table 3.5 should be combined with the mass balance obtained from Pilot plant I in order to determine the most realistic outcome. The predicted flow sheet is shown in Figure 3.4, which combines the most realistic outcomes from Pilot plants I and II, including the estimated water flow used for the process.

3.2.2.1 Process Water Balance

As BA is separated by a wet physical treatment, water is added in several steps. According to tests with Pilot plant I and some parts of Pilot plant II, the water mass balance was calculated as represented in Figure 3.4. The process water was collected in the process tank and reused as input water, totalling 160 t/h per 50 t/h of BA input. During the final separation steps, building products were rinsed with, on average, 7 t/h of fresh water. This fresh water should have

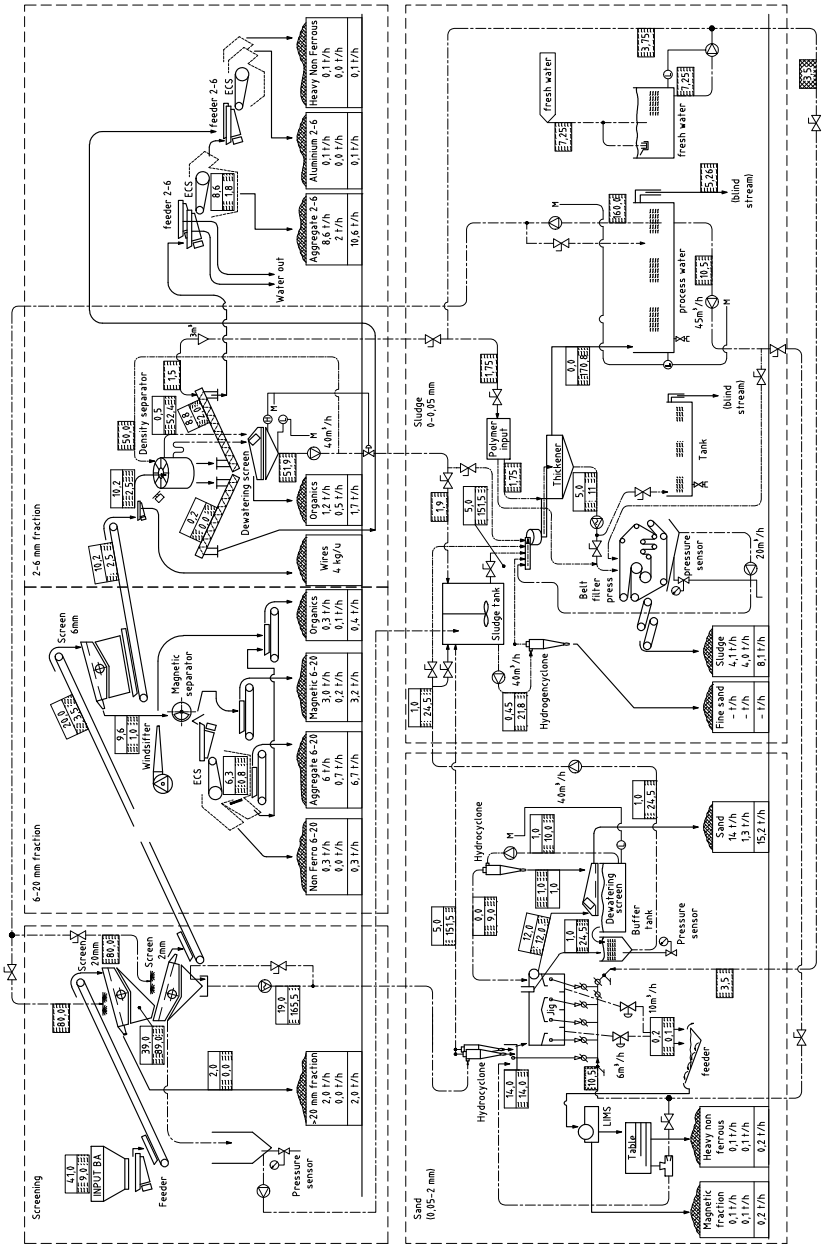

Figure 3.4: Scheme of Pilot II; after optimization, predicted flow.

decreased the leaching values (mainly salts) of the final products. The fresh water was collected and mixed with the process water. It is believed that such mixing of the process water and fresh water, should maintain the quality of the process water. The water losses were mainly caused by the increased moisture content of each final fraction. Ideally, the total water loss for 1 tonne of BA should not exceed 20 litres.

With an input of 50 t/h of BA , consisting of 41 tonnes of solids and 9 tonnes of water, 150 kg of Cl is present in the processed material. The average chloride content of BA is 3600 mg/kg, while the quality limit for building products is 600 mg/kg of chloride. Therefore, by using a process water and fresh water rinsing system it has been determined that Cl will be dissolved and remain in the process water, thereby reducing the solid Cl content in the BA. An example of chlorides in the water and solid phase distribution during the process is shown in Figure 3.5.

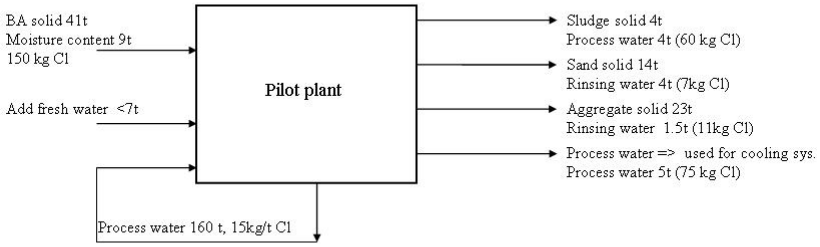

Figure 3.5: An example of chloride distributions during the wet physical separation at the AEB Pilot plant.

Figure 3.5 shows that some of the process water is always lost together with sludge, sand and aggregate. Some of the process water is also allocated for use in the cooling systems after incineration. The data in figure 3.5 indicate that the pilot installation with a capacity of 50 t/h requires approximately 160 t/h of process water and <7 t/h of fresh water to maintain a constant quality of the process water (with 15 g/l of Cl).

3.3 Separation Improvements for 0-40 mm Bottom Ash

The separation of BA is based on commonly used separation principles such as screening, eddy current separation, magnetic separation, and recently developed separation systems like a kinetic gravity separator (KGS), a special WECS for fine particles, a specially constructed jig and a wire separator. Therefore, the following section describes the optimal separation systems and separation

settings developed and implemented for each size fraction and product of AEB BA. The basic separation principles of known machines used and implemented in the pilot plants are explained in Annex C.

3.3.1 0-2 mm Fraction

The 0-2 mm fraction is the largest fraction from BA (>40%). It contains various products, such as non-ferrous metals, precious metals and sand, but also substances that have a negative effect on the final products such as organics and magnetic materials. The aim when processing it is to produce environmentally-clean sand that is comparable to natural sand and non-ferrous metals that could be sold to metal smelters. The first issue was to separate the <CCS material from the rest using a hydrocyclone because this fraction of fine particles cannot be used as building material since they have inappropriate properties in terms of size, composition, etc. (Figure 3.6).

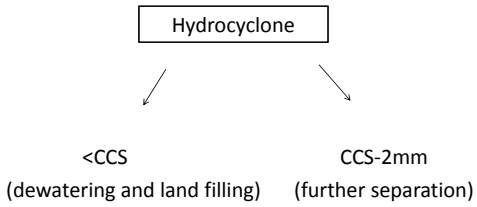

Figure 3.6: Mechanism of separation by a hydrocyclone.

The separation mechanism applied by a hydrocyclone is explained in Annex C. The overflow from the hydrocyclone, called sludge should be settled in a thickener, dewatered by a belt filter press and land filled (or alternatively used for building purposes, Chapter 6). The optimal settling velocity of the sludge (both with either of two polymers, one supplied by Sachleben and the other by Nalco, and with no polymer) and size of the settling tank were explored in several experiments, results of which are illustrated in Figure 3.7.

The settling velocity strongly depends on the polymer used. While designing the plant and calculating the required size of the settling tank a different polymer was used. Based on the settling velocity and amount of sludge generated in trials with Pilot plant II a settling tank area of 25 m^2 was calculated. However, this settling tank area was insufficient to handle the increased amount of sludge generated in later operations (from 2 t/h in 2003 to 4 t/h in 2004 and 7 t/h in 2007), which was mainly due to changing the cut-off point of the hydrocyclone and increases in the organic content of AEB BA.

The degree of dewatering of the sludge was calculated in terms of specific

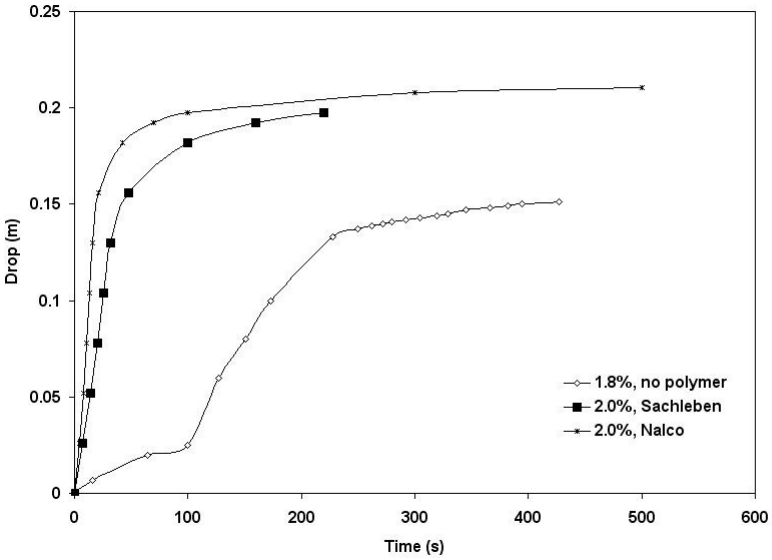

Figure 3.7: Settling velocities of the sludge with 1.8% solid content without added polymer, and sludge with 2% solid content in the presence of polymers from Sachleben and Nalco.

cake resistance (α). Different types of sludge have different specific cake resistances. The AEB BA cake resistance was calculated as $\alpha = 1.1012\,\mathrm{m/kg}$, a typical value for a sludge, indicating that BA sludge is relatively easy to dewater. A belt filter press (Annex C) was implemented for the dewatering, which showed positive results in terms of cake thickness.

The underflow of the hydrocyclone is the CCS-2 mm fraction which contains:

- heavy non-ferrous metals (product which can be sold to a smelter)
- precious metals (product which can be sold to a precious metals smelter),
- ferrous metals (waste stream due to their very fine size distribution)
- aluminium (waste or product)
- organics (waste stream)
- sand (product for building applications)

This fraction should be further separated by wet physical methods. The schemes of two optional separation steps for the CCS-2 mm fraction tested during the research are shown in Figure 3.8.

Heavy Metals Separation
The CCS-2 mm fraction was separated by a new system patented at TU Delft, in which the jig can separate, at the same time heavy particles (heavy non-ferrous and ferrous metals) from the organics and the residual sand product (Figure 3.9).

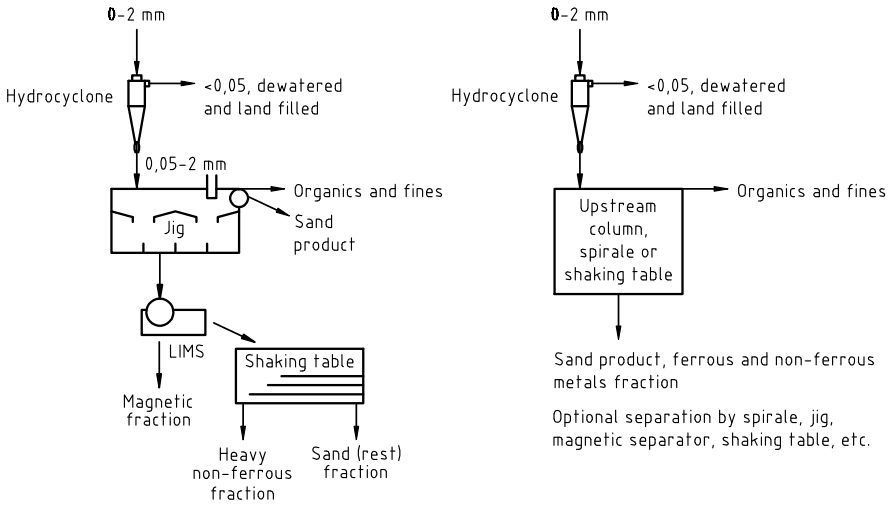

Figure 3.8: Separation systems for the 0-2 mm fraction. Scheme A (left), Scheme B (right).

The CCS-2 mm fraction is fed into the jig (A) where the denser particles (heavy non-ferrous, ferrous and larger stony particles) fall through the ragging and the screen into exits F and G (as in a conventional jig). A detailed explanation of jig principles is presented in Annex C. The sand product travels over the jig and is separated by the cylindrical drum, which helps to separate the light particles. The organic and very light particles are removed at exit H, which has an adjustable setting. The sand product is dewatered on the dewatering screen and if necessary to decrease the leaching of salts can be rinsed with extra clean water, then removed via exit M. The jig at Pilot plant II was constructed with a length of 2 m, width of 0.75 m and screen with rectangular, 3 mm openings. The recommended jig frequency and amplitude settings for the AEB BA 0.1-2 mm fraction are 2 Hz and 9.5 mm, respectively.

A jig is a highly complex machine with many parameters that influence its separation performance (Witteveen 2003). Experiments were conducted to identify suitable jig settings for the new separation system implemented in Pilot plant II, which focused mainly on:

- the size and material of the ragging,
- water flow,
- the organics removal system.

However, the jig was not further optimized and more research is needed to optimize its operation more thoroughly. Nevertheless, this research provided useful indicative information about this jig option.

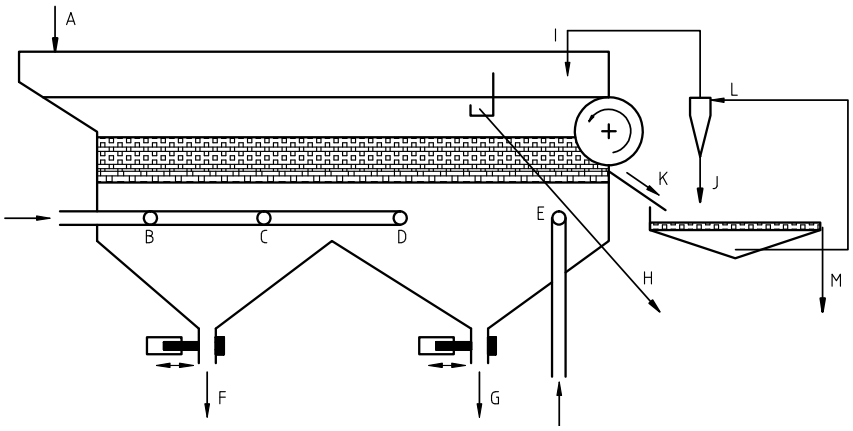

Figure 3.9: A new jig developed for the pilot plant in Amsterdam.

During the research three types of ragging (4-8 mm natural raw stone, 8-12 mm natural raw stone and 4-8 mm hematite) were tested with the same flow rate. The first kind (4-8 mm stone) was not suitable for the installation, since the flow of feeding material moved the fine ragging across the bed, and the ragging in the first part of the jig was completely displaced. The hematite was not suitable as ragging material either, because it was too heavy to allow sufficient fluidization of the bed. Consequently, most of the heavy fraction stayed in the jig and was removed together with the sand product. The best results were obtained using larger ragging (8-12 mm raw stone), therefore further tests were performed with this ragging.

In a second test series the parameters of the under flow water were varied (Figure 3.9, exits B, C, D and E) and the best grade and recovery results for the heavy fraction are shown in Figure 3.10. The underflow water influences the heavy metals separation, therefore two different underwater flow settings were tested: (i) B=C=D=E=4000 l/h, and (ii) B=C=4000 l/h and D=E=6000 l/h. The best results were obtained with the second option, which yielded a heavy fraction in which the grade of heavy metals was 49% and the recovery 62% (in this context, high recovery of the heavy fraction is more important than high grade). The grade of heavy metals in the sand product was measured several times during operation (with the flow rate settings of B=C=4000 l/h and D=E=6000 l/h) and found to be 0.08% for heavy non-ferrous metals and 4% for ferrous metals.

Magnetic Fraction Separation

The heavy fraction from the jig should be further separated by two additional separation steps where the magnetic particles and heavy non-ferrous particles

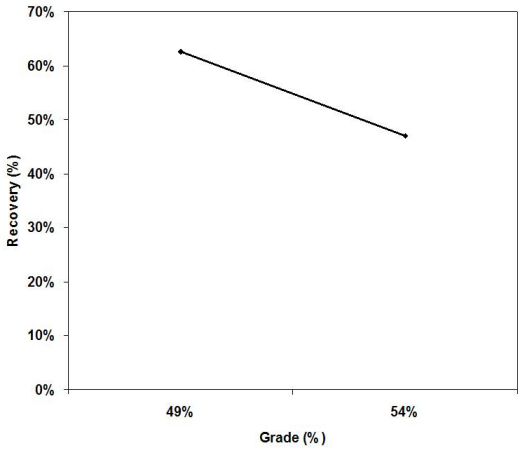

Figure 3.10: Grades and recoveries of heavy metals in the heavy sand fraction.

are separated from the residue. In this research a wet LIMS (low intensive magnetic separator), adjusted for the application, was used for the first step (see Annex C for description of its operational principles). Grade and recovery curves for the magnetics are shown in Figure 3.11. The highest recovery, 99%, is for a grade of 57%.

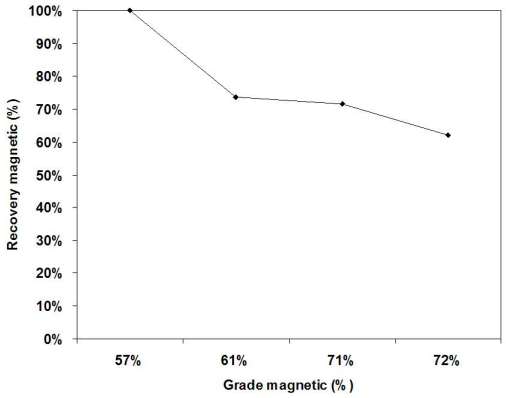

Figure 3.11: Grade-recovery curve for the magnetics in the heavy sand fraction.

The second separation step after the LIMS was by means of a shaking table (Figure 3.12), where the residue from the LIMS was separated into heavy non-ferrous metals and residual sand.

However, it would be preferable to separate the magnetic fraction by the LIMS before jigging, since the LIMS will reduce the mass of magnetic particles by ca. 3% and thus improve the efficiency of jigging for non-ferrous metals. This is because jigs are usually designed for a heavy mass output of 3%, but in Pilot plant II where the LIMS was used after jigging, the heavy mass output

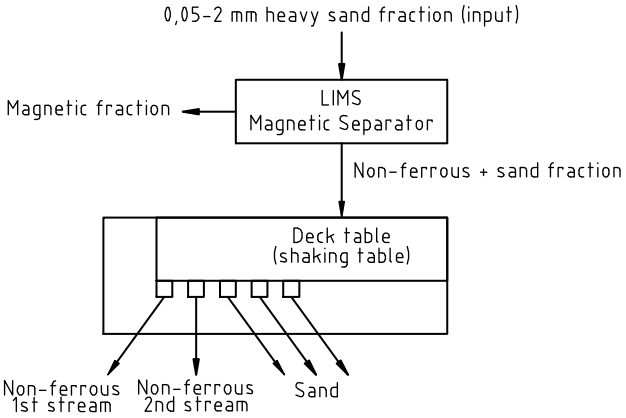

Figure 3.12: System of magnetic and non-ferrous metals separation by the LIMS and shaking table.

was between 6-7%, which adversely affected the efficiency of the jig.

Heavy Non-ferrous Metals Separation

The results obtained from Pilot plant II show that the heavy non-ferrous fraction can be concentrated by a jig (11%) and by removing the magnetic fraction via the LIMS the final heavy non-ferrous metal content of the input for the shaking table can reach 25-30%. Separation by a shaking table is an excellent method for separating non-ferrous metals up to sufficient grade. While no successful experiment was performed with the shaking table in the pilot installation, a similar experiment using a shaking table was conducted by Agacayak (Agacayak et al. 2007) with low rate chromite ores (grade, 20-25%). His results show that the metals grade can reach 51%, with a recovery of 85%. An experiment was performed in which the CCS-2 mm heavy fraction was processed by the shaking table. However, instead of using a jig, the heavy fraction was previously separated by a spiral and the magnetic fraction was removed by LIMS before the spiral process. In this experiment 143 tonnes of 0-40 mm bottom ash was processed by the spiral, resulting in 2.48 tonnes of heavy fraction. The masses and compositions of the fractions obtained in this experiment are shown in Table 3.6.

The results obtained by Agacayak using a shaking table are similar to those obtained in the experiment performed using a spiral and shaking table (3.6).

However, using a spiral in place of a jig has advantages as well as disadvantages. Jigs used for industrial processes pose more challenges for achieving constancy because they are sensitive to many parameters. Nonetheless, using a jig affords higher recoveries of metals than using a spiral. Recovery by a spiral (Wills and Napier-Munn 2006) for the very fine fraction is on average 36% while the measured recovery from the jig was 62% (Figure 3.10). Another problem

Table 3.6: Mass and composition of each sub-fraction obtained from the CCS-2 mm heavy fraction separated by the shaking table.

	Mass (kg)	Mass (%)	Cu (%)	Pb (%)	Ag (g/t)	Au (g/t)	Pd (g/t)	Pt (g/t)
Concentrate 1	0.68	1.3	27.76	15.95	2389	159	18	5
Concentrate 2	1.02	2.0	21.55	5.7	370	17	4	0.4
Middlings	3.3	6.4	5.76	1.02	62			
Tailings	46.8	90.4	0.32	0.1	8			
Total (d.s)	51.8	100.0	55.39	22.77	2829	176	22	5
Recovery of conc.(1+2)			54.55	67.4	77.5	100	100	100

with the spiral is the buildup of sediment on the surface of the spiral; over time, fine materials can collect and thereby reduce its efficiency.

Organic Separation

The second issue affecting separation of the CCS-2 mm fraction is the presence of fine and organic particles. Therefore, the CCS-2 mm fraction was analysed for contents of organic particles, very light particles (<1800 kg/m^3) and very fine particles (<100 μm), and the results are shown in Figure 3.13.

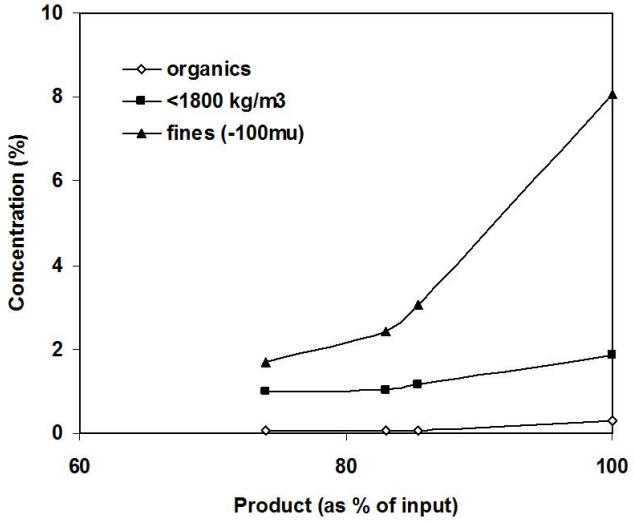

Figure 3.13: Contents of organic particles, very light particles (<1800 kg/m^3) and very fine particles in the CCS-2 mm fraction (measured in 2004).

Figure 3.13 shows that the main 'organic content' consists of particles less dense than 1800 kg/m^3 and very fine particles (<0.1 mm). The real organic content is very small. However, the whole 'organic content' has to be separated from the sand.

The new jig can also separate light particles (very fine particles and organics)

by a specially constructed cylindrical drum, which is placed at the end of the jig (Figure 3.9).

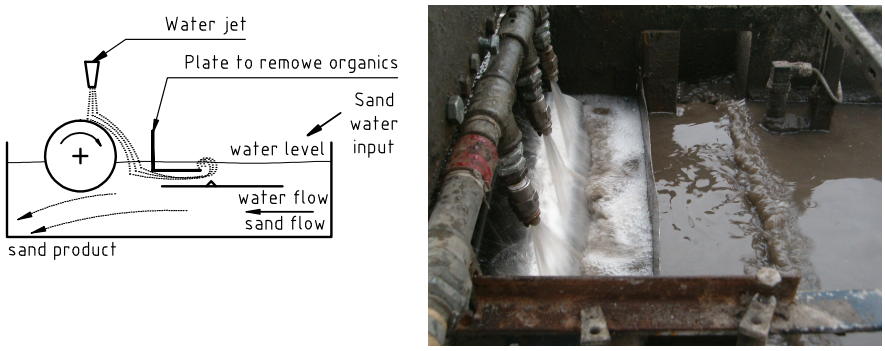

(a) Scheme of the separation. **(b)** Photo of the separation system.

Figure 3.14: An organic separator implemented on the jig.

The separation system is shown in Figure 3.14; the cylindrical drum rotates clockwise and water is sprayed on the top of the drum. The speed of the water flow and direction of the flow are adjustable. The water flow removes light particles (light, fine and organic) from the top of the bed by forcing them onto the plate. The output collected on the plate (waste and light residue) moves to the water tank where the fraction is dewatered together with the sludge.

This system was tested by varying the water flow (on the top of the cylindrical drum, called the water jet). The results are presented in Table 3.7. The sand input contained on average 2.5-3% of organics. The results of this experiment show that most of the organics were removed by a water flow of 5000 l/h. However, together with the organics, other solids (sand product) were removed and a large amount of water was required. Therefore, the best results obtained were with a flow of 2000 l/h, with which the organic content was decreased from 2.5% to 1.6% and the total solid mass removed together with organics was 582 kg/h with an input of 30 t/h of BA.

Table 3.7: Organic removal by indicated water flows over the cylindrical drum of the jig, with a total of 30 tonnes/h of BA input and the following jigging parameters: B=C=4000 l/h and D=E=6000 l/h (Figure 3.9).

Water flow (l/h)	Total solid removed (kg/h)	Total water collected (l/h)	Organic content in the sand product (%)	Organic content in the solid part (%)	Organic total in the sand input (%)
5000	2025	20486	0.5%	6.2%	2.4%
3000	913	17560	1.9%	10.1%	3.0%
2000	582	16321	1.6%	12.0%	2.5%

The first impressions obtained from this separation system are positive, however the system still has to be optimised, mainly to decrease the mass of sand

and water removed together with organics.

Other options for separating organics from the CCS-2 mm fraction are to use an upstream column, a spiral or a shaking table. The upstream column had already been used in Pilot plant I, therefore one of the first tests examined its recovery of the organics from the fraction. The organic content before and after upstream column separation was 1.6% and 0.7%, respectively. Thus, the upstream column both reduced the fine particles content (Figure 3.15) and more than halved the organic content.

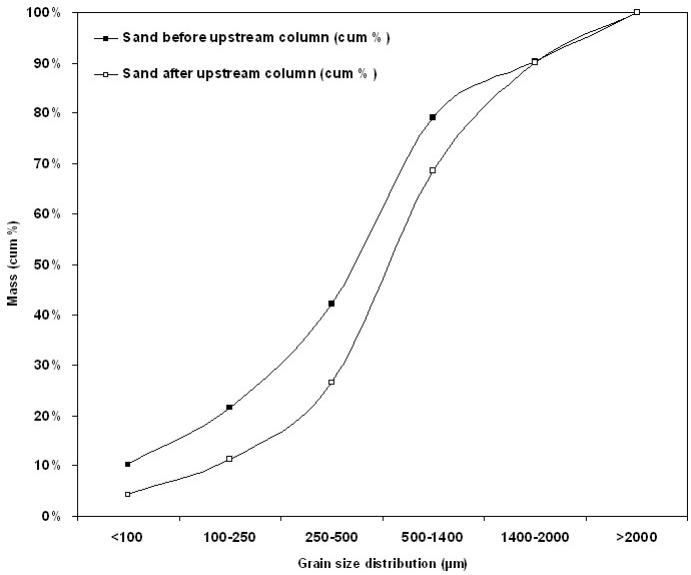

Figure 3.15: Grain size distribution before and after separation by the upstream column.

In another series of tests to identify ways to decrease the organic content, conducted in cooperation with the University of Aachen, laboratory tests with a spiral (Annex C) and shaking table were performed. Three different spirals were tested (one with low pulp density, a coal spiral with high pulp density and a coal spiral with low pulp density). The best results were afforded by the coal spiral with high pulp density, which reduced the organics (LOI) content by approximately 30%.

3.3.2 2-6 mm Fraction

The 2-6 mm fraction contains valuable products, similar to the CCS-2 mm fraction, therefore these products should be further separated into:

- aggregate (product for building applications)
- heavy non-ferrous metals (product which can be sold to a smelter)
- precious metals (product which can be sold to a precious metals smelter),

- ferrous metals (product which can be sold to a smelter)
- aluminium (product which can be sold to a metals smelter)
- organics (waste stream)

The main objectives for processing this stream are to produce environmentally-clean aggregate that has similar characteristics to natural aggregate and non-ferrous metals that can be sold to metal smelters. The products from the 2-6 mm fraction can be separated by a different system, according to their gravity, conductivity, size, shape and magnetization. The basic principles of these separators are explained in Annex C.

Heavy Metals, Aggregate and Organics Separation by the KGS
The heavy metals (ferrous and heavy non-ferrous), organics and aggregate/aluminium fraction can be separated in a single step by a KGS (Annex C). A KGS separates particles on the basis of differences in their terminal velocity, which depend not only on their density but also on their size and shape. The non-granular shape of flat particles and wires in the feed makes it difficult to separate these particles in currently available separators like jigs. For this reason, an alternative KGS was designed in which the solids concentration of the input is low and particles are separated strictly according to terminal velocity.

The prototype KGS, used in Pilot plant I, consists of a cylindrical shell with an inner diameter of 100 cm and a height of 100 cm surrounding a 60 cm diameter cylinder. Between the cylinders a paddle wheel is placed coaxially, with 65 radial paddles (Figure 3.16a). A double size kinetic gravity separator (Figure 3.16b) was constructed for Pilot plant II. This larger separator can handle about 10 t/h.

(a) Kinetic gravity separator (KGS) as used in the Pilot plant I.

(b) View of the gravity separator from the top-the material input, Pilot II.

Figure 3.16: Kinetic gravity separator (KGS).

The paddles of the kinetic gravity separator are key elements for suppressing the effects of the shape factor. They are placed close to each other to prevent horizontal fluttering of, for instance, flat particles. The inner space, where the paddle wheel is placed, is filled with water and rotates around its vertical axis. The water is, thus, forced to move at a constant angular velocity. At the bottom of the separator the particles are collected in six different compartments. When

a particle is fed from the top, its specific terminal velocity determines, together with the wheel speed and the height of the machine, the compartment in which it lands. By feeding particles of different sizes at different feeding points, particles of similar densities are collected in the same product compartment. The speed at which the paddle wheel rotates makes the heavy metals fall into the first compartment while the light metals, stones and glass are collected in the second and third compartments. Water jets are installed at the outlets underneath the first three compartments to remove the metal and stone particles from the kinetic gravity separator, transporting heavy metal particles to one WECS and light metal particles and stones to another WECS. The extremely light organic/ highly porous stone fraction is collected, together with the heavy organics, in the fourth, fifth and sixth compartments. Organic material with similar density to water is also collected in compartments four, five and six. The last group of particles, the light organics, flows over the top and is mixed together with the rest of the organic material.

An experiment was performed to examine the effects of the shape of BA particles (polished spheres, cylinders and discs) falling in water on their terminal velocity, and to determine the terminal velocities of heavy non-ferrous metal particles, light non-ferrous metal and granulate particles of different size ranges (Mooij 2004). The results are shown in Figure 3.17, where experimentally determined terminal velocity-curves for each size range are plotted. The aluminium curves are indicated in white and the heavy non-ferrous curves are indicated in black. The results suggest that aluminium and heavy non-ferrous particles can be separated on the basis of terminal velocity, using cut-offs ranging from approximately 0.3 m/s for the 2-4 mm particles to about 0.45 m/s for the 8-10 mm particles.

The average velocities for different shaped particles of copper/zinc and aluminium of different sizes have been combined and plotted in Figure 3.18. This figure also indicates the recovery values obtained when feeding at the beginning of the density separator (border compartment 1) and 40 mm upstream from the first point (40 mm back from the border), and the recovery of aluminium in the third and fourth compartments of the kinetic gravity separator in Pilot plant I.

Wire Separation

In most recycling operations the presence of wires complicates the separation process, which is often designed for granulate particles. The transport parameters of wires differ from those of granulate particles, due to their curved shapes and large length to diameter ratio. When no wire separator was used wires blocked the underflow of the KGS and caused a major problem by blocking the material flow. Another advantage of the wire separator is that removing wires enhances metal recovery and the collection of other long, thin materials such as various fragments of plastics and wood. A prototype wire separator was constructed and tested in the laboratory, and results obtained from trials with it were used to develop a cascade wire separator, as illustrated in Figure C.6. The principle of the wire separator is explained in Annex C.

Several parameters influence the wire separation recovery:

- the width and height of the gap
- the length of the wires

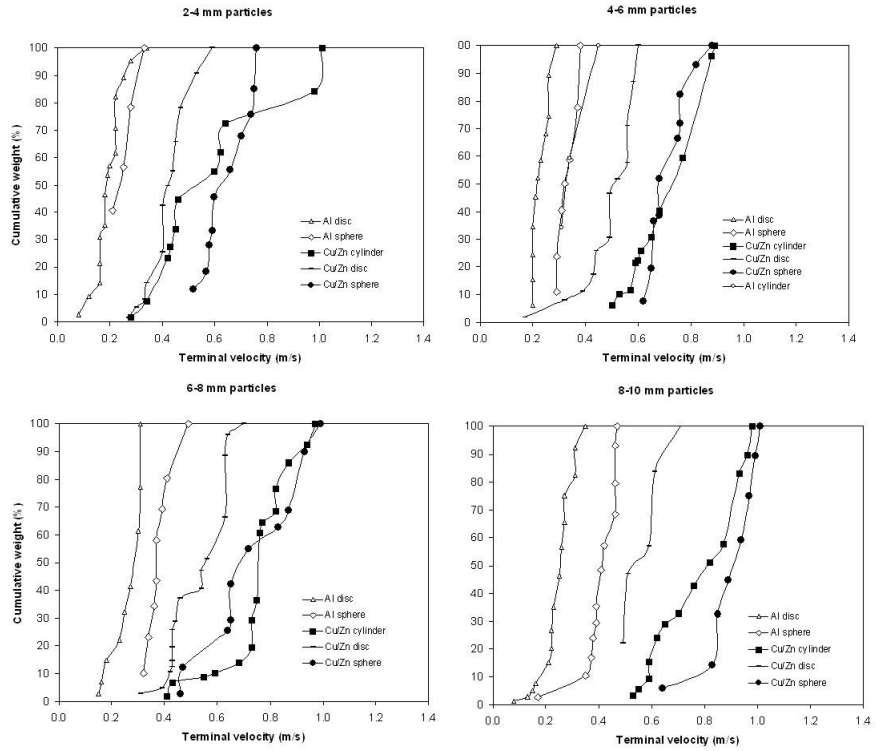

Figure 3.17: Experimentally determined distributions of terminal velocities for aluminium and heavy non-ferrous particles in the four size ranges. Data points for aluminium alloys and heavy non-ferrous alloys are shown in white and black, respectively (Mooij 2004).

- multiple step separation (cascade separation)
- the frequency and the amplitude of the feeder

During the development of the separator a set of experiments was performed to identify ways to improve and optimize the design for the 2-6 mm AEB fraction. Initially, a series of experiments were conducted with the single step separator mounted on a standard vibrating feeder with wires of three length categories. The primary initial goal was to optimise the width and height of the gap. Table 3.8 shows the wire recovery results obtained with gaps of three different dimensions. The recovery of wires increases with decreasing width and height, although there is a minimum dimension of the gap to ensure a limited loss of granulates to the wire fraction.

After optimization of the gap dimensions, the effects of varying the frequency and amplitude of the feeder were tested. In a second experimental series wires of four different categories (35-39, 40-44, 45-50 and 50-54 mm) were fed into the separator with a gap of 17 mm by 20 mm (width by height) at two feeder settings. The purpose of the experiments was to determine the relationship between the feeder settings and l50 (50% recovery).

Table 3.8: Recovery of wires using a separator with gaps of the indicated dimensions.

Gap size	Wires < 50 mm	50 mm < Wires < 80 mm	Wires > 80 mm
Width: 17.0 mm, Height: 20.0 mm	10.0%	66.0%	87.5%
Width: 17.0 mm, Height: 15.0 mm	40.0%	76.0%	93.8%
Width: 16.0 mm, Height: 15.0 mm	46.7%	89.8%	93.8%

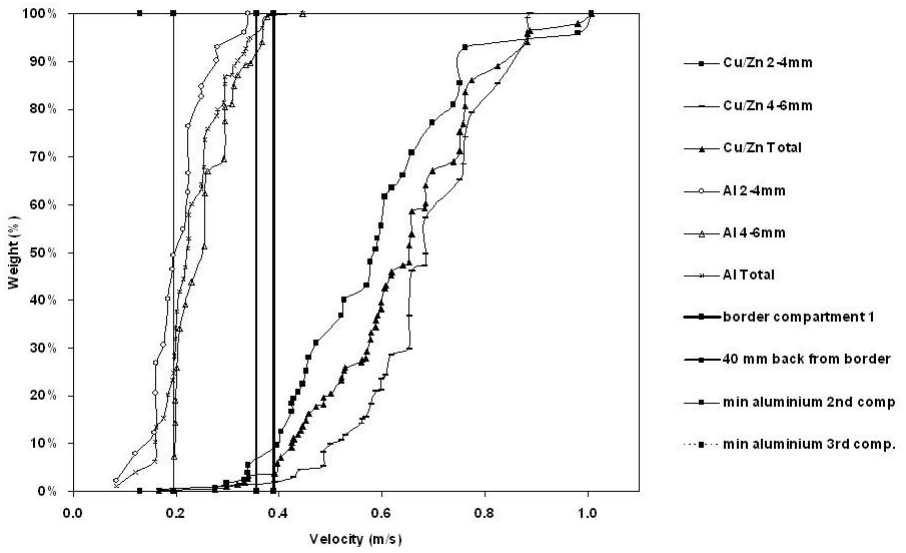

Figure 3.18: Experimentally determined distributions of terminal velocities for aluminium and heavy non-ferrous particles in the size ranges.

Data in black in Figure 3.19 show the experimental results, which were fitted to a sigmoid curve according to equation (3.1):

$$\frac{1}{1+\left(\frac{l_{50}}{l}\right)^{n}} \tag{3.1}$$

Where n was determined to be 4.

A final experiment was conducted to verify the theory using a 5 by 5 cascade, processing 700 kilograms of 2-6 mm BA containing 632 wires at least 35 mm long. The results of this experiment are shown in Table 3.9.

The recovery of the larger wires shows that the separation of larger wires is outstanding (100% recovery). A comparison of theoretical and experimental data for the 5x5 test separator is shown in Figure 3.20.

The experimental curve follows the shape of the calculated recovery curve, although the slope is less steep. It is believed that the decrease in steepness is due to changes in operating parameters during the separation: firstly in feeder amplitude (which was difficult to keep constant due to irregular pressure of the compressor), and secondly in the moisture content of the BA. The 700 kg sample was collected in a box that held a lot of water at the bottom. The top material was therefore drier than the material at the bottom.

The recovery of the larger wires shows that the separation of larger wires was outstanding (100% recovery). A cascade wire separator has been successfully applied to granular material from BA. The experimental recovery for wires longer than 50 mm was essentially complete. With increases in the speed of the wires (when the vibration amplitude or frequency is high) there is a higher

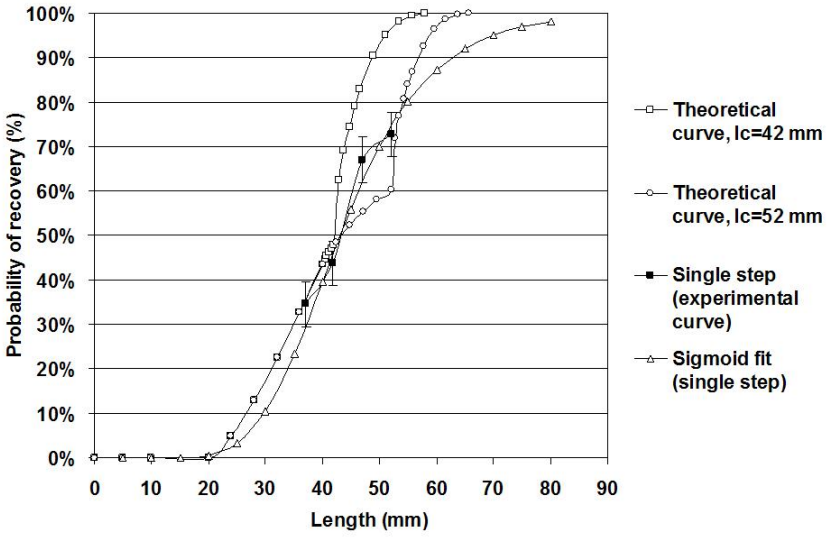

Figure 3.19: Experimental recoveries of a single-step operation and a sigmoid fit, compared to the theoretical recovery for the feeder setting corresponding to l_c =42 mm and l_c = 52 mm.

probability that wires will pass over the gap. The shape of the recovery curves depends on two factors: the critical length of the wires (the feeding speed) and the cascade system. These parameters define the position and steepness of the curve (Muchova et al. 2005).

Replacement of the KGS at the Position of the WECS

In Pilot plant I a separation system was developed according to Figure 3.21a. The 2-6 mm fraction was first separated by a WECS for fine particles, which separated the aggregate/magnetic fraction from the non-ferrous fraction. The non-ferrous fraction was then processed by a wire separator that removed long wires and the residue (non-ferrous metals fraction) was further separated by a KGS, which separated heavy metals from the aggregate/aluminium fraction.

In system A (Figure 3.21), a WECS was used with two tested rotor speeds (1000 rpm and 1500 rpm) and a belt speed of 1 m/s. The KGS was operated at a constant speed of 15.4 seconds per rotation. The moisture content of the 2-6 mm feed on the WECS belt was approximately 19% during each of the runs.

Increasing the rotor speed from 1000 rpm to 1500 rpm had a positive effect on the recovery of non-ferrous metals. The recovery curve of heavy non-ferrous metals versus recovery of aggregate measured by different experiments, by changing the rotor speed, is shown in Figure 3.22 (Mooij 2004).

The recovery of heavy non-ferrous metals increased from 65% to 67% and the measured recovery of aluminium was 56%. The grade of heavy non-ferrous metals was on average 82% and 77% in tests with the 1000 and 1500 rpm rotor speeds, respectively, while the grade of aluminium was 6% and 8%, respectively.

Table 3.9: Experimental results of the wire recovery verification experiment.

Length categories of wires	Wires in wire product (number)	Wires in tailings (number)	Total number of wires (number)	Average wire length of category	Recovery wires in product (%)
35-39 mm	147	64	211	37.0	69.7%
40-44 mm	145	26	171	41.8	84.8%
45-49 mm	85	3	88	47.0	96.6%
50-54 mm	55	0	55	52.2	100.0%
55-59 mm	30	1	31	57.2	96.8%
60-64 mm	29	1	30	61.9	96.7%
65-69 mm	15	1	16	67.6	93.8%
70-74 mm	8	0	8	72.5	100.0%
75-79 mm	7	0	7	76.7	100.0%
80-84 mm	3	0	3	82.7	100.0%
85-89 mm	4	0	4	87.5	100.0%
>90 mm	8	0	8	117.4	100.0%

The grade for aluminium was low, because it was not yet processed by a further separation step, in contrast to the heavy non-ferrous metals. The data suggest that the rotation speed has very little effect on the heavy non-ferrous metal grade, but it has a stronger effect on the aluminium grade. The experimental results also show that the preliminary treatment of BA by a WECS had no effect on the grade of heavy non-ferrous metals. The magnetic fraction remained in the aggregate stream with a grade of 10±2% and a recovery of 98%. Under these conditions, the organic fraction will be concentrated in the aggregate fraction and should be further separated.

In a second experiment in 2004 the WECS was replaced by the KGS (Figure 3.21b). The 2-6 mm fraction was fed to the wire separator and then, after removing the wires, into the KGS. This step resulted in three fractions depending on the gravity of particles. The KGS separates the 2-6 mm fraction into three fractions: the organic, light aluminium/aggregate and heavy non-ferrous/magnetic fractions. The total mass balance obtained in this experiment is shown in Table 3.10 (Mooij 2004).

The results of this experiment show that the system offers very promising grade and recovery for the aggregate/aluminium fraction, and high recoveries of both aluminium and heavy non-ferrous metals (Table 3.11).

During this experiment the organic stream was collected separately and it was not included in the mass balance. However, the organic fraction in every stream was separately analysed. The 2-6 mm fraction was found to contain 1.5% by mass (in 2004), according to hand-picking analysis. The organic distribution after the separation is shown in Table 3.12.

The organic material present in the BA can be divided into three groups. Approximately 1/3 of the organic material present in the feed is light and flows over, 2/5 floats and 1/4 is heavy organic material which is difficult to separate by KGS and will end up in the aggregate/aluminium fraction. Unfortunately all organic content was only analysed by hand picking, therefore 1.2% of organics which remains in the aggregate/aluminium fraction is not the accurate organic

Table 3.10: Total composition of the output streams from the KGS in kg (d.s.).

	Stone (kg)	Heavy non-ferr. metals (kg)	Al (kg)	Magnetic (kg)	Organics (kg)	Total (kg)
Wires	0.03	0.04	0.00	0.01	0.01[1]	0.08
Heavy NF/magnetic stream	2.20	1.20	0.01	0.53	0.14[1]	4.06
Al/aggregate stream	77.16	0.12	1.26	0.47	0.47[1]	79.47
Total out	79.38	1.35	1.27	1.00	0.61[1]	83.61

[1] The organic fraction was sorted by hand-picking, it was not measured according to procedures dscribed in Chapter 2.

Table 3.11: Grades and recoveries of the KGS from the operation B.

	Recovery (%)	Grade (%)
Aggregates in aggregate/aluminium fraction	97.2	97.1
Heavy non-ferrous metals in heavy non-ferrous/magnetic fraction	88.4	29.4
Aluminium in aggregate/aluminium fraction	99.6	1.6

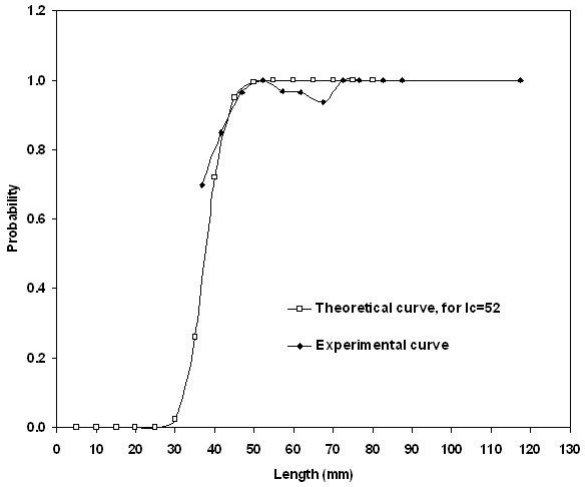

Figure 3.20: Cascade system (experimental data versus theoretical calculations).

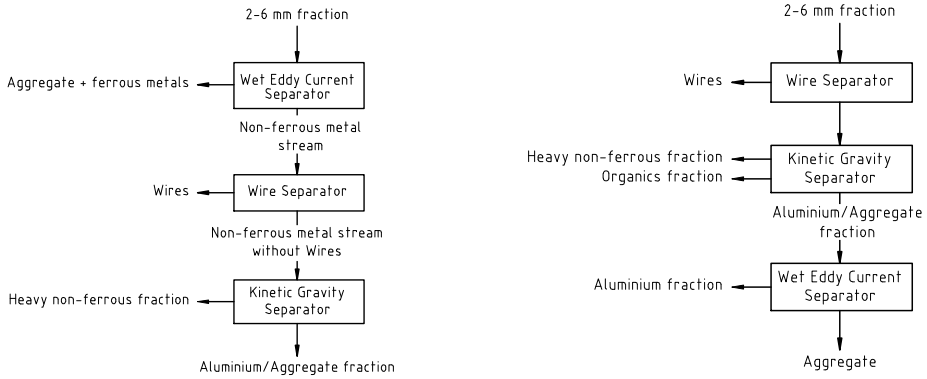

(a) First tested system. **(b)** New proposed system.

Figure 3.21: Two tested systems for the 2-6 mm fraction.

content. However, it can be concluded that the KGS can reduce the organic content (measured by hand-picking) by 67%. The organic content in the 2-6 mm aggregate fraction obtained from Pilot plant II was 1.8±0.2% (analysed by procedure 1, Chapter 2). This organic content is high, probably due to the increased organic content in the AEB BA resulting from incinerating sewage sludge together with the household waste. However, further research is needed to both assess the organic content, and its distribution more thoroughly, and to optimize ways to process it.

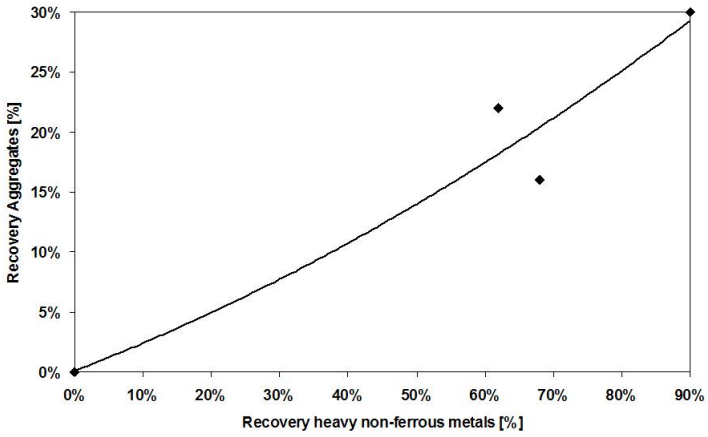

Figure 3.22: Recovery/recovery curve of 2-6 mm heavy non-ferrous metals and aggregate.

Table 3.12: Organic distribution after separation by the KGS.

Stream	Organics[1] (%)
Wires	0.2
Heavy non-ferrous/magnetic fraction	0.8
Aggregate/Aluminium fraction	32.7
Overflow	34.8
Organic fraction	24.6
Organics lost	6.9

[1] The organic fraction was sorted by hand-picking, it was not measured according to procedures described in Chapter 2.

System B shows more advantages than system A. The main improvements are:

- reducing the organics content of the aggregate stream by 67%
- increasing the recovery of heavy non-ferrous metals (from 67% using system A to 88.4% using system B)
- increasing the recovery of aluminium (from 56% using system A to 99.6% using system B)
- washing out very fine particles (sludge).

However, the grade of heavy non-ferrous metals in the heavy non-ferrous/magnetic fraction must be further treated by an extra WECS. Also, the aluminium should be separated from the aluminium/aggregate stream by a WECS. Therefore, the

performance of a WECS and a Magnus separator was compared to identify the best separation system and the optimal separation settings for aluminium separation.

Aluminium Separation, the WECS versus a Magnus Separator
The aggregate/aluminium stream resulting from the BA separation plant should be separated to recover aluminium from the aggregate fraction (glass, stone, ceramics). Therefore, the WECS and the Magnus separator were compared in terms of their ability to separate the aluminium content from the granulate stream (Figure 3.23).

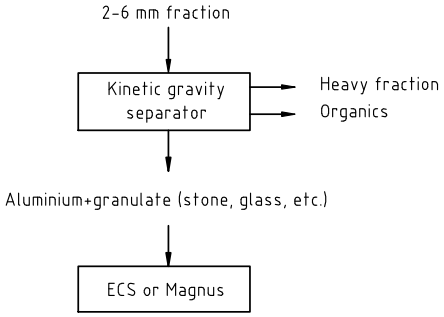

Figure 3.23: Scheme for separating 2-6 mm fraction by the WECS or Magnus separator.

The aluminium-granulate stream resulting from treatment by system A (Figure 3.21) contained 7% by mass of aluminium particles with sizes ranging between 2 and 6 mm. The WECS and Magnus separator were chosen for their high recovery of non-ferrous metals and for the advantage of wet separation. The moisture content of the aluminium/aggregate fraction was on average 15%. The goal was to obtain a high-grade aluminium fraction and a minimal grade of aluminium particles in the rejected aggregate fraction. The aggregate product (a mixture of glass, stone, ceramic, sinter) should be used for the building industry. The aluminium content in the aggregate product has a negative influence (due to oxidisation) on the quality of building materials, thus it is important to minimize the aluminium content in the aggregate product.

Both types of separator (WECS and Magnus) have been previously found to provide high recoveries of heavy non-ferrous metals (Settimo et al. 2004). The high recovery of small non-ferrous particles based on the eddy current torque was developed in TU Delft (Rem 1999). The principle of the wet eddy current separation (Annex C) is to add water at the feeding point to stick all the small particles to the belt surface. For small particles, typically <5 mm, this adhesive force is of the same order of magnitude as gravity. The rotating magnetic field

makes the conductive particles spin, causing the water bonds between these particles and the belt to break. The principle of the Magnus separator (Fraunholcz et al. 2002) is to exploit the rotation of particles that are deflected by the Magnus effect as they fall through the water (Annex C). The particle size for a wet Magnus separator is typically between 1 and 10 mm. Particles smaller than 1mm have a relatively low terminal velocity, which makes the process less effective (Rem 1999). Eddy current separation has proved to be effective in previous experiments with a non-ferrous <5 mm fraction (Köhnlechner et al. 2002). Another option to separate aluminium particles from the residue is to use a WECS with an inclined magnetic disc (Schlett and Lungu 2002). However, the Magnus separator and the WECS were selected for tests with the aluminium/aggregate fraction because of their potential for high product recovery and high capacity.

The experiments with the WECS (Bakker Magnetic BM 29.710/18) and the Magnus separator were performed in the laboratory and Pilot plant I. In the first experiments the effects of several factors affecting the performance of the WECS were examined:

- changes of the splitter position,
- changes of the rotor speed,
- the moisture content of the fraction
- the particle size of the fraction.

Results of the first tests, in which the splitter position of the WECS (Bakker magnetic) was varied, are shown in Figure 3.24.

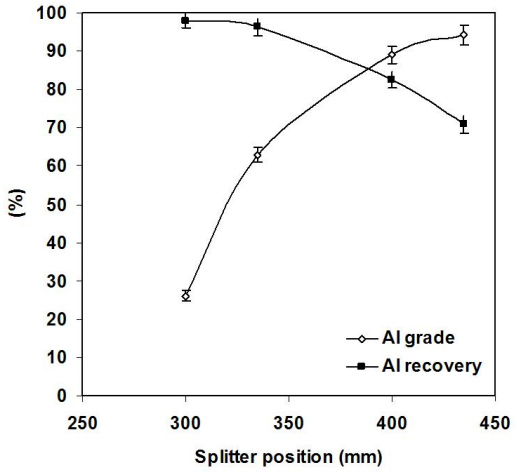

Figure 3.24: Splitter position of the WECS versus grade and recovery curve.

The results of these tests show that the grade and recovery of aluminium are optimal with the splitter position between 380-400 mm.
The optimal parameters found experimentally, when processing an artificial sample in the laboratory, were as follows:

- Splitter position, 380 × 600 mm

- Moisture content, 15%
- Belt speed, 1 m/s
- Rotor speed, 1500 rpm

Grade-recovery curves obtained from a separation performed in the laboratory with an artificial sample and a separation by a WECS at Pilot plant I in Amsterdam are compared in Figure 3.25.

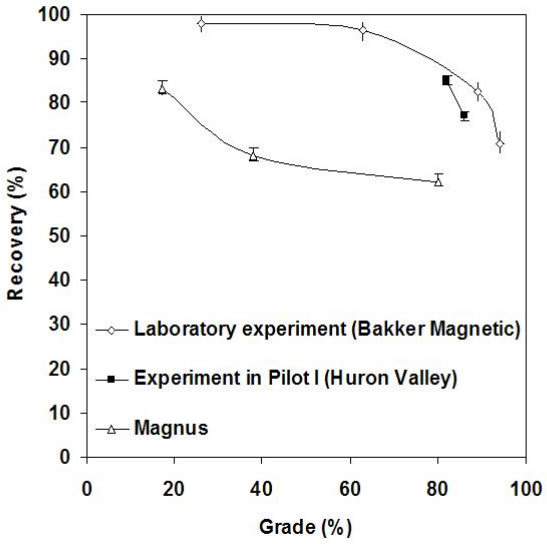

Figure 3.25: Grade recovery curve for aluminium from BA measured in the laboratory versus in the Pilot I in Amsterdam by WECS and by Magnus (measured in the laboratory).

The experiment at Pilot plant I performed using the WECS (a 24-pole drum eddy current separator manufactured by Huron Valley Steel Corp., US, Huron ECS, Model MK. IV-36/24) yielded similar results to the laboratory experiment performed with the WECS (Bakker Magnetics). The WECS can separate non-ferrous metals with both high recovery (>80%) and high grade (>80%). As a comparison of wet eddy current separation by using a traditional drum eddy current separator, a new industry design Magnus separator was utilized in our test. Experiments were carried out with the same artificial sample as in the wet eddy current separation. Figure 3.25 shows the grade-recovery curve obtained for Magnus separation. It can be seen that the grade of aluminium decreases rapidly with increases in aluminium recovery. The figure also shows that separation by WECS is more effective for recovery of fine aluminium particles than Magnus separation.

Ferrous/non-ferrous Metals Separation
The heavy fraction (heavy non-ferrous/magnetic fraction) from the KGS in system B (Figure 3.21) must be further separated by WECS to concentrate heavy non-ferrous metals (Cu, Zn, Pb, brass, precious metals) from the residue (magnetic particles, scrap iron, stone, glass). In the research reported here, the main interest focused on the heavy non-ferrous product quality and recovery. Pilot plant II is not yet complete, therefore a combination of data from previous laboratory experiments and new data from Pilot II were combined, and show measured and predicted grade-recovery curves for heavy non-ferrous metals from the pilot plant when fully commissioned (Figure 3.26).

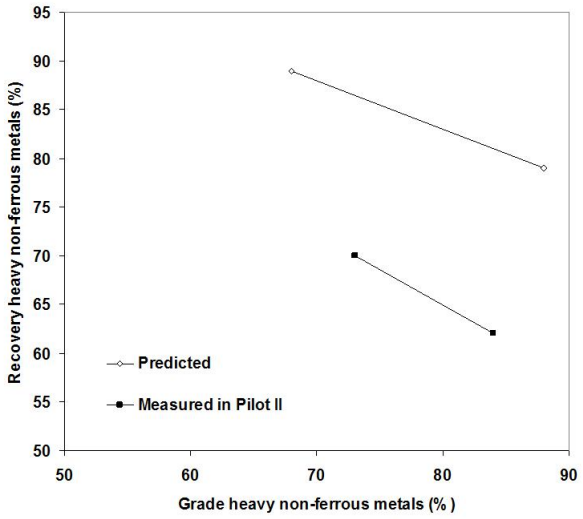

Figure 3.26: Grade/recovery curves of heavy non-ferrous metals, measured and predicted based on laboratory experiments.

The results from Pilot plant II were obtained using the WECS from Huron Valley with a non-optimized splitter position, therefore the results shown in Figure 3.25 are only initial indications, and results are likely to be better in the future.

3.3.3 6-20 mm Fraction

The 6-20 mm fraction contains approximately 1% non-ferrous metals, 5-8% ferrous metals and 1-2% organic particles (foil, paper, plastic, textile, bones). The ferrous and non-ferrous metals can be separated from the stream and sold to smelters, but the organics should be removed since they do not meet environmental and civil engineering quality criteria. The final fractions resulting after wet separation are the following:

- Non-ferrous metals fraction (product)
- Magnetic fraction (partly product)

- Aggregate fraction (product)
- Organic fraction (waste)

Ferrous Metals Separation
The 6-20 mm fraction was initially separated by a magnetic separator, which removed all magnetic particles (ferrous metals including magnetic stones, etc.). In the Pilot plant an AISI 304 trommel magnet made by Bakker Magnetics was used to separate the magnetic fraction. The principle of the magnetic separator is explained in Annex C. The magnet attracts all magnetic particles, including particles that are only slightly magnetic. Therefore, the 6-20 mm magnetic fraction could not be considered as scrap iron. This fraction was analyzed by milling to determine its scrap iron content, and the results indicate that only 20% of the 6-20 mm magnetic fraction could be regarded as valuable scrap iron. The grade of the magnetic fraction during all experiments was on average 62%, with 96% recovery.

Non-ferrous Metals Separation
The non-ferrous metals are removed by an eddy current separator (Bakker magnetic) which separates all non-ferrous metals from the residue (aggregate). The grade-recovery curve of the ECS separation is shown in Figure 3.27. The grade is a very important criterion for the metals smelters as they will accept only non-ferrous product with >75% grade. On the other hand, the aggregate must also meet proposed limits for metals content. Usually, for building applications large metallic particles are not permitted in the product and the metals content should not exceed 1% (Chapter 6).

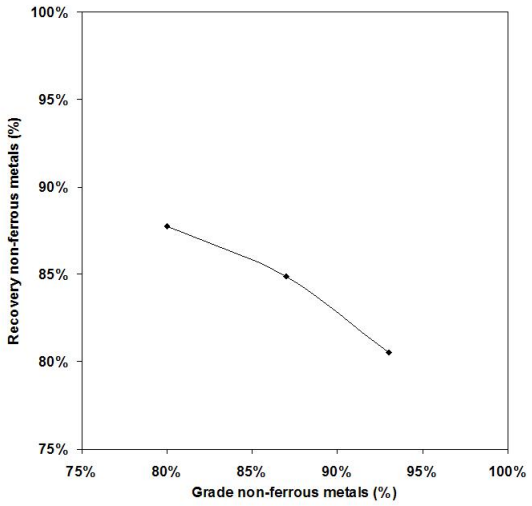

Figure 3.27: Grade-recovery curve of 6-20 mm non-ferrous metals in the non-ferrous fraction.

The amounts of non-ferrous particles in the aggregate fraction during the three phases of the experiment shown in Figure 3.27 correspond to 0.5% (of

which 0.3% is stainless steel), 0.7% and 0.9%.The optimal set-up for an ECS is 3000 RPM with a belt speed of 1 m/s.

Organic Separation
The organic particles (foil, paper, plastic etc.) in the 6-20 mm fraction must be separated out from the fraction due to their negative influence on the quality of the aggregate product. The organic particles can be separated by dry physical methods. Three different organic separators were placed in different locations in the pilot plant (Figure 3.28). First, a wind sifter blew the light particles (paper, foils) away from the rest of the 6-20 mm fraction.

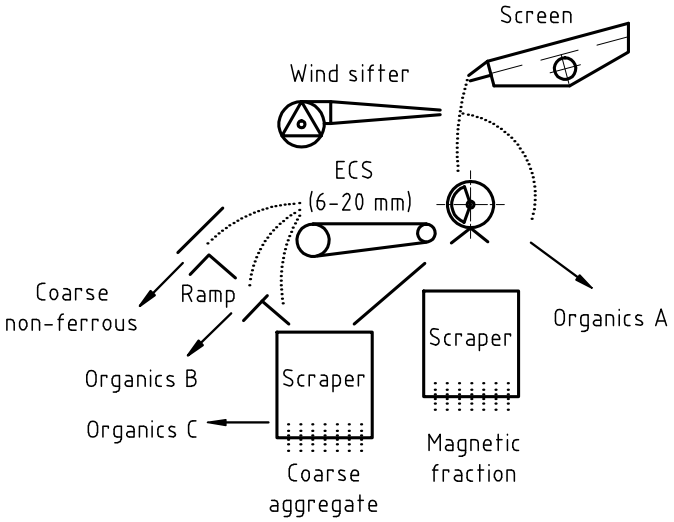

Figure 3.28: Separation of organics in the 6-20 mm fraction (scheme).

The second separator is the ramp under the ECS, which removes heavier (wet) organic particles, since they slide down through the ramp. The third separator is the scraper (a brush) installed under the conveyer belt where the aggregate fraction ends up. Particles stuck on the conveyer belt should be removed, otherwise they will end up in the granulate product.

In experiments in 2004 all three separators were used and the final 6-20 mm aggregate was analysed for organic content (Chapter 2, Procedure 1). The coarse organic particles left in the aggregate correspond only to 0.04% of organics where the fine organics were 0.6%.

The wind sifter can remove 80% (according to analysis by hand picking) of organic material from the coarse granulate fraction. The optimal set-up was built, tested and is shown in Figure 3.29.

A laboratory experiment in 2004 showed that the optimal position for the wind sifter is 300 mm from the falling particles, and it can provide a recovery

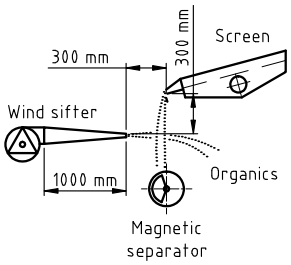

(a) Scheme of the wind sifter separation.

(b) Photo of the wind sifter separation.

Figure 3.29: The scheme of the separation by the wind sifter in Pilot II.

rate of 80% (Table 3.13). Together with the organic fraction 1.2% of the total mass of aggregate (stone, glass, etc.) is removed.

Table 3.13: Grade and recovery of organics separated by the wind sifter.

	Organic Grade	Organic Recovery	Aggregate in the organic fraction (% of the total mass)
340 mm (lab.)	68%	65%	0.6%
300 mm (lab.)	57%	80%	1.2%

An efficiency test with the wind sifter was performed in Pilot plant I and the recoveries of coarse organics were very similar to those observed in the laboratory test, between 70-80%.

The ramp can remove another part of the organic content from the coarse aggregate fraction (Figure 3.30).

The 6-20 mm fraction is first separated by an ECS, built into the covering (Figure 3.30). Aggregate falls straight down onto the conveyer belt and the non-ferrous metals fraction is propelled further away (Figure 3.30). The organic particles (paper, textile, foil) are therefore ejected from the ECS and slide down the opposite wall of the covering. Thus, a ramp placed precisely between the wall and the output of aggregate can separate out those organics (Figure 3.30). In January 2004 an experiment with the ramp was performed in which 0.2% (d.s.) of the total mass was removed by the ramp. The coarse organic content was found to be (by hand-picking) 6%, and the fine organic content analysed by hand picking was at most 19%. The experiment was subsequently repeated using material with a different total organic content. The loss on ignition of the fraction removed by the ramp was 14.5%. These two sets of results are consistent if we assume that the fine and coarse organic contents of the ramp product are about 13% and 6%, respectively.

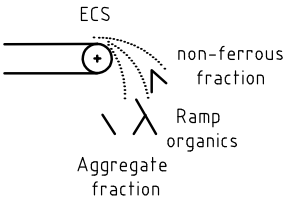

(a) Scheme of the separation by the ramp.

(b) Photo of the separation by the ramp at Pilot II.

Figure 3.30: Organic separation by ramp.

The scraper separator is the final organics remover, installed under the conveyer belt in order to remove organic particles (foil, textile) from the aggregate stream that are stuck to the conveyer belt. The material that was removed from the coarse granulate product by the scraper was sampled and analysed for loss on ignition (LOI). With an input of 50 t/h of BA, the scraper fraction amounted to 170.6 kg (d.s) per hour with 3.8% loss of ignition, equivalent to 6.5 kg/h of organics. It should be noted that some of the material in the 6.5 kg/h stream will be fine organics. The rest of the scraper fraction consists of stones, glass and sinter.

The data acquired during this experiment were compiled for these three separators (wind sifter, ramp and scraper) and an efficiency mass balance was calculated (Table 3.14).

Each separator removed some of the 6-20 mm stream, including organics and aggregate (Table 3.14, column 2). Each fraction was then analysed by hand-picking the organics (coarse and light), and the results indicated that there was a total of 2% of organics in the 6-20 mm aggregate fraction. This mass balance shows the efficiency of each separator; the wind sifter removes 80% of organics, the ramp 10% and the scraper 0.2%.

Table 3.14: Mass balance of the total mass removed by each organic separator and detailed organic contents (coarse and fine) analysed by hand-picking in each removed fraction. Calculated as percentages of the coarse granulate (10 t/h) for a throughput of 50 t/h of input BA.

	Dry mass removed total (%)	Organic content coarse (hand-picked) (%)	Organic content light (hand-picked) (%)
Wind sifter	2.8%	1.6%	n.m.
Ramp	1.1%	0.07%	0.14%
Scraper	1.7%	0.003%	
Aggregate	94.4%	0.25%	
Total	100.0%	1.9%	0.14%

A similar mass balance was calculated for each separator and the fraction it yielded by measuring LOI (Table 3.15). The LOI of the fraction removed by the wind sifter was estimated from previous experiments, the LOI values of the ramp and scraper fractions were 14.5% and 3.8%, respectively. The LOI of aggregate was divided into LOI of coarse organics and fine organics. The main LOI in the final aggregate product is mainly attributable to fine organics, which are impossible to remove by these separators. Another option for removing the fine organics is rinsing the final product.

The total mass of aggregate that was removed by the separators together with the organic fraction in 2004 was 3.8%, equivalent to a loss of 380 kg of material from processing 50 t/h.

3.4 Conclusion

The 0-40 mm fraction of BA can be separated by the wet physical system in order to separate more metals and improve the environmental quality of the residue. Conceptually, and in practice, wet separation appears to be superior to dry methods (Chapters 1 and 2). The wet system was tested during this research in Pilot plants I and II at AEB in Amsterdam, where the optimal separation configuration was proposed and tested. The main aim is to produce environmentally clean building products (aggregates, sand) from BA, which will comply with Dutch regulations (SQD). At the same time, the process should concentrate metals (non-ferrous metals, ferrous metals, stainless steel and precious metals) that can be sold to smelters. The system of wet treatment was developed and implemented at AEB Amsterdam. The main concept is based on dividing BA into several size categories: <CCS mm, CCS-2 mm, 2-6 mm, 6-20 mm and >20 mm fractions. Each fraction is then separately treated by wet or dry physical methods.

For the first step of separating the 0-2 mm fraction a hydrocyclone was proposed. The hydrocyclone can separate the <CCS mm fraction (sludge), which should first be settled in a thickener and then dewatered by a belt filter press.

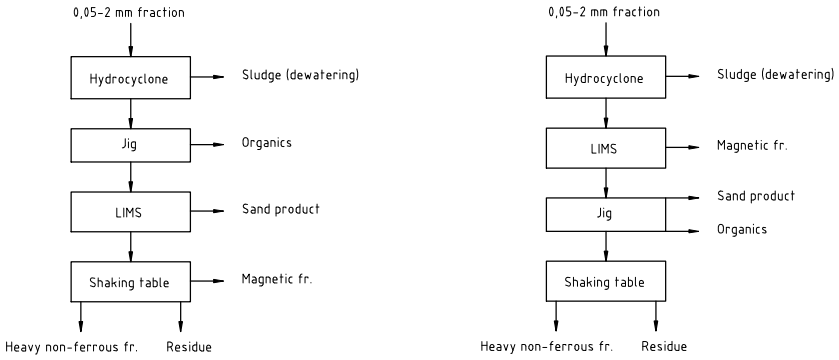

(a) The tested system. **(b)** The optimal system.

Figure 3.31: Tested and optimised set-ups for the CCS-2 mm BA fraction.

Table 3.15: Mass balance of the total mass removed by each organic separator and detailed organic content (coarse and fine) analysed by measuring LOI (according to procedure 2, Chapter 2) in each removed fraction. Calculated as percentages of the coarse granulate (10 t/h) for a throughput of 50 t/h of input BA.

	Dry mass removed total (%)	LOI of coarse organic (%)	LOI of fine fine organic (%)	LOI in each fraction removed by separator (%)
Wind sifter	2.8%	15%[1]	0.4%	
Ramp	1.1%	14.5%	0.2%	
Scraper	1.7%	3.8%	0.1%	
Aggregate	94.4%	0.04%	0.6%	0.6%
Total	100.0%	33%	0.6%	1.25%

[1] estimated value.

The CCS-2 mm fraction should be further separated by a LIMS, where the magnetic fraction will be separated from the non-ferrous/sand fraction (Figure 3.31b), but this step was not tested during this research. The LIMS was placed after the jig process (Figure 3.31a), however, it is highly recommended to place the LIMS before the jig in order to minimize the mass of heavy outputs that are processed by the jig.

Results obtained with the tested system shown in Figure 3.31a a demonstrate that the CCS-2 mm fraction processed by jigging can separate the heavy fraction, non-ferrous and ferrous metals, with a grade of 49% and recovery of 64%. The heavy fraction coming from the jig contains 11% heavy non-ferrous metals, 50% magnetic particles and 49% light particles (stone, aluminium and glass). The LIMS can separate 99% of magnetic particles with a grade of 57%. The residue fraction, heavy non-ferrous metals and the remaining sand from the LIMS, should be separated by a shaking table. The shaking table can separate heavy non-ferrous metals at high grade, which are suitable for selling to metal smelters. The organic content in the sand product can be decreased by 50% by using the cylindrical drum that is part of the jig separator. In 2004 the organic content in the CCS-2 mm fraction was 1.6%. In 2007 the organic content increased on average to 2.5%, but in one case the organic content was as high as 7%. However, for the final sand product, the jig can decrease the organic content by half. The jig can also create a sand product containing <0.1% of heavy non-ferrous metals and <4% of magnetic particles. This sand product can be used for building applications (Chapter 6). The magnetic fraction currently does not have any potential for utilization; it has to be land filled. The heavy non-ferrous metals fraction can be sold to a metal smelter or scrap company, which will further purify the metals content. The sand product contains between 1-2% metallic aluminium and the utilization options are discussed in Chapter 4.

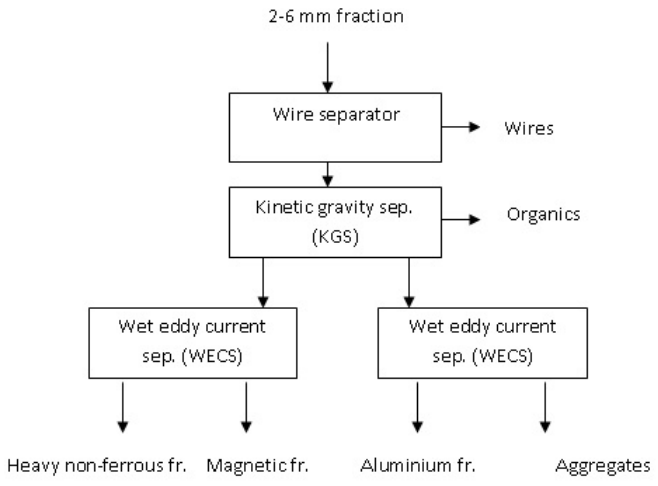

Figure 3.32: Optimised set-ups for the 2-6 mm BA fraction.

The 2-6 mm fraction should initially pass through a wire separator and then

be separated by a kinetic gravity separator (KGS), which can separate the heavy fraction (heavy non-ferrous/ferrous metals) from the aggregate/aluminium fraction and the organic fraction. The KGS can separate the heavy fraction with a grade of 29% and recovery of 88%. In this case the recovery of heavy non-ferrous metals should take priority over the grade of materials. The most important factor is to decrease the heavy non-ferrous metals content in the aggregate fraction due to their adverse leaching effects (Chapter 5). The heavy fraction should be further separated by a WECS, which can separate heavy non-ferrous metals from the magnetic material. A WECS can provide approximately 80% recovery with a grade of 70-75%. However, further research is needed because Pilot plant II has not yet been optimized. The heavy non-ferrous fraction should be separated in the future by MDS, which can separate the precious metals fraction (Au, Ag, Pb) from the heavy metals fraction (Cu, Zn, brass) and the light fraction (stone, aluminium) (Chapter 4).

The aggregate/aluminium fraction from the KGS should also be separated by another WECS. It is believed (based on laboratory experiments) that the recovery of aluminium, which is more important than the grade of aluminium, can be 80-90% with a grade between 70-80%. The aluminium fraction should be further milled and screened to concentrate the metallic aluminium from the rest of the aggregate and aluminium oxide. This treatment can create a metallic aluminium fraction that can be sold to metal smelters. The 2-6 mm fraction contains on average 1.5% of heavy metals, of which 88% can be recovered. Therefore, the aggregate/aluminium fraction will still have a heavy metals content of approximately 0.2%. This fraction can be further separated by WECS and thus the heavy metals and aluminium contents should each be reduced to <0.1%.

The organic content in the 2-6 mm fraction, which has a major influence on the aggregate quality, can be reduced by 67% (measured by hand-picking) by the KGS. However, the latest measurements in Pilot II show that the aggregate still contains 1.8±0.2% organics (data from 2007). The organic contents in 2007 were higher, on average, than those measured in 2003-2005. However, a previous laboratory experiment in 2004 with the 2-6 mm aggregate fraction, using a laboratory KGS, showed that gravity separation can decrease the organic content to 0.5% (measured according to procedure 1, Chapter 2).

The optimal proposed separation system for the 6-20 mm fraction is presented in Figure 3.33.

The 6-20 mm fraction should be first separated by a wind sifter, which can remove 80% of coarse organic particles (measured by hand-picking). The organic content must be minimized for two reasons: the large organic particles influence the mechanical and visual properties of the aggregate (Chapter 6) and the fine organic content has a negative influence on leaching values (Chapter 5). The organic content (mainly coarse organic particles) should be separated by a wind sifter, a ramp and a scraper. The combination of these three organic separators can remove 90% of organics (analysed by hand-picking), the most efficient being the wind sifter, which removes 80%. The total organic content (measured as LOI) can be reduced by 50% through use of these separators, however another 50% of LOI is composed of fine organics which cannot be removed in this way. However, rinsing of the final product may be an option. The loss on ignition of aggregate examined in 2004, was 0.64%. The loss of materials (aggregate)

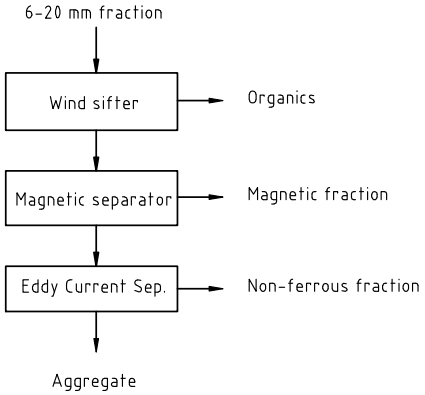

Figure 3.33: Optimal set-ups for the 6-20 mm BA fraction.

removed together with the organic fraction was less than 1%. The residue (non-ferrous metals/ferrous metals/aggregate) can then be separated by a magnetic separator, which can separate the magnetic fraction with a grade of 62% and recovery of 96%. The magnetic fraction should be further milled and screened to separate scrap iron from the magnetic residue because only the scrap iron has value. Further separation of the remaining fraction (aggregate/non-ferrous metals fraction) is done with an ECS, which can separate 88% of non-ferrous metals with a grade higher than 80%. Therefore, if the 6-20 mm fraction contains 5% of non-ferrous metals the non-ferrous metals content in the aggregate will be <1%. The metals content must be minimized to below a specific limit when used for building applications (Chapter 6) and to reduce the negative influence of leaching of heavy metals into the environment (Chapter 5).

Chapter 4

Advanced Separation Options

Summary

Additional value-adding separation steps after wet physical separation can be implemented to increase the price and quality of the final products. These options were considered for implementation in the pilot plant in Amsterdam, but they may also be used for processing other waste streams for which there are similar challenges.

One of the further separation steps imparting a high economic effect is the separation of precious metals from the heavy non-ferrous fraction using a magnetic density separator (MDS). This separation can increase the value of BA by 22%. Another important improvement is the separation of stainless steel from the 6-20 mm aggregate, since legislation standards limit the quantity of metals in aggregate. The stainless steel particles can be separated and can reach recovery rates of up to 90%. The last research presented in this chapter deals with the issue of fine metallic aluminium (1-2%) in the sand product. This sand-aluminium mixture can be optionally used as a replacement for building materials.

4.1 Introduction

Three additional separation treatment options were investigated in terms of their potential to improve the quality of products after wet physical separation of BA:

- Precious metals separation by a MDS (magnetic density separator)
- Utilizing the metallic aluminium content in the sand product, which can have a negative effect on buildings' materials quality.
- Separation of stainless steel from 6-20 mm aggregate to improve the quality of building products

Precious Metals in Bottom Ash
Composition analyses show that the heavy non-ferrous concentrates from MSWI BA contain interesting levels of precious metals, such as silver, gold, platinum and palladium. Precious metal particles have been found in all size fractions smaller than 20 mm. Figure 4.1 shows examples of gold particles found in the 2-6 mm heavy non-ferrous fraction.

Figure 4.1: An example of gold particles separated from the 2-6 mm HNF fraction.

In 2007 the London Metals Exchange (LME) value of precious metals in Amsterdam BA exceeded €10 per tonne of dry ash. One of the important issues in recycling MSWI BA is how to increase the value of its precious metals content in the most efficient way. This chapter discusses the challenges associated with accurately assessing levels of precious metals in various size fractions, detailing the many forms in which precious metals occur in the non-ferrous concentrates, and finally, producing optimal concentrates.

Fine Metallic Aluminium in the Sand Fraction (CCS-2 mm)
The CCS-2 mm fraction (called sand product) is the largest residue after jig separation, corresponding to 30-40% by mass of the BA input. The sand product contains metallic aluminium particles which are very difficult to separate

from the sand because they have a very similar size distribution and particle density. This aluminium causes problems if the sand product is to be used for a building application since it will oxidize and thus create cracks if used in lime-sand stone. However, the presence of aluminium can be advantageous because aluminium can be used as a source of hydrogen. Consequently several experiments were performed to explore the behaviour of metallic aluminium and its reactions (oxidation of aluminium in ambient conditions, kinetics of oxidization and their dependence on pH, etc.). The hydrogen generated from aluminium can be used for internal company uses (e.g. fuel for trucks). The second option is to use the sand product as a substitute material in the manufacture of aerated autoclave concrete (AAC), which is made from a mixture of sand, cement, lime and aluminium powder. The aluminium powder is an expensive additive; therefore using the sand mixture derived from BA, which already contains metallic aluminium particles may be economically attractive.

Stainless Steel Separation from 6-20 mm Aggregate
The presence of stainless steel (0.3%) in the 6-20 mm aggregate fraction also causes several problems for building applications, since building material standards impose limits for metals that must be complied with and, furthermore, if the material is to be used for concrete, for example, long stainless steel fragments will cause problems in production. Therefore, a new machine capable of separating stainless steel (SSS), based on the shape of particles (stainless steel is usually in the form of long, thin particles), was developed, providing SSS recovery rates of 80-90%.

4.2 Precious Metals Content and Separation by a Magnetic Density Separator

The non-ferrous metal fractions resulting from wet physical separation are the coarse non-ferrous (6-20 mm), fine non-ferrous (2-6 mm) and very fine non-ferrous (0-2 mm) fractions. These fractions amount to approximately 1%, 0.35% and 0.16% of the input of BA, respectively. Smelting tests show that one of the heavy non-ferrous fractions (2-6 mm) contains precious metals such as silver (3000 ppm) and gold (100 ppm) (Bakker et al. 2007b). Bakker proposed a system for separating the 2-6 mm heavy non-ferrous fraction (HNF) based on magnetic density separation (MDS). MDS can separate the heavy non-ferrous (HNF) fraction into three sub-fractions: a light fraction with residual glass and stone, a copper-zinc concentrate and a lead and precious metals concentrate. The process is essentially a sink-float operation in a medium containing nanometre-sized magnetite particles. For the separation of precious metals such as silver and gold (which have high densities: Ag 10490 kg/m^3, 19300 kg/m^{3*}, a cut-density of about 10000 kg/m^3) needs to be achieved. The value of BA can be increased by using a MDS system because different smelters (precious metals smelters, copper smelters, brass smelters) pay different prices, depending on the processes they apply. Precious metals smelters focus on the precious metals content and brass smelters do not pay for precious metals. Therefore,

*The golden particles from bottom ash were found as an alloy with other metals, therefore their density is lower than that of pure gold.

separating the HNF fraction into a precious metals product, which can be sold to a precious metals smelter, and a copper-zinc product to be sold to a copper or brass smelter, makes the BA economically more attractive.

The research described in this chapter focused on the HNF fractions of all sizes containing precious metals separated from Amsterdam BA. The chapter presents a statistical distribution of gold in all HNF fractions, and results of X-ray fluorescence (XRF) and microprobe analyses of the 0-2 mm HNF fraction. In addition, an economic overview of the MDS system and BA separation is presented, indicating optimal ways to valorise the precious metals content of BA.

4.2.1 Principle of Magnetic Density Separation

The basic principle of magnetic density separation is to use magnetic liquids as a separation medium. Such liquids have a relatively low density, ρ, comparable to that of water, but in a gradient magnetic field, B, the force on a volume of the fluid V is the sum of gravity and the magnetic force. Hence, by appropriate arrangement of the magnetic field, it is possible to make the liquid artificially light or heavy. For a fluid with magnetization, M, the force per unit volume is (Murariu et al. 2005, Svoboda 2004):

$$F/V = (\rho/g)\, g = \rho' g \tag{4.1}$$

Non-magnetic particles such as glass, stone, zinc and copper will float in the medium if their density is less than that of the artificial medium, ρ', given by Eq. (4.1).

Many designs of magnetic density separators have been presented (Kaiser 1969, Reimers et al. 1974, Vlasov et al. 1988, Svoboda 1998). The most common type consists of a cavity between two curved polar pieces of an electromagnet, in which the field contours are mainly horizontal and the concentration of the contours (the magnetic induction) increases towards the bottom of the cavity. If the induction was perfectly linear in the vertical direction and the magnetization of the magnetic liquid constant (which is nearly true for ferro-fluids), the effective density of the medium would be the same throughout the entire cavity. In reality, Maxwell's equations do not allow this, so the density is not entirely homogeneous in the cavity. Hence, the particles will converge at the middle of the cavity and this will lower the capacity. Another important point is the relatively complex geometry of the cavity. Iron particles are present in most waste streams and such iron will be collected at the surface of the magnet. The complex geometry of the cavity makes it is difficult to remove any iron present at the surface of the magnet, and to scale the separator to an industrial size.

The novel MDS approach to magneto-hydrostatic separation is to create a medium with a cut-density that is not a constant but varies with the vertical coordinate (Bakker et al. 2007b). For a magnetic induction that varies exponentially with vertical direction z,

$$|B|(x, y, z) = B_0 e^{-2\pi z/w} \tag{4.2}$$

the effective medium density also varies with z:

$$\rho_{\mathrm{cut}} = \rho + \frac{2\pi M B_0}{gw} e^{-2\pi z/w} \tag{4.3}$$

This is illustrated in Figure 4.2. The density is constant in the horizontal plane.

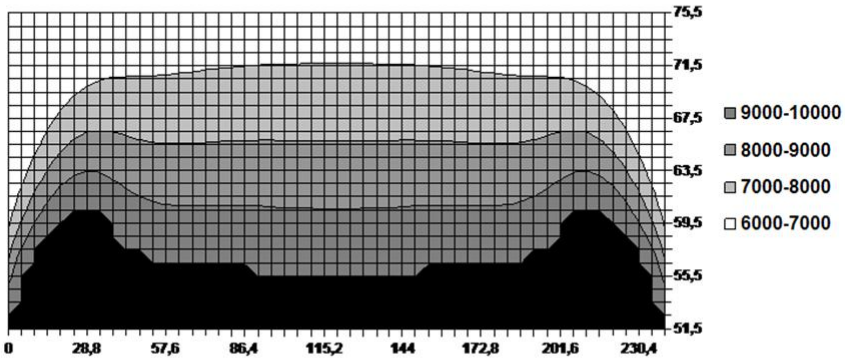

Figure 4.2: Cross-section of the effective medium density in the magnetic liquid above the magnet (which is situated below this figure). The magnetization of the liquid is 7817 A/m. The x and y values are in mm and the colours show the density in kg/m^3.

A field such as that modelled by Eq. (4.2) can be created by a series of alternating magnetic poles in a planar geometry:

$$B_x(x, y, z) = B_0 e^{-2\pi z/w} \sin(2\pi x/w) \tag{4.4}$$

$$B_z(x, y, z) = B_0 e^{-2\pi z/w} \cos(2\pi x/w) \tag{4.5}$$

The MDS separator segregates the feed into layers of different materials, with each material floating at a distance from the magnet corresponding to its density in Eq. (4.3). If two materials of density ρ_1 and ρ_2 need to be separated, the segregation distance is given by:

$$z_1 - z_2 = \frac{w}{2\pi} \ln\left(\frac{\rho_2 - \rho}{\rho_1 - \rho}\right) \tag{4.6}$$

Figure 4.3 shows the principle of the separation.

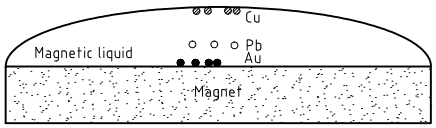

Figure 4.3: Principle of separation of Au (density 19300 kg/m^3), Pb (density 11340 kg/m^3) and Cu (density 8900 kg/m^3).

Because of the simple geometry of the MDS, in contrast with existing magnetic density separators, it is easy to eliminate any iron by using a conveyer belt. The MDS can be easily constructed at an industrial scale, because in the horizontal plane there are no size limitations. Figure 4.4 shows the layout of the prototype separator. A flow of ferro-fluid is passed over a plane magnet, producing a field like that expressed by Eq. (4.2) and an apparent density distribution in the fluid like that expressed by Eq. (4.3). The materials to be separated are fed into the fluid upstream. A conveyor belt between the flow and the magnet serves both to limit the flow in the lateral direction and to collect the materials that are either magnetic or heavy enough to sink to the surface of the belt. The remaining light non-magnetic materials flow with fluid into the light product.

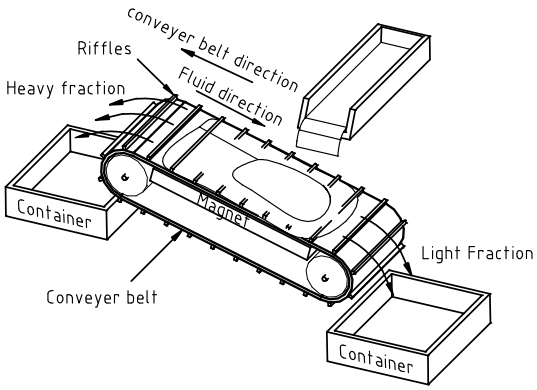

Figure 4.4: The prototype MDS separator.

4.2.2 Precious Metals Levels in Bottom Ash

The wet treatment facility for the separation of BA at the Amsterdam MSWI produces heavy non-ferrous concentrates in three size fractions: 0-2 mm, 2-6 mm and 6-20 mm. Most of the research on precious metals has been done on the 2-6 mm fraction (Bakker et al. 2007b, Bakker et al. 2007a, Muchova et al. 2008).

4.2.2.1 The 0-2 mm Fraction

The 0-2 mm heavy non-ferrous fraction is produced together with steel and coarse sand particles as a result of removing heavy contaminants from the sand fraction. The resulting heavy contaminant stream has a poor non-ferrous grade, but it may be upgraded to a sellable non-ferrous concentrate by removing the steel and coarse sand, e.g. by magnetic separation and tabling. Laboratory tests show that the stream yields about 1.6 kg of 0-2 mm heavy non-ferrous metal per ton of dry BA. Table 4.1 shows the amounts of non-ferrous and precious metals that can be recovered from the stream on the basis of an analysis of a smelt produced from the heavy contaminant in 145 kg of sand.

Preliminary applications of MDS to the 0-2 mm non-ferrous concentrate, intended to further concentrate the precious metals, were not successful, indicating that most of the precious metal is not composed of solid gold-alloys but of material with densities lower than or equal to that of copper. Microprobe analyses on a similar smelt detected significant levels of platinum and palladium, in addition to silver and gold (Table 4.2). The data therefore suggest that the precious metals in the 0-2 mm fraction are derived from electronic equipment. This hypothesis is consistent with the mass balance.

A recent study (Janz and Bilitewski 2007) showed that German household waste contains 1.4 to 2.8% of small items of waste electrical and electronic equipment (WEEE; shavers, hair-dryers, cell phones, etc.). Such levels are consistent with a UK study by Darby (Darby and Obara 2005), who found that UK WEEE accounts for 4% of household waste and that 23% -60% of UK citizens who responded to questionnaires stated that they put small WEEE in household waste. The maximum precious metals content in the 0-2 mm non-ferrous metal fraction resulting from WEEE can be computed as in equation (4.7):

$$X_{\text{precious}} = F_{NF0-2} F_{\text{ash}} F_{\text{WEEE}} F_{\text{PCB}} Y_{\text{precious}} \tag{4.7}$$

Here, Y_{precious} is the concentration of precious metals in the Printed Circuit Boards (PCB's) of small WEEE, which include 110 ppm of gold and 280 ppm of silver (Cui 2005), F_{PCB} is the mass fraction of PCB's in small WEEE (measured by Cui as 3%), F_{WEEE} is the mass fraction of small WEEE in household waste (taken as 1.4 to 2.8%), F_{ash} is the mass ratio of household waste to the resulting dry BA, which is known to be about 3:1 for the Amsterdam incinerator (AEB incinerates waste with about 60% household waste), and F_{NF0-2} is the mass ratio of dry BA to the 0-2 mm non-ferrous metal fraction, which is about 700:1. The resulting equation is:

$$X_{\text{precious}} = (1 \text{ to } 2) Y_{\text{precious}} \tag{4.8}$$

The precious metals concentrations found by XRF analysis in the 0-2 mm HNF were 80 ppm of gold and 1500 ppm of silver (Table 4.2). According to the previous calculation, based on average levels of precious metals found in PCB's of small WEEE, expected levels of gold and silver from WEEE are 100-200 ppm and 300-600 ppm, respectively. In fact, the smelt level for gold is of the expected order of magnitude, whereas the value for silver shows that WEEE is one of the important contributors.

Table 4.1: Amounts of 0-2 mm heavy non-ferrous and precious metals per ton of dry BA that can be recovered from the heavy contaminant stream from the sand cleaning operation.

Metal	g/t of dry BA
Cu	920
Pb	480
Zn	10
Sn	80
Ag	2.4
Au	0.1

4.2.2.2 The 2-6 mm Fraction

The 2-6 mm heavy non-ferrous concentrate contents 20-30% of large pieces of glass and stone, while the rest consists of metals; mainly copper, zinc and lead with traces of iron, tin, silver and gold. The stream contains about 2-3 kg of heavy non-ferrous metal per tonne of dry BA. Two batches of the 2-6 mm heavy non-ferrous concentrate, collectively weighing about 1600 kg, were smelted and the metal product was analysed. The results are shown in Table 4.3. A sample of less than 1 kg of the corresponding fraction from a German incinerator was also smelted and analysed for comparison. Samples of such small sizes do not show a consistent gold content, so only the silver content is presented in Table 4.3. The results suggest that German BA has similar heavy non-ferrous metal contents to Dutch BA.

A 75 kg batch of the 2-6 mm heavy non-ferrous concentrate of AEB BA was separated by MDS at a cut-density of approximately 10000 kg/m^3. The light and heavy products of this separation were each processed further to obtain fractions that could be smelted and analysed. The heavy MDS fraction (6.3 kg) was first separated magnetically to remove the steel (1.05 kg) and then the remaining non-magnetic heavy material was treated with HCl to change the colour of the brass particles from yellow to red. Finally, the non-magnetic heavy fraction was hand-picked to separate the yellow gold-containing alloys from the copper-alloys and the lead and silver. Table 4.4 shows results of the XRF analysis of the gold particles. The alloy compositions show that most of the particles originated from jewellery. In some cases, this was also apparent from the shapes of the particles. A minor amount of gold was present as a thin coating on copper particles (Table 4.4 shows five such particles).

The 19 solid gold particles obtained from the separation were combined with four solid gold particles found in earlier tests of the MDS separation on small samples (each of several kg) of 2-6 mm heavy non-ferrous concentrate. In total, the 23 particles had a gold mass of 5.04 g and represented 68.5 kg of metal from the 2-6 mm heavy non-ferrous concentrate, corresponding to a gold concentration $X_{\text{gold}} = 74$ ppm in the heavy non-ferrous metal content. Since one of the particles in the set of 23 contained almost 1 g of gold and particles containing up to 4 g of gold have been observed in the 2-6 mm fraction, this result has a significant statistical error.

Table 4.2: Results of microprobe spot analyses of 14 selected spots of a smelt of the 0-2 mm heavy non-ferrous concentrate. Values are in percent, by mass. Point-averaged values are indicated in bold.

Pb	Sn	Fe	Ni	Zn	Cu	Sb	Au	Ag	Pt	Pd
0.491	7.349	1.641	0.439	1.121	87.594	1.039		0.092		0.009
99.492		0.026			0.442				0.128	
0.099	3.156	1.407	0.442	1.503	93.893	0.376		0.027		
0.115		88.757	1.317	0.087	8.099		0.049	0.011	0.007	0.014
0.461		85.962	1.364	0.037	8.181		0.072	0.025	0.045	0.042
0.201	3.914	1.084	0.435	1.330	91.713	0.376		0.028		0.017
	4.942	0.604	0.490	1.407	92.660	0.568		0.020		0.022
0.411	4.201	2.195	0.462	1.442	90.880	0.510		0.127		0.032
0.006		87.165	1.573	0.051	7.408		0.061	0.007	0.005	
0.420	5.842	0.676	0.357	1.177	89.803	0.927		0.133		0.011
0.320	5.802	0.702	0.445	1.025	88.183	0.856		0.038		0.027
0.251		85.772	1.375	0.065	8.484		0.077	0.059	0.039	0.284
0.681		8.019		0.183	61.425	0.003		0.029		0.002
0.454		7.828	0.005	0.907	60.980	0.095		0.057		0.040
							0.019	**0.047**	**0.016**	**0.036**

Table 4.3: Composition of 2-6 mm heavy non-ferrous concentrates from BA in 2004.

		Dutch	German
Glass, stone, %		30	
Metal, %		70	
	Cu, %	73	74
	Ag, ppm	3600–3890	3800
	Au, ppm	100–107	
	Pt, ppm	14	

Table 4.4: Composition of the gold-alloy particles in the heavy MDS product.

Weight (g)	Mass% Au	Au (g)	Weight (g)	Mass% Au	Au (g)
0.258	61	0.157	0.887	47	0.417
0.148	51	0.075	0.123	0.68	0.001
0.544	46	0.25	0.157	29	0.045
0.439	24	0.105	0.484	23	0.111
0.435	55	0.239	0.312	31	0.097
0.857	54	0.463	1.415	30	0.424
0.087	40	0.035	0.352	28	0.098
0.12	37	0.044	0.249	40	0.1
0.079	0.32	0	0.268	0.7	0.002
0.103	0.37	0	0.336	41	0.137
0.743	68	0.505	0.178	0.11	0
0.732	41	0.3	0.09	16	0.015
Total			9.4		3.7

According to the sampling theory of Gy, the statistical error is:

$$\sigma_{\text{gold}} = \frac{\sqrt{\sum_i m_i^2}}{\sum_i m_i} X_{\text{gold}} = 21\,\text{ppm} \tag{4.9}$$

In order to reduce this error, the cumulative distribution of the gold mass of the particles was compared to and fitted to the lognormal distribution (Figure 4.5). The maximum deviation of the fit to the data in terms of cumulative probability is 0.07, which is well below the deviation that would be expected from Kolmogorov-Smirnov theory for a true lognormal distribution. According to the best fit, the logarithm of the gold content of the solid gold-alloy particles is normally distributed with a mean value $\mu = -1.926$ and standard deviation $\sigma = 1.077$. Assuming that the gold mass of the solid gold-alloy particles in BA is indeed distributed in this manner, the gold mass of N of these particles is expected to be:

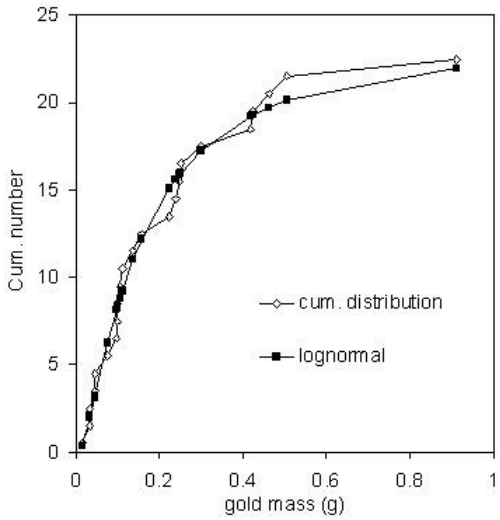

Figure 4.5: Cumulative distribution of the gold mass of the 23 pieces of gold-alloy that were found in 68.5 kg of heavy non-ferrous metal from the 2-6 mm heavy non-ferrous concentrate.

$$M_{\text{gold}} = \frac{N}{\sqrt{2\pi}\sigma} \int_0^\infty m e^{(\log(m)-\mu)^2/2\sigma^2} d\log(m) = N e^{\mu+\sigma^2/2} = N.26g \tag{4.10}$$

$$\mu = -1.926 \tag{4.11}$$

$$\sigma = 1.077 \tag{4.12}$$

or 0.26 g of gold per solid gold-alloy particle. A further small correction is required because the tails of the distribution extend into the 0-2 mm fraction for the small gold masses and into the 6-20 mm fraction for large gold masses. If we assume that the cut-point of the 2 mm screen is at 80% for the 2 mm particles, gold-alloy particles containing less than about 15 mg of gold should be missing from the 2-6 mm dataset presented in Table 4.4 and Figure 4.5. At the same time, particles with about 2 g of gold have been found in both the 2-6 mm and 6-20 mm fractions, indicating that this is roughly the cut-point of the 6 mm screen at the upper side of the distribution. Thus, together, the missing tails represent less than 3% of the particles, much less than the maximum deviation of the data from the lognormal fit that is due to randomness. Therefore, the missing tails of the 2-6 mm data set should not significantly affect the parameters of the lognormal fit. However the expected gold mass of a 2-6 mm particle may be significantly lower due to the finite particle size range:

$$\begin{aligned} M_{\text{gold}} &= N \int_{15mg}^{2000mg} m e^{-(\log(m)-\mu)^2/2\sigma^2} d\log(m) / \int_{15mg}^{2000mg} e^{-(\log(m)-\mu)^2/2\sigma^2} d\log(m) \\ &\approx N.24g \end{aligned} \tag{4.13}$$

The best guess for the solid gold-alloy content of 68.5 kg of 2-6 mm non-ferrous metal is then:

$$M_{\text{gold}} = N.24g \pm \sqrt{N}.24g = 5.6g \pm 1.2g \tag{4.14}$$

Hence, the concentration in the metal of the 2-6 mm non-ferrous concentrate is 82±17 ppm. This concentration is not entirely in agreement with the concentration measured in 2004 (Table 4.3) due to the changes of screen openings. Therefore, in 2004 more finer particles containing golden particles ended up in the 2-6 mm fraction. An upper threshold of 2 g of gold for the 2-6 mm fraction implies that about 8% of the gold in the form of solid gold-alloy particles ends up in the 6-20 mm fraction at the AEB wet treatment plant.

The results of the overall analysis of the light and heavy MDS products are summarized in Table 4.5. The recovery of the various non-magnetic materials in the heavy MDS product consistently increases with the material density, as expected.

Table 4.5: Summary of the overall analysis of the light and heavy MDS products.

	2-6 mm HNF	Light MDS		Heavy MDS	
	grade %	grade %	recovery %	grade %	recovery %
Glass, Stone	22.2	24.1	100	1.3	0
Iron	2.5	1	36	19.5	64
Zinc	20.2	21.3	96	8.7	4
Copper	43.3	44.2	94	33.1	6
Silver	0.21	0.2	86	0.364	14
Lead	7.8	6.3	74	24.5	26
Gold	0.006	0.001	12	0.058	88
Total	**96.2**[1]	**97.1**[1]	**91.7**	**87.51**[1]	**8.3**

[1] the missing mass (up to 100%) is for the elements present in small proportions (% by mass), e.g. aluminium, tin, etc.

Nevertheless, the recovery of silver and lead was less than satisfactory. This indicates that the cut-density applied in the experiment was slightly too high. Analysis of the relationship between material recovery and material density shows that lowering the cut-point by about 800 kg/m^3, would increase recoveries of silver and lead to about 26% and 45%, respectively, at the expense of losing 10% of the copper to the heavy MDS product. The measured grade and recovery values for the density of approximately 10000 kg/m^3 and 11000 kg/m^3 are shown in Figure 4.6.

The recovery value for gold in Table 4.5 was calculated on the basis of the gold mass of the 24 recovered pieces shown in Table 4.2 and the known gold content of the large smelts (Table 4.1). However, sampling theory shows that the limited sample mass of the MDS experiment results in an uncertainty of about 18% in the gold recovery value.

In addition to the precious metals 11 small diamonds were found in the 2-6 mm fraction, which probably came from the jewellery. However, the source and concentration of diamonds in bottom ash must be further investigated.

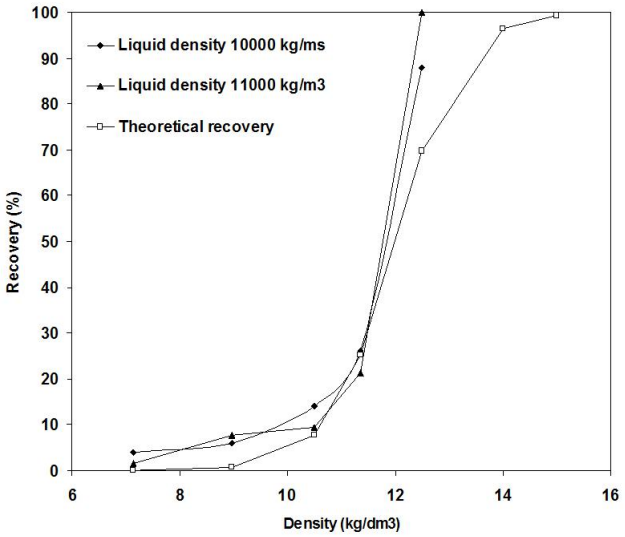

Figure 4.6: Recovery curves based on the density of metals from two experimental measurements and the theoretical recovery curve.

4.2.2.3 The 6-20 mm Fraction

The 6-20 mm non-ferrous concentrate contains both light alloys (aluminium) and heavy non-ferrous metals. About 5-6 kg of 6-20 mm non-ferrous metal can be produced per tonne of dry ash from Amsterdam BA, of which 2.9 kg consists of light alloys and 2 kg heavy alloys, excluding 0.1 kg of stainless steel. The best fit to the distribution of solid gold alloys presented above suggests that 8% of the solid gold-alloy mass is present in the 6-20 mm fraction. This corresponds to a gold content in the heavy non-ferrous alloys of 16 ppm. Since the solid gold alloy particles typically weigh 4 g, 1 tonne of heavy non-ferrous alloys of the 6-20 mm fraction typically contains only four of these particles. For this reason, only the silver content of the 6-20 mm fraction was assessed (Table 2.4). The silver content was found to be 0.1% of the 6-20 non-ferrous metal fraction. However, half of the mass was found in just one particle; the rest was found in smelt (see Table 2.4).

4.2.3 Economic Analysis

This analysis focuses on the 2-6 mm HNF fraction, for which two economic options were compared (Muchova et al. 2008). One option was to sell the original 2-6 mm HNF fraction to a precious metals smelter. A precious metals smelter pays for the gold (minimum 5 g of Au in 1 tonne), silver (minimum 100 g of Ag in 1 tonne) and the copper content. Table 4.6 shows the estimated price for one tonne of 2-6 mm HNF fraction when it is sold to a precious metals smelter without magnetic density separation. The smelter pays €2108 after charges and penalties. The metals prices are averages based on LME values in the second half of 2007, when prices of copper, gold and silver were €4000 per tonne, €15800 per kg and €300 per kg, respectively.

Table 4.6: Overview of values of metals in one tonne of the 2-6 mm non-ferrous fraction without further separation (sold to a precious metals smelter).

Revenue/costs	€/t
Treatment charge	-650
Silver	577
Gold	829
Copper	1715
Other charges and penalties	-363
Net revenue 2108	

The second option is to separate the fraction into three products: a stone-glass fraction, a copper-zinc concentrate for the copper or brass smelter and a precious metals concentrate for the precious metals smelter (Table 4.7). The copper-zinc concentrate can be sold to either a brass smelter or a copper smelter. Therefore, a copper smelter in Germany and a brass smelter in the Netherlands were contacted to bid for the light product. The copper smelter pays for the copper content, and the offered price for one tonne of the 2-6 mm copper-zinc fraction was between €455-637. Selling to the copper smelter was not considered an attractive option due to the low price offered. The brass smelter uses a different pricing strategy, based on current market prices for their metals of interest and the market situation for their final product. The prices offered by the brass smelter were between 80-96% of the LME value, including charges and penalties. The value for the fraction shown in Table 4.7 is between €1806-2167, assuming that the light 2-6 mm fraction has a 25% content. According to LME prices at the time of writing, the estimated price of the 2-6 mm fraction separated by MDS will be between €2357 to 2686 per tonne if sold to a precious metals smelter and a brass smelter.

The cost of the MDS process is calculated on the basis of an installation for a large incinerator (e.g. the Amsterdam incinerator) that produces 300 kilotonnes of BA, or about 1500 tonnes of the 2-6 mm HNF fraction per year. The cost of the process is a combination of investment costs (estimated at €67 per tonne) and operating costs (€123 per tonne).

The complete price revenue accrued from the whole wet physical separation process in Pilot plant II, including the MDS step is shown in Chapter 7. The profit accruing from the pilot plant without the MDS is approximately €6 per tonne and with the MDS €8 per tonne of BA. Hence, the MDS step increases the value of BA by approximately €2 per tonne.

4.2.4 Conclusion

Two HNF fractions (0-2 mm and 2-6 mm HNF) from Amsterdam BA were analyzed for their precious metals content. The source of the 0-2 mm precious metals is probably WEEE. The separation of this fine fraction is technically demanding and requires further research. The source of the gold in the 2-6 mm HNF fraction is jewellery. The statistical analysis of the gold particle masses shows that the cut size of 6 mm is optimal; only 8% of gold from the jewellery will be found in the >6 mm fraction. The experiment in which the 2-6 mm HNF

Table 4.7: Economic overview of the separation by MDS resulting in heavy and light fractions (selling the heavy fraction to a precious metals smelter and the light fraction to a brass smelter) according to the mass balance in Table 4.5

	LME (€/kg)	Other costs (€/t)	Heavy fraction (€)	Light fraction paid by brass smelter (€)
Treatment charge			-650	
Silver	292		1001	
Gold	15860		8743	
Copper	4		1311	
Zinc	2.3			
Other charges and penalties			-376	
Investment cost		-67		
Process costs		-123		
Net revenue per tonne			10029	1806-2167
Net revenue per fraction in ratio 9% x 91%			903	1644-1973
Net revenue total		-190	903	1644-1973

fraction was separated using the MDS system shows that 88% of the gold can be recovered in a precious metals concentrate, while 94% of the copper can be recovered in the copper-zinc fraction. The recovery of silver and lead from the precious metals fraction should be improved by lowering the density of the magnetic fluid. By adjusting the MDS settings the recovery of silver and lead in the precious metals fraction will increase. New technology based on magneto-hydrostatic separation is suitable, from an economic perspective, for recovering precious metals from the >2 mm HNF fraction of MSWI BA. The separation system is simple and cheap. An economic analysis was performed for a large incinerator producing about 1500 tonnes of this fraction per year, but the additional value of precious metals like platinum and palladium was excluded from the calculation. The MDS separates the fraction into a copper-zinc concentrate for the brass smelter and a precious metals concentrate for the precious metals smelter. The estimated price of the 2-6 mm HNF fraction increased from €2108 per tonne without the MDS to €2415-2735 per tonne with the MDS. Hence, use of the MDS and separating precious metals increased the value of MSWI BA by €2 per tonne.

4.3 Metallic Aluminium in the Sand Product

The presence of metallic aluminium in the sand product complicates its utilization as a building product (lime-sand stone). However, destroying the aluminium by allowing oxidization is not an attractive solution due to the high economic and environmental value of aluminium. Therefore other solutions were investigated. At first, several experiments were performed to measure the

mass of aluminium and elucidate the behaviour of metallic aluminium and its reactions (oxidation of aluminium in ambient conditions, kinetics of oxidization and their dependence on pH, etc.) (Muchova and Rem 2007b).

4.3.1 Materials and Methods

The sand product separated by wet physical methods from Amsterdam BA was used in all these experiments. The treated BA originated from incineration one day before being processed in the pilot installation (by wet physical separation). The separation removed ferrous and non-ferrous metals from the sand by gravity separation. The composition of the resulting sand (mainly silica and calcium, in addition to OH and CO_3 ions) was comparable to that of natural sand, aside from the aluminium content. The sand was at most two days old before it was dried in the laboratory oven at 110 °C for 5 hours. This sand was then split and used for the experiment.

In the laboratory, the metallic aluminium content in the sand fraction can be measured by the amount of hydrogen generated by the reaction of aluminium with acids or bases. Alkali environments were used in the experiments instead of acidic environments. One of the reasons for this is that the sand (after reaction with the base) will be used for building applications, and for civil engineering applications a basic environment is required. Another practical reason is that acid will liberate a mixture of CO_2 and H_2, whereas reaction with a base produces very pure H_2. Sodium hydroxide consumed in the hydrogen-generating reaction (4.16) is regenerated in reaction (4.17) and the overall process is reaction (4.15). Thus aluminium and water are the only raw materials consumed to produce hydrogen (Soler et al. 2007, Belitskus 1970).

$$2Al + 6H_2O \rightarrow 2Al(OH)_3 + 3H_2 \tag{4.15}$$

$$2Al + 6H_2O + 2NaOH \rightarrow 2NaAl(OH)_4 + 3H_2 \tag{4.16}$$

$$NaAl(OH)_4 \rightarrow NaOH + Al(OH)_3 \tag{4.17}$$

4.3.2 Experimental Procedures and Results

The sand product was characterized using five different tests:

- measuring the aluminium content and hydrogen production in the sand
- measuring the grain size distribution of the metallic aluminium in the sand
- measuring the reaction kinetics in ambient conditions
- determining kinetics of hydrogen production as a function of temperature and stirring
- determining kinetics of hydrogen products as a function of pH.

4.3.2.1 Measuring the Aluminium Content and Hydrogen Production

The aluminium content in the sand from BA was measured using a specially constructed set-up (Figure 2.4). The aim was react a NaOH solution and metallic aluminium, collect the hydrogen gas thereby created, and measure it. Several

experimental mixtures were monitored and the gas (hydrogen) generated was analyzed by a CP 9000 gas chromatograph. The results show that the gas consisted almost entirely (99%) of hydrogen gas, with a minor amount of water vapour. The aluminium content was calculated retrospectively from the volume of hydrogen generated. The average metallic aluminium content measured in the experiment was 1.9±0.2%. The composition of the sand product was also analysed by microprobe resulting in the same aluminium content which shows the result measured according to Procedure 1 (Figure 4.7).

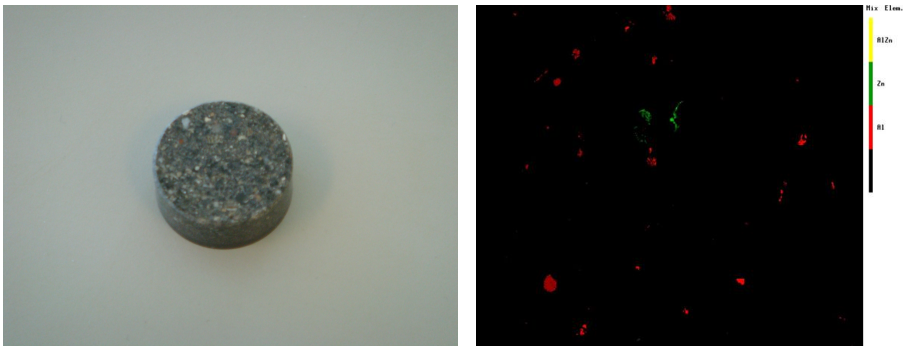

(a) A sample of sand product. **(b)** Microprobe result.

Figure 4.7: A sample of sand product (a) and the image analysed by a microprobe (b) recognizing metallic aluminium particles (red).

4.3.2.2 Grain Size Distribution of Metallic Aluminium in the Sand Product

The sand product was first investigated by grain size distribution to determine if certain portions of the fraction have a significant content of metallic aluminium. The results of screening two sand products, one collected in January 2007 and the second in April 2007, are shown in Table 4.8. The differences in aluminium content between the material collected in January 2007 and April 2007 were due to differences in the age of the bottom ash and delay in analyses.

These findings show that the aluminium in the sand is not concentrated in any particular size fraction, but is distributed throughout the entire sample.

4.3.2.3 Measuring the Aluminium Kinetics at Ambient Conditions

Previous tests were repeated on sand that had been stored for varying times at ambient conditions. The material used in the experiment was wet sand that had been stored in a closed bucket. After different time periods a sample of the sand was collected from the bucket, dried and its aluminium content was measured. The sand produced by wet separation was found to have a moisture content of 30% and pH of 10.3. The experimental set-up was the same as in the previous experiment (Figure 2.4). The amounts of hydrogen collected from the different samples (taken at different moments) reflect the degree of oxidation.

Figure 4.8 shows that the natural oxidation of aluminium at pH 10.3 and 20 °C is very slow; the aluminium content decreased from 2.3% to 1.5% over

Table 4.8: Grain size distribution and metallic aluminium content in each indicated size fraction in the sand product. The sand was previously separated by jigging in Pilot plant II in Amsterdam and collected in January and April 2007.

	January 2007			April 2007		
Size	Mass (g)	Mass (%)	Al (%)	Mass (g)	Mass (%)	Al (%)
<100μm	12.2	1.2%	0.5%	8.5	0.8%	0.2%
100μm−200μm	66.4	6.3%	1.2%	84.2	7.9%	0.8%
200μm-500μm	321.4	30.7%	1.5%	279.2	26.2%	0.6%
500μm-1 mm	269.8	25.7%	1.6%	283.7	26.6%	0.6%
1 mm-2 mm	303.2	28.9%	2.2%	353.8	33.2%	1.4%
> 2 mm	75.6	7.2%	0.4%	57.1	5.4%	1.3%
Total	1048.6	100.0%	1.6%	1066.5	100.0%	0.9%

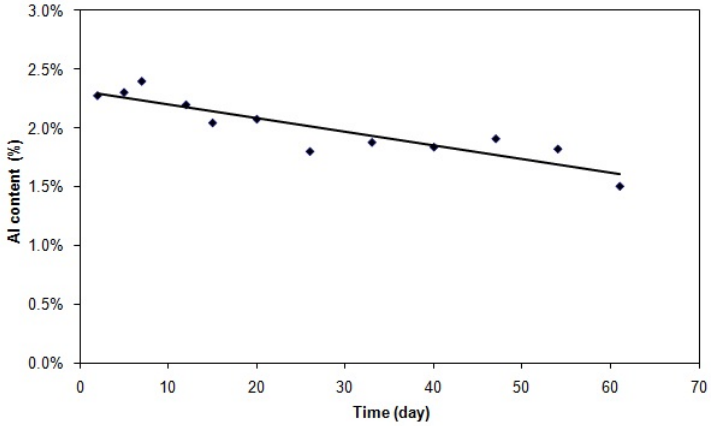

Figure 4.8: Aluminium oxidization time versus aluminium content.

60 days. A similar experiment performed by Ishii (Ishii et al. 2007) showed that the loss of metallic aluminium does not strongly depend on pH, but it is very sensitive to temperature.

4.3.2.4 Kinetics of Hydrogen Production as a Function of Temperature and Stirring

From an economic perspective, the oxidation of aluminium and the production of hydrogen should occur rapidly enough to decrease the delay before selling the sand, and avoid substantial hydrogen losses. The experiment used the same set up as in the previous experiment. In an attempt to identify appropriate conditions to achieve these goals, sand was subjected to four treatments (using the same experimental set-up as in the previous experiment), with different temperatures, with and without stirring by a laboratory magnet. In each case the solution was kept at pH 13. One sample was neither heated (22 °C) nor stirred by a magnet. A second sample was also not heated, but was stirred during the whole testing period. A third sample was heated to 40 °C and stirred, while a fourth sample was heated to 55 °C and stirred. In each case the hydrogen generated was monitored as a function of time. Results are shown in Figure 4.9.

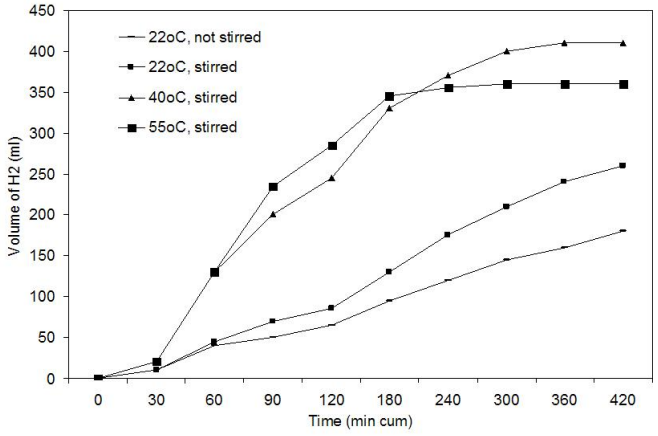

Figure 4.9: Kinetics of hydrogen production as a function of temperature and stirring.

The result of the experiment shows that the temperature has an important influence on the kinetics of hydrogen generated from aluminium. However, the change of temperature from 40 °C to 55 °C did not show a major difference; therefore it is economically better to use the lower temperature. In addition, stirring the sample had a significant effect, increasing the rate of the reaction and thus the rapidity of aluminium oxidation.

4.3.2.5 Kinetics of Hydrogen Generation from Aluminium as a Function of pH

The optimal pH of the NaOH-containing incubation medium for hydrogen production was investigated in this experiment. It should be noted that the pH should not exceed 13 otherwise the leaching of certain elements may also increase. If the sand is to be used for building applications in the future, it is required that the leaching is below certain limits.

The same set-up was used as in the previous experiment, except that the pH of the sodium hydroxide solution was varied for each sample. The results are shown in Figure 4.10. The sample used for this experiment was very small, therefore there was substantial uncertainty regarding the aluminium content (standard deviation ±0.2%). The reaction rate increased with increasing pH. The temperature was 55 °C during the experiments and each sample was stirred throughout the whole experimental period.

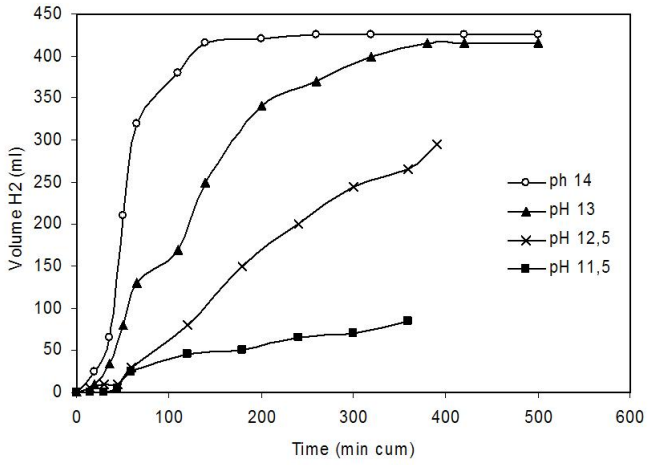

Figure 4.10: Kinetics of hydrogen production as a function of pH.

4.3.3 Utilization Options

The findings outlined above indicate that there are several options for utilizing the sand:

- Leaving it for a long period (3-4 months) and allowing the aluminium to oxidize in ambient conditions. Then the sand can be utilized in lime-sand stone, cement, etc.
- Increasing the oxidation of aluminium by adding base (pH 13) and allowing it to react for 250 minutes at 40 °C. The reaction can be accelerated by increasing the temperature of the solution. The sand after the reaction can be utilized for building applications (lime-sand stone, cement).

- In the third option the oxidation of the sand can be combined with collecting the hydrogen generated during the reaction. Therefore, the sand can be used for building applications and the hydrogen generated from the aluminium can be used for internal company uses (e.g. as fuel for trucks collecting waste in the city).
- Using the sand product as a substitute material for making aerated autoclave concrete (AAC), which is made from a mixture of sand, cement, lime and aluminium powder. The aluminium powder is an expensive additive, therefore using the sand mixture which already contains metallic aluminium particles can be economically attractive.

The last option for the utilization of sand has the highest environmental and economic potential.

Sand for Aerated Autoclave Concrete
The sand from BA containing metallic aluminium shows similar characteristics to that of the standard sand used for making AAC. Two fractions (Table 4.8), 100-200 μm and 200-500 μm , were analysed by XRF and the results show that its contents include 30-34% of SiO_2, 15-19% of $CaCO_3$, 7-8% of Al_2O_3, 6-7% of Fe_2O_3, 2-2.5% of $MgCO_3$ and the rest consists of small percentages (by mass) of Na_2CO_3, K_2CO_3, MnO, TiO. The metallic aluminium content in each size fraction was also analysed by Procedure 1 (Chapter 2) and the results are shown in Table 4.8. Each size fraction contained metallic aluminium particles at contents ranging between 0.2 and 2.2%. The total sand contained between 0.9-2% of metallic aluminium. Standard AAC is characterised by the NEN standard (NEN7714 2000) and should meet required limits for strength, density, dimensional accuracy, etc. The main components are hydraulic binders (cement or lime), siliceous material (sand), cell-generating material (Al) and water. The proportion of metallic powder is approximately 0.057%, depending on the AAC type. Water should be present in a ratio of 1:2 (water to solid). The main factor influencing the quality and cell-creating factors is the grain size distribution for all components. Regular producers of AAC in the Netherlands use sand with a grain size of approximately 100 μm and aluminium powder of max. 60 μm. This fine grain size distribution is essential for rapid aluminium expansion. The optimal expansion is approximately 460 ml/min. The sand from BA containing metallic aluminium is too coarse for optimal expansion and thus should be milled to below 100 μm.

Two sand fractions were sent to a producer of AAC in the Netherlands and a producer of aluminium powder in Sweden. Both of these companies showed interest only in the pure aluminium powder with a minimum purity of 90%. They showed no interest in the sand because they have traditionally employed a system in which the pure components are mixed in specific ratios. However, the mixture has high financial and environmental potential, since it is cheaper than natural concrete additives (sand and aluminium powder).

4.3.4 Economic Analyses

From an environmental perspective, BA sand conversion into AAC is very promising. Through this process, the Netherlands could save 6.6 ktonnes of metallic aluminium, corresponding to €14.5 mil. per year. The Amsterdam

(AEB) incinerator is producing 300000 tonne/year of BA, corresponding to 90000 tonne/year of sand product. If the sand contains approximately 1% of metallic aluminium and the current price of aluminium scrap is €2200 per tonne then AEB could save €2 mil per year.

Examples of original AAC components and prices are shown in Table 4.9. These are the average prices for the Dutch AAC producer, the most valuable component being aluminium powder (€5000 per tonne). In order to produce 6.18 m^3 (equivalent to 3350 kg of moulded material), 2 kg of aluminium powder is needed. This corresponds to 0.057% aluminium in the mixture. The composition of other components is shown in Table 4.9, where the missing 18.4% of material is the reused AAC material, which results from cutting. Because of the reaction of water and lime the amount will increase by ± 150 kg extra. The price for standard AAC is approximately €22.4 (Table 4.9). AAC can also be made from BA sand and, as shown in Table 4.10, when 4.6% of original sand is replaced by BA sand (with an aluminium content of 1%), it will provide the desired 0.057% metallic aluminium content for one tonne of sand, and the value of the BA sand can then reach €67 per tonne.

Table 4.9: Composition and prices of components for regular AAC in 2007.

	Mass (%)	€/t	€/t regular AAC
Cement	10.0%	75	7.5
Lime	8.5%	90	7.7
Sand	61.0%	6	3.7
Gypsum	2.0%	35	0.7
Aluminium	0.057%	5000	2.9
Total	81.6%		22.4

Table 4.10: Composition and prices of original components including a competitive price for the BA sand with 1% aluminium content for producing AAC with the same metallic aluminium content as regular AAC.

	Mass (%)	€/t	€/t BA AAC
Cement	10.0%	75	7.5
Lime	8.5%	90	7.7
Gypsum	2.0%	35	0.7
Sand	56.4%	6	3.4
BA sand (Al 0.057%)	4.6%	67	3.1
Total	81.6%		22.4

However, the optimal ratio of BA sand for AAC is still under investigation. The price of €67 per tonne of BA sand is probably optimistic because of the lower expansion parameters of metallic aluminium in BA sand. Therefore, an alternative (worst case) economic scenario is shown in Table 4.11. Under this scenario only 50% of the aluminium in BA is active and the price may then be approximately €13 per tonne.

Table 4.11: Masses and prices of original components, and value of ACC made using BA sand with 1% aluminium content to produce ACC with a final 0.5% metallic aluminium content.

	Mass (%)	€/t	€/t BA AAC
Cement	10.0%	75	7.5
Lime	8.5%	90	7.7
Gypsum	2.0%	35	0.7
Sand	20.3%	6	1.2
BA sand (Al 0.5%)	40.8%	13	5.3
Total	81.6%		22.4

The AAC market is large in the Netherlands, the biggest producer of AAC makes approximately 240000 m^3/year, and 50 other factories in other EU countries also make AAC products. Therefore, sand from BA after milling may be a good alternative for replacing the traditional mixture of regular sand and metallic aluminium powder.

4.3.5 Conclusion

The sand separated from BA has 1-2% metallic aluminium contents, which are currently lost from the aluminium cycle. This metallic aluminium is very difficult to separate from the sand, due to the similarities of its size distribution and particle density. Another problem is the oxidizing properties of aluminium if the sand is to be used as a building product (lime-sand stone, cement). Therefore, several options for utilizing this BA sand containing metallic aluminium were investigated.

The first option is to let the aluminium oxidize under ambient conditions. The aluminium is then lost and the sand can be reused for building applications. This solution takes time because the aluminium will naturally oxidize in >3 months. Furthermore, the loss of aluminium has a negative environmental and economic impact. The second option is to add base (NaOH) to increase the rate of oxidation, which allows the sand to be used, while the aluminium is lost, as in the first option. The oxidizing reaction will be much faster (300 min) but the environmental and economic issues still remain. The third option is to let the aluminium oxidize by adding base and at the same time collecting the hydrogen generated during the process. The hydrogen can then be used for internal applications (as fuels for tracks operated by AEB). This solution is environmentally friendlier and economically more attractive; however it poses practical challenges (safety, and the need to build a reactor). The last option is to use the BA sand containing the metallic aluminium particles in the manufacture of AAC. This option has environmental as well as financial benefits. For example, if there is 1% of aluminium in 90000 tonnes of sand (annual production at AEB), the hydrogen is worth about euro 150000 while the (secondary) aluminium is worth approximately €2 mil per year. Hence, it would be most profitable to use both the sand and the aluminium as materials for building applications.

Regular AAC contains approximately 0.057% of expensive aluminium pow-

der (€5 per kg), which can be replaced by BA sand. BA sand has similar characteristics to those of natural sand and contains approximately 1% of metallic aluminium. This fraction should be milled, resulting in an optimal replacement for sand and aluminium powder. This solution has high environmental and financial benefits, because the aluminium in the sand will be reused while the fraction can be sold as a high-price sand product containing aluminium. The BA sand can replace approximately 4.6% of the mass in regular AAC, thus up to €67 per tonne profit can be acquired. This is more attractive option than the first three options discussed, in which the aluminium is fully oxidized, leaving the sand with a value of €6 per tonne. The economic analyses of wet physical separation, including utilization options for sand product, are explained in Chapter 7.

4.4 Stainless Steel Separation from the 6-20 mm Aggregate Fraction

The 6-20 mm aggregate fraction (granulate fraction) contains approximately 0.3% of stainless steel. The stainless steel particles are difficult to separate by the wet physical separation systems (ECS, magnetic separation) used in the pilot plant in Amsterdam. The aggregate should be used as a building material, but the content of stainless steel particles, which are usually long, complicates the quality requirements for building products. The second issue is the high price of stainless steel, which can be recycled as a secondary metal product.

Therefore, a new machine for stainless steel separation (SSS) was developed and its ability to remove the stainless steel particles from the aggregate fraction was tested. Two laboratory experiments were performed and a new industrial SSS with a capacity of 10 t/h was built.

4.4.1 Principle of the Stainless Steel Separator

The SSS is composed of a cylindrical steel plate surrounded by an outer cylinder of wire screen with 22 mm openings (Figure 4.11). The whole cylinder rotates at an inclination of 25^o from horizontal. The 6-20 mm fraction is fed into the top of the device and is separated into long and spherical particles. Relatively spherical particles fall through holes in the screen between the two cylinders and are removed in the axial direction, down (fraction 1) while long particles fall over the screen and are removed on the other side (fraction 2), or are caught in the screen and are propelled by the rotating movement to the other side (fraction 3), or are stuck in the screen (fraction 4).

4.4.2 Experimental Measurements and Results

Two experiments were performed using a cylinder 53 cm wide and 78 cm long, with a rotating capacity of 10 t/h and screen opening of 18 mm (instead of 22 mm). In experiment 1, the feed was 214 kg of the 6-20 mm fraction, which was separated into four fractions. Fraction one was the aggregate product, while fractions 2, 3 and 4 were the stainless steel concentrate collected from three different positions after separation (Figure 4.11). The amounts of stainless

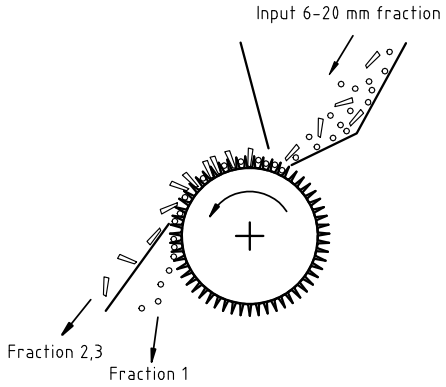

Figure 4.11: Operating principle of the stainless steel separator (SSS) for 6-20 mm aggregate.

steel and aggregate obtained in experiment 1 are shown in Table 4.12, and the recoveries in Table 4.13.

Table 4.12: Experiment 1; stainless steel separation by laboratory SSS with an input of 214 kg of 6-20 mm fraction in kg.

Experiment 1	Stainless steel (kg)	Aggregate (kg)
Fraction 1	0.35[1]	200
Fraction 2	0.145	13
Fraction 3 and 4	0.045	n.m.

n.m. not measured

[1] max. particle length 70 mm

The second experiment was performed with selected particles; in total 0.7 kg of long stainless steel particles were fed through the SSS (experiment 2). The results of this experiment are shown in Table 4.14.

The results of experiment 2 show 90% recovery of long stainless steel particles.

The 6-20 mm aggregate fraction contains long wooden particles and plastic particles as well as long particles of stainless steel. Therefore, during experiment 1 all long particles (of stainless steel, wood and plastic) were collected from the 6-20 mm fraction. The total recovery of all long particles in the 6-20 mm fraction is shown in Table 4.15.

Based on the laboratory results it was decided to build an industrial SSS containing a 2.5 m long cylinder with a 1 m diameter, an effective free surface of at least 0.4 m^2, and a rotating frequency of one turn per 3-6 seconds. The top of the cylinder contains large numbers of conical cups with a depth of 28 mm and an internal diameter 32-40 mm (Figure 4.12).

Table 4.13: Experiment 1; recoveries from stainless steel separation by the laboratory SSS with an input of 214 kg of 6-20 mm fraction in %.

Experiment 1	Stainless steel (%)	Aggregate (%)
Fraction 1	65%	94%
Fraction 2,3 and 4	35%	6%

Table 4.14: Experiment 2; recoveries of stainless steel from the laboratory SSS from an input of long stainless steel particles.

Experiment 2	Stainless steel (kg)	Stainless steel particles (amount)
Fraction 1	0.07[1]	7
Fraction 2	0.45	15
Fraction 3	0.135	6
Fraction 4	0.04	3

[1] max. particle length 50 mm

Table 4.15: Recovery (%) of all long particles and aggregate by the laboratory SSS.

	Long particles (stainless steel and wood) (%)	Aggregate (%)
Stainless steel concentrate	80%	2%
Aggregate	20%	98%

Figure 4.12: The SSS used in the Pilot II.

4.4.3 Conclusion

The laboratory results showed that the SSS can separate the 6-20 mm aggregate fraction with a capacity of 10 tonnes/hour, providing 80-90% recovery of particles longer than 50 mm and stone recovery between 94-96%. These results are satisfactory because they show that the SSS can reduce contents of stainless steel particles to below 0.1% in the aggregate fraction and at the same time remove long wooden particles, which also have a negative influence on the quality of building products. However, these measurements were performed solely in the laboratory, thus the industrial SSS must still be implemented and optimized in the field.

Chapter 5

Leaching of Bottom Ash Products

Summary

The value of high-end building materials produced from municipal solid waste incinerator (MSWI) bottom ash (BA) depends critically on its environmental quality, in particular on its emission values to the soil. Many EU countries have strict leaching limits and standard testing requirements for such materials. Leaching of bottom ash processed in a conventional dry manner often highly exceeds these leaching values, mainly for Cu, Mo, Sb, Pb, Cr, Cl, Br and SO_4. New wet physical separation techniques provide solutions for improving the quality of the final building products from BA by decreasing their leaching values (Chapter 1). This treatment is able to decrease leaching values to near or below the required limits in order to produce building materials from BA of a category where no extra isolation is needed. However, some elements (Cu, Mo, Sb, SO_4 and Cl) tend to exceed the required limits even after wet separation. Therefore the aim of the research reported here was to characterize the main factors that influence the leaching values by varying the separation settings of process equipment (splitter position, rotor speed, etc.), the composition of the final products (organic content, metals content, etc.) and composition of the input waste to the incinerator (sewage sludge). Furthermore, during this research another problem arose which conflicted with the industrial production of building materials. In order to maintain good quality control of building products from BA it is necessary to have an accurate and quick quality prediction system. Therefore, a further objective of this research was to develop a technique for predicting the final leachate values of the column test in a short period, 5 days, instead of the traditional 21 days. A prediction model was designed for high-end building products separated from raw BA by wet physical separation. Therefore this research shows that testing procedures for industrial practice can be accelerated significantly. The model is the first step towards quickly providing a prediction of environmental quality according to the column test.

5.1 Introduction

In many EU countries there are requirements to measure the leaching value of materials that will be used for building purposes. In the Netherlands the leaching values must be tested according to the SQD (Chapter 1), which stipulates that a column test must be used to measure the leaching values. The SQD (SQD 2007) introduced two limits for granulate materials: the 'Granulate construction materials limit' and 'IBC limits' (Chapter 1). The aim of the research presented here was to decrease the BA leaching values by using wet separation treatment to below the 'Granulate construction materials limit', allowing this material to be utilized without any isolation according to the SQD.

The leaching behaviour of samples of all the building material products was tested throughout the development of the technology to check whether the materials complied with the limits stipulated in the SQD. Table 5.1 shows the results of the leaching tests in 2004 and 2005 (averaged) and 2006 against the 'Granulate construction materials limit' and 'IBC limits' defined in this regulation applicable from 2008. All products proved to comply with the IBC limits; this means that they can be applied with certain restrictions. However, the leaching of SO_4 for fine aggregate and Cl for coarse aggregate remains above the 'Granulate construction materials limits' (Table 5.1). This is mainly due to the high concentrations of these components in the plant process water. The leaching values for antimony and copper are slightly above the limits.

The leaching results obtained in 2005 after wet physical separation resulted in very positive improvements. However, leaching values for some of the components still exceeded the limits. Therefore, experiments were conducted in which the input material (extra sewage sludge), separation settings (deep organic separation, deep metals separation by changing splitter position or rotor speed, etc.) and the quality of final materials (amount of fines, organic content, pH, conductivity, etc.) were tested. Two series of tests were performed: one in the laboratory pilot installation (mini-pilot plant) and corresponding tests in Pilot plant II in Amsterdam, where the quality of process water was also measured and correlated with the previously mentioned changes. The small laboratory tests gave indications of the quality improvement that wet separation affords, and the tests in Pilot plant II corroborated these results, and identified more correlating factors.

The column test is the most accurate for determining leaching behaviour, but unfortunately it is also expensive and slow. Therefore, an objective of this research was to predict column test leaching values on the basis of results at low L/S (liquid to solid ratios) and the specific leaching behaviour of the elements Cu, Sb, Mo, SO_4 and Cl. This system was intended to predict the leaching of those elements in a very short period (one week). The model can be adjusted and used for soil cleansing streams and other building streams that must meet similar environmental quality regulations.

Another experiment presented in this chapter was intended to identify correlations between results of the column test and the shaking test for leaching values of Cu, Mo, Sb, SO_4, Cl. The Dutch legislation (SQD) requires measurement of the quality values of building materials by the column test. Since the column test is time-consuming and expensive compared to the batch test (shaking test), which is fast but less comparable to natural leaching behaviour, finding a correlation of values between the shaking test and the column tests could save

Table 5.1: Leaching values of Amsterdam BA after dry separation (long-term averages) and the building material products obtained from the Amsterdam pilot plant, and SQD 'Granulate construction materials' and 'IBC' limits (Chapter 1).

Leachate	Bottom ash 2004 and 2005	Sand product 2004 and 2005	Sand product 2006	Fine aggregate 2004 and 2005	Fine aggregate 2006	Coarse aggregate 2004 and 2005	Coarse aggregate 2006	Granulate construction materials 2008	IBC 2008
Cu	5.4±3.2	**1**	0.7	**1**	**1.3**	0.9	**1.1**	0.9	10
Mo	1.2±0.4	0.2	**1.2**	0.9	0.5	0.5	0.5	1	15
Sb	0.21±0.13	**0.27**	**0.29**	**0.20**	**0.20**	**0.18**	**0.19**	0.16	0.7
SO_4	6100±1838	1600	**2633**	**3000**	1717	1550	1277	1730	20000
Cl	4150±495	165	**1282**	400	**692**	**800**	**975**	616	8800

Values between 'Granulate construction materials' and 'IBC' are indicated in bold.

time and help provide results more rapidly.

All performed experiments were checked by evaluating statistical error calculating the variance between two samples of the same measurements. Another test checked the accuracy of measurements in a regularly sized column with a column of double size.

5.2 Factors Influencing Leaching of AEB BA Products

It is difficult to obtain building products from AEB BA that meet the required leaching limits (below the 'Granulate construction materials limits') for Cu, Sb, Mo, Cl and SO_4. Therefore the aim of this research was to identify factors that influence leaching quality.

A mini-pilot plant was built in the laboratory which simulated the real pilot installation in Amsterdam. The main aim was to process BA under conditions similar to those in the actual pilot plant and to obtain three kinds of final products (sand, 2-6 mm aggregate and 6-20 mm aggregate). It is believed that these three fractions have similar qualities to the products from the actual pilot installation. This experimental work was repeated every week for 11 weeks in total. Each week, 100 kg of fresh bottom ash from the dry treatment plant was processed in the mini-pilot plant to remove 2-6 mm aggregate, 6-20 mm aggregate and sand product. The composition of the sample (in terms of organic and metal contents) was different every week. Changes were made to the control settings during the separations and to the final products by adding back part of the fractions already removed by separation (e.g. the density separator removed the organic content, but then a variable proportion of the organic content was added back to the samples).The resulting fractions were split and used for two kinds of leaching tests: column tests and batch tests (shaking tests) (Chapter 1). Data from the leaching experiments for Cu, Sb, Mo, Cl, SO_4, conductivity and redox (samples from the mini-pilot plant) are included in Annex B. The results from the experiments were correlated using SPSS software. The leaching values for all elements were measured at L/S=2 l/kg. The effects of three types of factors that may influence the leaching were then investigated:

- Input material. The input waste to the incinerator can be changed to improve the leaching quality of the final products. For example, extra sewage sludge was added to the incinerator together with the household waste. The mass of the sewage sludge added to the household waste during incineration was monitored, and the weekly average value was taken.

- Separation settings. Since separation performance can be improved by adjusting the parameters of the separation the settings were varied for each of the separators (e.g. splitter position, rotor speed, etc.), and every week, the amount of water that was used to wash the fractions was monitored. Other potentially influential factors that were monitored included the organic content removed by separation, metals content removed by separation, etc.

- Composition influences. The effects of final aggregate and sand composition (e.g. Cu, Pb, Mo, Fe contents, pH, redox, conductivity, etc.) are

difficult to control, but it is important to understand the interactions between elements during leaching.

Therefore, in the second series of experiments samples of products from Pilot plant II were analyzed, and the resulting data were examined for correlations between composition and input parameters. The aims were to check the correlations observed in the previous experiment from 2005 and identify the factors influencing leaching.

The types of variables (from mini-pilot and Pilot II) used for correlations are presented in Table 5.2. Significant linear correlations found between leaching values for all five elements (SO_4, Cl, Cu, Sb and Mo) and the quality of input material, separation settings and the composition of samples from the mini-plant and Pilot plant II in Amsterdam are described below.

5.2.1 Cu leaching

Sand

Samples from the mini-pilot did not show any significant linear correlations between Cu leaching values and any tested variable. Samples from Pilot plant II showed correlations between Cu leaching and conductivity, and between Cu leaching and SO_4 leaching; Cu leaching decreased with decreasing conductivity and SO_4 leaching (Figure 5.1).

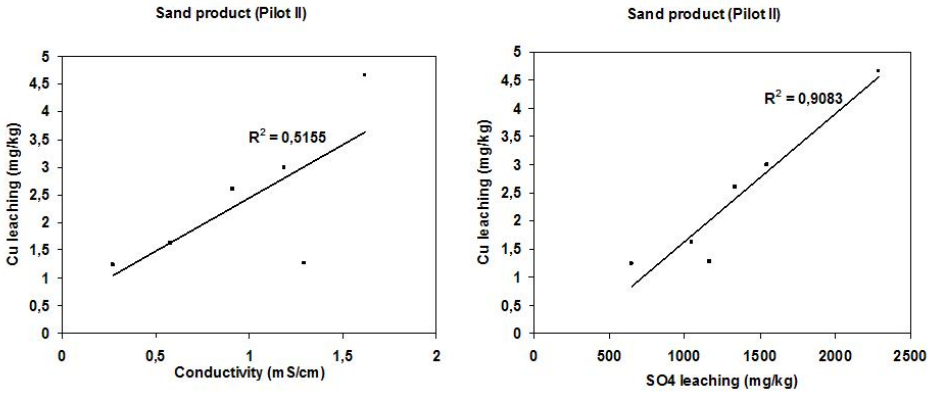

Figure 5.1: Cu correlations found from Pilot II samples, with conductivity and SO_4 leaching measured by column test for L/S = 2 l/kg.

2-6 mm fraction

No correlations were found between leaching values of any monitored substances and any other monitored variables.

Table 5.2: Parameters (variables) measured at the mini-pilot plant and Pilot II.

Variables measured	Mini-pilot	Pilot II
Mass of particles <70 m in the sample (analysed after leaching experiment)	yes	yes
Conductivity (for L/S=2 l/kg) of the eluate	yes	yes
Redox (for L/S=2 l/kg) of the eluate	yes	no
pH (for L/S=2 l/kg) of the eluate	yes	yes
Organic content (measured according to Procedure 1)	yes	yes
Mass of magnetic particles in the sample (analysed by magnet)	yes	yes
Mass of non-ferrous metals in the sample (total)	yes	yes
Mass of Fe, Cu, Ni, Zn, Pb metals in the sample (analysed by XRF)	yes	no
Amount of rinsing water (used during the separation process)	yes	no
Amount of sludge incinerated together with household waste	yes	yes
Leaching of SO_4 (L/S=2 l/kg) by column test and batch test	yes	yes
Leaching of Cl (L/S=2 l/kg) by column test and batch test	yes	yes
Leaching of Cu (L/S=2 l/kg) by column test and batch test	yes	yes
Leaching of Mo (L/S=2 l/kg) by column test and batch test	yes	yes
Leaching of Sb (L/S=2 l/kg) by column test and batch test	yes	yes
Leaching of NH_4 (L/S=2 l/kg) by column test and batch test	no	yes
Composition of process water - measured for SO_4, Cl, NH_4, Cu, Ca, Fe, Mo, Na and Sb	no	yes
DOC (L/S=10 l/kg) of the eluate	no	yes

6-20 mm fraction

Using samples from both the mini-pilot plant and Pilot plant II Cu leaching was found to increase with increasing conductivity. In addition, Cu leaching increased with Cl leaching. A further correlation was found between Cu leaching and the amount of sludge (Figure 5.2). When extra sludge was added during incineration, the shaking test showed it had a negative effect on Cu leaching. However, the column test showed a much weaker correlation between these two variables. Therefore further research is needed.

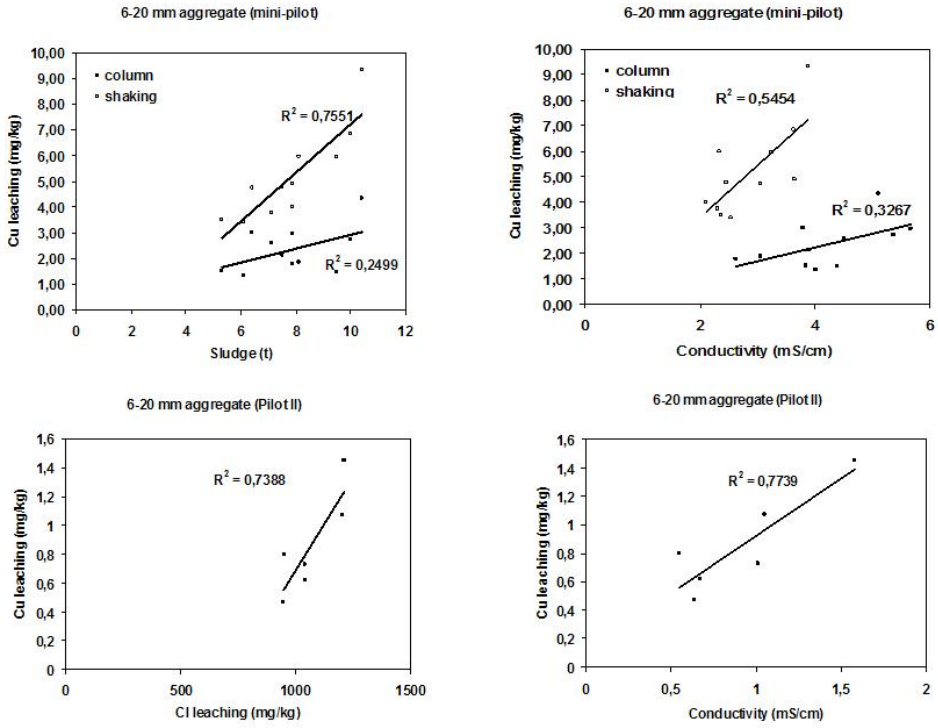

Figure 5.2: Correlations found between Cu leaching and other variables from mini-pilot and Pilot plant II samples. Measurements for the mini-pilot samples were conducted by shaking and column tests, while Pilot II samples were analysed solely by column tests (L/S=2l/kg)

5.2.2 Mo leaching

Sand

Only samples from Pilot II showed linear correlations. A correlation between Mo leaching and the non-ferrous metals content was found, as well as between Mo leaching and the leaching of NH_4; Mo leaching decreased when both of these variables (NH_4 and non-ferrous metals) decreased (Figure 5.3).

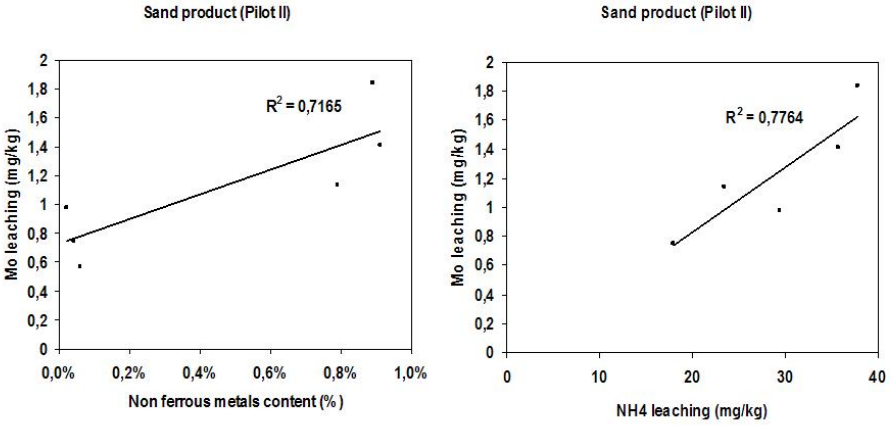

Figure 5.3: Mo correlations found from Pilot II samples (sand), measured by column test at L/S = 2 l/kg.

2-6 mm fraction

A weak negative linear correlation (in the data obtained from mini-pilot samples) between Mo leaching and Cl leaching was found (Figure 5.4). However, this correlation was not observed in analyses of samples from Pilot plant II, therefore further research is needed.

6-20 mm fraction

The leaching of Mo was positively correlated with the amount of fine particles (<75 μm) of the 6-20 mm fraction; when the amount of fines decreases, Mo leaching decreases (Figure 5.5). However, this correlation was not observed for samples from Pilot plant II.

The findings indicate that Mo leaching could be improved by reducing the amount of sludge added during incineration, since sludge increases the amount of fine particles, which have a negative influence on Mo leaching. Another influential factor is the amount of non-ferrous particles, which can be reduced by separation settings. The factors influencing Mo leaching from sand, fine aggregate and coarse aggregate remain to be investigated.

5.2.3 Sb leaching

Sand

There was only an indication of a positive correlation between Sb leaching and both SO_4 leaching and NH4 leaching (Figure 5.6). The Sb leaching increases with SO_4 leaching and when NH_4 leaching decreases Sb leaching also decreases.

The 2-6 mm and 6-20 mm fractions

No correlations between Sb leaching and any other monitored variables were

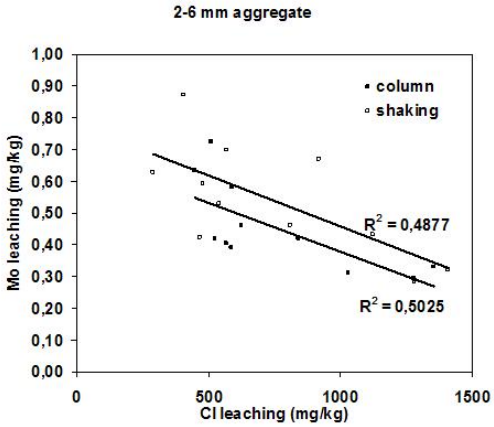

Figure 5.4: Mo correlation found from mini-pilot samples (2-6 mm), measured by column test and shaking test at L/S = 2 l/kg.

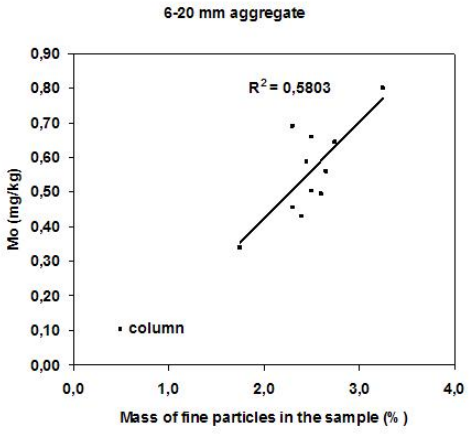

Figure 5.5: Mo correlation found from mini-pilot samples (6-20 mm), measured by column test at L/S = 2 l/kg.

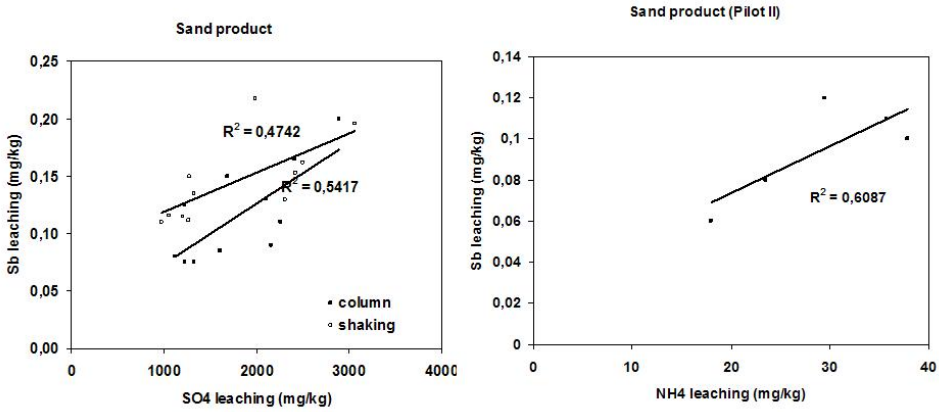

Figure 5.6: Correlations between Sb leaching observed in analyses of mini-pilot and Pilot plant II samples (sand). Measurements for the mini-pilot samples were conducted by shaking and column tests while Pilot plant II samples were subjected solely to column tests (L/S=2l/kg).

found of samples collected from the mini-pilot plant.

5.2.4 SO_4 leaching

Sand

SO_4 leaching showed the strongest linear correlations with conductivity and pH (Figure 5.7). With decreasing conductivity, SO_4 leaching decreased in analyses of samples from both plants. A positive correlation was also found between SO_4 leaching and Cl leaching; SO_4 leaching decreases when Cl leaching decreases (Figure 5.7). However this correlation was found only in analyses of samples from Pilot plant II (measured by the column test).

The 2-6 mm fraction

A correlation was found between SO_4 leaching and pH; with increasing pH, leaching of SO_4 decreased (Figure 5.8). However, this correlation was only observed in analyses of Pilot plant II samples.

The 6-20 mm fraction

The strongest correlation between SO_4 leaching from this fraction was with the organic content (in analyses of samples from Pilot plant II), which can be removed by physical separation. When the organic content decreased, SO_4 leaching decreased. In addition, when the level of NH_4 in the process water decreased the leaching of SO_4 decreased (Figure 5.9), and an indication of a positive correlation was found with hospital waste that was added to the incinerator together

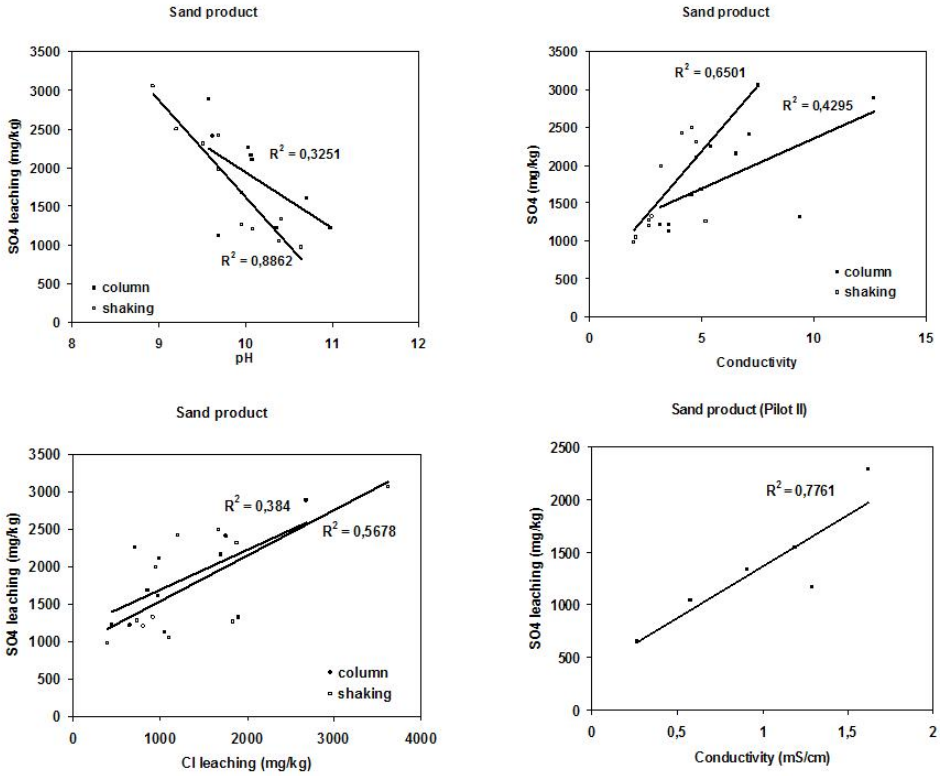

Figure 5.7: Correlations between SO_4 leaching and other monitored variables observed in analyses of samples (sand) from the mini-pilot and Pilot plant II. Measurements for the mini-pilot samples were conducted by shaking and column tests while Pilot II samples were subjected solely to the column test (L/S=2 l/kg).

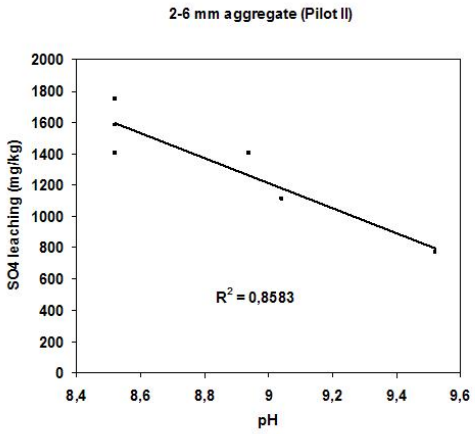

Figure 5.8: Correlations between SO_4 leaching and other monitored variables observed in analyses of samples (2-6 mm) from Pilot plant II measured by the column test at L/S=2 l/kg.

with household waste. When the mass of hospital waste increases, SO_4 leaching also increases.

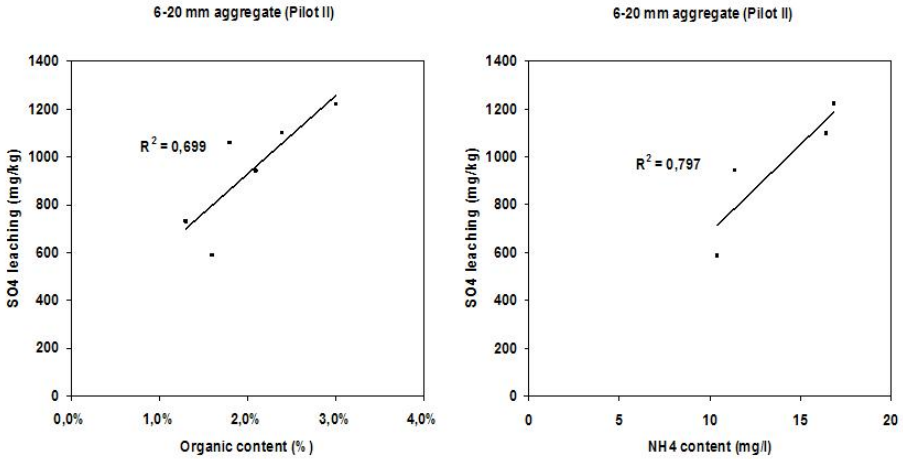

Figure 5.9: Correlations between SO_4 leaching and other monitored variables observed in analyses of samples (6-20 mm) from Pilot plant II measured by the column test at L/S=2 l/kg.

The findings indicate that organic content is the main factor influencing SO_4 leaching. The number of bigger organic particles can be reduced by physical separation and very fine organic particles can be washed out. The organic content can be decreased by appropriate adjustment of the separation settings, and the conductivity and pH can be monitored during separation.

5.2.5 Cl leaching

Sand

Leaching of Cl is strongly positively correlated to conductivity and strongly negatively correlated to the amount of fresh water rinsing (Figure 5.10). Leaching from the Pilot plant II samples also showed a positive correlation with the NH_4 content in the process water (Figure 5.10).

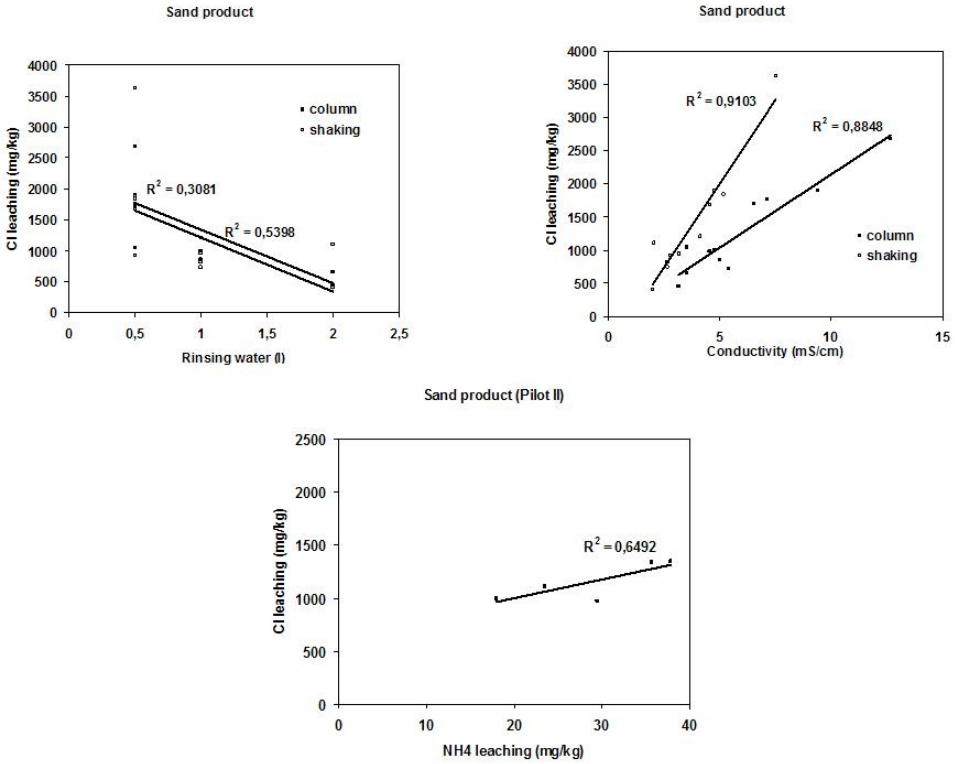

Figure 5.10: Correlations between Cl leaching and other monitored variables observed in analyses of samples (sand) from the mini pilot and Pilot plant II. Measurements for the mini-pilot samples were conducted by shaking and column tests while Pilot II samples were conducted solely by column test (L/S=2 l/kg).

The 2-6 mm fraction

Cl leaching from this fraction showed strong correlations to conductivity and redox (Figure 5.11); when conductivity increased Cl leaching increased. There

was also an indication of a positive correlation with the sludge added during incineration.

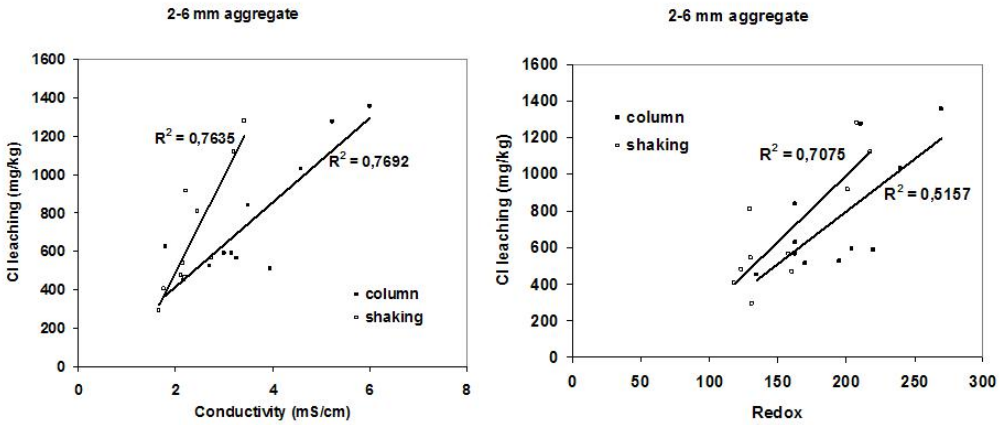

Figure 5.11: Correlations between Cl leaching and other monitored variables observed in analyses of samples (2-6 mm) from the mini pilot plant, measured by shaking and column tests with L/S=2 l/kg.

The 6-20 mm fraction

The main correlation for Cl leaching from this fraction was with conductivity; all samples from the mini-pilot and Pilot plant II showed a strong positive correlation between Cl leaching and conductivity (Figure 5.12). In addition, a negative correlation was found with the amount of rinsing water, and another correlation was with the NH_4 content in the process water. Sewage sludge contains urea which resulted in increasing leaching of NH_4 and thus it has a negative influence on Cl leaching.

5.2.6 Result and Discussion

The main factors influencing leaching of Cu, Sb, Mo, SO_4, Cl of the BA products after wet physical separation are:

- Organic content, fine particles and sludge, all of which could be reduced by rinsing the final products.
- Leaching of salts could be controlled by keeping conductivity and pH within appropriate limits.
- Cu leaching can be controlled by keeping conductivity within appropriate limits and by checking SO_4 leaching, which was correlated with Cu leaching.

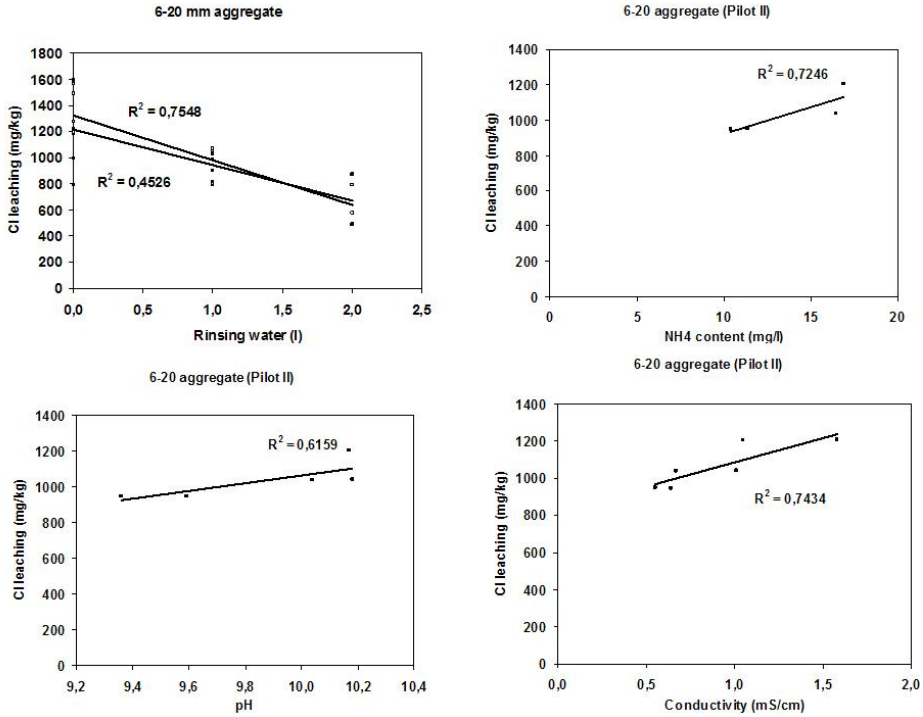

Figure 5.12: Correlations between Cl leaching and other monitored variables observed in analyses of samples (6-20 mm) from the mini pilot and Pilot plant II. Measurements for the mini-pilot samples were conducted by shaking and column tests while Pilot II samples were conducted solely by column test (L/S=2 l/kg).

- Mo leaching could be controlled by reducing fine particles ($< 75\mu$m) in the fraction and by reducing the non-ferrous content.

- Sb leaching was correlated with SO_4 leaching and NH_4 leaching. No other significant correlations with Sb leaching were found, but there was an indication of a possible correlation with pH; Sb leaching tended to decrease as pH increased.

5.3 Leaching Prediction System

In recent years, there have been several industrial initiatives to produce high-end granular building materials from MSWI BA (Rem et al. 2004, VITO n.d.). In these installations, sized granular materials are produced by means of wet classification followed by a series of physical separation steps to remove metals and organics. The process involves a considerable financial investment, which is compensated by the higher value of the metals and mineral products (building materials) that are produced from the ash. However, the value of the mineral products is particularly sensitive to their environmental quality, so their quality must be continuously controlled. More specifically, MSWI BA separated by wet physical separation (Muchova and Rem 2006a, Muchova and Rem 2007c) can be used as high quality building products only when the producer guarantees the stable quality of those products. The column test is not suitable for direct process control because the quality of products from BA is sensitive to input and process parameters, and therefore fluctuates over relatively short timescales, whereas the test results are available only after 21 days. This long period causes difficulties if the producer needs to react rapidly to separation changes or changes in input material. Therefore, a quicker test is required. The objective of this research was to find a model based on early leachate measurements capable of providing accurate predictions of the final eluate. A previous study by Lopez Meeza (Lopez Meza et al. 2008) showed that results from the shaking tests and column tests are generally comparable, but for some contaminants the shaking test indicated that substantially higher amounts are released than the column test.

Column tests are designed to evaluate the release of constituents under advection conditions as a function of time or L/S (Lopez Meza et al. 2008). In the NEN 7373 test a column is used (in our case 20 cm long, with a 5 cm internal diameter) filled with material that has been previously crushed to a particle size below 4 mm. The column is percolated with distilled water from bottom to top with a maximum water flow of 2 cm/h, and according to the Dutch Soil Quality Decree, the cumulative liquid to solid ratio (L/S) must be 10 and in the course of time seven fractions are collected corresponding to L/S ratios of 0.1 (K1), 0.2 (K2), 0.5 (K3), 1 (K4), 2 (K5), 5 (K6) and 10 (K7). The leaching behaviour of copper, antimony, molybdenum, sulphate and chloride is the result of a combination of chemical and physical processes in the column during the leaching period. Since the details of the chemical processes cannot be known a priori for industrially produced materials, an accelerated predictive model should simulate the effects of the physical processes and fit the unknown parameters to early leachate measurements. Parameters used in this model are the total amount of contaminants, dissolved contaminants and the dissolving factor. By fitting

these parameters to the known concentrations of the K3-K5 eluates, the model should accurately predict the concentrations in the K7 eluate. Based on the first three points, the final K7 value could be predicted, therefore the future results of the K7 value could always be based solely on the first 3 data points. This would decrease the measuring time and reveal the final parameter in a short period of time. This system could be put into practice at the installation in order to control the quality of the materials for the reason that the result of the K3-K5 leachates will already be known after 5 days instead of the regular 21 days. Furthermore, based on the leaching result, if needed, the separation setting could be appropriately adjusted in order to improve the quality of the products.

5.3.1 Model development

The time-dependent leaching behaviour generally varies amongst contaminants. Chloride, for example, is usually completely dissolved during the leaching test. On the other hand, contaminants like molybdenum and antimony are not dissolved during the leaching period. This is because contaminants can be present in several phases: chemically bound, adsorbed or dissolved in the liquid phase. Contaminants that are dissolved can be present in dead zones, where the liquid is not able to reach them, or in parts of the liquid that are continuously refreshed as a result of channelling. The constructed model therefore discriminates between three different physical situations in the column:

- free contaminant is completely dissolved in the water during leaching
- contaminant is partly dissolved in the water during leaching
- channelling or no channelling

At any time, the total amount of a contaminant in the bed is equal to Cm_s. Since contaminants are distributed over liquid and solid in a ratio $f : (1 - f)$, the amount of contaminant in the liquid phase is equal to $Cm_s f$. The volume of liquid inside the bed is:

$$V_l = \frac{\epsilon}{1-\epsilon}\frac{m_s}{\rho_s} \approx 0.6\frac{m_s}{\rho_s} \tag{5.1}$$

So, an infinitesimal volume dV_l of water added to the column will remove an amount of contaminant equal to:

$$d(Cm_s) = -\frac{dV_l}{V_l} fCm_s = -\frac{1-\epsilon}{\epsilon}\rho_s fCdV_l \approx -1.7\rho_s fCdV_l \tag{5.2}$$

This means that the amount of leachable contaminant in the column decreases according to the differential equation:

$$\frac{d(Cm_s)}{dV} = \frac{dC}{d(L/S)} = -1.7\rho_s fC \tag{5.3}$$

(Water in the column is completely distributed; fraction f of the element is dissolved.)

At the start of the leaching test, the concentration of the contaminant in the liquid phase is assumed to be homogeneous. If the water in the column does not

remain completely mixed due to channeling, then the water that is replaced will have an increasingly lower concentration than average for the entire column. This can be modeled by replacing C in the right hand side of equation (5.1) with $C\ (C/C_o)^{1/n}$, where C_o is the amount of leachable contaminant at the start of the process. $n = \infty$ corresponds to the case of no channeling, and for lower values the effect of channeling is increasingly important.

$$\frac{dC}{d(L/S)} = \frac{-1.7\rho_s f C^{1+1/n}}{C_o^{1/n}} \tag{5.4}$$

The solution to this equation is:

$$C = \frac{C_o}{\left(1 + \alpha\frac{(L/S)}{n}\right)^n} \tag{5.5}$$

where:

$$\alpha = 1.7\rho_s f \tag{5.6}$$

The amount of contaminant that has leached L from the column is then $(C_o - C)$:

$$L = C_o \left[1 - \frac{1}{\left(1 + \alpha\frac{(L/S)}{n}\right)^n}\right] \text{ for } n > 0 \tag{5.7}$$

The model has three parameters (n, α and C_o) that need to be estimated for a particular column test. It can be argued that the parameter n depends on the detailed spatial distribution of the contaminant and the grain size of the sample, and not on the particular case. Therefore, full data from thirty samples analysed in 2004 were used to fix the value of n (the effect of dead zones or channelling) for each combination of grain size (sand, fine granulate or coarse granulate) and contaminant (copper, antimony, molybdenum, sulphate and chloride). To this end, the K3, K4, K5, K6 and K7concentrations were measured then the theoretical curve described by equation 5.7 was fitted to the data by minimizing least squares. All five points were used in the fit, resulting in optimal values for the parameters n, α and C_o. Then, for each contaminant and each size category, the value of n was fixed to a best value. In the second part of the study, the same data were used to fit the theoretical curve only to the first three points (K3, K4 and K5) to estimate α and C_o. The goal of this procedure was to use the main equation 5.7 as a predictor of the leaching behaviour from K5 to K7. Finally, data acquired in 2005 and 2006 were used as an independent check of the prediction procedure, using the values for n derived from the 2004 data. Figure 5.13 shows examples of all measured contaminant values and theoretical fitting curves for the 2-6 mm fraction from 2005.

Tables 5.3, 5.4, 5.5, 5.6, and 5.7. show the measured and predicted values for all size fractions and all five contaminants measured in 2005 and 2006.

The tables also show the root mean square differences between the measured values and the theoretical values. Values of the factor n are shown in Table 5.8.

The channelling described by the physical model can also be interpreted as limited solubility. In either case, the contaminant cannot be reached by the liquid and enters the liquid phase only by diffusion. The higher n indicates a

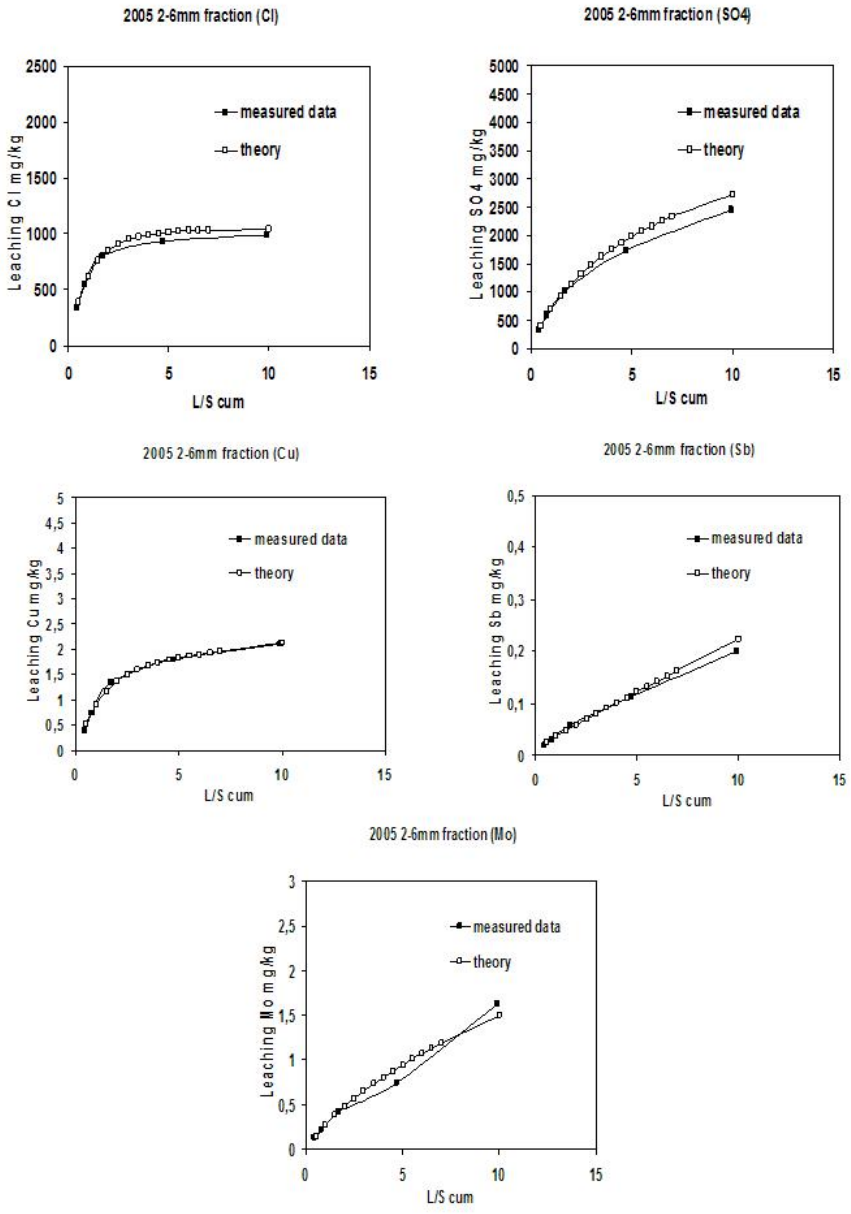

Figure 5.13: Cumulative release of copper, antimony, molybdenum, sulphate and chloride from the 2-6 mm fraction collected in 2005 (measured and theoretically fit data).

Table 5.3: Measured cumulative leaching values of chloride from 2004 until 2006 in mg/kg, predicted values according to equation 5.9 (cumulative, mg/kg) and their standard deviations in %.

		K3 cum (mg/kg)	K4 cum (mg/kg)	K5 cum (mg/kg)	K6 cum (mg/kg)	K7 cum (mg/kg)
Sample 1 (sand)	Measured	106.4	125.8	134.6	149.9	160.2
	Exp. fit	105.7	127.6	133.4	133.9	133.9
Sample 2 (sand)	Measured	97.2	131.4	142.6	158.1	168.8
	Exp. fit	97.6	130.6	143.0	146.0	146.0
Sample 3 (sand)	Measured	443.3	779.0	1324.4	1859.1	1901.9
	Exp. fit	439.9	781.9	1323.8	1919.9	1974.0
Sample 4 (sand)	Measured	354.7	723.9	1379.1	1943.3	1998.0
	Exp. fit	336.2	736.8	1376.6	2557.1	2847.2
Sample 5 (sand)	Measured	1219.6	1654.8	2469.8	3398.8	3537.9
	Exp. fit	1178.2	1699.1	2459.0	3416.3	3471.3
Sample 6 (sand)	Measured	1471.0	2181.2	2988.5	3283.8	3417.5
	Exp. fit	1434.9	2222.8	2974.9	3733.5	3764.6
Sample 7 (sand)	Measured	1433.9	2163.8	2773.5	3020.0	3140.1
	Exp. fit	1452.7	2141.3	2781.0	3244.8	3258.4
Sample 8 (sand)	Measured	795.4	1522.3	2514.3	2877.9	2956.3
	Exp. fit	638.8	1629.8	2483.9	2913.2	2923.2
Standard deviation between measured and experimentally fitted values (%)		7.4%	2.9%	0.6%	13.4%	17.5%
Sample 1 (2-6 mm)	Measured	247.5	306.3	345.8	386.5	399.2
	Exp. fit	246.2	308.7	344.6	359.0	360.2
Sample 2 (2-6 mm)	Measured	141.0	241.5	327.1	378.1	390.4
	Exp. fit	147.5	234.2	329.4	473.6	520.9
Sample 3 (2-6 mm)	Measured	394.8	707.4	923.8	1067.9	1089.7
	Exp. fit	405.1	695.5	928.2	1139.8	1171.5
Sample 4 (2-6 mm)	Measured	318.6	540.1	768.1	878.8	910.7
	Exp. fit	327.2	531.1	770.6	1005.5	1037.9
Sample 5 (2-6 mm)	Measured	343.6	556.7	802.4	929.9	989.2
	Exp. fit	352.6	547.3	804.8	1011.9	1046.4
Standard deviation between measured and experimentally fitted values (%)		2.8%	1.9%	0.5%	12.0%	13.8%
Sample 1 (6-20 mm)	Measured	540.5	677.2	750.8	769.7	786.6
	Exp. fit	538.8	680.2	749.2	767.8	767.8
Sample 2 (6-20 mm)	Measured	777.3	842.4	875.2	897.0	917.0
	Exp. fit	774.4	852.0	868.3	869.2	869.2
Sample 3 (6-20 mm)	Measured	684.1	855.1	970.1	1018.2	1029.4
	Exp. fit	680.4	861.1	967.3	996.0	996.2
Sample 4 (6-20 mm)	Measured	408.1	437.8	447.1	469.4	478.0
	Exp. fit	407.5	440.5	444.9	445.0	445.0
Sample 5 (6-20 mm)	Measured	611.3	792.3	854.5	884.2	891.2
	Exp. fit	614.1	786.9	857.4	870.9	870.9
Sample 6 (6-20 mm)	Measured	337.6	666.5	838.9	896.6	923.1
	Exp. fit	359.0	641.5	848.8	1114.4	1259.8
Sample 7 (6-20 mm)	Measured	518.6	782.1	916.2	997.6	1042.9
	Exp. fit	529.1	767.6	922.2	987.5	987.7
Standard deviation between measured and experimentally fitted values (%)		2.4%	1.8%	0.6%	7.8%	11.0%

Table 5.4: Measured cumulative leaching values of sulphate from 2004 until 2006 in mg/kg, predicted values according to equation 5.9 (cumulative, mg/kg) and their standard deviations in %.

		K3 cum (mg/kg)	K4 cum (mg/kg)	K5 cum (mg/kg)	K6 cum (mg/kg)	K7 cum (mg/kg)
Sample 1 (sand)	Measured	228.5	412.6	692.5	1236.5	1610.4
	Exp. fit	232.4	421.8	684.7	1325.6	1916.1
Sample 2 (sand)	Measured	204.7	391.7	624.5	1126.7	1511.4
	Exp. fit	210.5	396.0	619.3	1224.3	1801.7
Sample 3 (sand)	Measured	409.0	766.0	1451.2	3330.4	4155.4
	Exp. fit	415.2	768.4	1447.4	3072.4	4042.5
Sample 4 (sand)	Measured	336.2	745.4	1466.6	3349.0	4432.0
	Exp. fit	348.5	763.1	1452.5	3242.5	4626.3
Sample 5 (sand)	Measured	333.8	526.2	1584.7	3210.5	4343.2
	Exp. fit	491.9	772.1	1325.7	3426.7	5699.8
Sample 6 (sand)	Measured	401.9	705.6	1234.9	2729.5	4202.3
	Exp. fit	417.7	744.3	1221.4	2939.1	4574.3
Sample 7 (sand)	Measured	386.9	703.3	1143.5	2323.6	8693.1
	Exp. fit	380.6	677.2	1176.3	2975.9	5654.7
Sample 8 (sand)	Measured	149.0	441.9	981.7	1999.1	7240.4
	Exp. fit	137.0	441.6	980.7	2559.5	4589.3
Standard deviation between measured and experimentally fitted values (%)		17.2%	16.7%	5.9%	15.3%	23.1%
Sample 1 (2-6 mm)	Measured	494.5	717.7	1040.2	1663.5	2234.7
	Exp. fit	484.3	731.3	1035.4	1553.8	2022.7
Sample 2 (2-6 mm)	Measured	364.2	559.7	922.1	1861.1	2723.5
	Exp. fit	351.7	590.8	905.6	1695.0	2438.0
Sample 3 (2-6 mm)	Measured	448.8	894.2	1339.3	2312.4	3139.2
	Exp. fit	461.8	875.7	1347.3	2367.2	3251.6
Sample 4 (2-6 mm)	Measured	292.3	562.6	963.4	1686.4	2134.6
	Exp. fit	308.8	554.7	962.2	1923.8	2455.8
Sample 5 (2-6 mm)	Measured	330.2	581.8	1011.1	1725.1	2442.7
	Exp. fit	335.7	570.9	1016.0	1907.7	2720.9
Standard deviation between measured and experimentally fitted values (%)		3.3%	2.9%	0.9%	8.8%	10.1%
Sample 1 (6-20 mm)	Measured	253.2	356.5	494.9	782.9	1026.7
	Exp. fit	256.2	365.8	483.8	722.5	905.0
Sample 2 (6-20 mm)	Measured	101.4	134.4	184.0	294.2	429.2
	Exp. fit	99.0	137.9	182.8	263.3	326.7
Sample 3 (6-20 mm)	Measured	597.0	805.5	1122.9	1626.8	1912.4
	Exp. fit	595.8	827.4	1104.8	1598.3	1974.2
Sample 4 (6-20 mm)	Measured	769.5	1064.5	1421.4	2016.6	2319.0
	Exp. fit	746.4	1078.3	1427.6	2077.0	2592.4
Sample 5 (6-20 mm)	Measured	619.4	910.4	1234.9	1884.1	2289.1
	Exp. fit	618.8	916.9	1229.7	1825.6	2252.5
Sample 6 (6-20 mm)	Measured	127.1	254.7	350.3	457.3	605.8
	Exp. fit	149.2	255.1	336.5	472.0	667.2
Sample 7 (6-20 mm)	Measured	208.9	360.1	532.0	964.0	1271.4
	Exp. fit	229.4	364.6	515.6	872.2	1082.4
Standard deviation between measured and experimentally fitted values (%)		6.7%	1.9%	2.2%	6.7%	13.2%

Table 5.5: Measured cumulative leaching values of copper from 2004 until 2006 in mg/kg, predicted values according to equation 5.10 (cumulative, mg/kg) and their standard deviations in %.

		K3 cum (mg/kg)	K4 cum (mg/kg)	K5 cum (mg/kg)	K6 cum (mg/kg)	K7 cum (mg/kg)
Sample 1 (sand)	Measured	0.58	0.80	0.91	1.07	1.32
	Exp. fit	0.59	0.79	0.92	1.09	1.34
Sample 2 (sand)	Measured	0.52	0.87	1.06	1.21	1.46
	Exp. fit	0.54	0.84	1.07	1.34	1.58
Sample 3 (sand)	Measured	1.70	2.78	4.16	5.69	6.04
	Exp. fit	1.56	2.70	4.32	5.75	5.94
Sample 4 (sand)	Measured	1.28	2.47	3.85	5.44	5.97
	Exp. fit	1.18	2.40	3.95	5.56	5.83
Sample 5 (sand)	Measured	1.85	2.49	3.29	3.97	4.39
	Exp. fit	1.84	2.51	3.29	3.95	4.19
Sample 6 (sand)	Measured	2.41	3.44	4.28	4.75	5.14
	Exp. fit	2.39	3.46	4.28	4.90	5.12
Sample 7 (sand)	Measured	2.15	3.13	3.87	4.29	4.60
	Exp. fit	2.17	3.10	3.88	4.44	4.71
Sample 8 (sand)	Measured	0.99	2.07	2.98	3.36	3.68
	Exp. fit	0.91	2.13	2.96	3.30	3.48
Standard deviation between measured and experimentally fitted values (%)		5.1%	2.1%	1.7%	3.9%	4.0%
Sample 1 (2-6 mm)	Measured	0.13	0.18	0.22	0.35	0.61
	Exp. fit	0.13	0.17	0.22	0.36	0.61
Sample 2 (2-6 mm)	Measured	0.05	0.07	0.11	0.26	0.51
	Exp. fit	0.05	0.07	0.11	0.26	0.51
Sample 3 (2-6 mm)	Measured	0.20	0.40	0.52	0.67	0.93
	Exp. fit	0.21	0.38	0.53	0.75	1.01
Sample 4 (2-6 mm)	Measured	0.33	0.66	1.16	1.52	1.63
	Exp. fit	0.41	0.70	1.06	1.51	1.67
Sample 5 (2-6 mm)	Measured	0.39	0.74	1.34	1.79	2.10
	Exp. fit	0.47	0.77	1.25	1.81	2.12
Standard deviation between measured and experimentally fitted values (%)		12.3%	4.0%	5.3%	4.9%	3.9%
Sample 1 (6-20 mm)	Measured	0.54	0.57	0.61	0.77	1.03
	Exp. fit	0.54	0.57	0.61	0.77	1.03
Sample 2 (6-20 mm)	Measured	0.91	0.93	0.97	1.11	1.36
	Exp. fit	0.91	0.93	0.97	1.11	1.36
Sample 3 (6-20 mm)	Measured	0.29	0.36	0.41	0.57	0.82
	Exp. fit	0.32	0.35	0.39	0.55	0.81
Sample 4 (6-20 mm)	Measured	0.23	0.27	0.31	0.47	0.74
	Exp. fit	0.24	0.27	0.31	0.46	0.73
Sample 5 (6-20 mm)	Measured	0.33	0.41	0.45	0.61	0.86
	Exp. fit	0.37	0.39	0.43	0.59	0.84
Sample 6 (6-20 mm)	Measured	1.06	1.94	2.33	2.49	2.60
	Exp. fit	1.20	1.87	2.22	2.50	2.67
Sample 7 (6-20 mm)	Measured	1.74	2.63	3.21	3.71	4.06
	Exp. fit	1.75	2.60	3.23	3.73	4.02
Standard deviation between measured and experimentally fitted values (%)		6.9%	2.7%	2.8%	1.5%	1.5%

Table 5.6: Measured cumulative leaching values of antimony from 2004 until 2006 in mg/kg, predicted values according to equation 5.11 (cumulative, mg/kg) and their standard deviations in %.

		K3 cum (mg/kg)	K4 cum (mg/kg)	K5 cum (mg/kg)	K6 cum (mg/kg)	K7 cum (mg/kg)
Sample 1 (sand)	Measured	0.013	0.027	0.049	0.135	0.272
	Exp. fit	0.016	0.027	0.046	0.111	0.210
Sample 2 (sand)	Measured	0.013	0.027	0.046	0.127	0.264
	Exp. fit	0.015	0.027	0.044	0.107	0.206
Sample 3 (sand)	Measured	0.023	0.042	0.081	0.156	0.241
	Exp. fit	0.022	0.041	0.082	0.203	0.299
Sample 4 (sand)	Measured	0.012	0.033	0.059	0.135	0.237
	Exp. fit	0.015	0.032	0.059	0.142	0.240
Sample 5 (sand)	Measured	n.m.	0.013	0.039	0.148	0.341
	Exp. fit	0.011	0.018	0.032	0.109	0.247
Sample 6 (sand)	Measured	0.031	0.054	0.085	0.216	0.427
	Exp. fit	0.027	0.051	0.089	0.272	0.543
Sample 7 (sand)	Measured	0.033	0.056	0.087	0.202	0.446
	Exp. fit	0.028	0.051	0.092	0.262	0.602
Sample 8 (sand)	Measured	0.010	0.032	0.063	0.153	0.279
	Exp. fit	0.008	0.028	0.065	0.195	0.422
Standard deviation between measured and experimentally fitted values (%)		15.9%	13.8%	6.7%	24.0%	30.1%
Sample 1 (2-6 mm)	Measured	0.021	0.039	0.069	0.156	0.289
	Exp. fit	0.030	0.041	0.060	0.116	0.221
Sample 2 (2-6 mm)	Measured	0.017	0.029	0.046	0.100	0.198
	Exp. fit	0.018	0.029	0.046	0.107	0.205
Sample 3 (2-6 mm)	Measured	0.017	0.039	0.060	0.119	0.202
	Exp. fit	0.026	0.038	0.055	0.116	0.222
Sample 4 (2-6 mm)	Measured	0.016	0.032	0.056	0.116	0.170
	Exp. fit	0.023	0.032	0.050	0.112	0.167
Sample 5 (2-6 mm)	Measured	0.018	0.032	0.059	0.113	0.201
	Exp. fit	0.024	0.033	0.053	0.115	0.221
Standard deviation between measured and experimentally fitted values (%)		28.5%	2.9%	10.7%	11.8%	12.1%
Sample 1 (6-20 mm)	Measured	0.014	0.027	0.043	0.107	0.213
	Exp. fit	0.012	0.022	0.038	0.102	0.208
Sample 2 (6-20 mm)	Measured	0.007	0.016	0.033	0.100	0.205
	Exp. fit	0.011	0.020	0.036	0.094	0.194
Sample 3 (6-20 mm)	Measured	0.006	0.011	0.022	0.063	0.125
	Exp. fit	0.013	0.023	0.042	0.106	0.208
Sample 4 (6-20 mm)	Measured	0.013	0.021	0.037	0.099	0.164
	Exp. fit	0.011	0.021	0.038	0.100	0.208
Sample 5 (6-20 mm)	Measured	0.019	0.033	0.055	0.133	0.208
	Exp. fit	0.011	0.021	0.038	0.102	0.202
Sample 6 (6-20 mm)	Measured	0.013	0.024	0.034	0.049	0.079
	Exp. fit	0.007	0.014	0.022	0.042	0.096
Sample 7 (6-20 mm)	Measured	0.022	0.042	0.065	0.142	0.217
	Exp. fit	0.011	0.022	0.040	0.130	0.246
Standard deviation between measured and experimentally fitted values (%)		79.4%	67.5%	50.7%	28.9%	27.9%

Table 5.7: Measured cumulative leaching values of molybdenum from 2004 until 2006 in mg/kg, predicted values according to equation 5.10 (cumulative, mg/kg) and their standard deviations in %.

		K3 cum (mg/kg)	K4 cum (mg/kg)	K5 cum (mg/kg)	K6 cum (mg/kg)	K7 cum (mg/kg)
Sample 1 (sand)	Measured	0.16	0.24	0.29	0.45	0.69
	Exp. fit	0.17	0.22	0.30	0.50	0.77
Sample 2 (sand)	Measured	0.12	0.20	0.24	0.39	0.64
	Exp. fit	0.13	0.18	0.24	0.44	0.71
Sample 3 (sand)	Measured	0.14	0.25	0.44	1.06	1.41
	Exp. fit	0.14	0.24	0.44	0.88	1.18
Sample 4 (sand)	Measured	0.13	0.28	0.52	1.33	2.13
	Exp. fit	0.13	0.28	0.53	1.19	1.76
Sample 5 (sand)	Measured	0.35	0.58	1.04	2.57	3.94
	Exp. fit	0.77	1.10	1.62	2.97	4.08
Sample 6 (sand)	Measured	0.49	0.89	1.47	2.78	4.03
	Exp. fit	0.95	1.44	1.99	3.30	4.26
Sample 7 (sand)	Measured	0.45	0.85	1.41	2.50	3.69
	Exp. fit	0.61	0.97	1.44	2.57	3.72
Sample 8 (sand)	Measured	0.16	0.55	1.24	2.32	3.30
	Exp. fit	0.24	0.67	1.25	2.37	3.39
Standard deviation between measured and experimentally fitted values (%)		57.5%	39.9%	23.3%	12.4%	10.3%
Sample 1 (2-6 mm)	Measured	0.34	0.52	0.76	1.19	1.91
	Exp. fit	0.34	0.52	0.76	1.23	1.78
Sample 2 (2-6 mm)	Measured	0.03	0.06	0.10	0.25	0.49
	Exp. fit	0.03	0.05	0.09	0.24	0.49
Sample 3 (2-6 mm)	Measured	0.04	0.09	0.13	0.28	0.54
	Exp. fit	0.05	0.09	0.14	0.30	0.57
Sample 4 (2-6 mm)	Measured	0.07	0.13	0.20	0.38	0.60
	Experimentally fit	0.08	0.13	0.20	0.41	0.57
Sample 5 (2-6 mm)	Measured	0.12	0.22	0.42	0.75	1.63
	Exp. fit	0.12	0.22	0.42	0.90	1.49
Standard deviation between measured and experimentally fitted values (%)		4.1%	4.0%	1.2%	9.1%	6.2%
Sample 1 (6-20 mm)	Measured	0.25	0.31	0.38	0.54	0.80
	Exp. fit	0.25	0.31	0.38	0.58	0.86
Sample 2 (6-20 mm)	Measured	0.27	0.32	0.36	0.51	0.76
	Exp. fit	0.27	0.31	0.37	0.53	0.79
Sample 3 (6-20 mm)	Measured	0.11	0.16	0.25	0.41	0.76
	Exp. fit	0.11	0.17	0.25	0.45	0.74
Sample 4 (6-20 mm)	Measured	0.16	0.24	0.29	0.44	0.71
	Exp. fit	0.17	0.23	0.30	0.48	0.77
Sample 5 (6-20 mm)	Measured	0.11	0.13	0.22	0.38	0.63
	Exp. fit	0.10	0.15	0.21	0.40	0.66
Sample 6 (6-20 mm)	Measured	0.12	0.25	0.35	0.47	0.76
	Exp. fit	0.13	0.24	0.35	0.55	0.92
Sample 7 (6-20 mm)	Measured	0.22	0.38	0.59	1.08	1.72
	Exp. fit	0.22	0.38	0.59	1.18	1.65
Standard deviation between measured and experimentally fitted values (%)		4.2%	5.1%	1.9%	9.4%	8.0%

Table 5.8: Optimal n-values, derived from data obtained in 2004.

	Chloride	Sulphate	Copper	Antimony	Molybdenum
Sand	1000	0.04	100	0.01	0.1
Fine granulate	5	0.04	100	0.001	0.1
Coarse granulate	100	0.02	100	0.000001	0.5

better (faster) solubility during the leaching test. The best dissolving behaviour is shown by chloride, the worst by antimony. A smaller particle size led more rapidly to steady state leaching conditions except for molybdenum in the coarse fraction. The lower n-value for sulphate compared to chloride is probably due to the limited solubility of gypsum and ettringite (Todorovic and Ecke 2006). Copper leaching may be related to the presence of dissolved humic and fulvic acids (van Zomeren and Comans 2004). However, more research is needed to investigate the behaviour of antimony, copper and molybdenum in general and the mechanisms controlling their solubility.

In practice, the prediction of the leaching has one further complication. The analyses of the eluates have a finite detection limit. For this reason, the measured behaviour has the general form:

$$L = C_0 \left[1 - \frac{1}{\left(1 + \alpha \frac{(L/S)}{n}\right)^n} \right] + \text{detection limit } x(L/S) \tag{5.8}$$

The leaching prediction was summarised in three equations, 5.9, 5.10 and 5.11. The differences are due to differences in the detection limit. In the analyses of K6 and K7 values from 2004 the detection limits were usually 0.05 or 0.02.

Chloride and sulphate

$$L = C_0 \left[1 - \frac{1}{\left(1 + \alpha \frac{(L/S)}{n}\right)^n} \right] \text{ for } n > 0 \tag{5.9}$$

Copper and molybdenum

$$L = C_0 \left[1 - \frac{1}{\left(1 + \alpha \frac{(L/S)}{n}\right)^n} \right] + 0.05(L/S) \text{ for } n > 0 \tag{5.10}$$

Antimony

$$L = C_0 \left[1 - \frac{1}{\left(1 + \alpha \frac{(L/S)}{n}\right)^n} \right] + 0.02(L/S) \text{ for } n > 0 \tag{5.11}$$

5.3.2 Results and Discussion

The final leachate, K7, for concentrations of copper, antimony, molybdenum, sulphate and chloride measured by the column test can be predicted from K3, K4 and K5 concentrations by three different equations. The model was validated against measured values for BA samples separated by dry and wet physical separation processes in the Amsterdam incinerator collected at different times over a period of 11 weeks. Therefore, there were substantial variations in the composition of the modelled samples. Nevertheless, the model provided accurate predictions for the test set. This model can be used for any quality bottom ash samples and is able to show the result of final eluate in 5 days.

5.4 Column Versus Shaking Tests

The aim of this experiment was to explore the correlations between values measured by the column and shaking tests for Cu, Mo, Sb, SO_4 and Cl leaching. The leaching values obtained using these leaching tests often vary widely, but if correlations between their results could be found, both the measuring time and costs of compliance tests could be reduced. Figure 5.14 shows a plot of the results obtained with the shaking test and column test for Cl and SO_4 leaching from samples collected in 2005 and 2006 from the mini-plant built in the laboratory (which was intended to simulate the wet pilot plant in Amsterdam) and the wet pilot plant in Amsterdam, respectively.

Significant correlations were found between SO_4 leaching values for the coarse (6-20 mm) and fine fractions (2-6 mm) obtained from the shaking and column tests. For these fractions, the values obtained from the shaking test were on average 36% and 22% higher than the values obtained from the column test, respectively. However, for the sand fraction a significant correlation between the SO_4 leaching values yielded by the two tests was only observed for the samples collected from the mini-plant, and in this case the column test provided higher leaching values than the shaking test.
The correlations between the shaking and column test values for Cl leaching require further investigation. The leaching of Cl is correlated with the amount of organics, thus the results show unexpected relationships, partly because the organic content was higher in 2006 than in 2005. No correlations between leaching values obtained from the two tests for metals (Cu, Mo, Sb) were observed.

5.5 Evaluation of the Statistical Error During Experiments

5.5.1 Standard Deviation Between Two Samples

Samples (sand product, 2-6 mm aggregate and 6-20 mm aggregate) collected from the mini-plant in 2005 were analysed by column tests and shaking tests in duplicate. One sample of the sand (approximately 4 kg), one sample of the 2-6 mm aggregate (approximately 4 kg) and one sample of the 6-20 mm aggregate (approximately 10 kg) were milled to below 4 mm and then each split into two parts. This experiment was intended to evaluate the precision of the tests by

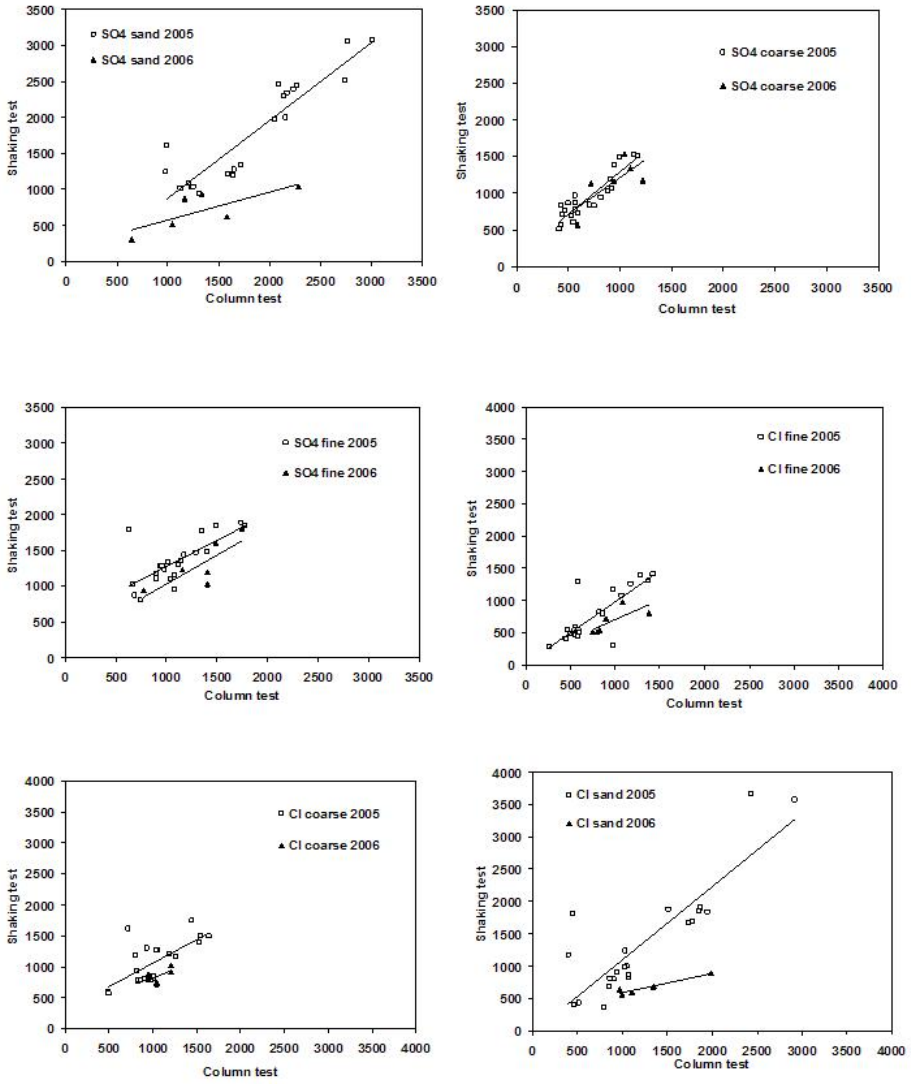

Figure 5.14: Correlation between values obtained from the shaking and column tests in 2005 (for samples produced from the mini-plant) and in 2006 (for samples collected from Pilot plant II in Amsterdam) for SO_4 and Cl leaching.

determining standard deviations of duplicate based on their homogeneity (Table 5.9).

Table 5.9: Standard deviations (%) between leaching values obtained for duplicate samples of the sand product, 2-6 mm aggregate and 6-20 mm aggregate by the column and shaking tests.

	Column test			Shaking test		
	Sand	2-6 mm	6-20 mm	Sand	2-6 mm	6-20 mm
Cl	4.7%	12.6%	2.0%	6.2%	9.4%	21.7%
SO_4	7.2%	0.8%	1.4%	1.8%	15.5%	1.6%
Cu	8.9%	3.7%	13.2%	3.8%	14.2%	5.8%
Sb	12.1%	23.1%	11.2%	2.9%	14.6%	3.6%
Mo	7.7%	5.3%	9.1%	5.7%	5.3%	8.0%

The standard deviations for the duplicate samples was, in many cases, very small. The highest errors were for Sb (measured by column test) and for Cu and Cl in the 2-6 mm and 6-20 mm aggregate. The error for Sb was also high in the prediction procedure, probably due to the complex chemical reactions that Sb participates in. The values from the shaking test show that the variance of leaching values for metals tend to be highest in the fine fraction, which can be explained by the small size of the sample, before milling, used for the tests.

5.5.2 Small Column Versus Large Column

In 2006 another experiment was performed to evaluate the accuracy of the column test. Four columns: two standard-sized columns according to NEN 7343, measuring 5x20 mm (NEN7343 2004), and two larger, 5x40 mm columns were used in the experiment. Sand product collected from Pilot plant II was split into four sub-samples, two of which (sand a and sand b) were placed in the regular sized columns and the other two (sand a and b big column) were placed in the bigger columns. The experiment was performed according to the standard method, but for a longer period. The regular column test should run until L/S=10 l/kg, but this experiment ran until L/S=13 l/kg except for sample sand b (big column), which was only run until L/S=10 l/kg due to problems with the pump during the measurement.

The results show (Figure 5.15) that the size of the column does not significantly influence the leaching values. However, the leaching behaviour of metals (Cu, Sb and Mo) did not reach equilibrium until L/S=10 l/kg. Probable reasons for this were mentioned in section 5.4.

5.6 Conclusions

The Cu, Sb, Mo, SO_4, Cl leaching values of the BA products after wet physical separation are strongly influenced by the quality of the process water and the amount of water used in the last step during the rinsing of the final products. Increasing the amount of water decreases the free ions, the organic content and reduces the amount of fine particles. These factors decrease the leaching of Cl

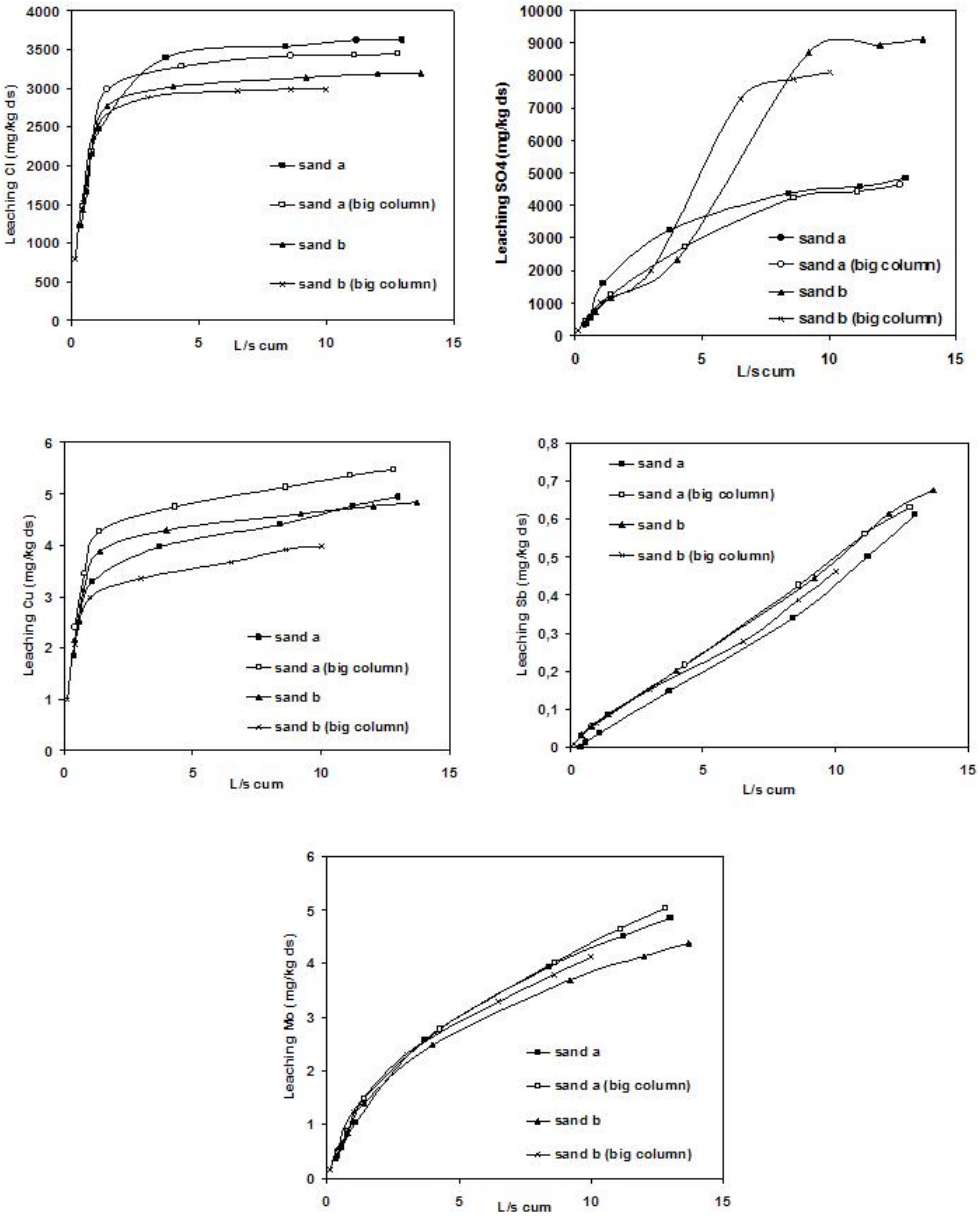

Figure 5.15: Results of column leaching tests performed with columns of two sizes (standard and big) and duplicate sand samples collected from Pilot plant II in Amsterdam in 2006.

and SO_4, and this appears to be accompanied by reductions in the leaching of metals. Amounts of fine particles ($< 75\mu$m) and small organic particles are correlated with amounts of sludge added to the household waste. Sludge has been recently (since 2005) incinerated together with household waste, therefore due to its incomplete incineration, the sludge remains in the bottom ash fraction and has a negative influence on leaching.

Chlorides are highly soluble, hence their leaching is not constrained by solubility limitations (Sloot et al. 1997). Further, leaching of this freely soluble ion can be controlled by simply measuring the conductivity and rinsing if necessary; when the conductivity is < 3 mS/cm the leaching of Cl will be below the leaching limit (616 mg/kg). For washing out Cl, the L/S ratio is a key factor (Boddum and Skaarup 2000, Kim et al. 2003). The L/S ratio affects the removal of salt, but it must be minimized due to the treatment costs. Kim (Kim et al. 2003) found that with a L/S=2.5 l/kg and 5 minutes of washing, 77% of the Cl could be removed. Increasing the L/S ratio or washing time did not increase the removal of chlorides. This result could be further improved by washing continuously. Sulphates are incorporated in a number of minerals, they are involved in numerous reactions (including highly undesirable reactions), and are released at rates that depend on the solubility of these minerals. Sulphates could be released through substitution, for instance with oxyanions. Significant leaching due to decomposition of ettringite can be limited by decreasing the pH or by carbonation (Todorovic and Ecke 2006). SO_4 leaching can be also controlled by reducing the conductivity sufficiently. According to the acquired measurements, the conductivity should be <6 mS/cm in order for the 1730 mg/kg limit to be met. Soluble SO_4 can be easily removed by washing, especially from fine particles. However, the solubility of sulphate depends upon the minerals in which it is bound, so (for instance) treating the coarse fraction is more problematic due to the presence of relatively insoluble minerals such as gypsum or ettringite.

Cu leaching can also be controlled by reducing the conductivity to below a critical threshold, since it was found to be correlated with SO_4 leaching: if the copper content has to be <0.9 mg/kg (according to the SQD), SO_4 leaching should be <1000 mg/kg and the conductivity <1 mS/cm. Other possibly influential factors that have been noted by other authors, but were not found during this research include: Cu complexation with organic matter (Sloot et al. 1997), adsorption to Al- and Fe-(hydr)oxides (Meima and Comans 1998) and pH dependency, with a reported minimum at pH 9-10.

The Mo leaching can be decreased by reducing the fine particles (<75 μm) in the fraction and the non-ferrous metal content. When the mass of fine particles is reduced to below 4-5%, Mo leaching will also be reduced to below 1 mg/kg (the limit stipulated by the SQD).
Sb leaching was correlated with SO_4 leaching and NH_4 leaching. No other significant correlations with Sb leaching were found, but there was an indication of a possible correlation with pH; Sb leaching decreased as pH increased. A similar pH effect was found by Comans (Comans et al. 1993). Thus, Sb leaching can possibly be predicted using a conductivity meter. High conductivity indicates that SO_4 and Sb leaching will be high. Metals can be reduced by reducing pH by adding CO_2 to the suspension of water (Svensson et al. 2005). After the formation of carbonates, an excess addition of CO_2 leads to their decomposition and mobilization of carbonate formers (Ecke 2001). Carbonic acid (H_2CO_3) dissolves calcite ($CaCO_3$) that buffers at a moderate alkaline level and decreases

the pH to an acidic level where the solubility of metals is increased (Todorovic and Ecke 2006).

Levels of the critical elements in the AEB BA products can be reduced to below the leaching limits by reducing levels of fines, organics and salts by modifying the separation settings, using an adequate amount of water, and using an extra washing system at the end of each separation of each building product. The quality of the process water should be controlled by measuring the conductivity, and taking steps to reduce it if necessary. Similarly, the quality of building products can be controlled by using sensors to measure their organic and metals contents, and taking appropriate steps when needed. Cu and Mo leaching can be reduced by reducing the amount of sewage sludge incinerated with household waste. However, these are preliminary conclusions from analyses of samples from mini-plant and Pilot plant II. Therefore, further research should be performed to determine the optimal parameters and levels for reducing the leaching.

Modelling showed that the final concentrations of elements in eluate K7 can be predicted for L/S=10 l/kg from their concentrations in the first three eluates from the column test, K3-K5. The model obtained provides robust indications for five critical elements (SO_4, Cl, Cu, Mo, Sb), the behaviour of which is adequately described by an empirically derived formula, based on their physical behaviour in the column. The model provides accurate predictions for all of the considered elements except Sb. An advantage of this model is that it can be used of BA products of any quality.

The experiment in which correlations between leaching values obtained from the shaking and column test found correlations for some ions. Notably, a correlation was found for SO_4. The leaching of metals (Cu, Mo, Sb) did not show any correlation between the results from the shaking test versus the column test. Therefore, the column test can be replaced by the shaking test (which is faster and cheaper) for measurements of SO_4. The results obtained by the shaking test for the coarse fraction were on average 36% higher than corresponding results obtained by the column test. The leaching of the fine fraction showed a similar relationships; the results of the shaking test were on average 22% higher. However, for the sand fraction a correlation between SO_4 values from the two tests was only found in analyses of samples collected from the mini-plant in 2005, and there was no significant correlation between the results of the two tests for this fraction. The correlations between the values yielded by the shaking and column tests for Cl leaching need to be further investigated, partly because the leaching of Cl is correlated with the organics content of the material (which was higher in the samples examined in 2006 than in those examined in 2005). In addition, the leaching values of metals (Cu, Mo, Sb) obtained from the shaking and column tests showed no significant correlations.

The last two experiments examined the statistical error between values obtained from the shaking test and column tests for duplicate samples, and the potential difference in leaching measurements obtained using a column of regular size and a larger column. The variance of leaching values for duplicate samples measured by the column test and the duplicates measured by the shaking test was in many cases very small, generally <10%. The highest variance was for Sb (measured by the column test) and for Cu and Cl in the 2-6 mm and 6-20 mm aggregate. The values from the shaking test show that the variance of leaching values for metals tend to be higher in the fine fraction, which can be explained

by the small size of the sample, before milling, used for the tests. The results of measurements of duplicate samples in two differently sized columns show that the size of the column does not significantly influence the leaching values.

5.7 Discussion of the Results

- The correlations in the data acquired in this study were examined by SPSS software using binary correlation analysis to obtain preliminary indications of relationships amongst leaching values of the monitored elements in fractions from mini-pilot and Pilot plant II. Further research is needed to determine more comprehensively the optimal process settings for reducing leaching values of these fractions to below target limits.
- Results obtained from mini-plant samples from 2005 and samples from the pilot plant in Amsterdam in 2006 generally showed little correspondence. The process at the mini-plant was less consistent and resulted in generally higher leaching values. The results of analyses of samples from the pilot plant in Amsterdam should be considered as the most relevant.
- Results obtained from the same leachant, but different grain sizes (sand, 2-6 mm, 6-20 mm) showed little correspondence.
- It is generally not easy to identify simple process parameters that could effectively reduce leaching. The one exception is rinsing, which directly reduces chloride levels, and is important for building application since it reduces conductivity, which in turn reduces several other leaching mechanisms.
- Leaching limits can be modified by adjusting the separation settings, reducing amounts of fines, organics and salts by using an adequate amount of water and by using an extra washing system at the end of each separation of every building product.
- The quality of the process water should be controlled by taking conductivity measurements, and making appropriate adjustments if necessary.
- The quality of building products can be checked by using sensors to monitor their organic and metals contents.
- Cu and Mo leaching can be reduced by reducing the amount of sewage sludge incinerated with household waste.

Chapter 6

Building Products from Bottom Ash

Summary

The sand, fine aggregate and coarse aggregate fractions that result from wet physical separation of bottom ash (BA) show potential as raw materials for lime-sand stone, asphalt and concrete. Together, the three fractions comprise 80% of the input, hence optimization of their quality and applications is important from both ecological and economic perspectives.

The most common use of the mineral fraction of BA in Western Europe is unbound, as road filler. Provided that its ferrous metal and aluminium contents are not too high, the material is particularly suitable for this application because it is slightly pozzolanic. At present, the road filler application is limited to dry-treated BA due to environmental problems (Chapter 5). In countries where the material needs to be isolated by an impermeable lining, the mineral fraction of dry-treated BA has a negative economic value, i.e. incinerators typically pay users €5 to €10 per tonne to take it. However, if BA is separated by wet separation and the contents of organics, metals and fines are sufficiently reduced to solve the environmental problems, the material can compete with granulated EOL concrete, and its application as a road filler may have a small positive value up to €7 per tonne. Leaching results for wet-treated BA indicate that this route is viable if there is stable legislation and unfavourable leaching limits are not imposed.

The mineral fractions from wet-separated BA show similar qualities to those of natural aggregate and sand. Therefore, they can be utilized as a substitute for natural aggregate and sand in many bound applications, depending on the market situation and the criteria imposed by the relevant building legislation. The main problems are related to the composition (metals content, LOI) and the mechanical properties (elasticity, strength, etc.) of the resulting product.

One of the simplest solutions for direct utilization of the mineral fractions of wet-treated BA is to certify them according to the relevant building legislation and directly sell them as certified aggregates to customers. If this course of action is adopted, customers will determine the future utilization of the aggregates (e.g., in asphalt, concrete, lime-sand stone, etc.), depending on their characteristics and quality requirements.

This chapter relates quality requirements to measured properties of mineral BA products for various utilization options and building applications. All three

AEB building fractions (6-20 mm aggregate, 2-6 mm aggregate and CCS-2 mm sand) were characterized according to standard tests for aggregates. Furthermore, these upgraded building products were utilized in concrete, asphalt and lime-sand stone. The results show their chemical, geometrical and mechanical properties and demonstrate the advantages and disadvantages of the utilization of these products.

6.1 Introduction

Improved BA aggregates can be utilized in many ways, based on relevant specifications stipulated by building legislation. In recent years BA has been tested as an alternative material for both concrete (Pera et al. 1997, Bertolini et al. 2004) and cement (Saikia et al. 2007, Pan et al. 2007). Results of these investigations show that BA has similar mechanical properties to natural building materials (Bertolini et al. 2004).

There are specific quality requirements for aggregates used in concrete and asphalt. The general EU regulations for building materials are set out in the European Construction Products Directive (89/106/EG), which applies to construction products and requirements for construction work. However, the European Construction Product Directive is mainly concerned with technical criteria, rather than environmental or health criteria. If secondary building material is used in the Netherlands, it must also fulfil the environmental rules imposed by the Soil Quality Decree (SQD).

The Dutch government has also passed national legislation for building materials, including: RAW 2005 (specific testing requirements) and certification requirements according to BRL 2506 BSA for aggregates, BRL 9311 for asphalt and concrete, BRL 9320 for asphalt and BRL 9321 for sand and gravel, etc. In 2002 the first Dutch standards for aggregates were harmonized with European standards (Table 6.1).

Table 6.1: Dutch standards for building materials harmonized with European standards.

EU product standards	Dutch standards	Subject
NEN-EN 12620	NEN 5905 and testing standards NEN 5905-5945	Aggregates for concrete
NEN-EN 13139	NEN 3835 (only parts for building materials & mortar)	Aggregates for mortar
NEN-EN 13055-1	NEN 3543	Lightweight aggregates for concrete, mortar and grout
NEN-EN 1304	NVN 6240 & NEN 3975 & testing NEN/NVN 6241-6251 and NEN 3975-3984	Aggregates for bituminous mixtures and surface standards treatments for roads, airfields and other trafficked areas
NEN-EN 13450		Aggregates for railway ballast
NEN-EN 13242		Aggregates for unbound and hydraulically bound materials for use in civil engineering work and road construction
NEN-EN 13383-1	NEN 5180 and testing standards NEN 5181-5188	Armourstone

Due to this harmonization the products can be certified with the CE, which is important if the material is to be used in EU countries. The Dutch certification system (for example KOMO, the Dutch quality mark for building products administrated by the Dutch foundation for quality for the construction sector) works on a voluntary basis. The system of legal and market requirements for

building products in the Netherlands is summarized in Table 6.2.

Table 6.2: Legal requirements for building products in the Netherlands.

	Building product	Buildings/works
Legal requirements in EU/Netherlands	EU Construction Products Directive = apply EU testing methods and required form of attestation or conformity. Required: CE	SQD=level of requirements set for buildings. Demonstrate via: KOMO (BRL) or demonstrate it oneself
	Netherlands SQD for stony building products. Demonstrate via: KOMO (BRL) or NL BSB (BRL) or Demonstrate it oneself	
Market requirements in Netherlands	BRL; selection on private requirements. Agreements between clients-providers concerning aspects such as color, evenness, transport, storage, durability: KOMO	BRL; section on private requirements. Agreements between clients-providers concerning applications in building structures, such as processing, installation, connection: KOMO

BRL = nationale Beoordelingsrichtlijn (National Assessment Guideline) accepted by the Harmonization Commission for the Building Industry.

Each regulation for utilization in asphalt, concrete etc. has specifications for composition of aggregates.
For example, EN 12620:2002+A1:2008 (aggregates for concrete) describes proportions of constituent materials permitted in coarse aggregate (e.g. amounts of floating materials in volume, and miscellaneous materials such as metals, non-floating wood, plastic and rubber).

For example, the certification according to BRL 9311 (BRL 9311, 2005), recycled materials for the production of asphalt and concrete are required to have the following physical properties:

- natural mineral, minimum content 97% (m/m)
- other mineral, maximum content 2% (m/m)
- non-mineral materials (plastics, metals, rubber, etc.) 1% (m/m and V/V)
- digestible organic material, maximum content 0.1% (m/m)

According to NEN 3543 (pertaining to coarse lightweight aggregates for lightweight concrete) the limits are:

- loss on ignition, maximum 5% (m/m),
- particles smaller than 0.063 (fines) maximum 2%.
- Chloride, maximum content 0.02%
- Sulphate (measured as SO_3) maximum content 1%

The limits for MSWI BA according to BRL 2307 are 5% for loss on ignition and 3% for organic content.

The main problems associated with building materials from untreated or dry treated BA are their high organic content and presence of metals. Dry-

processed BA from the Amsterdam incinerator contains 1 to 5%, by mass, of organics. Analysis of the organics in BA shows that two kinds of organic materials contribute to its organic matter content. One kind consists of plastics, wood and rubber particles of a comparable particle size to that of the stony fraction in which they are found (mainly in 6-20 mm aggregate). The second material is fine organics, which contribute to the loss on ignition (LOI). It is believed that the two types of organics may have different effects on the quality of building material products. The fine organics are potentially chemically reactive and are related to the leaching of heavy metals, while the coarse organics adversely affect the mechanical properties of the products. High organic content is detrimental to the strength of concrete and is believed to increase leaching values of aggregates. Another negative aspect of high organic content is that it adversely affects the resilient modulus of concrete in which the material is used, which is mainly important for road construction. The Swedish geotechnical institute found that the resilient modulus increased by 50% (from approximately 80 MPa to 120 MPa) when the content of organic matter was halved from 8% to 4%, (Arm 2004). An earlier Swedish study (Arm 2004) also showed that the E-modulus of concrete was considerably reduced by the presence of 6%, by weight, of organic matter in the material with a grain size less than 2 mm.

The second problem with utilizing BA for building products is the presence of metallic particles like ferrous metals and non-ferrous metals. The most problematic are ferrous metals and aluminium, which expand during oxidation and create cracks. Another problem is the visual effect of large metallic particles in the concrete.

BA aggregates after wet physical separation can often meet technical and environmental criteria for such an application. However, they must be cheaper to compete with natural aggregates. Average prices of natural aggregates in various countries (in 2007) are shown in Figure 6.1.

Another economic issue is the additional cost related to the higher moisture content and porosity of the materials. Due to the high moisture content there are additional costs for drying the material before utilization in concrete, asphalt, etc. With regard to porosity, problems arise when aggregates are utilized in asphalt, because the material requires more bitumen. The price of bitumen was around €250 per tonne in 2007, and around €400 per tonne in 2008.

The studies presented in this chapter investigated the quality of AEB building products (sand, fine aggregate and coarse aggregate) that were separated from Amsterdam BA. The aim was to demonstrate that AEB building products are comparable to natural materials and thus can meet European quality criteria. The quality challenges associated with those BA products, mainly the oxidizing effects of iron and aluminium, were eliminated by the advanced wet separation system described in the preceding chapter. Several tests (Table 6.3) were performed on AEB building products that had relatively high organic and metals contents since the pilot plant settings had not yet been fully optimized. Therefore, the results gave only initial indications of the characteristics and suggest aspects that require further research. The aggregates were further tested for utilization in concrete, lime-sand stone (LSS) and high density asphalt (DAC). The principal investigation focused on asphalt created from all AEB building products, including the sludge fraction (0-CCS mm). Several tests were performed to assess the durability and mechanical properties (density, grading, Marshall Test, ITT, etc.) of AEB asphalt.

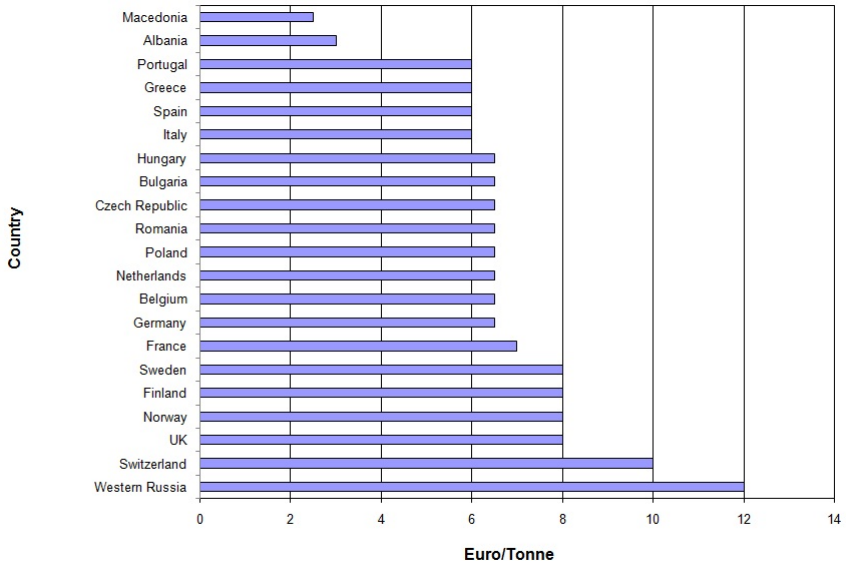

Figure 6.1: Average prices of natural aggregates in 2007 (Umweltbundesamt n.d.)

.

6.2 Characterization of AEB Building Products

AEB products (0-CCS mm sludge, CCS-2 mm sand, 2-6 mm fine aggregate and 6-20 mm coarse aggregate) were characterized using samples collected in 2006 from AEB Pilot plant II. It should be noted that the composition of these samples was not optimal at this time, since the plant had not been fully developed. AEB products were tested according to the standard for aggregates NEN-EN 12620 (Dutch version NEN 5905), see Table 6.3. Tests on all the fractions were performed by a certified laboratory except the sludge fraction, which was analyzed by TU Delft.

6.2.1 AEB Sludge

The sludge was evaluated in terms of grain size distribution, loss on ignition (LOI), organic content and leaching values (as determined by the column test according to NEN 7343). The grain size distribution results are shown in Table 6.10. The LOI measured in 2005 and 2006 was 31.6%±0.9% and 20%±0.5%, respectively. The leaching values for the sludge from 2002 and 2006 measured by the column test are shown in Table 6.4.

In some cases the leaching values in Table 6.4 from 2006 exceeded those measured in 2002. This could be because in 2005 sewage sludge started to be incinerated together with household waste. The sewage sludge is probably the reason for increased leaching values for Mo, F, Se, SO_4, Cl and Cu. The characteristics of the sludge relevant to its utilization as an asphalt additive were also examined, and the results are discussed in section 6.3.3.

Table 6.3: Tests applied for analyzing aggregates from BA.

Analysis	Technique	Standard
Quartering (sample reduction)		NEN-EN 932-2
Loose bulk density and voids		NEN-EN 1097-3
Susceptibility for alkali-aggregate reaction		NEN 5925 (1988)
Water-soluble chloride salts	titration	NEN-EN 1744-1 par. 8
Humus content	visual	NEN-EN 1744-1 par. 15.1
Fulvo acid content	visual	NEN-EN 1744-1 par. 15.2
Laboratory samples reduction		NEN-EN 932-2
Fines content	gravimetric	NEN-EN 933-1
Highly expanding clay minerals content		NEN 5941 (1988)
Grading	gravimetric	NEN-EN 933-1
Density 4-31.5 mm (particle density)	gravimetric	NEN-EN 1097-6
Water absorption (24 hours)	gravimetric	NEN-EN 1097-6

6.2.2 AEB Sand and Aggregates

The AEB sand and aggregate were tested to determine their density, chloride contents, fines contents, water absorption, and various other relevant parameters, as shown in Table 6.5, and their grain size distributions, as plotted in Figures 6.2, 6.3 and 6.4.

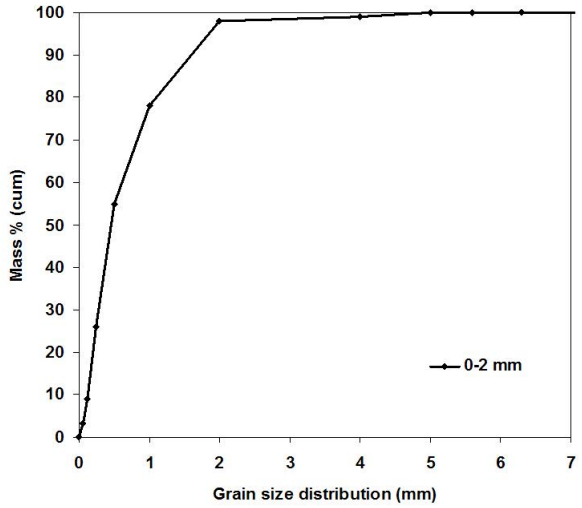

Figure 6.2: Grain size distribution of AEB sand product measured in 2006.

For the sand product, neither the alkali silica reaction nor the fulvo acidic content were measured. A first conclusion is that the AEB sand (particle density) was less dense than regular sand, presumably due to the higher organic content in the sand product at this time.
One of the organic constituents that was over the limit at this time was hu-

Table 6.4: Leaching values (column test) for sludge samples collected in 2002 and 2006.

	2002		2006	
	$L/S = 1.8$	$L/S = 10$	$L/S = 1$	$L/S = 10$
Cu	3.5	8.4	**14**	31
Mo	0.38	1.17	**3.4**	9.6
Sb	0.35	1.8	<0.03	<0.03
Br	4.7	6.4	n.m.	n.m.
As	<0.04	<0.2	<0.03	<0.03
Ba	<0.2	<0.8	0.4	1.2
Cd	<0.003	<0.007	<0.02	<0.02
Cl	2100	2200	5490	7205
Cr	<0.6	<1	1	3
Co	<0.01	<0.07	n.m.	n.m.
F	<0.53	<2.2	234	**<u>348</u>**
Hg	<0.001	<0.005	<0.03	<0.03
Pb	<0.05	<0.3	<0.05	<0.05
Ni	<0.06	<0.2	0.2	0.3
Se	0.048	0.083	**1.2**	**<u>4.4</u>**
SO_4	4300	14000	3188	19213
Sn	0.36	1	n.m.	n.m.
V	<0.05	<0.3	n.m.	n.m.
Zn	<0.1	<0.7	<0.02	<0.02

Values in bold exceed the Dutch landfill directive limits indicating that the sludge must be land filled, category C2 (Chapter 1).
The underlined values in bold exceeded European land fill directive limits for non-hazardous waste (Chapter 1).

mus (which is formed in the ground by the decomposition of animal and plant residues). The content of humus is estimated from the resulting colour when a test portion is shaken in a sodium hydroxide solution. For 2-6 mm aggregates, neither the alkali silica reaction nor the fulvo acidic and humus contents were measured. However, the density of the particles was lower than that of regular aggregates. The AEB 6-20 mm aggregate was also tested to determine its values for the properties that were determined for the sand and fine aggregates, including sulphur, light materials and organic contents, reactive iron sulphide particles and Los-Angeles test values. The results show that AEB 6-20 mm aggregate has similar characteristics to those of natural aggregates except that the particles are less dense due to their higher porosity.

6.3 Products from AEB Aggregate

6.3.1 Concrete

Several studies performed on concrete made from MSWI BA have shown that the major problems of poor durability and workability are caused by the presence of metallic aluminium particles (Bertolini et al. 2004, Müller and Rübner 2006) and glass (Müller and Rübner 2006). The reaction of aluminium with cement

Table 6.5: Results of analyses of AEB sand and aggregate products according to NEN-EN 12620.

	CCS-2 mm	2-6 mm	6-20 mm
Bulk density of particles	0.961 Mg/m	1.050 Mg/m^3	1.077 Mg/m^3
Water soluble chloride salts	0.20% (m/m) d.s.	0.05 % (m/m) d.s.	0.04% (m/m) d.s.
Humus	Over the limit	not measured	No fine particles
Fines content	3.2% (m/m)	1.2%(m/m)	0.6%(m/m)
Sharpness of fine materials	Not dangerous	Not dangerous	Not dangerous
Density of the fraction	2.10 Mg/m^3	2.2 Mg/m^3	2.16 Mg/m3
Water absorption (24 hours)	5.6%	7%	4.8%
Light materials (LPC)	not measured	not measured	6.0% (m/m)
Organic content (LOPC)	not measured	not measured	0.0% (m/m)
Sulphate, measurement (SO_3)	not measured	not measured	0.3% (m/m) d.s.
Fulvo acid content	not measured	not measured	Not influence
Reaction iron sulfide particles	not measured	not measured	None
Fines content	not measured	not measured	0.6% (m/m)
Los-Angeles coefficient	not measured	not measured	41% (m/m)

paste forms aluminium hydroxide, aluminates and hydrogen. The reaction can proceed long after the concrete hardens and if it occurs near the surface region at a high rate, spalling (crumbling) will occur. Glass particles cause problems because of the potential for silica gel formation. In our case the aluminium in aggregate was separated by an eddy current separator (Chapter 3) thus, the potential for adverse reactions was minimized. A mixture of fine and coarse AEB aggregates was used to create the first aggregate concrete, in 2004 when the process was still not fully optimized, thus this test was a provisory test which will be repeated in the future. The results showed that the aggregate contained large foreign particles, mainly of stainless steel and organics (wood, plastics, bones), which reduce its quality (especially visual). Another problem was the low particle density, but this could be circumvented if the mixture was used as a light-weight aggregate. The concrete mixture was made by adding 30% of AEB aggregate, the rest was regular aggregate. An example of concrete made using the aggregate is shown in Figure 6.5.

A sample was made to test the compressive strength. The results show that the compressive strength of AEB concrete after 28 days was 41.5 MPa, while that of a reference concrete without BA, according to (Müller and Rübner 2006) (2006), was 36.2 MPa after 28 days.

The preliminary tests indicate there is scope for using AEB aggregates in concrete. It is recommended for the next testing to improve the quality of aggregates by optimizing the settings of the installation in order to decrease the amount of large organic particles and stainless steel, and use the recommended test methods according to standards. The focus of the tests should be on checking the grain size distribution, density and shape of the particles and their organic and metal contents. If those parameters are in accordance with the limits then tests on workability and durability can be applied.

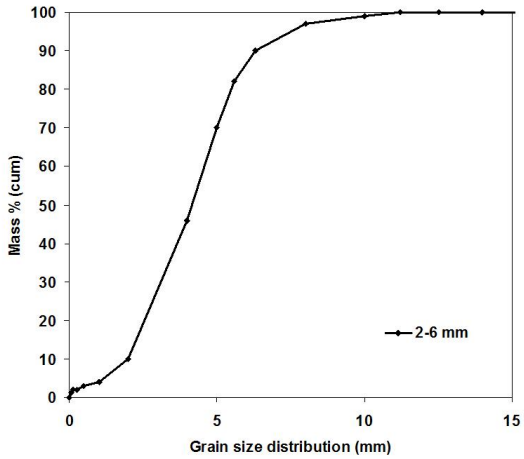

Figure 6.3: Grain size distribution of AEB 2-6 mm aggregate measured in 2006.

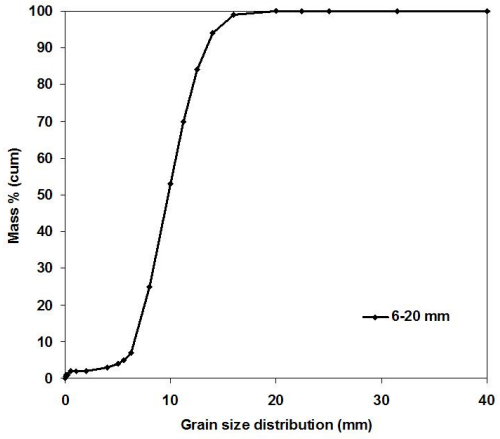

Figure 6.4: Grain size distribution of AEB 6-20 mm aggregate measured in 2006.

6.3.2 Lime Sand Stone

In another experiment, sand products obtained after wet physical separation of BA from the plant and the laboratory (using jigging, magnetic and a shaking table) were used to make lime-sand stone (LSS). A sample of the LSS was investigated by the diffusion test (NEN7345 1995), and the results are shown in Table 6.6.

The results show that all of the measured elements meet SQD limits. The LSS was not further investigated by mechanical tests because the visual quality revealed the presence of metallic aluminium. The surface was destroyed by cracks due to aluminium oxidation (Figure 6.6).

Therefore, the quality of AEB sand must be improved by oxidizing the alu-

Figure 6.5: Concrete sample made with 30% of AEB aggregate mixture.

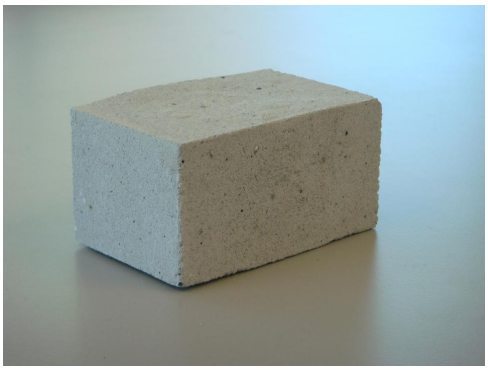

Figure 6.6: Lime-sand stone made from AEB sand product (in 2004).

minium before making LSS, or it should be used in other products, e.g. aerated autoclave concrete (AAC) in which the presence of aluminium is advantageous (Chapter 4).

6.3.3 Asphalt

Various types of asphalt mixtures (porous asphalt, stone mastic asphalt, dense graded asphalt concrete, open graded asphalt concrete, crushed gravel asphalt concrete, gravel asphalt concrete etc.) are used for different pavement layers (a base layer, a binder layer and a top layer). An asphalt mixture can be considered to consist of two phases, a mineral aggregate phase (stone skeleton, sand skeleton, filler skeleton or some intermediate between these types of skeletons) and a binder phase (mastic - i.e. a mixture of sand, filler and bitumen or mortar) (Molenaar 2003). To assess the potential for using AEB products in asphalt, dense asphalt (DAC) containing a stone skeleton mixture filled with AEB products (0-CCS mm sludge, CCS-2 mm sand product and 2-20 mm aggregates), and a mastic containing AEB sludge (0-CCS mm fraction) were also made and tested.

Dense asphalt mixtures (DAC) are suitable for application in wearing courses (top layers). Dense mixtures are durable and require higher quality because they form the top pavement layer for traffic classes 3 or 4 (RAW bepalingen 2005). The extremely dense mixture provides high resistance to deformation and has a low voids content, which is important for minimizing the disintegrating influ-

Table 6.6: Results of the diffusion test (NEN 7345-1995)(NEN7345 1995) applied to the LSS (in 2004) and limits for moulded construction materials in mg/m^2 according to the SQD (SQD 2007).

	Sample average E_{64d} in mg/m^2	Moulded cons. mat. limits (E_{64d}) in mg/m^2
Cu	1.2	98
Mo	1.2	144
Sb	n.m.	8.7
Br	n.m.	670[2]
As	n.m.	260
Ba	n.m.	1500
Cd	1.2	3.8
Cl	227.4	110000[2]
Cr	1.2	120
Co	n.m.	60
F	n.m.	2500[2]
Hg	n.m.	1.4
Pb	1.2	400
Ni	1.2	81
Se	n.m.	4.8
SO_4	810.0	165000[2]
Sn	n.m.	50
V	n.m.	320[1]
Zn	1.2	800

1 Requirement of 460 mg/m^2 for vanadium applies in the case of the use of solid building materials in large surface water and a requirement of 4.6 mg/kg dry matter applies in the case of granulate materials.

2 The following applies to the use of building materials in places where direct contact is possible with seawater or brackish surface water with a natural chloride content of more than 5.000,mg/l: a) No emission requirements for chloride and bromide, and b) the emission requirements given in the table for fluoride and sulphate multiplied by a factor of 4.

ences of penetrating water. The dense wearing course should provide protection against penetration of the lower asphalt layer. The mastic is applied mainly for its durability and resistance to permanent deformation. It also affords higher noise reduction and drainage capacity in comparison to sensed asphalt.

The first part of the research focused on the characteristics of AEB products (density, porosity, grading and characteristics of fillers) that were used to make high density asphalt (DAC). The mechanical properties of each of the mixtures were investigated, and the results have been presented in a TU Delft internal report (van de Ven et al. 2006). The most important results of this research are outlined below for:

- Marshall test (2x75 blows and 2x50 blows)
- Indirect tensile strength (ITS) and ITSR
- Indirect tensile test (ITT)
- Dynamic uniaxial compression creep test

6.3.3.1 Characteristics of the AEB Products Used for the Asphalt

Grain Size Distribution
The grain size distributions of the first three size fractions (CCS-2 mm, 2-6 mm and 6-20 mm) were analyzed, and the results are shown in Tables 6.9, 6.8 and 6.7, respectively.

Table 6.7: Grain size distribution of the AEB 6-20 mm aggregate measured in 2006.

Screen size (mm)	Weight (g)	Oversize (%)	Oversize cum (%)
20	6.3	0.32	0.32
16	5.6	0.28	0.60
11.2	503.9	25.21	25.80
8	1020.8	51.07	76.87
5.6	417.9	20.91	97.77
2	28.5	1.43	99.20
>0.063	16	0.80	100.00

Table 6.8: Grain size distribution of the AEB 2-6 mm aggregate measured in 2006.

Screen size (mm)	Weight (g)	Oversize (%)	Oversize cum (%)
20	0	0.00	0.00
16	0	0.00	0.00
11.2	2.2	0.15	0.15
8	42	2.80	2.95
5.6	243.8	16.27	19.22
2	1054.5	70.37	89.59
1	122.3	8.16	97.75
0.5	19.9	1.33	99.08
0.25	5.7	0.38	99.46
0.125	3.2	0.21	99.67
0.063	2.5	0.17	99.84
<0.063	2.4	0.16	100.00

The 6-20 mm and 2-6 mm fractions were screened to the following sizes: 11.2-16 mm, 8-11.2 mm, 5.6-8 mm and 2-5.6 mm according to RAW (RAW bepalingen 2005). The grain size distribution of the AEB sand was difficult to determine due to its high organic content (which resulted in an accumulation of masses that could not be screened).

The grain size distribution of sludge was investigated by the hydrometer test. This sludge contains very light materials (organics) which caused problems in measuring the grain size distribution (as for the sand fraction). Due to the structure of the sludge it was not possible to determine the correct grain size distribution by either dry or wet screening.

Table 6.10 shows that approximately 10% of the material was smaller than 2 μm. Due to the high very fine particles content it was decided not to use the

Table 6.9: Grain size distribution of the AEB sand product (CCS-2 mm) measured in 2006.

Screen size (mm)	Weight (g)	Oversize (%)	Oversize cum (%)
2	36.5	7.30	7.30
1	132.6	26.53	33.83
0.5	116.9	23.39	57.22
0.25	124.1	24.83	82.05
0.125	76.5	15.31	97.36
0.063	11.6	2.32	99.68
>0.063	1.6	0.32	100.00

sludge in the asphalt (as a substitute for regular filler). Therefore, AEB sludge was used to make mastic, to obtain a better understand of its behaviour in this kind of application (van de Ven et al. 2006).

Density
The maximal densities of six different size fractions of AEB products were measured by a pyknometer. The results are shown in Table 6.11.

The density of the largest fraction was difficult to measure due to the high porosity of the particles. Therefore, the bulk density of this fraction was measured. These measurements gave more accurate results (Table 6.12) and showed it to have similar bulk density to those of normal raw aggregates used in DAC 0/16.

6.3.3.2 Asphalt Mixture

A DAC was made from a mixture of AEB products that was heavier than the standard mixture according to RAW (RAW bepalingen 2005). The composition of the regular mixture according to RAW 2005 is shown in Table 6.13.

The AEB asphalt mixture (Table 6.14) was made according to the mixture shown in Table 6.13.

In DAC 0/16 (for class 4 traffic), 6% of bitumen 40/60 is needed. However, when this mixture was produced with the AEB aggregate some bitumen was absorbed, resulting in a very dry mixture. Therefore the bitumen content needs to be increased to 7% if AEB aggregate is used with no other aggregate, but increasing the bitumen content means that the DAC does not meet regulations concerning its composition (RAW bepalingen 2005).

6.3.3.3 Mechanical Tests

All mechanical tests were performed on the sample mixture shown in Table 6.14.

Marshall Test
Asphalt mixture design is officially standardized in the Netherlands, and is based on the Marshall method according to RAW. This is intended to optimize the binder content in the mixture. The Marshall test was performed on three different asphalt samples (cylindrical sample with height of 60 mm and diameter

Table 6.10: Grain size distribution of the sludge <CCS mm collected in 2006.

Size (mm)	Mass through (%)
37.5	100.00
20	100.00
10.0	100.00
6.3	100.00
3.35	100.00
2.00	100.00
1.180	100.00
0.600	100.00
0.300	100.00
0.150	100.00
0.077	100.00
0.063	60.63
0.05605	53.35
0.04049	45.11
0.02916	37.83
0.01573	26.68
0.01232	23.28
0.00612	17.46
0.00341	13.10
0.00160	8.73

of 101.4 mm) made from AEB products. The aim was to create DAC 0/16 for class 4.

Three asphalt samples were made of three different mixtures, designated T1, T2 and T3:
T1. mixture according to Table 6.4, AEB sludge, and a higher binder percentage.
T2. mixture according to Table 6.4 and AEB sludge.
T3. mixture according to Table 6.4 and regular filler.

Two Marshall tests were performed, in each case using 2 x 75 blows and 2 x 50 blows. The goal was to create a high density asphalt (DAC), therefore according

Table 6.11: Densities of particles in different size fractions of AEB products measured by pyknometer.

Fraction	Particle density (g/cc)
11.2-16	2.55
8-11.2	2.63
5.6-8	2.70
2-5.6	2.76
Sand	2.77
Sludge (<0.063 mm)	2.41

Table 6.12: Bulk density of four size fractions.

Fraction	Bulk density (g/cc)
11.2 - 16	2.24
8 - 11.2	2.32
5.6 - 8	2.33
2 - 5.6	2.27

Table 6.13: Regular asphalt 0/16 in % (m/m) according to RAW (RAW bepalingen 2005).

Screen	Recommended	Min.	Max.
C16	-	0.0	6.0
C11.2	-	5.0	25.0
C8	-	-	-
C5.6	-	30.0	55.0
2 mm	60.0	57.0	63.0
63 μm	-	y-0.5	y+1.0
Bitumen (class 4)	-	6.0	6.4

to RAW standards the 2 x 75 blows Marshall test is required. Standard (for example binder layer) asphalt should be tested by a 2 x 50 blows Marshall test. The results of applying the Marshall test using 2 x 75 blows and 2 x 50 blows to each of the three asphalt mixtures are shown in Tables 6.15 and 6.16, respectively.

The results of the 2 x 75 blow tests show that all three asphalt samples met the requirement for class 4, and the T3 sample met the requirement for class 5 according to the 2 x 50 blows test. The findings indicate that the optimal mixture for AEB DAC is that shown in Table 6.17.

The T3 sample after the Marshall test (2 x 50 blows) was screened to investigate how many particles in each fraction were crushed. Results for two samples

Table 6.14: AEB DAC (based on the composition in Table 6.13 and data presented by Ghile (Ghile 2006).

Fraction	% (m/m)
22.4 - 16	0.0%
16 - 11.2	11.5%
11.2 - 8	10.5%
8 - 5.6	11.5%
5.6 - 2	20.8%
Sand	39.0%
Wigro	6.7%
Bitumen 40/60	6.0%
	106.0%

Table 6.15: Results of applying the Marshall test (2 x 75 blows) to three samples: T1, T2 and T3.

	Class 4				
	Min.	Max.	T1	T2	T3
Marshall stability P_m (N)	7500	-	8600	8900	9600
Marshall flow F_m (mm)	2.0	4.0	2.6	2.2	2.0
Marshall quotient Q_m (N/mm)	3000	-	3308	4045	4800

Table 6.16: Results of applying the Marshall test (2 x 50 blows) to sample T3.

	Class 4		
	Min.	Max.	T3 50 blows
Marshall stability P_m (N)	7500	-	8100
Marshall flow F_m (mm)	2.0	4.0	2.4
Marshall quotient Q_m (N/mm)	3000	-	3375

(I and II) are shown in Table 6.18.

The results of this experiment show that approximately 20% of the larger fraction (16-11.2 mm en 11.2-8 mm) was crushed. This was due to the glass, ceramic and porous particles in the AEB aggregate, which increased the amount of fines.

Other Mechanical Tests (ITS, ITT, ITSR)

Indirect Tensile Strength Test (ITS) and Indirect Tensile Strength Ratio (ITSR)

The AEB DAC 0/16 mixture was subjected to ITS tests in dry and wet conditions to assess the effects of water, ITT (influence on water) and ITSR.

Table 6.17: Optimal mixture for DAC made from AEB products.

Fraction	Mass (g)
16-11.2	110.60
11.2-8	102.61
8-5.6	113.41
5.6-2	200.37
Sand	406.28
Sludge (<0.063 mm)	66.72
Bitumen*	70.00
Total	1070

* the mass of bitumen is too high according to RAW 2005, hence the composition should be further investigated.

Table 6.18: Input mixture used to make AEB DAC and the mixture following the Marshall test after extraction and screening.

Fraction	Mass (g)		
	Original mixture	After extraction	
		I	II
16-11.2	110.6	72.2	88.3
11.2-8	102.6	83	80.9
8-5.6	113.4	117.7	106.7
5.6-2	200.4	234.5	232.1
Sand	406.3	420.6	419.2
Filler	66.7	72	72.8
Total	1000.0	1000.0	1000.0

The results of the ITS tests are shown in Table 6.19.

Table 6.19: ITS tests results under dry and wet conditions for AEB DAC 0/16.

Temperature °C	ITS_{dry} (MPa)	ITS_{wet} (MPa)	ITSR (%)
5	2.04	1.27	62.39
15	1.14	0.74	64.64
25	0.69	0.36	52.44
35	0.34	0.22	65.37

The results in Table 6.19 indicate that the AEB samples, at all temperatures, had lower tensile strength than regular DAC (RAW bepalingen 2005). The ITSR ratio for the AEB DAC asphalt mixture was between 50% and 65%, which is lower than that of regular DAC (80% usually).

Indirect Tensile Test (ITT)

The ITT test was performed at four temperatures: 5, 15, 25 and 35°C, and five frequencies (0.5, 1, 2, 4 and 8 Hz). The results for the AEB DAC gave a maximal stiffness modulus of 10000 to 12000 MPa at 5°C and frequency of 8 Hz. This result is lower than the highest modulus according to the reference (Ghile 2006).

The results of indirect tensile fatigue tests (ITT fatigue) are shown in Table 6.20 for AEB DAC 0/16 and in Table 6.21 for regular DAC according to Ghile (Ghile 2006).

The results indicate that the AEB DAC is less resistant to ITT fatigue than the reference mixture (Ghile 2006). To understand and improve the AEB DAC in this respect further research is needed.

Dynamic uniaxial compression creep test

The dynamic uniaxial compression creep test was performed at two temperatures (40 and 50°C) with three stress levels (100, 200 and 300 kPa), a signal of one pulse per 200 msec and a pause period of 800 msec.

Table 6.20: Results of ITT fatigue tests at 5°C for the AEB DAC 0/16.

Sample	Density (kg/m^3)	σ (kPa)	N
AEB039	2029	852.2	27754
AEB036	2036	693.8	178920
AEB032	2014	537.0	320176
AEB031	1988	769.0	28280
AEB021	1988	613.7	32472
AEB040	2030	619.8	184016
AEB045	2024	730.0	46024
AEB037	2013	693.8	37112
AEB035	2025	650.8	26104
AEB044	2018	615.2	93592
AEB041	2021	539.6	191720

Table 6.21: Results of ITT fatigue tests at 5°C for reference DAC 0/16 samples.

Sample	Density (kg/m^3)	σ (kPa)	N
DACS-II-54	2431	759.0	204672
DACS-II-86	2451	890.0	113536
DACS-II-56	2438	1065.0	66240
DACS-II-87	2433	1246.1	31664
DACS-II-9	2446	1436.3	16248
DACS-II-48	2451	1597.5	11584
DACS-II-105	2433	1890.6	5296
DACS-II-61	2451	2179.5	2720

Figure 6.7 shows the K-slopes obtained for AEB DAC and regular DAC (Ghile 2006), which are similar at 40°C for 100 and 200 kPa, however the other deformations are substantially higher than those of the reference asphalt mixture.

6.3.3.4 Mastic from AEB Sludge

A mixture in which AEB sludge replaced regular filler in mastic was subjected to two mechanical tests: a rheological test using a dynamic shear rheometer (DSR) and the direct tension test (DTT). In comparative rheological tests, AEB mastic with a filler/bitumen ratio of $f/b = 0.5$ was found to have similar rheological properties to Wigro mastic (van de Ven et al. 2006) although its f/b ratio was lower than that of Wigro mastic ($f/b = 1.12$). Therefore, AEB sludge should be used in a lower concentration if used to make mastic. However, further research is needed. The DTT results show that AEB mastic has similar tensile strength to Wigro mastic. In one case the AEB mastic was even found to have higher tensile strength than Wigro mastic, but a greater tendency to break. This aspect should also be further investigated.

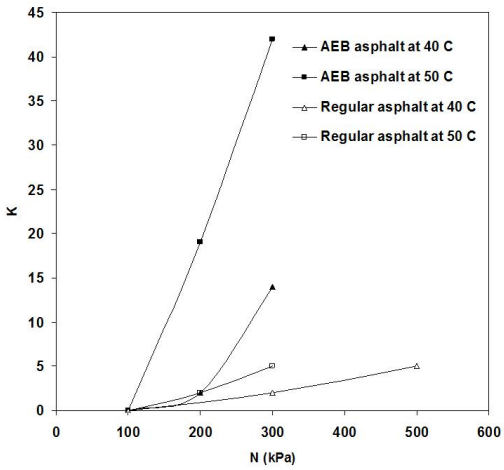

Figure 6.7: Permanent deformations observed in dynamic uniaxial compression creep tests at indicated temperatures of the AEB asphalt and the reference asphalt mixture (regular asphalt).

6.4 Conclusion

The AEB building products separated from MSWI BA by wet physical methods show improved quality (lower organics and metals contents) than MSWI BA separated by dry methods and MSWI BA that has not been treated at all. A critical aspect was that its aluminium content was too high to meet quality criteria (to avoid problems with oxidization in the concrete, etc.). The aluminium content of the >2 mm fraction was reduced, thereby improving the quality of AEB products. However, during this experiment, AEB building products were not completely optimized because the pilot plant still requires improvements that should greatly reduce the stainless steel and organic content of the BA.

AEB aggregates (2-6 mm, 6-20 mm) and sand (CCS-2 mm) show good characteristics. Their grain size distributions are similar to those of standard aggregates, but they are less dense than regular aggregates and have higher porosity, especially the 6-20 mm aggregate fraction. Porosity can create several problems for asphalt as well as for concrete in terms of durability and workability.

Two AEB aggregates (2-6 mm and 6-20 mm) were used to obtained first indications of the properties of concrete made with it. The mechanical properties were tested by compressive strength tests, which showed that the compressive strength after 28 days was 41.5 MPa; comparable to that of regular concrete (made using natural aggregates), even though the AEB aggregate was not fully optimized (especially in terms of its organic and stainless steel contents, which were too high).

The sand product was used to make lime-sand stone (LSS) in 2004, but the results were poor. The visual test indicated that the high aluminium content has a negative influence on the quality of LSS. Therefore an alternative is to use the AEB sand containing aluminium in aerated autoclave concrete (AAC). The AAC made in this way warrants further research; the economic and environmental impacts are described in Chapter 4. Most tests were performed on

aggregate, sand and sludge in high density asphalt (DAC). The results show that the size distribution of AEB aggregates is suitable for asphalt, but the AEB aggregate is less dense than normal aggregates.

Marshall tests (at 40°C and both 100 and 200 kPa) of the mechanical properties of DAC made from AEB aggregates and sand indicated that the deformation of AEB asphalt is comparable to that of reference DAC (Ghile 2006). However, tests of the influence of water found that the AEB DAC had an ITSR of 50-65%, substantially lower than that of regular DAC, which is usually 80%. This is due to the high porosity and presence of glass and ceramics in AEB aggregate. All values for AEB asphalt obtained in the tests were compared to those of regular DAC, which has higher quality requirements. Therefore, using AEB aggregate as a different quality asphalt for different applications (e.g. in a binder or base layer) may be an option.

Tests of an asphalt made using sludge as a filler did not yield promising results, therefore the sludge was excluded in further tests of AEB fractions in asphalt. Instead, the possibility of using the sludge as a filler in mastic was examined. The direct tension test (DTT) and dynamic shear rheometer (DSR) tests showed positive results for AEB mastic. AEB mastic with a filler to bitumen ratio of $f/b = 0.5$ proved to have similar rheological properties to Wigro mastic with an $f/b = 1.12$ ((van de Ven et al. 2006)). Therefore, AEB sludge has high potential for use in mastic.

Based on the initial tests with BA sand product and aggregates, its most promising applications appear to be in low quality asphalt and concrete. In addition, the BA aggregates products and sand could be utilized in the cement industry, although this possibility has not been examined during this study. In order to use the aggregates and sand for higher quality construction materials additional improvements are needed, such as reductions in the contents of organics (coarse and fine) and metals (especially iron and aluminium).

Chapter 7

Economic Overview of the Process

Summary

Wet physical separation processes are generally more expensive than dry treatments. However, the wet system can separate more metals from bottom ash and produce a higher quality building materials. The issue is the higher cost of the wet system, due to the extra equipment required for the distribution and treatment of process water, the dewatering and disposal of sludge and the associated labour costs. The investment costs of a wet bottom ash treatment are, on average, about €3 million for a capacity of 50 t/h. This high cost is due to the complex machinery required to separate BA into high quality products such as metals and materials for building purposes. The estimated process cost of the wet plant in Amsterdam is, on average, €20 per tonne; approximately double the costs of a conventional dry process.

The wet plant produces about 17 kg of non-ferrous metals per tonne of BA input, which is worth about €20. In addition, aggregate remaining after wet separation has a value of up to €7 per tonne, while the dry process may create products with costs rather than profits when utilized for road fillers (€-5 to €-10) or deposited in land fills (€-30 to €-80). The additional value of the products of the wet system compensates for the higher investments and running costs. Hence, despite the high process costs the overall outcome may be financially advantageous, depending on the utilization and separation options adopted, and product quality requirements.

This chapter discusses the investment and process costs of the wet system used at the pilot plant in Amsterdam under three scenarios. The first, basic, scenario is based on the current situation at AEB, which results in non-ferrous metals, ferrous metals, aggregate and sand products. The second scenario shows the financial benefit of applying an additional separation step to recover precious metals to be sold independently as additional products. The third scenario shows the financial benefits of using the sand product in the manufacture of aerated autoclave concrete (AAC), rather than as a regular sand product.

7.1 Introduction

The economic costs and benefits of wet and dry systems strongly depend on local factors and current prices of metals. Important local factors are the possibilities for using granulate (aggregate) in high-end building applications and dry-treated ash in road works, because in some European countries there are limitations on the use of BA as road filler.

An influential factor is the capacity of the plant in which the BA is to be separated. The high investment costs of the wet process become economic if the capacity is sufficiently high (>200000 t/y). For example, there will not be major differences in investment costs of wet plants with capacities of 50 t/h or 100 t/h, but the additional capacity increases the production of products from BA, thus resulting in higher profits.

The prices of metals have major impacts on the revenue. Metal prices rapidly increased from 2004 until mid-2008, then declined to 2002 prices and subsequently increased. Average LME prices for metals used in the calculations presented in this chapter are shown in Table 7.1. The prices of the non-ferrous metals fractions also vary depending on the sort of smelter they are sold to (brass, copper or precious metals smelters).

Table 7.1: Average LME prices from mid-2007 in €/kg.

	Average €/kg
Cu	4
Zn	2.3
Pb	2.5
Al	2.6
Au	15861
Ag	292

Other influential factors are the prices of other products and waste streams. Prices for such residues are calculated using prices of €5 per tonne for aggregates, €7 per tonne for sand, €100 per tonne for ferrous scrap and €30 per tonne for land filling aand are summarised in Table 7.2.

Table 7.2: Summary of prices used in the cost-benefit analysis presented in this chapter.

	Range €/tonne
Building products	5-7
Ferrous scrap metals	80-120
Land filling cost	30-80

Conventional dry physical separation treatment yields less ferrous and non ferrous metals than the wet system, and disposing of its residues incurs costs rather than making profits. These residues cannot be used as secondary building products without incurring extra costs for isolation. The residues can be used

as road fillers (at €-5 to €-10 per tonne costs) or land filled (at €-30 to €-80 per tonne costs). On the other hand, the dry physical treatment requires lower investment costs and running costs since it involves fewer separation steps and consumes less energy and water. The investment costs will depend on the complexity of the plant and, thus, it is very difficult to estimate such costs. However, running costs of an illustrative dry process are shown in Table 7.3.

The data for dry separation are based on parameters of the basic dry separation plant in the Netherlands (AEB Amsterdam) and the estimated prices of metals are based on LME prices in the second half of 2007. The price for non-ferrous metals differs from that shown in Table 7.1 to the poor quality of the non-ferrous product (which is compromised by oxidation and dirt) and mixture of alloying elements. The €2000 per tonne value was based on the price offered by one of the smelters in the Netherlands.

Wet physical separation can generate more products and the aggregates obtained can be used as secondary building products, thereby eliminating the costs associated with disposing of the residues from dry separation. The disadvantages of the wet system are higher investment costs and running costs. Therefore its use will only be viable in large plants, e.g. the Amsterdam incinerator, which is one of the biggest incinerators in Europe (producing 200000 tonnes of BA in 2006, and in 2007 a fourth generation waste-fired power plant was installed, which will eventually incinerate more household waste, after which approximately 280000 tonnes/y of BA will be generated). At the time of writing, with wet physical separation, Pilot plant II should be able to separate 120000 tonnes/y of BA.

The investment costs of the pilot plant, which has a capacity of 50 t/h, are on average 3 million, including costs of installation and machinery in the plant. The operational costs of the plant include costs of employing six people, electricity and water costs (Table 7.4).

Table 7.4 shows the costs for processing 1 tonne of BA, depending on the capacity of the installation. With a capacity of 50 t/h, the total cost for treating 1 tonne of BA is on average €12 for returns calculated over six years.

The wet separation system at the pilot plant in Amsterdam hosts basic dry and wet separation systems that can separate non-ferrous metals (CCS-2 mm, 2-6 mm and 6-20 mm), ferrous metals products (2-6 mm, 6-20 mm) and building products (sand product, 2-6 mm aggregate and 6-20 mm aggregate).

The wet separation process also yields residue fractions, which for the time being are land filled, such as sludge, the CCS-2 mm magnetic fraction and the organic fractions (CCS-2 mm, 2-6 mm and 6-20 mm) which could be incinerated. The 20-40 mm fraction, which is not currently separated at the pilot plant in Amsterdam, will be shredded and re-processed in the future by the wet installation. This fraction was not included in the financial calculation. However, it is rich in stainless steel (5%) and non-ferrous metals (0.5%), therefore it will create additional profit, although this will be partly offset by the costs of shredding.

The non-ferrous metals products and sand products can also be further separated. The non-ferrous fraction contains valuable precious metals, which can be further separated by MDS (Table 7.7). The sand product contains metallic aluminium and this mixture can be used for AAC (Table 7.8). Therefore three possible financial scenarios, shown below, were examined to obtain indications of the extent to which each of these products could improve the economic value of BA.

Table 7.3: Dry physical separation, costs and returns, base on the AEB dry BA treatment.

	Dry separation	Cost €/t (d.s.)	Fraction of input (%)	Grade (%)	Cost total (€/t)	Returns total (€/t)
0-40 mm	Sorting	-15	100%		15	
	Non-ferrous product (alloys)	2000	1%	80%		17.6
	Ferrous scrap	100	7%	98%		7
	Organics (mixture of organics and sand)	-30	5%		1.5	
	Waste (granulate, organic, etc.)	-10 to -30	87%		8.7-26.1	
Total					25.2-42.6	24.6

Table 7.4: Investment and production costs of the wet separation plant (Pilot plant II).

Production at the plant	20-30 t/h	50 t/h
Production of BA/y	60000	120000
	3000000	3000000
Direct costs (installation and machines)		
Fixed operational costs (personnel costs, 6 people including laboratory empl.) per year	300000	300000
Variable operational costs (electricity, water) per year	300000	600000
Total costs/tonne BA, return in 6 years	18	12
Total costs/tonne BA, return in 6 years with interest of 10%	20	13

7.1.1 Base Case

The basic financial scenario presented in this section is based on the mass balance from 2004-2005 (Table 3.4), which is shown in a simplified form in Table 7.5. The mass balance from 2004-2005 was chosen because it represents the most realistic scenario of products separation.

The masses of the metallic fractions (the aluminium, non-ferrous metal and magnetic fractions) shown in Table 7.5 are the total masses, which include residues such as stonnee, sludge etc. For example, the heavy non-ferrous metals content of the CCS-2 mm heavy non-ferrous fraction was only 40%, therefore for the financial calculations a mass of 0.1% was used (Table 7.6), based solely upon the heavy non-ferrous metals content. A similar correction was applied to the 2-6 mm heavy non-ferrous fraction, in which the non-ferrous metals grade was 70-80%, therefore Table 7.6 shows a mass of 0.2%.The amount of the 6-20 mm heavy non-ferrous fraction shown in Table 7.6 was reduced for the same reason to 0.5%. The magnetic fraction (CCS-2 mm) cannot be sold due to its fine particle sizes, and should be considered as a waste stream. However, the 2-6 mm and 6-20 mm magnetic fractions can be further milled and sold as iron scrap. The masses of the 2-6 mm and 6-20 mm magnetic fractions were reduced, due to the milling, to 0.1% and 2%, respectively (Table 8.5). The residue after milling the magnetic fraction is included in the mass balance shown in Table 7.6 as an additional fraction 'land filling residue from magnetic'. This fraction has a negative value at the time of writing because it is considered as waste, which must be land filled. The amount of the 2-6 mm aluminium fraction was reduced from 0.3% (Table 7.5) to 0.2% (Table 7.6) partly because the aluminium grade within it was 70% and partly because of the oxidation of the aluminium. The >20 mm fraction can be further milled and separated, however for these calculations this fraction was not included.

Each fraction shown in Table 7.6 was divided into products and waste streams. The land filling cost generally varies between €30-80 per tonne in Western Europe, and in the Netherlands the land filling price was €30 per tonne in 2007. The organic fraction (a mixture of organics, sludge and minerals) could be incinerated. The prices for aggregates and sand were taken as average building product prices. For non-ferrous metals the estimated prices were based

Table 7.5: Masses of each fraction generated by wet physical separation, based on the optimal separation scenario. Experimentally determined in 2004 and 2005 at Pilot plant II and in the laboratory (Chapter 3).

		Mass total (%)
2-20 mm	Basic washing plant	100%
<CCS mm	Dewatering	10%
	Disposal of sludge cake	10%
CCS-2 mm	Heavy non-ferrous fraction	**0.24**%
	Heavy magnetic fraction	0.30%
	Sand product	33.80%
	Organic fraction	2.00%
	Two polishing steps	36.34%
2-6 mm	Heavy fraction	**0.30**%
	Scrap Iron (estimated)	**0.40**%
	Aggregate	21.00%
	Aluminium fraction	**0.30**%
	Organics	3.00%
	Fine fraction sorting	25.00%
6-20 mm	Non-ferrous fraction	**0.70**%
	Scrap Iron (estimated)	**7**%
	Aggregate	15%
	Organics	0.80%
	Coarse fraction sorting	23.50%
20-40 mm	Total	5%
Total		100%

Values in bold indicate that the fraction is a mixture of metals and residue (minerals, organics, etc.).

Table 7.6: Wet physical separation, the costs and returns per fraction and total costs and return per 1 tonne of BA. The mass balance is based on data from 2004-2005 from Pilot I in Amsterdam.

		Mass total (%)	Cost €/t	Return €/t	Cost tot. (€/t)	Return tot. (€/t)
0-20 mm	AEB wet treatment	100%	13		13	
<CCS mm	Disposal of sludge cake	10%	30		3	
CCS-2 mm	Heavy non-ferrous fraction	**0.1**%		1500		1.5
	Heavy magnetic fraction	0.3%	30		0.1	
	Sand product	34%		7		2.4
	Organic fraction	2%	30		0.6	
2-6 mm	Heavy fraction	**0.2**%		2108		4.2
	Scrap iron (estimated)	**0.1**%		100		0.1
	Aggregate	21%		5		1.1
	Aluminium fraction	**0.2**%		1500		3
	Organics	3%	30		0.9	
	Land filling residue from magnetic	**0.3**%	30		0.1	
6-20 mm	Non-ferrous fraction	**0.5**%		2000		10
	Scrap iron (estimated)	**2**%		100		2
	Aggregate	15%		5		0.8
	Organics	0.8%	30		0.2	
	Land filling residue from magnetic	5%	30		1.5	
20-40 mm	Total	5%			?	?
Total					19	25

The numbers in bold indicate the pure metal content in the mass of the fraction.

on the copper price and offers from brass and copper smelters. The highest price offered for the 2-6 mm heavy non-ferrous metals fraction was €2108 per tonne, by a brass smelter. Table 7.6 shows that the cost of separating 1 tonne of BA is €19, and the returns from the product separated from the BA are €25. Therefore, there is a profit of €6 per tonne of BA.

7.1.2 Precious Metals Recovery

The 2-6 mm heavy non-ferrous fraction resulting after wet separation can be further separated by magnetic density separation (MDS). This fraction contains mainly copper and small amounts of gold and silver. By using the MDS, this fraction can be separated into two parts: a precious metals concentrate and a heavy non-ferrous metals fraction (Table 7.7). The copper concentrate can be sold for €2167 per tonne, and the precious metals concentrate fraction for a higher price, approximately €10029 per tonne (Chapter 4).

Table 7.7 shows the same values as Table 7.6, but for a scenario with an additional step to separate precious metals. The metals prices are averages based on LME prices from mid-2007. The MDS separation and investment costs were estimated to be €190 per tonne (Muchova et al. 2008).

The profit after wet physical separation, including MDS for the 2-6 mm heavy non-ferrous metals fraction, amounts to €8 per tonne of BA (Table 7.7). Hence, the additional precious metals separation increased the profit by €2 per tonne of BA.

7.1.3 Sand Utilization

The sand product containing metallic aluminium resulting from wet physical separation can be further valorised. Regular sand can be sold for €7 per tonne. However, AEB sand containing metallic aluminium (1%) could be used for the production of aerated autoclave concrete (AAC). The price of the sand/aluminium product was calculated in Chapter 4, as €67 per tonne for this fraction. This utilization in AAC requires an extra milling step because the optimal size of the fraction is <0.1 mm, the milling cost will be on average €45 per tonne, based on the estimated investment and process costs shown in Table 7.8.

A financial overview of this extra valorisation step, including basic wet physical separation and precious metals separation, is shown in Table 7.9.

Table 7.9 shows the costs of this scenario, which are approximately €35 per tonne of BA with a revenue of €49 per tonne, therefore the profit is €14 per tonne of BA.

7.2 Conclusion

The products of wet physical separation can provide financial benefits and minimize the amounts of residue that are land filled. At the time of writing, land filling in the Netherlands costs €30 per tonne. With a production of 120,000 tonnes/y of BA this amounts to €3.6 mil. per year. The wet system can also improve the quality of building products and recover more metals, which can be sold to metals smelters. The costs and benefits of the basic scenario for

Table 7.7: Costs and returns per fraction of BA separated by the wet physical system (including MDS separation to recover precious metals from the 2-6 mm heavy non-ferrous fraction) and total costs and return per tonne of BA. The mass balance is based on data from 2004-2005 from Pilot plant I in Amsterdam.

		Mass total (%)	Cost €/t	Return €/t	Cost tot. (€/t)	Return tot. (€/t)
0-20 mm	AEB wet treatment	100%	13		13	
<CCS mm	Disposal of sludge cake	10%	30		3	
CCS-2 mm	Heavy non-ferrous fraction	0.1%		1500		1.5
	Heavy magnetic fraction	0.3%	30		0.1	
	Sand product	34%		7		2.4
	Organic fraction	2%	30		0.6	
2-6 mm	Heavy fraction	0.2%		2167		4.3
	Precious metals	0.03%		10029		3
	Scrap Iron (estimated)	0.1%		100		0.1
	Aggregate	21%		5		1.1
	Aluminium fraction	0.2%		1500		3
	Organics	3%	30		0.9	
	Precious metals separation	0.3%	190		0.6	
	Landi filling residue from magnetic	0.3%	30		0.1	
6-20 mm	Non-ferrous fraction	0.5%		2000		10
	Scrap Iron (estimated)	2%		100		2
	Aggregate	15%		5		0.8
	Organics	0.8%	30		0.2	
	Landi filling residue from magnetic	5%	30		1.5	
20-40 mm	Total	5%			?	?
Total					20	28

Table 7.8: Investment costs of a milling unit with a capacity of 21600 t/y of sand containing aluminium.

Production at the plant	15
Production of BA/y	21600
Direct costs (installation and machines)	3500000
Fixed operational costs (personnel cost, 3 people) per year	150000
Variable operational costs (electricity, water) per year	150000
Total costs/tonne BA, return in 6 years	41
Total costs/tonne BA, return in 6 years with interest 10%	45

Table 7.9: Costs and returns per fraction of BA separated by the wet physical system (including MDS separation to recover precious metals from the 2-6 mm heavy non-ferrous fraction and the sand product used as AAC) and total costs and return per tonne of BA. The mass balance is based on data from 2004-2005 from Pilot I in Amsterdam.

		Mass total (%)	Cost €/t	Return €/t	Cost tot. (€/t)	Return tot. (€/t)
0-20 mm	AEB wet treatment	100%	13		13	
<CCS mm	Disposal of sludge cake	10%	30		3	
CCS-2 mm	Heavy non-ferrous fraction	0.10%		1500		1.5
	Heavy magnetic fraction	0.30%	30		0.1	
	Sand product	34%		67		23
	Organic fraction	2%	30		0.6	
	Sand product milling	34%	45		15.3	
2-6 mm	Heavy fraction	0.2%		2167		4.3
	Precious metals	0.03%		10029		3
	Scrap Iron (estimated)	0.1%		100		0.1
	Aggregate	21%		5		1.1
	Aluminium fraction	0.2%		1500		3
	Organics	3%	30		0.9	
	Precious metals separation	0.3%	190		0.6	
	Landi filling residue from magnetic	0.3%	30		0.1	
6-20 mm	Non-ferrous fraction	0.5%		2000		10
	Scrap Iron (estimated)	2%		100		2
	Aggregate	15%		5		0.8
	Organics	0.8%	30		0.2	
	Landi filling residue from magnetic	5%	30		1.5	
20-40 mm	Total	5%			?	?
Total					35	49

wet physical separation of BA (i.e. the system currently applied in Pilot plant II, in which the sand and aggregates building products, non-ferrous metals and ferrous metals are separated) are shown in Table 7.6. The financial balance of the wet system (Table 7.6) should be combined with the financial overview of the dry system (Table 7.3) to calculate the profitability of the overall BA separation. The dry system recovers 7% of scrap iron, 1.1% of non-ferrous metals and creates a waste stream of organics, which comprise 5% of the total mass. The residual fraction (87%) after the dry treatment will be separated by the wet system. Therefore, only 87% of the costs and revenues shown in Table 7.3 were used for the overall financial calculations (for both dry and wet systems) shown in Table 7.10. Table 7.10 shows that this combination yields a profit of €14 per tonne of BA.

Table 7.10: Overall costs and returns of the dry and wet system at AEB for one tonne of BA d.s. (combined data from tables 7.3 and 7.6).

	Total costs (€/t)	Total Returns (€/t)
Dry separation	16.5	24.6
Wet separation (Pilot II)	19	25
Total	35.5	49.6

The wet and dry treatment is financially superior to dry separation alone. The combined system can also recycle more materials while reducing land filling and/or other negative environmental impacts that can arise from utilizing BA as road filler (Chapter 8).

The wet physical separation concept implemented in AEB Amsterdam Pilot plant II can be improved by including an additional separation step, magnetic density separation (MDS), which can separate the 2-6 mm heavy non-ferrous fraction into a precious metals concentrate and a heavy non-ferrous metals concentrate. Each product can be sold separately, thus the revenue from these products will increase the BA value by €2 per tonne of BA. An overall financial overview of the dry and wet combination including precious metals separation is shown in Table 7.11.

Table 7.11: Overall costs and returns of the dry and wet system at AEB, including precious metals treatment by MDS, for one tonne of BA (d.s.), (combined data from tables 7.3 and 7.7).

	Total costs (€/t)	Total Returns (€/t)
Dry separation	16.5	24.6
Wet separation (Pilot II)	20	28
Total	36.5	52.6

The financial scenario presented in Table 7.11 shows a profit of €16 per tonne of BA.

The last financial scenario considers costs and returns for the wet physical separation system in Pilot plant II, including precious metals separation and

an additional utilization system for the sand/aluminium fraction (which can be milled to below 0.1 mm and sold to producers of AAC, to replace the mixtures of sand and aluminium powder that are currently used to make AAC). The financial outcome under this scenario is shown in Table 7.12.

Table 7.12: Overall costs and returns of the dry and wet system at AEB (including precious metals treatment by MDS and use of the sand/aluminium product for AAC) for one tonne of BA (d.s.), (combined data from tables 7.3 and 7.9).

	Total costs (€/t)	Total Returns (€/t)
Dry separation	16.5	24.6
Wet separation (Pilot plant II)	35	49
Total	51.5	73.6

The financial scenario presented in Table 7.12 shows a profit of €22 per tonne of BA. This scenario will bring returns in two years on investment and process costs.

All of these (and other) scenarios are sensitive to prices of metals, building products and land filling. However, even the basic concept (the current system at Pilot plant II in Amsterdam) is currently an interesting option when all factors, including sustainability and environmental benefits, are taken into account.

Chapter 8

Life Cycle Assessment of the Wet Physical Separation System

Summary

The environmental impacts of municipal solid waste incineration (MSWI) BA treatment employing a wet separation system are compared here with the existing commonly used dry separation system, by Life Cycle Assessment (LCA). The reference dry system produces ferrous metals, non-ferrous metals and road construction material as outputs. The wet system shows a higher recovery of metals and an improved quality of residue fractions (sand and aggregate). It is assumed that all products fulfil specific quality standards pertaining to the primary materials they will replace. At present, the wet separation system produces a small amount of sludge, which will eventually diminish in quantity as technologies progress. The wet system also uses water and consumes more energy than the dry system. It is concluded that the production of valuable outputs by the wet system more than compensates for its higher energy and water consumption.

This chapter provides the first LCA end-results, based on data collected during dry and wet separation at the Amsterdam incinerator (AEB). Based on these results it is concluded that bottom ash (BA) management employing the new wet system is environmentally superior to the commonly used dry system in terms of resource depletion, global warming, eco-toxicity, photo-oxidant formation, acidification, and eutrophication impacts. This conclusion is, however, subject to a number of caveats. Sensitivity analyses for three parameters (system boundaries, impact category modelling principles, and Life Cycle Inventory, LCI, data for economic inflows) showed that changing the system boundary of the alternatives by including the sludge land filling step for the wet separation, while leaving the boundary of the dry system unchanged, reduced the environmental advantages of the wet system. However, even for this perhaps unrealistically negative choice (including sludge within the boundary), BA separated by the wet process still showed lower environmental impacts compared to the dry system for all categories, except fresh aquatic ecotoxicity and eutrophication impacts.

8.1 Introduction

In Western Europe MSWI BA has long been recycled as a source of road construction materials instead of being land filled (Chapter 1). However, this recycling option is based on dry separation processes, and, while ranking higher in the waste hierarchy than land filling, it nevertheless has its own environmental problems. The problems of dry processing the BA into road construction materials are loss of useful materials that can be used as secondary raw materials (e.g. metals) and leaching of metals that contaminate soil and ground water.

For this reason, a more efficient system, wet physical separation, has been implemented as a demonstration pilot plant in the Amsterdam (AEB) incinerator (Chapter 3). The wet separation system makes more efficient use of resources by separating the metals with higher recovery and separating potential construction materials into higher quality building products (sand and aggregates, Chapters 3 and 4). In addition, the wet separation system contributes to reducing dependence of the EU on imported ores and concentrates. The wet physical separation system has strong economic advantages (Chapters 3, 4 and 7) compared to the existing dry system, not only because of the more effective removal of valuable metals, but also because the building materials obtained have lower metal contents, and thus are easier to apply in high value end products.

Life cycle assessment (LCA) is one of the most useful methodologies for comparing waste management solutions. Especially since the European Waste Directive came into force in 2008, the LCA methodology for assessing waste management practices has become increasingly important in waste management decision-making. However, a major problem arises when assessing the waste stages in a product LCA or when using LCA to analyze a waste management system. This is due to the so-called multi-functionality problem, in cases where the function of the management system is not only waste treatment, but also concurrent generation of energy and production of a variety of secondary raw materials. The problem is to decide what proportion of the environmental burdens of the activity should be allocated to each of the products investigated (Ekvall and Finnveden 2001). The general solution is to allocate the environmental burdens associated with a particular multi-functional process over the various functional flows of the process (Heijungs and Guinee 2007).

The aim of the research presented in this chapter was to obtain initial indications of the differences in energy and resources use and environmental impacts arising from processing BA by the two MSWI BA processing options: the standard dry separation system and the innovative wet separation system. Using LCA, it is possible to identify and quantify the differences in environmental impacts between processing BA by dry and wet separation systems. Therefore the LCA was carried out through the whole life cycle of BA. In order to be able to compare the performance of the two alternatives on the basis of functional equivalence, a functional unit was defined, as "waste management of 1 million tonnes of Amsterdam's MSWI BA (d.s)", to better illustrate the impacts values because this amount corresponds to the annual production of BA in the Netherlands. The service under examination is the waste management of MSWI BA, with particular consideration of the recovery of the materials obtained from the wet system compared to the dry system.

8.2 Methodology

LCA involves the compilation and evaluation of the material and energy flows as well as the potential environmental impacts of these flows throughout the life cycle of a product or service (ISO definition).

8.2.1 Dry Versus Wet Separation Treatment

8.2.1.0.1 Alternative A (dry separation treatment) In alternative A the scrap iron and coarse non-ferrous metals are separated, and the residue is a mixture containing a variety of compounds such as glass, sand, iron, copper, aluminium, lead, zinc, and even gold, which is used in road construction. This residue forms approximately 86.9% (dry mass) of the BA.

The LCA takes into account the electricity used for running the equipment of the process. The materials and energy used for the construction of the process were not taken into account in the study, as it is considered negligible due to the long life span of the process.

8.2.1.0.2 Alternative B (wet separation treatment) This process also starts with the dry separation system (analysed following the same procedure as in alternative A). The remaining part of the mixture, 86.9% d.s. of the original mass entering the dry separation step, instead of being used as road construction material, goes to the wet separation step. This fraction is thereby efficiently separated into scrap iron, non-ferrous metals, aluminium, stainless steel, sand, and aggregate. Only a small amount of sludge is left, approximately 5-13% (dry mass) of the input; this residue is presently land filled. The wet system results in a high recovery of metals and better quality building materials. The LCA takes into account the production of electricity and water used in the wet systems. For the reasons given above, the materials and energy used for the construction of the wet system were not taken into account in the LCA. In addition, the wet system has not yet been fully scaled up and optimized.

The analyses of both alternatives start after the production of MSWI BA. The composition of waste incinerated in 2007 contained approximately 47% municipal waste, 24% office waste, 1% hospital waste, 9% sewage sludge, re-incinerated BA in amounts ranging from 4 to 9%, and the rest was miscellaneous waste.

8.2.2 System Boundaries and flow diagram

The selected system boundary starts from the BA resulting from the incineration process. While the system is performing a comparative LCA, this study was restricted to a difference analysis. This analysis does not take the previous steps of treatment into account, as they are qualitatively and quantitatively identical.

The holistic approach of LCA is intended to avoid problem shifting, so it is important not to solve one environmental problem by shifting it to another stage in the life cycle of BA. Thus, it is important to consider possible problem shifting when defining the system boundaries. Concerning where the system ends, it was considered whether to include the road construction material (RCM) in the system of Alternative A and the sludge in the system of Alternative B. The decision was not to include either of them in their respective systems. The reason

for not including the products coming from the dry separation step, which is commonly used as RCM, was that no LCI-data is available for such materials in LCA databases. Sludge was not included in the system as this was considered an 'unfair' comparison with RCM. While sludge is contained within well-designed and monitored depots, RCM is not, and sometimes simply deposited over very large road-forming surfaces, where it leaches uncontrolled into ground water. System boundaries play an important role in the way environmental impacts are calculated in LCA. Therefore, this problem is discussed as part of a sensitivity analysis, in which the sludge was included in the system.

Figure 8.1 shows the system boundaries of both alternatives as rounded rectangular boxes. The wet separation system includes the dry separation step and the wet separation step.

8.2.3 Multi-functionality and Allocation

The management of MSWI BA provides for more than one function, not only eliminating municipal waste BA, but also providing for the production of energy and useful materials (e.g. scrap iron). Therefore, a realistic form of allocation had to be carried out. This study initially considered three allocation methods: partitioning, substitution, and system expansion.

The essential rationale of the partitioning method is that a multi-functional process is split into a number of mono-functional processes. The impacts are then allocated to the various processes by assuming an allocation factor based on physical or economic parameters, or on the number of physical flows. Although the partitioning is a logical method and presents no theoretical problems, it was not found suitable for the analysis presented here since some pertinent data were not available, which would have increased the uncertainty of the assumed allocation factors.

In the system expansion method, the boundaries of the system investigated are expanded to include the alternative production of the materials obtained from the new method and the alternative method. A central feature of the substitution method is the concept of avoided processes. In this method the impacts avoided by the normal production of these materials are included in the system by subtracting these impacts from the total impacts of the BA management system. The reason for considering system expansion and substitution is that these two approaches appear to be frequently applied in the context of waste management (Heijungs and Guinee 2007). For clarity, system expansion and substitution, are schematically illustrated in Figure 8.2.

In the substitution method, the impacts of producing materials in the 'normal way' are considered to be avoided because the separation processes produce them through BA treatment. These inventories are subtracted from those arising from the BA management. In the system expansion method, the dry separation system does not create some materials that are produced by the wet separation system. Accounting for these materials requires expansion of the system to include their normal way of production; this is done by adding their inventories to those arising from the management of BA by the dry separation system. The same procedure was applied to the wet separation system, which does not produce RCM, as shown in Figure 8.2.

The results are only presented for system expansion, as it is the recommended aproach according to ISO 14041 (Ekvall and Finnveden 2001); cite-

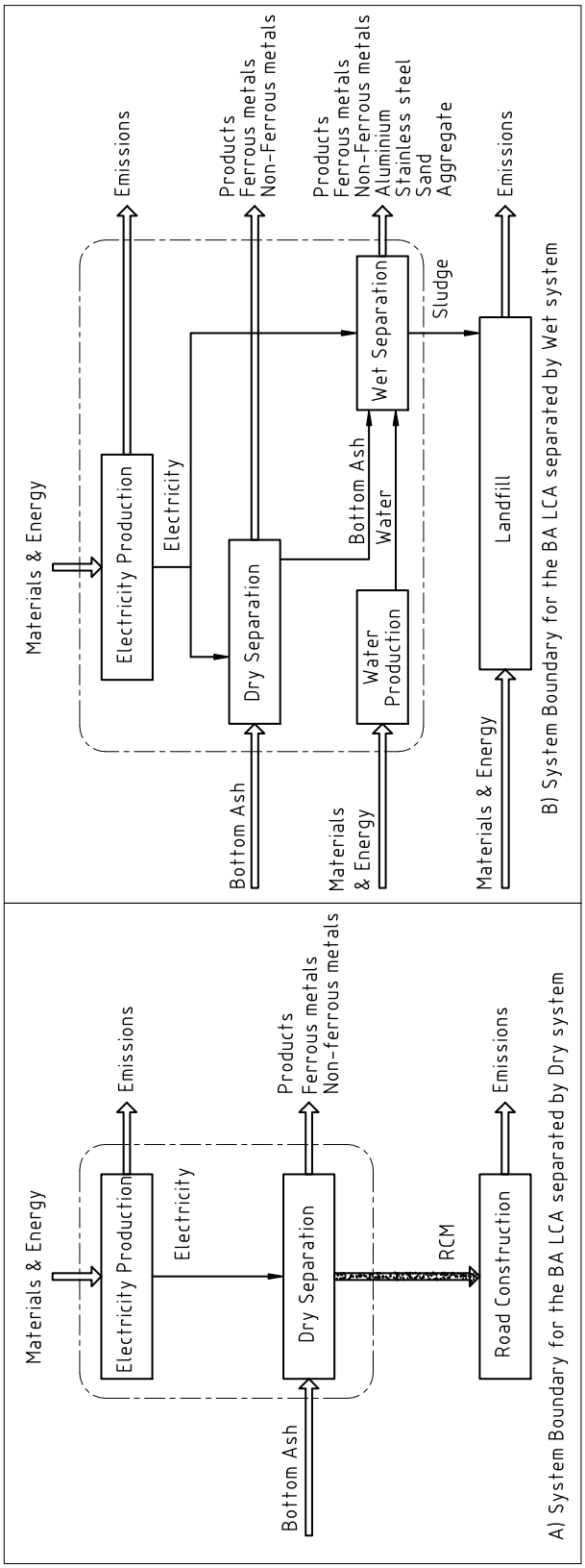

Figure 8.1: Case I, System boundaries of the two processes and their life cycle stages.(RCM-road construction material)

'Allocation should be avoided, wherever possible, either through division of the multifunction process into sub-processes, and collection of separate data for each sub-process, or through expansion of the systems investigated until the same functions are delivered by all systems compared.'

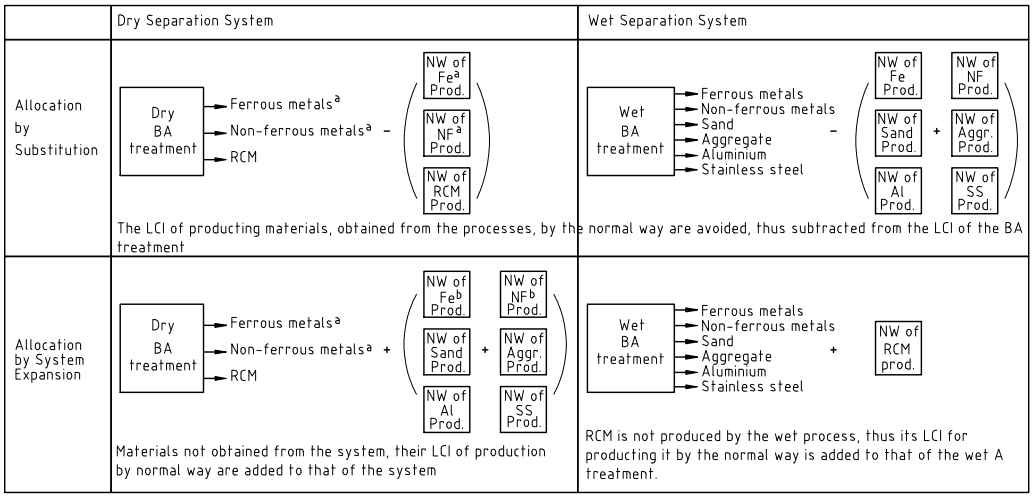

[a] Amount of Fe and non-Fe obtained from the Dry separation step

[b] Amount of Fe and non-Fe obtained from the Wet separation step only (e.g. Fe^b=Fe-Fe^a)

NW: represents the LCI of the 'normal way' of producing these materials

BAT: BA treatment

The rectangular boxes represent the life cycle inventory (LCI)

Figure 8.2: Allocation methods used in the study applied for the dry and wet systems.

8.2.4 Data Sources and Collection

Primary data were collected for the foreground processes, i.e. the dry separation step and the wet separation step. For the dry separation system data came from analyses of materials produced, in practice, at the Amsterdam plant. For the wet separation system data came from analyses of materials produced by the Amsterdam pilot plant, which currently consists of the existing dry separation system followed by a wet system. The dry system removes most of the ferrous scrap and the very coarse non-ferrous metals (larger than about 2 cm) by means of screening, shredding and magnetic separation. The <40 mm residue of the dry separation output is used as RCM. For the wet separation system this residue material is the input. The wet system further separates more materials according to differences in size and density to produce the products shown in

Table 8.1 (Muchova and Rem 2006b, Muchova and Rem 2006a). At the time of writing the sludge represents 13%, by weight, of the BA. This amount, however, could be reduced by optimizing separation settings, which will be done in the future. Both processes produce some organic materials, which are reincinerated. These organic materials are not taken into account in the scope of the study, nor are certain materials obtained by the wet separation system (e.g. the fine magnetic fraction), the utilization of which is still under investigation. Table 8.1 shows the economic outputs obtained from processing BA by the two alternatives. The dry separation system requires 8 kWh per tonne of BA input; the combined dry and wet separation steps require 20 kWh plus approximately 16 kg of water per tonne of BA input.

Table 8.1: Mass percentages of economic outputs of processing BA by the two alternatives (dry and wet systems). Please note that the last column represents additionally recovered materials.

Economic outputs	Dry system	Wet system
Scrap Iron	7%	0%
Iron 65%	0%	5.4%
Non-Ferrous Metals (Brass)	1.1%	0.6%
Aluminium		0.5%
Road Construction Material	86.9%	0%
Stainless Steel*	0%	0.6%
Sand	0%	18.7%
Aggregate	0%	48.9%

* The 20-40 mm fraction contains stainless steel, aggregate and non-ferrous metals; these fractions have not yet been separated. Because it is planned to separate them in the near future, this study considered them to be separated by estimating a realistic amount of energy needed for their separation.

For the rest of the data concerning the background processes, secondary data were utilized, from the Ecoinvent database * (Table 8.2). The background processes for the systems under investigation are: the electricity used to run the processes (which is generated at the waste incineration plant), the industrial water used for the wet separation, and the disposal of sludge in the landfill. The Ecoinvent database was also used to obtain data for allocation (Table 8.3).

In order to perform the allocation step, i.e. to solve the multi-functionality problem, life cycle inventory data for producing the materials obtained from each of the alternatives by the normal way of production are required. The selection criteria for inventory data were based on the quality and type of applications. This was an important issue, since in the database inventory data are available for various ways of producing iron. Thus, for choosing the most suitable type of iron to replace the one produced by the wet or dry system, similar quality and type of applications appropriate to the iron from the two systems were taken into consideration. However, in some cases, the exact product cannot be found (waste streams for which no inventory data exist). For

*The Ecoinvent database is a collection of data for over 2600 processes producing over 2700 economic outflows and almost 2400 environmental flows, compiled by a Swiss-based life cycle research institution. Source: http://www.ecoinvent.ch.

Table 8.2: Background process data from the Ecoinvent database.

Background Process	Process from database
Industrial Water production	Water, decarbonized, at plant [RER]
Electricity production	Electricity from waste, at municipal waste incineration plant [CH]
Land filling (for sludge)[1]	Disposal, average incineration residue, to residual material landfill [CH]

[1] Used for the first sensitivity analysis.

these cases approximations and reasonable estimations were made, for example for aggregate and sand products.

Table 8.3: Materials produced by the normal way selected from the Ecoinvent database for each material obtained from the processes, for which LCI data were used for the allocation methods.

Products	Alternative for Allocation (their normal way of production)
Sand	Sand, at mine [CH]
Aggregate	Lightweight concrete block, expanded clay, at plant [CH][1]
Stainless Steel	Steel, electric, chromium steel 8/18, at plant [RER]
Aluminium	Aluminium, primary, at plant [RER]
Non-ferrous	Copper, primary, at plant [CH]
Scrap Iron	Scrap Iron, at plant [RER]
Ferrous (content 65%)	Iron ore, 65% Fe, at beneficiation [GLO][2]
Road Construction Material	Concrete, sole plate and foundation, at plant [CH]

[1] Similar application and quality of aggregate, however, in different form, extra energy has been added to compensate for this difference.

[2] Similar % Fe content, which is less ready to use than scrap iron applications.

The letters in brackets represents the name of the country or region where the LCI data in the software was collected and calculated. CH is from Switzerland, RER is Western Europe, and GLO is global.

8.3 Results

8.3.1 Impact Assessment

Characterization gives meaning to the data generated by LCA by converting it into a number of environmental impacts. To do this, environmental flows are converted and aggregated into various impact categories using characterization models and factors. For this research the Problem Oriented Approach was used, Baseline (CML n.d.), shown in Table 8.4. Data are presented for the system expansion method.

Definitions and descriptions of these impact categories are given in Guinee (Guinee 2002).

The results were normalized to better understand the relative importance of

Table 8.4: Impact Categories and characterisation factor for the Problem Oriented Approach, baseline (CML n.d.)

Impact Category	Characterization factor
Abiotic Depletion (AD)	Abiotic Depletion Potential (ADP)
Global Warming (GW)	Global Warming Potential (GWP100)
Ozone Layer Depletion (OD)	Ozone Depletion Potential (ODP∞)[1]
Human Toxicity (HT)	Human Toxicity Potential (HTP∞)[1]
Freshwater Aquatic Ecotoxicity (FAET)	Freshwater Aquatic Ecotoxicity Potential (FAETP∞)[1]
Marine Aquatic Ecotoxicity (MAET)	Marine Aquatic Ecotoxicity Potential (MAETP∞)[1]
Terrestrial Ecotoxicity (TET)	Terrestrial Ecotoxicity Potential (TETP∞)[1]
Ozone creation (POC)	Photochemical Ozone Creation Potentials (high NOXPOCP)
Acidification (A)	Acidification Potential (AP; based on RAINS)
Eutrophication (E)	Eutrophication Potential (EP)

[1] These impact factors are based on infinity time interval.

the impact categories scores obtained in the characterization step. ISO 14042 defines normalization as "calculation of the magnitude of indicator results relative to reference information". In this study the Netherlands is taken as a reference for all impact categories. The reference information used refers to 1997, because this was the most recent year for which a complete list is available in the CML-IA database for the normalization factors.

Table 8.5 shows the characterization scores for selected impact categories.

Figure 8.3 shows the normalized impact assessment results for the two separation systems, which indicate their proportions of the impacts in the Netherlands. It shows clearly that the wet separation system is environmentally superior to the dry system for all impact categories.

Table 8.5: Characterization scores of the two alternatives (dry and wet systems).

Impact Category	Dry System	Wet System	Unit
AD	1.78	0.14	kg antimony eq.
GW	316	58.2	kg CO_2 eq.
OD	$25 \cdot 10^{-06}$	$24.2 \cdot 10^{-07}$	kg CFC-11 eq.
HT	3220	4.16	kg 1.4-dichlorobenzene eq.
FAET	148	1.08	kg 1.4-dichlorobenzene eq.
MAET	366000	3260	kg 1.4-dichlorobenzene eq.
TET	29.5	0.15	kg 1.4-dichlorobenzene eq.
POC	0.4	0.02	kg ethylene eq.
A	5.11	0.12	kg SO_2 eq.
E	0.17	0.02	kg PO_4 eq.

The contributors to the impact scores of the wet system are, firstly, the impacts of production of the required utilities for the wet separation system (electricity and water), and, secondly, the impacts resulting from the normal way for producing RCM (as explained for the system expansion allocation method in Figure 8.2).

Although the wet separation system requires more utility inflows (e.g. water and more electricity), it is nevertheless more environmentally friendly than the dry system. In fact, the difference in impacts of the two alternatives in one impact category (MAET) amounts to more than 10% of the total national impact. This is because the wet system generates more products than the dry system. The RCM is the only material that must be obtained by the normal way, and its impact is significantly smaller than the sum of all the impacts generated by the normal ways of producing aluminium, stainless steel, sand, aggregate, and some metals, none of which are obtained from the dry separation system.

8.3.2 Interpretation

In this study the interpretation step included a contribution analysis and a sensitivity analysis. A contribution analysis was carried out to calculate the contribution of the impacts of specific functions to the environmental impact categories scores for both alternatives. Utility needs (energy and water) were also considered for both processes. Additionally, a sensitivity analysis was performed by varying system boundaries. On the basis of the results of the sensitiv-

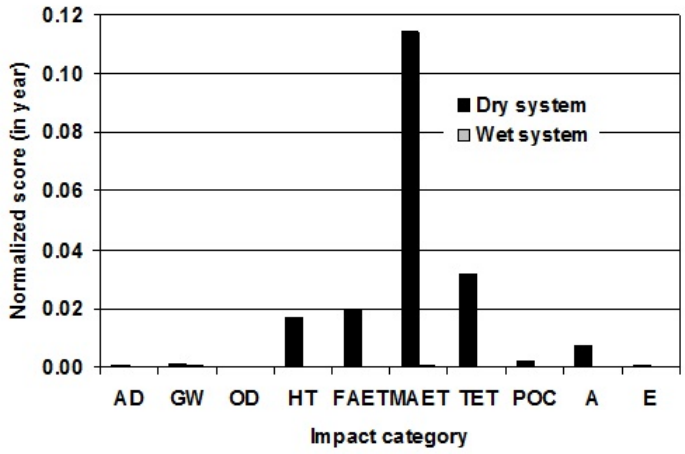

Figure 8.3: Normalized results of the two alternatives (dry and wet) for one million tonnes of BA, for a comparative analysis using the system expansion method.

ity analysis, a further sensitivity analysis was performed by changing the time horizon of some impact categories concerning toxicity and ecotoxicity; i.e. limiting them to 100 years instead of an infinite time interval. A sensitivity analysis was also carried out to compare the relative impact scores when changing the data sources for electricity used in the separation processes.

8.3.2.1 Contribution Analysis

The impact scores come from the impacts arising from the normal way of producing the materials that are not obtained from the dry system. Figure 8.4 shows that the electricity needed for dry processing impacts none of the environmental categories. This is because the Ecoinvent database assumes that electricity generated in a MSWI is impact-free, as all emissions are allocated to the service of treating waste, and none to generating electricity. In the sensitivity analysis outlined below, this assumption was modified.

The wet BA system requires more electricity than the dry system, and it also requires water. Electricity is also obtained from the incineration plant. Use of water has a negligible impact compared to that of the RCM produced by the normal way. In fact, the absolute amount of water used per tonn of BA is insignificant even in very dry climates.

Abiotic Depletion (AD)

The wet separation system almost has virtually zero abiotic depletion scores, whereas the dry system depletes a small amount (1.78 kg) of antimony equivalents. The 1.78 kg antimony equivalent is due to the depletion of light weight concrete (61%), aluminium (21%), stainless steel (11%) and heavy non-ferrous metals (copper, brass) (8%).

Global Warming (GW)

The global warming (GW) scores for the dry and wet systems are 316 and 58 kg

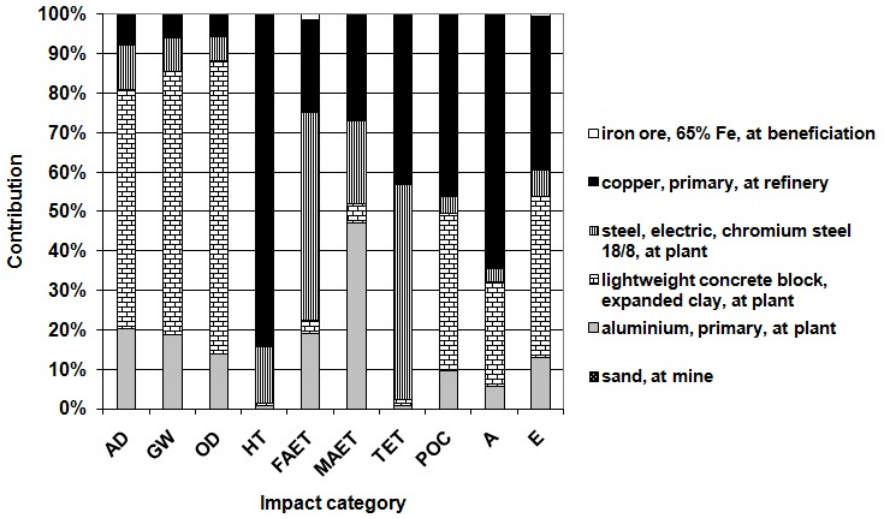

Figure 8.4: The contributions of materials not obtained and energy to the dry system LCA scores.

CO_2 eq., respectively. For the dry process, 67% of the GW comes from the non-production of aggregates, 19% from aluminium production, 9% from stainless steel production and 5% from heavy non-ferrous metals (copper, brass). The GW score for the wet process comes mainly from the non-production of RCM, while the rest comes from the water production.

Ozone Layer Depletion (OD)
The ozone depletion scores were very low for both alternatives.

Human Toxicity (HT)
The HT score for the dry process comes mainly (85%) from the production of heavy non-ferrous metals (copper, brass), while the rest comes from stainless steel production via the release of arsenic, cadmium, copper and zinc to air in brass (non-ferrous metals) production, and hexochlorobenzene, nickel, and mercury from stainless steel production. For the wet system most of the HT score comes from the production of aggregates, and the rest from water production.

Freshwater Aquatic Eco-toxicity (FAET)
The FAET score for the dry system comes mainly (53%) from the production of stainless steel and the rest from the production of heavy non-ferrous metals and aluminium, via the release of metal ions to fresh water in the production of metals. For the wet system, the main FAET potential comes from the production of road construction material and the rest from the production of water.

Marine Aquatic Eco-toxicity (MAET)
The MAET score for the dry system comes mainly (47%) from the production of aluminium, 27% from the production of heavy non-ferrous metals (copper, brass) and the rest from the production of stainless steel (21%), largely via the release hydrogen fluoride to air in the production of aluminium and stainless

steel. For the wet system the MAET score comes from the production of road construction material and the rest from the production of water.

Terrestrial Eco-toxicity (TET)
For the dry system the TET score comes mainly from the production of stainless steel (55%) followed by non-ferrous metals production, with a very small contribution from iron ore (65% content), aggregate and aluminium production, mainly via the release of mercury to air in the production of stainless steel. For the wet system most of the TET score comes from the production of road construction material and the rest from the production of water.

Photo-oxidant Formation (POC)
The POC score for the dry system comes mainly from the production of heavy non-ferrous metals (copper, brass) followed by production of light weight aggregates and aluminium. For the wet system the POC score comes from the production of road construction material and the rest from the production of water.

Acidification
The acidification score for the dry system comes mainly from the production of heavy non-ferrous metals (copper and brass) (65%), light weight aggregates (27%) and aluminium (6%). For the wet system the score comes from the production of road construction material and the rest from the production of water.

Eutrophication (E)
The eutrophication score for the dry system comes mainly from the production of light weight aggregates and heavy non-ferrous metals (copper and brass) followed by the production of aluminium (13%) and stainless steel (7%). The acidification score for the wet process comes mainly from the production of aggregates and road construction material and the rest from the production of water. For both alternatives A and B the eutrophication potential is largely attributable to the release of nitrogen oxides to air from the production of aggregate and RCM, respectively.

8.3.2.2 Sensitivity Analysis

Sensitivity analysis was conducted to identify the parameters that most strongly influenced the results. The effects of three different types of parameters were analyzed, the boundary setting and system definition, the model parameters selected for impact categories, and the utilities (electricity) data.

The effect of toxic substances on the environment appear for alternative A (dry system) and B (wet system) in the use of RCM and the sludge land filling stages, respectively. If the RCM is considered as a product, then it will be excluded from the system boundary of the study, but the sludge waste to landfill will be included. This may show superiority for the dry separation system for the toxicity-related impact categories. However, this approach may be unrealistic, as the toxic effect for the dry system is then merely shifted outside the boundary. Because of this problem, it was decided to perform a sensitivity analysis considering RCM as a product. This required a change in the system

boundary for the wet separation system by including the sludge-landfilling step, as shown in Figure 8.5. The impacts associated with the transport of the sludge to the landfill were not included in the study.

The results of the analysis are shown in Table 8.6 and the normalized scores in Figure 8.6. The wet system is still superior to the dry system in all impact categories except for those related to toxicity and the eutrophication potential.

Table 8.6: Characterization results for dry and wet systems (changed system boundaries; Case II in Figure 8.5, not normalized).

Impact Category	Dry system	Wet system	Unit
AD	1.78	0.25	Kg antimony eq.
GW	316	102	Kg CO_2 eq.
OD	$25 \cdot 10^{-06}$	$45.5 \cdot 10^{-07}$	Kg CFC-11 eq.
HT	3220	851	Kg 1.4-dichlorobenzene eq.
FAET	148	236	Kg 1.4-dichlorobenzene eq.
MAET	366000	206000	Kg 1.4-dichlorobenzene eq.
TET	29.5	0.72	Kg 1.4-dichlorobenzene eq.
POC	0.4	0.04	Kg ethylene eq.
A	5.11	0.19	Kg SO_2 eq.
E	0.17	0.75	Kg PO_4 eq.

Including the sludge land filling step affects all impact categories. However, the main increases are for human toxicity, freshwater aquatic ecotoxicity, marine aquatic eco-toxicity, and eutrophication potentials. These impact scores all increase for the wet separation system due to the leaching of metal ions into the environment.

The HT score increases due to the release of antimony (81% of the total HT score) and selenium (13%), to the fresh water. The releases of vanadium (32%), nickel (28%), and copper ions (28%) to fresh water all affect the FAET score. The MAET score is increased because of the dispersion of vanadium (36%), selenium (28%), and nickel ions (23%) to fresh water. The TET score rises due to the dispersal of mercury to fresh water, and the release of phosphate to water increases the eutrophication score. However, these values are fraught with many uncertainties, partly because the composition of the sludge from the wet separation system to be land filled is not similar to that of the land filled incinerated residue for which data are available in the database. Additionally, there is much uncertainty concerning the correctness of toxicity-related impact categories.

Changing modelling principles (model parameters) of an impact category may significantly influence results. In particular, the way in which life cycle impact assessment (LCIA) treats metals has been criticized e.g. (Heijungs et al. 2004). One parameter in question is the effect of metals' toxicity over given time intervals, and whether human toxicity should be considered over a 100-year period rather than an infinite time period. The 100-year time parameter was selected for this study. This analysis was performed on the basis of the results of Case II (wet system), which includes the sludge-land filling step in the system boundaries. The results of the analysis are shown in Table 8.7 (where the values for the wet system, case II, with infinite and 100-year time intervals

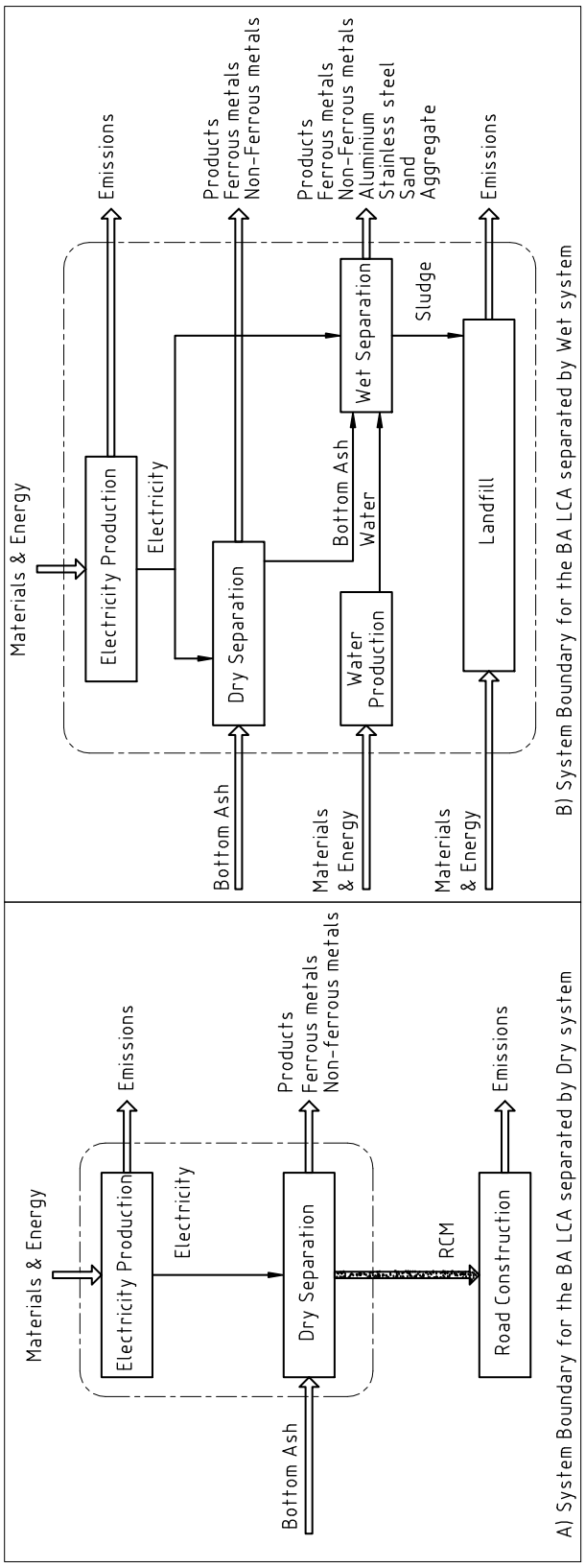

Figure 8.5: Case II, system boundaries of the two systems (dry and wet) and the life cycle stages.

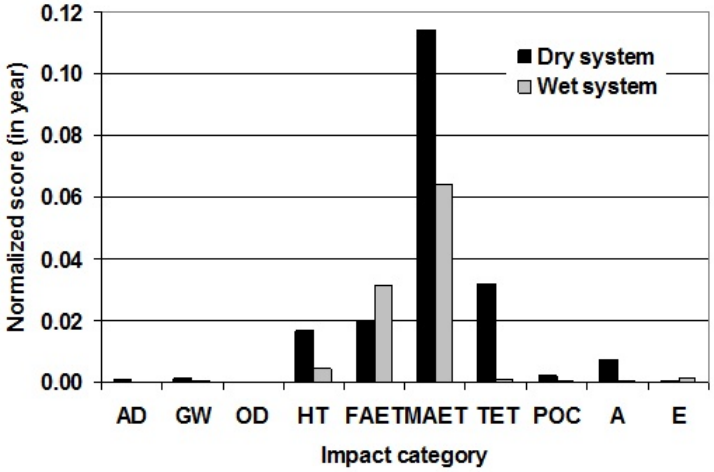

Figure 8.6: Normalized results for the dry and wet systems with changed system boundaries (Case II, Figure 8.5).

Table 8.7: Characterization scores for the alternatives according to modeling principles.

	CaseII		
Category	Wet System	Wet System (100 years)	Unit
HT	$4.48 \cdot 10^{-03}$	$-4.15 \cdot 10^{-03}$	kg 1.4-dichlorobenzene eq.
FAET	$3.15 \cdot 10^{-02}$	$1.8 \cdot 10^{-02}$	kg 1.4-dichlorobenzene eq.
MAET	$6.44 \cdot 10^{-02}$	$1.13 \cdot 10^{-04}$	kg 1.4-dichlorobenzene eq.
TET	$7.77 \cdot 10^{-04}$	$-2.72 \cdot 10^{-04}$	kg 1.4-dichlorobenzene eq.

are compared) and the normalized scores in Figure 8.7.

Changing to a 100-year time interval significantly reduces the absolute scores for all four impact categories.

Effects of Utilities Data (electricity)

The electricity used for the processes was calculated on the basis of LCI data for electricity produced from incineration, which has weaker impacts than electricity obtained from the grid. In this sensitivity analysis, the LCI data for electricity produced from waste incineration was replaced with that obtained from the grid. Changing the source of electricity to the grid only affected the global warming score. This effect was very small, i.e. contributions of 0.34% and 0.2% for the wet separation system for Cases I and II, shown respectively in Figures 8.1 and 8.4. For the dry system electricity from the grid contributes 0.032% and 0.028% to the global warming scores of Cases I and II, respectively. It had no influence on other impact category scores. Thus, impacts of electricity data hardly influence the results.

The sensitivity analysis showed that boundary setting and system definition had the most significant influence on the results, e.g. including or not including

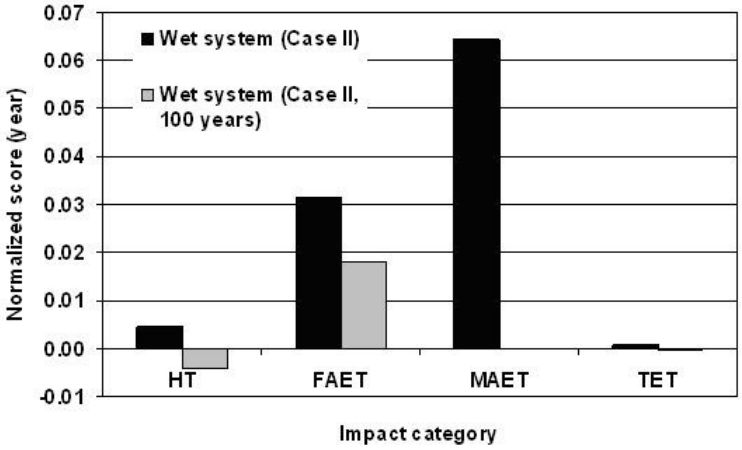

Figure 8.7: Normalized results for the wet Case II and wet Case II after 100 years and infinite time alternatives, derived by changing the modelling time parameter of the impact categories.

RCM within the system boundaries. It should be noted that contaminants in RCM, which is deposited over the huge surface areas of roadways, do in reality leach into ground water and thus adversely affect the environment. Therefore, including RCM in the systems boundary in this case seems to be a preferable option. However, no LCI data are available for BA used as RCM. Fortunately, a Danish study (Birgisdottir et al. 2007) is available, which compares the disposal of MSWI BA when recycled in road construction as a sub-base layer in an asphalted secondary road and when land filled in a coastal landfill in Denmark 8.8. The results of the cited study showed that the highest impacts during a 100-year period were (for both scenarios) eco-toxicity in water, with 30 PE (Person Equivalents) for the landfill scenario and 40 PE for the road scenario. The second highest impacts during the 100-year period for both scenarios were human toxicity via soil, with approximately three PE for the landfill scenario and 10 PE for the road scenario. Assuming that these findings are applicable, it can be concluded that the wet system impacts will be weaker than those of the dry system in these two impact categories.

In reality, the results are likely to be even more positive for the wet system, because the relative mass of material generated by the wet system to be land filled (the sludge) amounts to only 13% of the land fill mass considered by Birgisdottir. Therefore, it is likely that the impacts are also reduced, although to what extent is not easy to estimate.

8.4 Conclusions

First impressions based on the results of the LCA with carefully considered allocation procedures indicate that the wet system is environmentally friendlier than the dry system in all impact categories for processing 1 million tonnes (d.s.) of Amsterdam BA, for the following reasons:

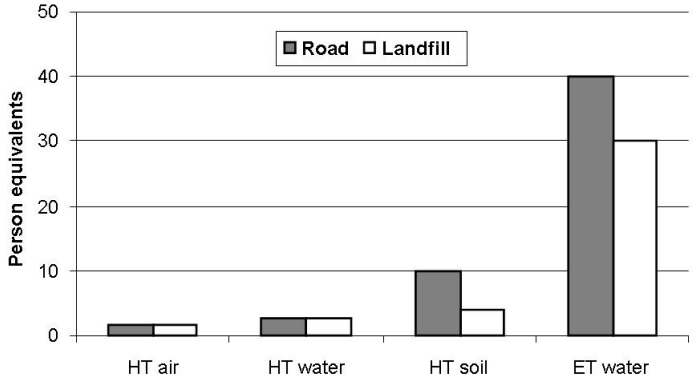

Figure 8.8: Results of the study by Birgisdottir, showing that using MSWI BA for road construction causes toxicity-related environmental impacts that are larger than (or equal to) those of land filling.

- The more efficient separation of the new wet system yields more valuable outputs, namely iron, stainless steel, heavy non-ferrous metals, aluminium, sand, and aggregate, all of which are pure enough to replace primary materials. Thus, the wet system is also superior to the dry system from the waste hierarchy perspective (Waste Framework Directive), as materials obtained from the wet system are effectively re-used (e.g. aluminium is separated and used, replacing aluminium produced otherwise, thus avoiding the amounts of energy needed to produce aluminium from ore and the large emissions resulting from aluminium production).
- The dry system separates a limited amount of mixed non-ferrous metals (aluminium, heavy non-ferrous metals) the remaining metals are mis-recycled or mis-used, because they are lost in road foundations. Thus, the economic value of the metals is zero. Additionally, their use as road construction materials has an adverse environmental impact due to the leaching of metal ions into the environment. Thus, while the wet system requires water and uses more electricity than the dry system, its production of valuable metals and other materials more than compensates for its higher energy and water consumption.

This conclusion is, however, subject to a number of caveats. While LCA can theoretically handle all process inputs and outputs, in reality not all the necessary information was available in existing LCA databases. Therefore certain assumptions had to be made. The second issue was that the wet system is still undergoing process development and optimization, hence further development will almost certainly result in greater efficiency and thus even more positive results.

Chapter 9

Conclusions and recomendations

Wet treatment technology has significant positive impacts on the economics and recycling efficiency of MSWI bottom ash. For the time being, the choice of wet or dry separation will be determined by the local market for aggregates and sand versus the cost of landfilling the residue or of the isolation measures required for using it in roads. In the future, the superior metal recovery, particularly in terms of copper and precious metals, the improvement of the mineral product to high quality building materials, the smaller amount of residue and the flexibility with respect to the moisture content of the input ash may become crucial points in favour of wet treatment technology.

Changes in legislation in the Netherlands have created a challenge to improve the separation of bottom ash. As a result, a wet physical separation pilot plant was built in Amsterdam. The pilot installation used a combination of screening, metals recovery and washing. Wet technology can recover most metals of a particle size >0.3 mm and remove organic and fine particles from the mineral fraction resulting in an improved grade of building materials. The high recovery of metals is not only financially appealing but it is also essential for the quality of the building products if used for high value construction applications. The focus of the research was on optimising the pilot installation in order to improve the environmental quality of the large mineral products (the aggregates) and at the same time produce metals which would sell to smelters. The main findings of the research are related to the composition, system of analysis, the best physical-separation options, economic aspects, utilization systems and environmental issues. Each of these subjects was investigated in order to get an overall understanding and to see if further research could be implemented based on these findings in the future.

The major components of bottom ash are aggregates and metals. Due to rising metal prices in the past few years, the recovery of metals from bottom ash is an increasingly interesting option. The composition of bottom ash is relatively constant throughout Western Europe. The Amsterdam BA contains 8-13% of ferrous metals, 2.3% of non-ferrous metals and 0.001% of precious metals. This study presented three different financial scenarios based on the separation options. All of these scenarios are sensitive to prices of metals, building products and land filling. However, even the basic concept (the current system at Pilot plant II in Amsterdam) is currently an appealing option when all factors, includ-

ing sustainability and environmental benefits, are taken into account. The second financial scenario is based on a new magnetohydrostatic separation system which is suitable for recovering precious metals from the >2mm HNF fraction of MSWI BA. This system separates the fraction into a copper-zinc concentrate for use in the brass smelter and a precious metals concentrate for use in the precious metals smelter. Subsequently, by selling two different metal products to a precious metals smelter and a brass smelter there will be an increase in the value of MSWI BA by €2 per tonne. The third financial scenario focused on the presence of metallic aluminium in the sand product because the sand separated from BA has a metallic aluminium content of 1-2%. If this sand-aluminium mixture can be marketed, the third scenario provides a more financially attractive option than the first two options, due to the high price of aluminium.

An important aspect concerning wet physical separation which needs to be taken into consideration is the capacity of the plant in which the BA is to be separated. The high investment costs of the wet process become economically acceptable at high capacities (>200000 t/y). There are no major differences in investment costs of wet plants with capacities of 50 t/h or 100 t/h, but the additional capacity increases the production of products from BA, thus resulting in higher profits. This capacity factor could play an essential role in the use of wet installations because not many incinerators in Europe need such a capacity.

Another focus of this research was on measuring the content of precious metals and proposing possible separation solutions. New developments in sink-floating using a magnetic density separator (MDS) could concentrate precious metals and produce non-ferrous metal fractions that are directly suitable for smelting. It was found that the source of the 0-2 mm precious metals is probably WEEE and the source of the gold in the 2-6 mm HNF fraction is jewellery. The experiment in which the 2-6 mm HNF fraction was separated using the MDS system shows that 88% of the gold can be recovered in a precious metals concentrate, while 94% of the copper can be recovered in the copper-zinc fraction.

Bottom ash without deep separation of metals and organics and washing steps is usually difficult to use as building material in many western European countries due to the high leaching values of some elements. The Amsterdam BA has difficulties with Cu, Sb, Mo, SO_4 and Cl. This research showed that the Cu, Sb, Mo, SO_4, Cl leaching values of the BA products after wet physical separation are influenced by the quality of the process water and the amount of water used in the last step during the rinsing of the final products. These factors decrease the leaching of Cl and SO_4, and this appears to be accompanied by reductions in the leaching of metals. Leaching of these freely soluble ions can be controlled and decreased by simply measuring the conductivity and rinsing if necessary. Another issue which has a negative influence on leaching is the amount of fine particles (<75 μm) and small organic particles. These are correlated to the amounts of sludge added to the household waste during incineration. Therefore if the amount of sludge incinerated with household waste is reduced, the leaching of critical elements will also be reduced. Cu leaching showed a correlation with SO_4 leaching. Therefore it can be controlled by reducing the conductivity to below a critical threshold. The Mo leaching can be decreased by reducing the

fine particles (<75 μm) in the fraction and the non-ferrous metal content. Sb leaching was correlated with NH_4 leaching and SO_4 leaching. No other significant correlations with Sb leaching were found, but there was an indication of a possible correlation with pH. Thus, Sb leaching can possibly be predicted using a conductivity meter. High conductivity indicates that SO_4 and Sb leaching will be high.
Decreased leaching of Cu, Sb, Mo, SO_4, Cl in the AEB BA products can be regulated by reducing levels of fines, organics and salts by modifying the separation settings, using an adequate amount of water, and using an extra washing system at the end of each separation of aggregate. The quality of the process water should be controlled by measuring the conductivity. Similarly, the quality of aggregates can be controlled by using sensors to measure their organic and metal contents, and by taking appropriate steps to control it.

In order to maintain good quality control of building products from BA it is necessary to have an accurate and quick quality leaching prediction system. Therefore another objective of this research was to develop a technique for predicting the final leachate values of the column test in a short period, 5 days, instead of the established 21 days. Modelling showed that the final concentrations of elements in the final eluate can be predicted from their concentrations in the first three eluates from the column test. The model obtained provides robust indications for five critical elements (SO_4, Cl, Cu, Mo, Sb), the behaviour of which is adequately described by an empirically-derived formula, based on their physical behaviour in the column.

The AEB building products separated from MSWI BA by wet physical methods show improved quality, lower organics and metals contents than MSWI BA separated by dry methods and MSWI BA that has not been treated at all. The grain size distribution of bottom ash after separation is similar to those of standard aggregates, but they are less dense than regular aggregates and have higher porosity, especially the 6-20 mm aggregate fraction.
Most of the research presented in the thesis was performed on aggregate, sand and sludge in high density asphalt (DAC). The results show that the size distribution of AEB aggregates is suitable for asphalt, but the density of AEB aggregate is less than normal aggregates. Tests done on asphalt made using sludge as a filler did not yield promising results. Positive results were shown using the sludge as a filler in mastic.
However, porosity of the mineral product can create problems for asphalt as well as for concrete in terms of durability and workability. Two AEB aggregates (2-6 mm and 6-20 mm) were tested in concrete to obtain initial indications of their quality. Mechanical properties, tested by compressive strength tests, showed that the compressive strength is comparable to that of regular concrete (made from natural aggregates), even though the AEB aggregate was not fully optimized (especially in terms of its organic and stainless steel contents, which were too high).
A critical aspect of aggregates separated by wet methods was that its aluminium content is too high to meet quality criteria, hence it was not possible to produce lime-sand stones. The presence of metallic aluminium should be avoided in order to minimize problems with oxidization in the concrete or in the lime-sand stone. An alternative solution is to use the AEB sand containing aluminium in

aerated autoclave concrete (AAC).
The most promising applications of the mineral product appear to be in low quality asphalt and concrete. Furthermore, BA aggregates products and sand could be utilized in the cement industry, although this possibility has not been examined during this study. In order to use the aggregates and sand for higher quality construction materials, additional improvements are needed, such as reductions in the contents of organics (coarse and fine) and metals (especially iron and aluminium).

LCA indicates that the wet system is environmentally friendlier than the dry system in all impact categories when the processing of 1 million tonnes of Amsterdam BA is taken as the functional unit. Dry systems separate only a partial amount of mixed non-ferrous metals and the remaining metals are mis-recycled or mis-used. Additionally, their presence in road construction materials has an adverse environmental impact due to the leaching of metal ions into the environment. Thus, while the wet system requires water and uses more electricity than the dry system, its production of valuable metals and other materials more than compensates for its higher energy and water consumption. This conclusion is, however, subject to a number of caveats due to the limited available information in existing LCA databases. Another issue in the LCA study was that the wet system is still undergoing process development and optimization, which means further development will almost certainly result in greater efficiency and thus even more positive results.

Appendix A

Particles Distribution

The average weight of BA particles was experimentally measured and is shown in Tables A.1, A.2, and A.3.

Table A.1: Average particle size of fine fraction (2-6 mm) for aluminium, copper-zinc, stone, ferrous metals, organics and glass.

Fine fraction (2-6 mm)	
Material and size	Particle weight (g)
Al $<$ 4 mm	0.29
Al $>$ 4 mm	0.63
Cu/Zn $<$ 4 mm	0.67
Cu/Zn $>$ 4 mm	1.77
Stone $<$ 4 mm	0.29
Stone $>$ 4 mm	0.63
Fe $<$ 4 mm	0.67
Fe $>$ 4 mm	1.77
Organics $<$ 4 mm	0.30
Organics $>$ 4 mm	0.40
Glass $<$ 4 mm	0.11
Glass $>$ 4 mm	0.36

Table A.2: Average particle size of coarse fraction (6-20 mm) for aluminium, copper-zinc, stone, ferrous metals, organics and glass.

Coarse fraction (6-20 mm)	
Material and size	Particle weight (g)
Al <13 mm	1.01
Al >13 mm	2.77
Cu/Zn < 13 mm	1.81
Cu/Zn > 13 mm	4.54
Stone < 13 mm	1.72
Stone > 13 mm	5.13
Fe < 13 mm	1.44
Fe > 13 mm	4.11
Organics < 13 mm	0.26
Organics > 13 mm	0.26
Glass < 13 mm	1.39
Glass > 13 mm	3.79

Table A.3: Average particle size of very coarse fraction (20-40 mm) for non-ferrous metals, stone, ferrous metals, organics and glass.

Very coarse fraction (20-40 mm)	
Material and size	Particle weight (g)
NF < 30 mm	6.82
NF > 30 mm	20.15
Fe < 30 mm	4.94
Fe > 30 mm	9.54
Stone < 30 mm	8.26
Stone > 30 mm	13.71
Organics < 30 mm	1.92
Organics > 30 mm	1.92
Glass < 30 mm	6.20
Glass > 30 mm	12.95

Appendix B

Leaching Data

	Sample sand 1		Sample sand 2		Sample sand 3		Sample sand 4		Sample sand 5		Sample sand 6		Sample sand 7		Sample sand 8		Sample sand 9		Sample sand 10		Sample sand 11	
Conductivity	**A**	**B**	**A**	**B**	**A**	**B**	**A**	**B**	**A**	**B**	**A**	**B**	**A**	**B**	**A**	**B**	**A**	**B**	**A**	**B**	**A**	**B**
K3 (L/S= 0.5)	10.66	9.25	8.37	10.74	13.64	13.73	10.28	9.1	5.9	5.41	n.m.	n.m.	6.24	6.91	6.16	6.27	3.85	3.33	4.28	2.7	3.13	3.33
K4 (L/S=1)	6.65	6.41	4.61	4.4	7.06	5.9	5.25	4.91	3.64	4.07	4.99	7.83	4.14	4.72	3.6	3.81	3.23	2.63	1.81	2.92	3.23	3.75
K5 (L/S=2)	4.63	5.33	1.79	1.64	5.22	2.86	2.4	1.86	1.33	0.98	3.29	5.32	3.4	3.47	2.2	2.51	1.83	1.64	0.98	2.32	1.93	2.91
K6 (L/S=5)	2.04	1.95	n.m.	n.m.	n.m.	n.m.	n.m.	n.m.	n.m.	n.m.	n.m.	n.m.	n.m.	n.m.	n.m.	n.m.	n.m.	n.m.	n.m.	n.m.	n.m.	n.m.
K7 (L/S=10)	0.78	0.71	n.m.	n.m.	n.m.	n.m.	n.m.	n.m.	n.m.	n.m.	n.m.	n.m.	n.m.	n.m.	n.m.	n.m.	n.m.	n.m.	n.m.	n.m.	n.m.	n.m.
pH																						
K3 (L/S= 0.5)	8.11	7.93	5.45	3.02	7.67	7.62	7.89	7.92	8.52	8.18	n.m.	n.m.	7.88	7.71	8.55	8.44	7.9	8.47	8.63	8.13	8.72	8.33
K4 (L/S=1)	8.71	8.6	8.92	8.78	8.01	8.02	8.03	8.2	8.84	8.42	8.32	8.06	8.17	8.05	9.05	8.87	10.36	9.36	8.74	7.73	8.92	8.47
K5 (L/S=2)	8.8	8.71	9.76	9.98	8.14	8.05	7.95	8.24	9.26	9.23	8.22	8	8.47	8.19	9.15	8.87	9.72	9.44	9.08	8.06	8.89	8.65
K6 (L/S=5)	9.4	9.45	n.m.	n.m.	n.m.	n.m.	n.m.	n.m.	n.m.	n.m.	n.m.	n.m.	n.m.	n.m.	n.m.	n.m.	n.m.	n.m.	n.m.	n.m.	n.m.	n.m.
K7 (L/S=10)	9.04	9.16	n.m.	n.m.	n.m.	n.m.	n.m.	n.m.	n.m.	n.m.	n.m.	n.m.	n.m.	n.m.	n.m.	n.m.	n.m.	n.m.	n.m.	n.m.	n.m.	n.m.
Redox																						
K3 (L/S= 0.5)	155.1	156.8	402	223	215	222	315	300.5	238.5	237.1	n.m.	n.m.	205.1	215.1	186.5	196.1	210.1	202.8	133.7	164.8	137.2	153.7
K4 (L/S=1)	132.2	130.2	141.6	143.5	236.3	236.3	195.8	189.8	246.6	250	209	220.8	256.8	181.3	185.6	185.5	145	171.6	181.8	174.1	124.7	133.5
K5 (L/S=2)	110.2	108.9	80.8	80.5	293.1	296	177.6	192.8	258.7	255.2	234.9	325.3	264	287.5	184.5	190.8	185.1	205	172.7	182.3	141.9	126.2
K6 (L/S=5)	119.4	118.9	n.m.	n.m.	n.m.	n.m.	n.m.	n.m.	n.m.	n.m.	n.m.	n.m.	n.m.	n.m.	n.m.	n.m.	n.m.	n.m.	n.m.	n.m.	n.m.	n.m.
K7 (L/S=10)	132.8	134	n.m.	n.m.	n.m.	n.m.	n.m.	n.m.	n.m.	n.m.	n.m.	n.m.	n.m.	n.m.	n.m.	n.m.	n.m.	n.m.	n.m.	n.m.	n.m.	n.m.

Figure B.1: Values for pH, conductivity (in mS/cm) and redox measured by column tests for sand fraction separated from bottom ash in the mini-pilot plant in different time periods and for different L/S ratios (in l/kg). All samples have been duplicated (duplicate refers to A and B). (Note: n.m. means not measured)

	Sample 2-6 mm 1		Sample 2-6 mm 2		Sample 2-6 mm 3		Sample 2-6 mm 4		Sample 2-6 mm 5		Sample 2-6 mm 6		Sample 2-6 mm 7		Sample 2-6 mm 8		Sample 2-6 mm 9		Sample 2-6 mm 10		Sample 2-6 mm 11	
Conductivity	**A**	**B**	**A**	**B**	**A**	**B**	**A**	**B**	**A**	**B**	**A**	**B**	**A**	**B**	**A**	**B**	**A**	**B**	**A**	**B**	**A**	**B**
K3 (L/S= 0.5)	3.58	3.8	6.56	5.81	5.53	5.07	5.25	4.26	2.55	2.73	n.m.	n.m.	3.31	2.79	3.06	1.39	3.01	3.16	1.75	1.8	2.06	2.24
K4 (L/S=1)	2.94	2.96	4.23	3.64	4.08	3.15	4.83	3.17	2.25	1.77	3.59	3.19	2.37	2.4	2.18	3.59	2.32	1.97	1.49	1.25	1.83	1.72
K5 (L/S=2)	1.82	1.78	2.22	1.79	2.31	1.55	4.31	3.16	2.03	2.85	2.31	1.67	1.52	1.36	1.35	1.67	1.6	1.31	0.99	0.72	1.18	0.94
K6 (L/S=5)	0.66	0.69	n.m.	n.m.	n.m.	n.m.	n.m.	n.m.	n.m.	n.m.	n.m.	n.m.	n.m.	n.m.	n.m.	n.m.	n.m.	n.m.	n.m.	n.m.	n.m.	n.m.
K7 (L/S=10)	0.47	0.42	n.m.	n.m.	n.m.	n.m.	n.m.	n.m.	n.m.	n.m.	n.m.	n.m.	n.m.	n.m.	n.m.	n.m.	n.m.	n.m.	n.m.	n.m.	n.m.	n.m.
PH																						
K3 (L/S= 0.5)	8.43	7.15	2.61	3.65	8.2	8.25	7.56	7.82	8.71	8.78	n.m.	n.m.	7.96	8.45	8.49	7.85	8.5	8.67	8.56	8.56	8.53	8.59
K4 (L/S=1)	8.76	8.79	8.52	8.81	8.35	8.56	7.65	8.03	8.95	9.02	8.74	8.73	8.49	8.32	8.73	9.2	9.38	9.48	8.31	8.69	8.56	8.73
K5 (L/S=2)	9.05	9.2	8.96	9.2	8.56	8.88	8.1	8.3	9.19	8.84	8.86	8.82	8.89	8.72	8.91	8.87	9.55	9.5	8.35	8.71	8.51	8.57
K6 (L/S=5)	9.44	9.44	n.m.	n.m.	n.m.	n.m.	n.m.	n.m.	n.m.	n.m.	n.m.	n.m.	n.m.	n.m.	n.m.	n.m.	n.m.	n.m.	n.m.	n.m.	n.m.	n.m.
K7 (L/S=10)	8.64	8.95	n.m.	n.m.	n.m.	n.m.	n.m.	n.m.	n.m.	n.m.	n.m.	n.m.	n.m.	n.m.	n.m.	n.m.	n.m.	n.m.	n.m.	n.m.	n.m.	n.m.
Redox																						
K3 (L/S= 0.5)	151.7	191.3	514	426	206	212	289	290	204.3	202.8	n.m.	n.m.	207.3	208.9	189.4	191.2	215.3	215.7	162.1	157.8	130.3	123
K4 (L/S=1)	124	124.2	147.5	143.6	236.4	236.5	189.9	195.6	246.2	248.3	195.2	183.2	158.6	171.2	176.2	144.8	177	178.3	162.4	121.6	108.9	92.5
K5 (L/S=2)	93.4	88.2	110.2	103.2	283.6	296.4	130.8	198.5	255.4	283.2	289.7	248.2	269.8	261	193.2	199.1	214.2	214.1	192.6	106.1	102.3	104.3
K6 (L/S=5)	122.2	112.9	n.m.	n.m.	n.m.	n.m.	n.m.	n.m.	n.m.	n.m.	n.m.	n.m.	n.m.	n.m.	n.m.	n.m.	n.m.	n.m.	n.m.	n.m.	n.m.	n.m.
K7 (L/S=10)	155.2	148.1	n.m.	n.m.	n.m.	n.m.	n.m.	n.m.	n.m.	n.m.	n.m.	n.m.	n.m.	n.m.	n.m.	n.m.	n.m.	n.m.	n.m.	n.m.	n.m.	n.m.

Figure B.2: Values for pH, conductivity (in mS/cm) and redox measured by column tests for 2-6 mm fraction separated from bottom ash in the mini-pilot plant in different time periods and for different L/S ratios (in l/kg). All samples have been duplicated (duplicate refers to A and B). (Note: n.m. means not measured)

	Sample 6-20mm 1		Sample 6-20mm 2		Sample 6-20mm 3		Sample 6-20mm 4		Sample 6-20mm 5		Sample 6-20mm 6		Sample 6-20mm 7		Sample 6-20mm 8		Sample 6-20mm 9		Sample 6-20mm 10		Sample 6-20mm 11	
Conductivity	**A**	**B**	**A**	**B**	**A**	**B**	**A**	**B**	**A**	**B**	**A**	**B**	**A**	**B**	**A**	**B**	**A**	**B**	**A**	**B**	**A**	**B**
K3 (L/S= 0.5)	4.14	3.74	5.21	5.47	4.88	5.38	6.07	5.97	4.74	4.42	n.m.	n.m.	4.02	3.82	3.54	3.51	3.95	4.49	3.11	3.23	2.96	2.61
K4 (L/S=1)	3.58	2.31	3.66	3.39	4.98	4.08	5.49	4.77	2.97	2.12	4.7	4.79	3.76	2.61	3.38	1.99	3.13	2.67	n.m.	1.31	3.02	2.04
K5 (L/S=2)	2.05	1.13	2.79	1.98	2.66	1.96	3.44	2.85	1.34	0.87	2.99	1.85	2.42	1.15	1.72	0.82	2.4	1.09	2.02	0.63	1.73	1.09
K6 (L/S=5)	0.54	0.41	n.m.	n.m.	n.m.	n.m.	n.m.	n.m.	n.m.	n.m.	n.m.	n.m.	n.m.	n.m.	n.m.	n.m.	n.m.	n.m.	n.m.	n.m.	n.m.	n.m.
K7 (L/S=10)	0.27	0.29	n.m.	n.m.	n.m.	n.m.	n.m.	n.m.	n.m.	n.m.	n.m.	n.m.	n.m.	n.m.	n.m.	n.m.	n.m.	n.m.	n.m.	n.m.	n.m.	n.m.
PH																						
K3 (L/S= 0.5)	9.32	9.84	7.22	7.49	8.54	8.67	8.8	8.54	9.23	9.44	n.m.	n.m.	8.27	8.79	8.55	8.92	8.5	8.86	8.78	9.06	8.99	9.33
K4 (L/S=1)	9.97	10.49	9.15	9.24	8.74	8.93	8.36	8.62	9.21	9.64	8.7	8.89	8.22	8.81	8.73	9.22	9.02	9.59	n.m.	9.44	8.71	8.94
K5 (L/S=2)	10.15	10.54	9.19	9.12	8.81	9.02	8.55	8.74	9.61	9.88	8.77	9.09	8.5	9.09	8.93	9.31	9.07	9.45	8.41	9.48	8.46	8.62
K6 (L/S=5)	9.67	10.54	n.m.	n.m.	n.m.	n.m.	n.m.	n.m.	n.m.	n.m.	n.m.	n.m.	n.m.	n.m.	n.m.	n.m.	n.m.	n.m.	n.m.	n.m.	n.m.	n.m.
K7 (L/S=10)	9.87	10.23	n.m.	n.m.	n.m.	n.m.	n.m.	n.m.	n.m.	n.m.	n.m.	n.m.	n.m.	n.m.	n.m.	n.m.	n.m.	n.m.	n.m.	n.m.	n.m.	n.m.
Redox																						
K3 (L/S= 0.5)	115.5	103.9	235	225	215	236	286	275.8	218.2	200.1	n.m.	n.m.	183.1	175.4	180.1	177.1	223	221.1	176.4	181.5	93.5	91.9
K4 (L/S=1)	89	70.5	142.3	133.5	235.8	227.7	180.2	190.4	249	244.7	245.1	246.5	175.8	135.3	153.7	133.2	188.2	176.8	n.m.	186.6	93.4	56.1
K5 (L/S=2)	63.2	54.3	100.8	102.2	210.3	249.4	210.3	191.9	230	179.8	303	272.2	269.7	214.2	182.3	148.8	223.4	232.1	194	141.7	201.8	94.9
K6 (L/S=5)	113.3	82.7	n.m.	n.m.	n.m.	n.m.	n.m.	n.m.	n.m.	n.m.	n.m.	n.m.	n.m.	n.m.	n.m.	n.m.	n.m.	n.m.	n.m.	n.m.	n.m.	n.m.
K7 (L/S=10)	130.1	110.2	n.m.	n.m.	n.m.	n.m.	n.m.	n.m.	n.m.	n.m.	n.m.	n.m.	n.m.	n.m.	n.m.	n.m.	n.m.	n.m.	n.m.	n.m.	n.m.	n.m.

Figure B.3: Values for pH, conductivity (in mS/cm) and redox measured by column tests for 6-20 mm fraction separated from bottom ash in the mini-pilot plant in different time periods and for different L/S ratios (in l/kg). All samples have been duplicated (duplicate refers to A and B). (Note: n.m. means not measured)

	Samples sand			Samples 2-6mm			Samples 6-20mm		
Sample nr.	Conductivity	pH	Redox	Conductivity	pH	Redox	Conductivity	pH	Redox
1 A	4.75	9.43	121.8	2.41	9.48	128.4	3.02	9.36	137.2
1 B	4.8	9.59	124.3	2.49	9.57	130.7	3.07	10.18	120.2
2 A	5.06	5.72	202	7.32	2.07	452	4.59	2.84	415
2 B	5.33	4.39	261	6.1	2.33	450	3.16	9.2	267
3 A	7.46	8.95	223.6	3.45	9.28	217.2	3.29	10.04	206.5
3 B	7.59	8.92	227.7	3.38	9.27	199	3.97	9.93	228.6
4 A	4.59	9.18	222.1	3.32	9.21	217.6	3.65	9.76	215.1
4 B	4.63	9.2	224	3.14	9.2	217.5	3.58	9.81	224.1
5 A	2.66	10.14	129.1	2.1	9.9	123.4	2.32	10.37	121.1
5 B	2.7	10.03	126.4	2.11	9.86	124.2	2.29	10.38	123.1
6 A	4.05	9.71	158.5	2.76	9.84	160.6	3.04	10.45	153.2
6 B	4.21	9.68	161.1	2.75	9.91	155.4	3.47	10.36	158.1
7 A	3.28	9.7	193.5	2.28	9.83	196.8	2.6	10.21	212.2
7 B	3.12	9.68	197.2	2.14	9.81	206.4	2.46	10.29	208.1
8 A	2.79	9.9	133.7	2.16	9.87	130.2	2.48	10.2	128.5
8 B	2.55	10.02	129.9	2.13	9.8	131.1	2.27	10.19	133.4
9 A	2.14	10.35	148	2.17	10.19	154.9	2.49	10.49	174.5
9 B	2.02	10.43	148.9	2.2	10.26	166.6	2.43	10.56	189.2
10 A	1.89	10.6	127.4	1.66	10.15	133.4	2.06	10.85	129.2
10 B	2.13	10.69	130	1.65	10.37	128.8	2.14	10.89	132.8
11 A	2.87	10.31	127.5	1.78	10.41	118.8	2.41	10.77	123.8
11 B	2.67	10.53	123.4	1.73	10.5	118.2	2.26	10.78	131.3

Figure B.4: Values for pH, conductivity (in mS/cm) and redox measured by batch test (shaking test) for sand fraction, 2-6 mm fraction and 6-20 mm fraction separated from bottom ash in the mini-pilot plant in different time periods and for L/S=2 l/kg. All samples have been duplicated (duplicate refers to A and B).

	Sample 1		Sample 2		Sample 3		Sample 4		Sample 5		Sample 6		Sample 7		Sample 8		Sample 9		Sample 10		Sample 11	
	A	B	A	B	A	B	A	B	A	B	A	B	A	B	A	B	A	B	A	B	A	B
Samples Sand																						
Cl	1518.36	1870.55	1947.33	1862.06	2924.24	2440.53	1742.61	1778.33	908.28	1065.76	402.82	1037.21	1052.59	938.80	865.93	849.77	446.26	463.72	795.98	515.30	1026.72	1073.84
SO_4	2170.30	2142.43	980.71	1656.10	2761.20	3011.62	2082.87	2737.00	1626.72	1589.00	2237.89	2269.78	2160.05	2057.32	1714.07	1645.97	1204.80	1232.93	1312.68	1126.52	987.28	1253.84
Cu	4.26	4.39	5.14	6.43	4.67	5.66	4.09	5.17	7.99	8.43	2.75	3.16	3.32	3.32	4.86	4.62	5.33	3.96	5.25	4.76	5.05	4.01
Sb	0.11	0.07	0.08	0.07	0.19	0.21	0.16	0.17	0.07	0.10	0.11	0.11	0.16	0.10	0.15	0.15	0.15	0.10	0.07	0.08	0.08	0.08
Mo	0.73	0.81	0.56	0.72	0.61	0.71	0.83	0.86	0.97	0.83	0.92	0.46	1.45	1.40	0.88	0.82	0.73	0.49	1.41	1.38	1.31	1.38
Samples 2-6 mm																						
Cl	820.73	857.93	1425.33	1283.14	1375.55	1176.50	982.60	1075.04	554.20	497.14	463.86	555.59	586.27	593.31	587.53	542.51	596.49	578.71	980.81	266.20	447.55	448.67
SO_4	1114.85	1142.50	942.31	984.48	1398.58	1294.68	1496.40	1352.74	961.85	1011.00	1744.73	1773.87	1173.02	1084.46	904.54	899.17	1035.30	1081.35	634.35	668.92	683.70	745.64
Cu	1.41	1.64	1.19	1.18	1.93	1.56	1.11	1.27	0.43	0.67	1.57	1.76	0.87	0.83	1.18	1.30	1.68	1.44	0.45	0.56	0.63	0.66
Sb	0.07	0.06	0.05	0.06	0.07	0.07	0.06	0.06	0.06	0.05	0.05	0.07	0.05	0.05	0.09	0.09	0.07	0.08	0.06	0.07	0.07	0.11
Mo	0.36	0.48	0.33	0.33	0.31	0.28	0.33	0.29	0.41	0.43	0.74	0.71	0.62	0.54	0.34	0.47	0.39	0.39	0.45	0.47	0.61	0.66
Samples 6-20 mm																						
Cl	1056.88	926.60	1258.67	1185.40	1534.48	1447.01	1638.64	1544.11	1005.68	974.83	822.73	797.88	1041.42	1012.46	964.97	829.14	907.29	836.54	484.22	494.78	862.48	717.30
SO_4	563.13	563.45	425.22	415.13	877.41	902.72	1168.35	1135.46	546.33	530.86	948.09	1002.47	924.36	819.44	565.27	472.18	703.53	752.17	442.98	587.77	504.84	430.46
Cu	2.73	3.23	4.23	4.43	2.08	3.38	3.16	2.74	2.33	2.85	1.28	1.69	1.16	1.51	1.25	1.76	1.89	2.37	1.16	2.42	2.06	1.67
Sb	0.05	0.06	0.04	0.05	0.06	0.08	0.05	0.06	0.04	0.04	0.04	0.05	0.05	0.05	0.06	0.07	0.05	0.05	0.04	0.05	0.05	0.05
Mo	0.59	0.59	0.50	0.51	0.39	0.47	0.64	0.65	0.47	0.44	0.79	0.81	0.78	0.60	0.35	0.33	0.51	0.48	0.50	0.62	0.72	0.60

Figure B.5: Leaching values for Cl, SO_4, Mo, Sb, Cu (in mg/kg) measured by column tests for sand fraction, 2-6 mm fraction and 6-20 mm fraction separated from bottom ash in the mini-pilot plant in different time periods and for L/S=2l/kg. All samples have been duplicated (duplicate refers to A and B).

	Sample 1		Sample 2		Sample 3		Sample 4		Sample 5		Sample 6		Sample 7		Sample 8		Sample 9		Sample 10		Sample 11	
	A	B	A	B	A	B	A	B	A	B	A	B	A	B	A	B	A	B	A	B	A	B
Samples Sand																						
Cl	1528.76	2087.03	2075.40	1878.19	3010.99	2445.37	1781.63	1824.21	922.52	1208.08	403.72	1050.41	1124.02	954.34	874.25	858.86	464.07	499.23	796.02	672.11	1523.69	1657.33
SO_4	4278.17	4215.27	2617.28	3604.57	4954.86	5191.92	4172.68	4894.55	3590.10	3514.68	4358.61	4365.81	4265.88	4112.78	3706.54	3591.10	2982.20	2924.54	3146.04	2840.17	2628.53	3037.16
Cu	4.73	5.00	5.66	7.01	5.42	6.51	4.87	6.65	8.65	9.99	3.30	3.60	3.85	3.84	5.59	5.24	6.59	4.84	5.72	9.65	6.53	5.78
Sb	0.32	0.25	0.31	0.23	0.65	0.66	0.53	0.65	0.24	0.37	0.35	0.33	0.46	0.29	0.47	0.49	0.34	0.33	0.27	0.38	0.30	0.38
Mo	1.74	2.09	1.54	2.33	1.93	2.26	2.40	2.74	2.96	2.53	2.57	0.92	5.05	4.68	3.08	3.05	2.14	1.62	2.84	4.93	4.68	4.70
Samples 2-6 mm																						
Cl	1008.76	1055.54	1756.20	1450.14	1630.09	1304.44	1067.46	1289.32	681.94	538.47	504.63	591.85	665.94	734.00	679.16	607.45	686.60	632.69	1713.97	298.71	586.97	527.21
SO_4	2840.08	2865.47	2550.78	2607.13	3271.98	3098.29	3411.07	3183.65	2584.78	2651.83	3746.79	3758.60	2932.60	2772.75	2484.03	2459.12	2709.67	2694.88	1959.59	2020.65	2062.57	2174.02
Cu	3.33	4.76	1.61	1.61	2.64	2.09	1.55	1.79	0.83	1.08	2.12	2.30	1.31	1.27	1.83	1.91	3.37	2.21	0.85	0.96	1.03	1.06
Sb	0.25	0.22	0.21	0.22	0.23	0.24	0.22	0.22	0.22	0.22	0.21	0.23	0.21	0.21	0.30	0.33	0.23	0.25	0.22	0.28	0.23	0.33
Mo	1.05	1.50	1.41	1.41	1.06	0.90	1.09	1.06	1.76	1.33	2.19	2.04	2.34	1.77	1.45	1.81	1.65	1.29	1.39	1.33	2.19	1.81
Samples 6-20 mm																						
Cl	1199.08	993.72	1418.63	1276.82	1871.62	1599.07	1866.39	1714.95	1032.08	991.79	864.89	806.70	1217.37	1125.64	1101.10	867.79	996.77	850.91	516.26	495.88	1043.67	834.99
SO_4	1448.32	1439.57	1206.48	1180.36	1911.83	1932.50	2280.70	2225.71	1420.51	1385.74	2005.38	2061.34	1974.31	1820.40	1451.83	1284.63	1666.94	1679.60	1239.56	1478.79	1350.04	1209.02
Cu	3.27	3.92	4.68	4.88	2.50	3.89	3.98	3.29	2.73	3.26	1.68	2.09	1.58	1.93	1.85	2.24	2.31	2.78	1.56	2.82	2.47	2.07
Sb	0.21	0.22	0.20	0.21	0.23	0.24	0.21	0.22	0.20	0.20	0.20	0.21	0.21	0.21	0.22	0.23	0.21	0.21	0.20	0.21	0.21	0.21
Mo	1.80	1.51	1.84	1.84	1.55	1.43	2.14	2.12	1.12	1.05	1.62	1.54	2.93	1.39	1.48	1.37	1.79	1.11	1.81	1.28	2.09	1.40

Figure B.6: Leaching values for Cl, SO_4, Mo, Sb, Cu (in mg/kg) measured by column tests for sand fraction, 2-6 mm fraction and 6-20 mm fraction separated from bottom ash in the mini-pilot plant in different time periods and for L/S=10 l/kg. All samples have been duplicated (duplicate refers to A and B).

	Sample 1		Sample 2		Sample 3		Sample 4		Sample 5		Sample 6		Sample 7		Sample 8		Sample 9		Sample 10		Sample 11	
	A	B	A	B	A	B	A	B	A	B	A	B	A	B	A	B	A	B	A	B	A	B
Samples Sand																						
Cl	1868.07	1896.41	1831.77	1850.16	3578.44	3665.51	1678.8	1681.06	797.87	826.75	1175.67	1233.27	990.23	904.43	799.5	676.2	1811.18	393.48	370.54	432.97	983.49	861.36
SO_4	2331.96	2287.43	1241.51	1279.29	3043.82	3066.72	2464.14	2518.82	1209.85	1202.68	2398.11	2440.35	2002.27	1970.16	1347.48	1192.54	1080.5	1021.88	937.67	1013.19	1619.28	1035.13
Cu	6.62	6.62	7.21	7.21	4.95	4.95	4.4	4.59	6.86	7.62	5.75	6.11	4.72	4.72	5.67	4.91	6.9	6.3	6.23	6.6	7.52	7.33
Sb	0.13	0.13	0.11	0.12	0.19	0.2	0.16	0.16	0.11	0.12	0.16	0.15	0.22	0.21	0.15	0.15	0.11	0.12	0.11	0.11	0.15	0.12
Mo	0.9	0.8	2.06	0.55	0.51	0.51	0.66	0.66	0.53	0.57	0.85	0.88	1.1	1.1	0.66	0.64	0.69	0.65	1.26	1.3	1.45	1.33
Samples 2-6 mm																						
Cl	816.84	799.73	1414.64	1399.4	1305.99	1255.02	1168.42	1076.15	462.68	490.82	554.2	578.58	1298.32	533.98	538.57	539.59	499.34	435.45	289.62	285.86	412.08	400.29
SO_4	1301.3	1355.2	1277.96	1233.57	1481.06	1464.35	1855.17	1773.66	1281.56	1331.41	1885.16	1841.86	1431.94	1153.59	1168.93	1106.39	1092.6	949.98	1789.74	1026.08	872.31	803.14
Cu	1.13	1.27	1.88	2.25	1.85	1.89	1.99	1.76	0.93	1.29	1.69	1.69	1.43	1.58	1.66	2.1	1.67	1.84	1.65	1.81	0.87	1.35
Sb	0.07	0.08	0.08	0.08	0.08	0.08	0.09	0.08	0.1	0.08	0.06	0.06	0.07	0.08	0.08	0.09	0.11	0.1	0.06	0.08	0.14	0.11
Mo	0.52	0.4	0.34	0.3	0.28	0.28	0.46	0.41	0.59	0.59	0.72	0.68	0.68	0.66	0.58	0.48	0.42	0.42	0.62	0.64	0.97	0.77
Samples 6-20 mm																						
Cl	1256.99	1295.95	1166.2	1194.26	1386.54	1742.64	1490.35	1495.88	802.79	782.66	932.03	1178.49	1277.69	851.97	839.41	758.61	795.95	793.01	593.19	563.05	776.7	1607.93
SO_4	878.15	974.52	569.85	507.33	1025.98	1202.36	1521.07	1527.8	603.3	698.75	1383.3	1495.4	1071.3	944.29	777.79	762.04	847.01	835.21	713.82	734.15	867.23	835.9
Cu	4.75	4.75	8.78	9.89	6.16	7.55	4.71	5.1	3.76	3.76	5.35	6.54	3.39	3.39	3.79	3.19	4.88	4.69	3.8	4.2	6.77	5.18
Sb	0.11	0.12	0.11	0.1	0.13	0.15	0.12	0.11	0.1	0.1	0.11	0.13	0.18	0.18	0.14	0.14	0.09	0.09	0.12	0.12	0.17	0.16
Mo	0.63	0.71	0.52	0.63	0.58	0.64	0.67	0.71	0.65	0.67	1.15	1.35	0.82	0.78	0.62	0.28	0.59	0.61	0.84	0.82	1.02	1.04

Figure B.7: Leaching values for Cl, SO_4, Mo, Sb, Cu (in mg/kg) measured by batch test (shaking test) for sand fraction, 2-6 mm fraction and 6-20 mm fraction separated from bottom ash in the mini-pilot plant in different time periods and for L/S=2 l/kg. All samples have been duplicated (duplicate refers to A and B).

Appendix C

Machinery

C.1 Belt Filter Press

A belt filter press (Figure C.1) is a continuous feed sludge dewatering machine with two porous moving belts that has a gravity drainage zone and mechanically applied pressure zones. The sludge is fed onto the gravity section of the belt via a feed chute. The solids-water mixture sits on the moving porous belt, allowing the water to drain through it. The water is collected in drain pans and routed to a sump. As the slurry moves on the belt, it is turned by plow blades. The plows greatly accelerate the gravity drainage process by clearing places for water to drain and by turning the solid mass on the belt. The slurry is stopped from running off the sides of the belt by restrainers and rubber seals. At the end of this gravity drainage section, the solids are usually in the form of a loosely structured cake. From the gravity drainage section, the cake falls onto the bottom belt and begins to be compressed between the belts, forming a wedge. The sandwiched solid material then passes over a series of rollers, which apply pressure to the solids at a gradual rate to expel nearly all the free water from the slurry. At the last roller, the belts separate and the cake is removed from the belts by scrapers (Turovskiy and Mathai 2006).

C.2 Hydrocyclone

The separation action in hydrocyclone is based on the centrifugal effect created within the cyclone body. Figure C.2 shows a functional scheme of a hydrocyclone. The cylindrical part is closed at the top by a cover, through which a liquid overflow pipe (vortex finder) protrudes some distance into the cyclone body. The slurry enters the hydrocyclone through a tangential inlet located near the top of the cyclone. Most of the incoming fluid moves in an outward, downward moving primary vortex. Some of the downward flow that carries most of the solids leaves through the underflow orifice at the bottom of the hydrocyclone, while vertical direction of the rest reverses and it moves upward in a secondary vortex, exiting via the overflow orifice. The strong centrifugal effect within the cyclone causes the particles in the slurry to migrate to the wall of the cyclone. Working against this is the flow of water from the primary to the secondary vortex, towards the overflow. The result of these opposing factors is that the coarse particles remain at the cyclone wall whilst the finer particles remain with the water and exit the cyclone in the overflow fraction. The coarse material is forced through the conical section of the cyclone to exit

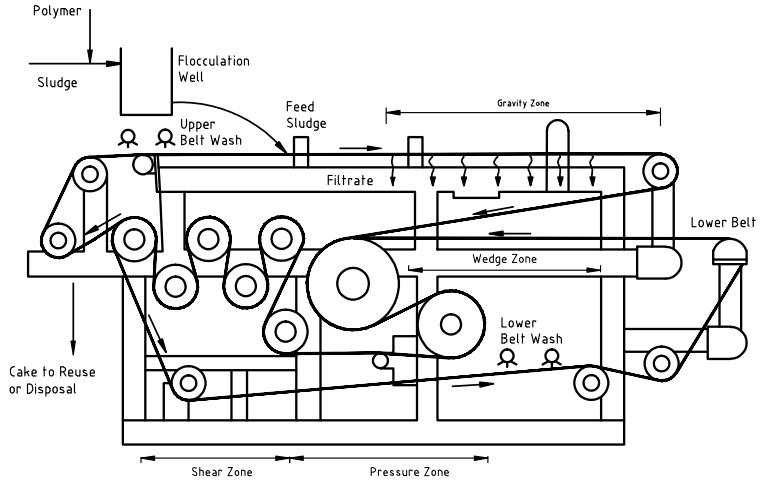

Figure C.1: Schematic of a belt filter press.

via the spigot (Svarovsky and Them 2002).

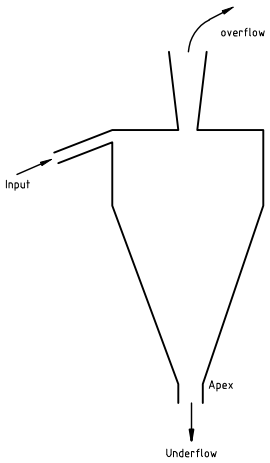

Figure C.2: Functional scheme of a hydrocyclone.

C.3 Jig

The jig operation consists of two actions. One is the effect of 'hindered settling', meaning that a heavier particle will settle faster than a light particle. The other is the separation process in an 'upward flow of water', which separates the particles by their density. These two actions are combined in a jig by slurry pulses generated mechanically or by air. The principle of the jig separation is explained by a layer of mixed particles lying on a perforated plate or screen creating a 'bed'. During the upward and downward stroke of the fluid, parts of the jig bed will be fluidized and particles are able to move. During this stage the heavy particles will have a greater velocity downward than the light particles. After equilibrium is reached, layers with different densities will be present on the screen. The density will increase with decreasing distance from the screen (Witteveen 2003). The jigging is influenced mainly by the following factors:

- The jigging speed (number of strokes per second)
- The stroke length (two times the amplitude of the stroke)
- The bed thickness
- The diameter and density of the particles
- The shape of the particles

For the pilot plant a specially constructed jig was developed and implemented that also allows the separation of organics (Chapter 3, 0-2 mm separation).

C.4 Shaking Table

A shaking table (Figure C.3) consists of small riffles over which a fine slurry is passed (Wills and Napier-Munn 2006). The heavy, dense particles settle into the riffles and through a vibrating action are directed to one side of the table where they are collected. The tailings are passed across the middle of the table or remain in suspension. Middlings, material that is partially settled, may be collected. Heads and middlings are commonly reprocessed on multi-stage tables. Shaking tables can handle materials from 15 μm to 3.0 mm.

C.5 Spiral

A spiral concentrator uses gravity to separate particles of different densities. The lighter minerals are more readily suspended by the water and attain relatively high tangential velocities so that they climb toward the outer rim of the spiral trough. At the same time, the heavier non-suspended grains migrate by saltation (defined as non-linear motion that is a combination of rolling and bouncing) along the lowest part of the spiral cross-section and are selectively directed with the adjustable product splitter into the product discharge outlet ports (Wills and Napier-Munn 2006).

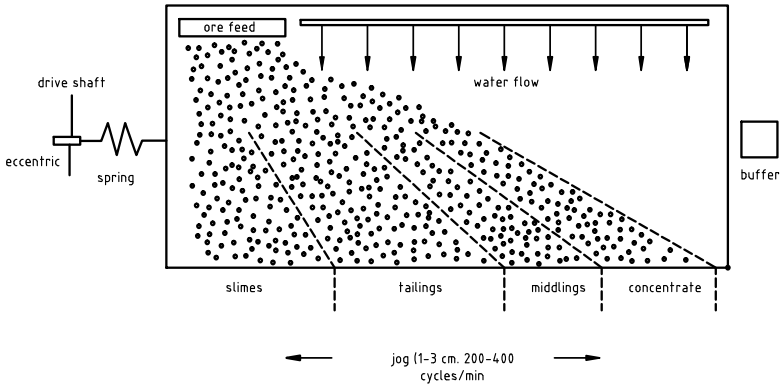

Figure C.3: System of separation by a shaking table.

C.6 Kinetic Gravity Separator

The principle of kinetic gravity separation is that particles that are fed at some point into a horizontal flowing fluid stream reach their terminal velocity rapidly after being released (Figure C.4). The particles then have a horizontal velocity component that equals that of the fluid and a vertical velocity component depending on their density, size and shape. The particles can be collected in compartments that are placed in line. The particles with a high terminal velocity end up in the compartment close to the feeding point, while particles settling at a lower speed are collected further downstream. It is practical to use a circular rotating design as shown in Figure C.4 (Kooy et al. 2004).

For the pilot plant an alternative, prototype kinetic gravity separator was designed in which particles are separated strictly according to terminal velocity. The prototype KGS, consists of a cylindrical shell with a cylinder placed inside it. Between the cylinders a paddle wheel is placed consisting of several paddles. These paddles are placed close to each other to prevent horizontal fluttering of the particles. The paddles rotate around the separator's vertical axis and due to their rotation, water in the separator is forced to move at a constant angular velocity. Particles are fed from the top and based on their specific terminal velocity, the wheel speed and the height of the machine, these particles will be separated into several compartments, located at the bottom of the KGS. The speed of the paddle wheel rotation makes the heavy particles (metals) fall into the first compartment while the lighter particles (stone, aluminium, glass) are collected in the second and third compartments. The light particles (organics, highly porous stone) are collected in the fourth, fifth and sixth compartments. The extremely light particles (organics coating on top of the water), flow over the top, where they are collected.

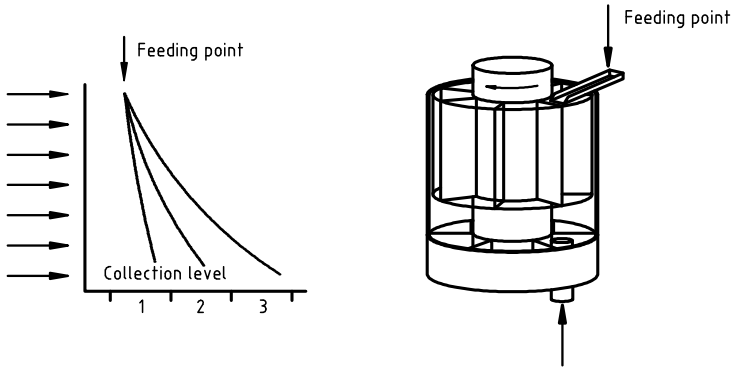

Figure C.4: Principle of kinetic gravity separation.

C.7 Wire Separator

The basic concept of the wire separator is that elongated particles can pass over a gap or slot of appropriate size, while granular particles of the same diameter will not (Figure C.5). By placing the construction on top of a conventional vibrating feeder a single step separator is created.

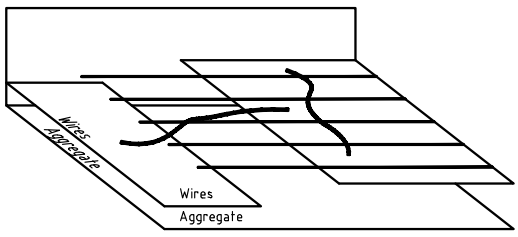

Figure C.5: A single step of the wire separator.

Wires move along the top level of the separator while the granulate particles fall down through the 'fingers' in the gap to a lower level. The 'fingers' are positioned over the gap with a parallel orientation, to prevent wires that have

a different orientation from falling through the gap. A single step separation can be sufficient for applications with wires that are long compared to the size of the granular particles and for low capacities. At higher loads, the granular particles form a thick layer on the separator and may fill the gap, while short wires occasionally fall through the gap, nullifying the effect of the apparatus. Therefore, positioning multiple gaps in a cascade system is the solution for applications with a need for high capacity and precise separation based on wire length. Such a design is shown in Figure C.6 (Muchova et al. 2005).

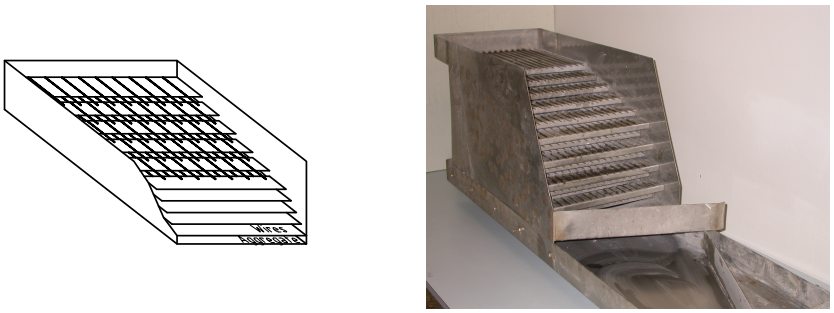

Figure C.6: Scheme of a 5 x 5 cascade wire separator.

C.8 Eddy Current Separator

The rotor of the ECS is based on a multi-pole magnet, consisting of an even number of poles, rotating at a very high speed in the same direction as the belt (see Figure C.7).

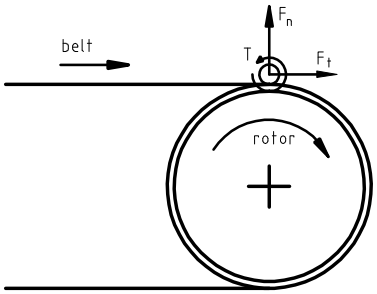

Figure C.7: Standard eddy current separator: the torque T and the forces F_n and F_t that work on a particle are shown.

When a metal particle approaches the rotor several processes occur (Rem 1999). The fast rotation of the rotor makes the field change very rapidly in such a way that at a certain position it can be experienced as a rotating field. A non-ferrous metal particle within a magnetic field tend to keep the magnetic flux inside the particle constant. A particle that approaches the rotor experiences a torque that makes it rotate in the same direction as the field. Besides the torque there are a number of forces working on the metal particle (e.g. normal Fn and tangential force Ft). The normal and tangential forces make the non-ferrous metal particles jump away from the belt, while the torque makes them spin (Figure C.7). In this way non-ferrous metals jump further than mineral particles (stone, glass), which fall by gravity closer to the belt while magnetic particles are removed below the belt.

C.9 Eddy Current Separator for Fine Particles

A wet eddy current separator (WECS) is, in contrast with the standard ECS, suitable for particles with sizes below 6 mm. The separator itself is not different from an ECS. The difference is that the feed is slightly wet (with a moisture content preferably around 10-15%) and the rotor of a WECS rotates, unlike an ECS, against the direction of the conveyor belt. The water sticks all the particles to the belt surface and the adhesive force acting on the small particles is similar to gravity (Rem 1999). The torque caused by the rotating field of the rotor breaks the adhesive force that makes the non-ferrous metal particles adhere to the belt and makes them spin (Figure C.8). The same processes affect the ferrous metal particles. However, if the magnetic attraction acting on these ferrous particles is sufficiently strong they will stay on the belt. The non-ferrous metal particles are disengaged from the belt and are collected in front of the separator while the non-metal and ferrous particles remain on the belt and are released below the separator.

C.10 Magnus Separator

Magnus separation is similar to separation by a WECS and is a relatively new process that is suitable for the separation of particles with sizes up to 6 mm (Haeser 2002, Fraunholcz et al. 2002). Like a WECS, a Magnus separator is used to separate non-ferrous metal particles from non-metal and magnetic particles. However, a Magnus separator separates non-ferrous metal particles using the lift force acting on rotating particles, which is called the Magnus effect. In a Magnus separator the particles are fed at the top (Figure C.9). They are dropped into the separator, which is filled with water, while the feeding water flows over. Inside the separator a rotor with a dipole magnet turns with an extremely high rotation speed. Around the rotor of the Magnus separator a conveyor belt is stretched with a strip that moves magnetic particles away from the rotor. This conveyor belt rotates in the opposite direction to the rotor to improve the separation. When a non-conducting particle falls down into the separator, it will only experience the usual forces like the drag, buoyancy and gravity force. When a non-ferrous metal particle, for example an aluminium particle, falls into the separator the particle starts to turn around.

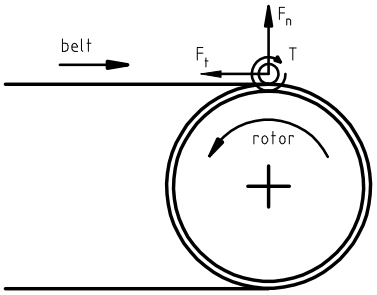

Figure C.8: Wet eddy current separator with torque T and forces F_n and F_t that work on a particle are shown. The F_t and the torque T are due to the change in rotor direction as compared to figure C.7.

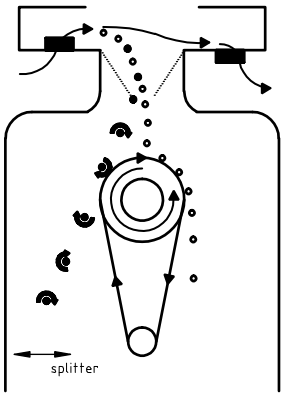

Figure C.9: Side view of a Magnus separator. The non ferrous metal particles are indicated by black spheres while the stone particles are indicated by white spheres.

This is the same as eddy current separation, caused by rotation of the rotor. The combination of falling and turning of the particles causes a lift force and alters the direction of their motion. When a particle rotates around its axis while moving through a fluid in a direction perpendicular to its axis, it experiences a force perpendicular to both the direction of motion and the axis. This lift force is called the Magnus effect.

C.11 Low Intensity Magnetic Separator

A LIMS consists of a rotating non-magnetic drum containing stationary magnets of alternating polarity. The material is fed together with water at the top of the drum and magnetic particles are lifted by the magnets and separated to one side by a splitter, while the non-magnetic particles are removed at the other side. The LIMS used in experiments described in Chapter 3 was adjusted by adding a specially constructed plate, to keep particles closer to the magnet (Figure C.10) and on the other side of the drum water was sprayed to free the sand particles from the magnetic particles.

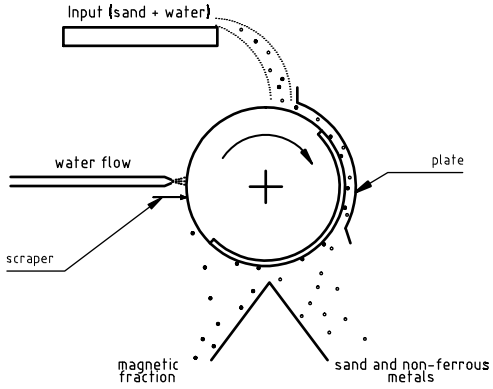

Figure C.10: An adjusted LIMS, used for an experiment with MSWI BA from Amsterdam.

C.12 Drum Separator

A drum separator consists essentially of a rotating non-magnetic drum containing three to six stationary magnets of alternating polarity. Separation is effected by the pick-up principle; by creating a magnetic force, a gravitational force and a drag force magnetic particles can be separated from non-magnetic particles because they are lifted by the magnets and pinned to the drum and

then conveyed out of the field, while non-magnetic particles exit in the tailing compartment.

C.13 Wind Sifter

Light particles (paper, foil) can be separated based on their density and shape from the residue by a wind sifter. The wind sifter is placed at a certain distance from the stream and air is blown at a certain velocity in an opposite orientation to the stream. The light particles are blown away from the residue and collected.

Appendix D

Acknowledgements

I would like to thank all of the people who in one way or another have helped me during my study at Delft University of Technology.

I gratefully acknowledge Peter Rem, who supervised, advised and helped throughout the entire research work concerning the wet physical separation of bottom ash. His knowledge of separation and physics was of great importance. His innovative ideas were stimulating and taught me that kindness and generosity are the cornerstones of higher education. I also want to express my gratitude to Klaas van Breugel and Marcus Reuter for allowing me to carry out this research and for the trust they had in me, which was crucial to the successful completion of this Ph.D. project.

I want to thank Afval Energie Bedrijf (AEB) and all the people involved in this project for their great cooperation and contributions to this research. I would also like to thank the laboratory group from AEB for their assistance during my laboratory work as well as the team involved in Pilot plant II and DWR.

Special thanks are due to SenterNovem, Life and Steenkorrel for their sponsorship.

I would also like to thank the following companies, Umicore, Outokumpu and Xella, for their valuable cooperation in determining utilization options and values of BA. I would like to thank Jan Schreurs from Schreurs b.v. for his excellent comments and advice about the soil quality decree and bottom ash leaching.

During my stay at the Resources Engineering section I was very well received by all of my colleagues and I have made very good friends. This list is quite long, so I wish to collectively thank all of you who supported me in one way or another.

I would also like to thank to all the students who were involved in this project as part of their master's or bachelor's degree for their great contributions.

Many thanks to Sees-editing Ltd., Gregory Suden and Anuja Ghate for their editing work on my thesis and to Michiel Nieuwenhuijse for his creativity in designing my cover.

Finally, I would like to thank all of my friends, especially Erwin Bakker who

has been my big supporter and is always available in any situation to help. Also, Simon Honingh who helps me realize what is important in life and because without him I would have never started this research. Many thanks to my wonderful partner, Fredo and to my loving parents Alena and Karel.

Appendix E

Curriculum Vitae

Personal

Name: Lenka Muchova
Date of Birth: 8 May 1978
Place of Birth: Opava, the Czech Republic

Education and working experience

2008-now: Researcher at the European Commission, JRC-IPTS, Seville, Spain.

2003-2008: Doctoral research (promovendus) at Delft University of Technology, Faculty of Civil Engineering and Geosciences, The Netherlands. Research subject: Wet physical separation of MSWI bottom ash.

2002-2003: Internship at Corus, IJmuiden, the Netherlands.

1996-2001: Master Degree (Commercial Engineering in the Field of Raw Materials), VŠB-TU Ostrava, Faculty of Mining and Geology, The Czech Republic.

Publications

Muchova, L., Mooij, M., Van Kooy, L., Berkhout, P., A cascade wire separator, International journal of mineral processing, 78 (2005), pp.40-48

Muchova, L. and Rem, P.C., (2006). Metal content and recovery of MSWI bottom ash, Waste Management and the Environment III, proceeding from the Waste Management Conference in Malta, 211-216pp.

Muchova, L., and Rem, P., (2006). Pilot plant for wet physical separation of MSWI bottom ash, Conference proceeding MMME 2006, Cape Town (South Africa), 14-15 November, pp.12

Muchova, L. and Rem, P.C., (2007). Hydrogen from bottom ash. Conference proceeding from CEMEPE, 24-28.7.2007 in Skiathos Island, Greece, pp.6.

Muchova, L. and Rem, P.C., (2007). Leaching improvement for separated bottom ash by wet physical techniques, Conference proceeding from the 3rd International Conference on Environmental Science and Technology 2007, 6 to 9 August 2007, Houston, Texas, United States, pp.6.

Muchova, L., Rem, P., Van Berlo, M. (2007). Innovative Technology for the Treatment of Bottom Ash. Conference proceeding from ISWA/NVRD World Congress 2007, Amsterdam, The Netherlands, 24-27 September 2007.

Muchova, L., Rem, P., (2007). Management of bottom ash in Europe. Waste Management World, November 2007, Vol. 8, issue 6. pp. 4.

Muchova, L., Bakker. E., Rem, P. (2008). Precious metals in municipal solid waste incineration bottom ash, Water, Air, and Soil Pollution, 2008.

Bakker, E.J., Muchova, L., Rem, P.C. (2007). Separation of precious metals from MSWI bottom ash, Conference proceeding from 6th international industrial mineral symposium, 1-3 February, Izmir, Turkey, pp.6.

Bakker, E.J., Muchova, L., Rem, P.C. (2007), Economic recovery of precious metals from MSWI bottom ash, Conference proceeding from CEMEPE, 24-28.7.2007 in Skiathos Island, Greece, pp.5.

Abayazid, J., Muchova, L., Lemkowitz, S., Heijungs, R., Rem, P., van Berlo, M. Comparative life cycle assessment of bottom ash management: Wet ver-sus Dry treatment, submitted to Resources, Conservation and Recycling in 2008.

Muchova, L., Bakker, E.J., Characterization and utilization of MSWI sand fraction containing aluminium, submitted to Waste Management Research in 2009.

Bibliography

1993/31/EU: 1993, Waste disposal act.

2001/118/EC: 2001, European waste list.

2003/33/EC: 2003, Council decision from 2002. establishing criteria and procedures for the acceptance of waste at landfills pursuant to article 16 of and annex ii to directive 1999/31/ec.

2008/98/EC: 2008, Waste framework directive.

Agacayak, T., Zedef, V. and Aydogan, S.: 2007, Benefication of low-grade chromite ores of abandoned mine at topraktepe, *Acta Montanica Slovaca, 12*, Beyşekir, Turkey, pp. 323–327.

Arm, M.: 2004, Variation in deformation properties of processed MSWI bottom ash: results from triaxial tests, *Waste Management* **24**, 1035–1042.

ASTMD3682-01: n.d., Standard test method for major and minor elements in combustion residues from coal utilization processes.

Autret, E., Berthier, F., Luszezanec, A. and Nicolas, F.: 2007, Incineration of municipal and assimilated wastes in France: Assessment of latest energy and material recovery performances, *Journal of Hazardous Materials, B* **139**, 569–574.

Bakker, E. J., Muchova, L. and Rem, P. C.: 2007a, Economic recovery of precious metals from MSWI bottom ash, *Proceedings of the CEMEPE*, Skiathos Island, Greece, p. 5.

Bakker, E. J., Muchova, L. and Rem, P. C.: 2007b, Separation of precious metals from MSWI bottom ash, *Proceedings of the 6th International Industrial Mineral Symposium*, Izmir, Turkey, p. 6.

Belitskus, D.: 1970, Reaction of aluminum with sodium hydroxide solution as a source of hydrogen, *J. Electrochem. Soc.* pp. 1097–1099.

Bertolini, L., Carsana, M., Cassago, D., Curzio, A. Q. and Collepardi, M.: 2004, MSWI ashes as mineral additions in concrete, *Cement and Concrete Research* **34**(10), 1899–1906.

Birgisdottir, H., Bhander, G., Hauschild, M. Z. and Christensen, T. H.: 2007, Life cycle assessment of disposal of residues from municipal solid waste incineration: Recycling of bottom ash construction or landfilling in denmark evaluated in the ROAD-RES model, *Waste Management* **27**, 75–84.

BMD: 1989, Building materials decree, http://www.vrom.nl/.

Boddum, J. K. and Skaarup, J.: 2000, Pilot and full scale washing of incinerator bottom ash, *Sustainable construction: Use of incinerator ash*, Thomas Telford Publishing, pp. 111–123.

Chandler, A. J., Eighmy, T. T., Hartlen, J., Hjelmar, O., Kosson, D. S., Sawell, S. E., van der Sloot, H. A. and Velow, J.: 1997, Municipal solid waste incinerator residues, Elsevier studies in environmental science 67, Elsevier, Amsterdam, 1997.

Chimenos, J. M., Segarra, M., Fernandez, M. A. and Espiell, F.: 1999, Characterization of the bottom ash in municipal solid waste incinerator, *Journal of Hazardous Materials* **64**, 211–222.

Chung, Y.-S., Moon, J.-H. and etc.: 2007, Determination of the elementar composition of the bottom ash of a municipal incinerator by instrumental neutron activation analysis, *Journal of Radioanalytical and Nuclear Chemistry* **271**(2), 339–244.

CML: n.d., n. 148. Leiden university.

Comans, R. N. J., van der Sloot, H. A. and Bonouvrie, P. A.: 1993, Speciatie van contaminanten tijdens uitloging van avi-bodemas, *Technical report*. In Dutch.

Cui, J.: 2005, Mechanical recycling of consumer electronic scrap. ph.d. thesis 2005:36, issn: 1402-1757, *Technical report*.

Darby, L. and Obara, L.: 2005, Household recycling behaviour and attitudes towards the disposal of small electrical and electronic equipment, *Resources, Conservation and Recycling* **44**(1), 17–35.

DIN38414S4: 1984, German standard procedure for water, wastewater and sediment testing. group s (sludge and sediment). determination of leachability (s4).

Ecke, H.: 2001, *Carbonation for fixation of metals in municipal solid waste incineration (MSWI) fly ash*, PhD thesis, Department of environmental engineering, Lulea, Sweden.

Ekvall, T. and Finnveden, G.: 2001, Allocation in ISO 14041 - a critical review, *Journal of Cleaner Production* **9**, 197–208.

EN12457/1: 2002, Characterisation of waste - leaching - compliance test for leaching of granular waste materials and sludges - part 1: One stage batch test at a liquid to solid ratio of 2 l/kg for materials with high solid content and with particle size below 4 mm (without or with size reduction).

EN12457/2: 2002, Characterization of waste - leaching - compliance test for leaching of granular waste materials and sludges - part 2: One stage batch test at a liquid to solid ratio of 10 l/kg for materials with particle size below 4 mm (without or with size reduction).

EN12457/3: 2002, Characterization of waste - leaching - compliance test for leaching of granular waste materials and sludges - part 3: Two stage batch test at a liquid to solid ratio of 2 l/kg and 8 l/kg for materials with high solid content and with particle size below 4 mm (without or with size reduction).

EN12457/4: 2002, Characterization of waste - leaching - compliance test for leaching of granular waste materials and sludges - part 4: One stage batch test at a liquid to solid ratio of 10 l/kg for materials with particle size below 10 mm (without or with size reduction).

Fraunholcz, N., Rem, P. C. and Haeser, P. A. C. M.: 2002, Dry magnus separation, *Minerals Engineering* **15**, 45–51. Presented at MEES'01, Falmouth, UK - June 2001.

Ghile, D. B.: 2006, *Effects of Nanoclay Modification on Rheology of Bitumen and on Performance of Asphalt Mixtures*, PhD thesis, Delft, The Netherlands. MSc thesis.

Guinee, J. B.: 2002, *Life Cycle Assessment, An operational guide to the ISO standards, CMLCA Handbook, part 2a*, Kluwer Academic Publishers.

Gy, P.: 1999, *Sampling for analytical purposes*, John Wiley & Sons.

Haeser, P. A. C. M.: 2002, Dry magnus separation. The modelling, construction and testing of a dry magnus pilot separator, *Technical Report GT2002A01.*

Heijungs, R., de Koning, A., Ligthart, T. and Korenromp, R.: 2004, Tno-report: Improvement of lca characterization factors and lca practice for metals, *Technical Report R 2004/347*, Apeldoorn, The Netherlands.

Heijungs, R. and Guinee, J. B.: 2007, Allocation and 'what-if' scenarios in the life cycle assessment of waste management systems, *Waste Management* **27**, 997–1005.

Ishii, K., Ozaki, R., Kaneko, K., Fukushima, H. and Masuda, M.: 2007, Continuous monitoring of aluminium corrosion process in deaerated water, *Corrosion Science* **49**(6), 2581–2601.

Janz, A. and Bilitewski, B.: 2007, The contribution of small electric and electronic devices to the content of hazardous substances and recyclables in residual household waste, *Proceedings of the International Conference on Environmental Management, Engineering, Planning and Economics*, Skiathos, p. 1576.

Kaiser, R.: 1969, Patent us 3,483,968.

Kim, S. Y., Matsuto, T. and Tanaka, N.: 2003, Evaluation of pre-treatment methods for landfill disposal of residue from municipal solid waste incineration, *Waste Management Research* **21**(5), 416–423.

Köhnlechner, R., Schlett, Z. and Lungu, M.: 2002, A new wet eddy-current separator, *Resources, Conservation and Recycling* **37**(1), 55–60.

Kooy, L. A. v., Mooij, M. A. and Rem, P. C.: 2004, Kinetic gravity separation, *Physical Separation in Science and Engineering* **13**(1), 25–32.

Kooy, L. v., de Vries, C. and Rem, P.: 2002, Verwerking bodemas van de AVI-A'dam fase II: Pilot plant, *Technical Report TA.GT.2002.20*, TU Delft, Delft, The Netherlands.

Lopez Meza, S., Garrabrants, A., van der Sloot, H. and Kosson, D. S.: 2008, Comparison of the release of constituents from granular materials under batch and column testing, *Waste Management* **28**, 1853–1867.

Meima, J. A. and Comans, R. N. J.: 1998, Application of surface complexation/precipitation modelling to contaminant leaching from weathered municipal solid waste incinerator bottom ash, *Environ. Sci. Tech.* **32**(5), 688–693.

Molenaar, J. M. M.: 2003, *Performance related characterisation of the mechanical behaviour of asphalt mixtures*, PhD thesis.

Mooij, M. A.: 2004, *Wet treatment of bottom-ash 2-6 mm fraction*, PhD thesis, TU Delft, Delft, The Netherlands. MSc thesis.

Muchova, L., Bakker, E. J. and Rem, P. C.: 2008, Precious metals in MSWI bottom ash. Submitted to the International Journal of Water Air and Soil Pollution.

Muchova, L., Mooij, M., Kooy, L. v. and Berkhout, P.: 2005, A cascade wire separator, *International journal of mineral processing* **78**, 40–48.

Muchova, L. and Rem, P.: 2006a, Pilot plant for wet physical separation of mswi bottom ash, *Proceedings of MMME 2006*, Cape Town, South Africa, p. 12.

Muchova, L. and Rem, P.: 2007a, Management of bottom ash in Europe, *Waste management worlds* p. 4.

Muchova, L. and Rem, P. C.: 2006b, Metal content and recovery of mswi bottom ash, waste management and the environment iii, *Proceedings of the Waste Management Conference*, Malta, pp. 211–216.

Muchova, L. and Rem, P. C.: 2007b, Hydrogen from bottom ash, *Proceedings of CEMEPE 2007*, Skiathos Island, Greece, p. 6.

Muchova, L. and Rem, P. C.: 2007c, Leaching improvement for separated bottom ash by wet physical techniques, *Proceedings of the 3rd International Conference on Environmental Science and Technology 2007*, Houston, Texas, p. 6.

Müller, U. and Rübner, K.: 2006, The microstructure of concrete made with municipal waste incinerator bottom ash as an aggregate component, *Cement and Contrete Research* **36**, 1434–1443.

Murariu, V., Svoboda, J. and Sergeant, P.: 2005, The modeling of the separation process in a ferrohydrostatic separator, *Min. Eng.* **18**, 449–457.

NEN7343: 2004, Leaching characteristics of solid earthy and stony building and waste materials - leaching tests - determination of the leaching of inorganic components from granular materials with the column test.

NEN7345: 1995, Leaching characteristics of solid earthy and stony building and waste materials - leaching tests - determination of the leaching of inorganic components from buildings and monolithic waste materials with the diffusion test.

NEN7373: 2004, Leaching characteristics - determination of the leaching of inorganic components from granular materials with a column test - solid earthy and stony materials.

NEN7375: 2004, Leaching characteristics - determination of the leaching of inorganic components from moulded or monolithic materials with a diffusion test - solid earthy and stony materials.

NEN7383: 2004, Leaching characteristics - determination of the cumulative leaching of inorganic components from granular materials with a simplified procedure of the columm test - solid earthy and stony materials.

NEN7714: 2000, Specification for masonry units, autoclaved aerated concrete masonry units.

NFX31-210: 2004, French standard procedure for batch extraction test.

NPR6416: 1995, Atomic absorption spectrometry - flame analysis - general guidelines.

NPR6417: 1997, Atomic absorption spectrometry - graphite furnace technique - general guidelines.

Pan, J. R., Huang, C., Kuo, J. and Lin, S.: 2007, Recycling MSWI bottom ash and fly ash as raw materials for portland cement, *Waste Management* . Accepted 18 April 2007.

Pera, J., Coutaz, L., Ambroise, J. and Chababbet, M.: 1997, Use of incinerator bottom ash in concrete, *Cement and Concrete Research* **27**(1), 1–5.

prEN 14405: n.d., The percolation test.

RAW bepalingen: 2005, Raw bepalingen, CROW, ede. In Dutch.

Reimers, G. W., Rholl, S. A. and Khallafalla, S. A.: 1974, Patent us 3,788,465.

Rem, P. C.: 1999, *Eddy current separation*, Uitgevery Eburon, Delft, The Netherlands.

Rem, P. C., de Vries, C., van Kooy, L., Bevilacqua, P. and Reuter, M.: 2004, The Amsterdam pilot on bottom ash, *Minerals Engineering* **17**.

RIVM: 1994, Report 1994/13, http://www.rivm.nl/.

Saikia, N., Cornelis, G., Mertens, G., Elsen, J., Balen, K. V. and van Gerven, T.: 2007, Assessment of Pb-slag, MSWI bottom ah and boiler and fly ash for using as a fine aggregate in cement mortar, *Journal of Hazardous Materials* . Accepted 25 October 2007.

Schlett, Z. and Lungu, M.: 2002, Eddy-current separator with inclined magnetic disc, *Minerals Engineering* **15**(5), 365–367.

Schmelzer, G., Wolf, S. and Hoberg, H.: 1996, New wet treatment for components of incineration slag, *AT Augbereitungs Technik* **37**.

Settimo, F., Bevilacqua, P. and Rem, P. C.: 2004, Eddy current separation of fine non-ferrous particles from bulk streams, *Physical Separation in Science and Engineering* **13**(1).

Sloot, H. A., Heasman, L. and Quevauviller, P.: 1997, *Harmonization of Leaching/Extraction Test*, Vol. 70, Elsevier Science B.V., Amsterdam, The Netherlands.

Soler, L., Macanas, J., Munoz, M. and Casado, J.: 2007, Aluminum and aluminum alloys as source of hydrogen for fuel cell applications, *Journal of Power Sources* . In press.

Song, G., Kim, K., Seo, Y. and Kim, S.: 2004, Characteristics of ashes from different locations at the MSW incinerator equipped with various air pollution control devices, *Waste management* **24**(1), 99–106.

SQD: 2007, Dutch legislation, soil quality decree, http://www.vrom.nl/.

Statistics, E.: 2007, Structural indicators: Municipal waste, http://europe.eu.int/.

Svarovsky, L. and Them, M. T.: 2002, *Hydrocyclones analyses and applications*, Kluwer Academic Publishers.

Svensson, M., Herrmann, I., Ecke, H. and Sjöblom, R.: 2005, Selective mobilization of critical elements in incineration ashes, *Technical Report Q4-104*, Värmeforsk Service AB, Stockholm, Sweden.

Svoboda, J.: 1998, Patent ep 0 839 577.

Svoboda, J.: 2004, Magnetic techniques for the treatment of materials. magnetic techniques for the treatment of materials.

Todorovic, J. and Ecke, H.: 2006, Treatment of MSWI residues for utilization of secondary construction minerals: A review of methods, *Minerals & Energy* **20**(3–4), 45–59.

Turovskiy, I. S. and Mathai, P. K.: 2006, *Wastewater sludge processing*, Jonh Willey & Sons, Inc.

Umweltbundesamt: n.d., Aggregates case study, final report.

van de Ven, M. F. C., Khedoe, R. N., Poot, M. and Moraal, J.: 2006, Asfalt met aeb granulaat, *Technical Report 7-06-142-1*, TU Delft, Delft, The Netherlands. In Dutch.

van der Sloot, H. A.: 2002, *Harmonisation of Leaching/Estraction Procedures for Sludge, Compost, Soil and Sediment Analyses. Methodologies for soil and sediment fractionation studies*, Royal Society of Chemistry.

van Gerven, T., Geysen, D., Stoffels, L., Jaspers, M., Wauters, G. and Vandecasteele, C.: 2005, Management of incinerator residues in Flanders (Belgium) and in neighbouring countries. A comparison, *Waste Management* **25**, 75–87.

van Zomeren, A. and Comans, R. N. J.: 2004, Contribution of natural organic matter to copper leaching from municipal solid waste incinerator bottom ass, *Environ. Sci. Tech.* **38**, 3927–3932.

VITO: n.d., Beste beschikbare technieken (bbt) voor behandeling van bodemas van huisvuilverbranding. report from vlaams kenniscentrum voor beste beschikbare technieken (vito) 2008/ims/r/(in dutch language).

Vlasov, V. N., Gubarevich, V. N., Zaskevich, M. V., Kravchenko, N. D., Zelenchuk, V. A. and Alipov, A. I.: 1988, Patent ep 0 362 380.

Waterman, M. and van Houwelingen, J.: 1997, Economische terugwinning van aluminium uit bodemassen van afvalverbrandingsinstallaties (AVI's), *Aluminium* **5**. In Dutch.

WBB: 1986, Soil protection act, http://www.vrom.nl/.

Wills, B. A. and Napier-Munn, T. J.: 2006, *Wills' Minerals Processing Technology*, Elsevier Ltd.

Witteveen, H. J.: 2003, *The response of a uniform jig bed in terms of the porosity distribution*, PhD thesis, TU Delft, Delft, The Netherlands.

WVO: 1969, Surface water protection law, http://www.vrom.nl/.